UNITED STATES DISTRICT COURT
SOUTHERN DISTRICT COURT OF FLORIDA
Miami Division

Case No.: 1:16-cv-23017-DPG

SOUTHERN ALLIANCE FOR CLEAN ENERGY
TROPICAL AUDUBON SOCIETY INCORPORATED,
and FRIENDS OF THE EVERGLADES, INC.,

Plaintiffs,

v.

FLORIDA POWER & LIGHT COMPANY,

Defendant.

EXPERT REPORT OF E.J. WEXLER, P.ENG. (Ontario)

I am offering expert testimony on behalf of Plaintiffs in this matter. Pursuant to Fed. R. Civ. P. 26(a)(2)(B), the following is my written report:

My opinions are based on data on the hydrogeology, hydrology, and water quality of both surface water and groundwater available to me as of May 14, 2018, and on my numerical modelling studies and reviews described in the attached technical reports. I will continue to search for new data and to update and refine our models to inform my opinions as set forth below.

OPINIONS

1. Analysis of Salt Water Movement in the South Dade Area

In 2010, Earthfx developed and calibrated a three-dimensional density-dependent groundwater flow/solute transport model for the area surrounding the Atlantic Civil Incorporated (ACI) property as part a cumulative impact assessment conducted on behalf of EAS Engineering and ACI. (The report is included as Attachment 2. A report describing a 2014 update to the model is included as Attachment 3). The model development followed procedures similar to those employed in previous USGS modeling studies of groundwater flow and saltwater encroachment (e.g., Merritt (1997) and Langevin (2001)). The primary focus of the modelling effort was to examine the impact of the quarry development on the position of the saltwater front. To assess cumulative impacts, other water uses and influences were also simulated including other permitted water takings, other quarry lakes, the SFWMD canal system and other irrigation canals, and the FPL Cooling Canal System (CCS).

A significant effort was directed to recreating the hydrologic history of the study area starting in 1945 to the present (2010 in the original work and extended in 2015) and on representing the migration of the FW/SW interface over time. Model simulations indicated that the current position of the FW/SW interface is the result of historical climate conditions and, more importantly, the sequence of man-made changes that altered the natural groundwater and surface water flow systems in the study area. These simulations showed that the hydraulic heads along with canal and wetland stage responded quickly to change, but movement of solutes is much slower. The response of the FW/SW system is slow but it is never static; it is constantly responding to external change as well as to wet season/dry season variations in rainfall and ET and year-to-year variations.

Simulations have also shown that since its inception, the FPL Cooling Canal System (CCS) has significantly affected the dynamics of freshwater/saltwater in the vicinity of the ACI property. As salinities in the CCS have increased over time, the simulations showed a corresponding westward migration of the freshwater/saltwater interface from the CCS towards the ACI property.

The model was updated in 2015 to reflect changes in rainfall and salinity in the CCS between 2010 and 2015. Figure 1 shows the simulated concentration (red contour lines) versus the observed data, showing that the model was able to match the observed concentrations in the Biscayne aquifer west of the CCS by simulating the history of the area starting pre-1940. It should be noted that the observed and simulated chloride concentrations close and beneath the CCS are above 19,400 mg/L, the average concentration of seawater (i.e., hypersalinity). Figure 2 and 3 show simulations of the dissolved solids concentrations in Fall of 2015 with the CCS and under a hypothetical case with similar climate and canal level history but where the CCS was never constructed.

The model has since been employed from 2015 to 2017 in a predictive manner to assess the impacts of various remedial measures at the ACI site (e.g., slurry walls and pumping/injection wells) and proposed remedial and dilution schemes for the CCS including extracting water from wells along L-31 at various rates and a “do-nothing” scenario to serve as a baseline. The model was used to assess whether the addition of large volumes of water to the CCS would allow or prevent continued westward movement of saline water already in the aquifer towards the ACI property.

As an example, output from the FPL Salt Water Balance model (in terms of an increase in relative heads in the CCS and a time series of monthly salinity values) was used as input to our three-dimensional density-dependent groundwater flow and transport model. The goal of the simulations was to determine whether the addition of water to the CCS would allow or prevent continued westward movement of saline water already in the aquifer towards the ACI property. Results of the simulations showed that dilution of water in the CCS (30, 60, or 100 MGD maximum takings from L-31) would reduce salinities in the aquifer compared to the “do-nothing” scenario. However, migration of saline water towards the ACI property would continue. That is, while the concentrations of new water seeping into the aquifer was reduced and mixing of this water occurred along the edges of the hypersaline plume, the body of saline water already introduced into the aquifer would continue to move westward driven by a combination of concentration gradients, density differences, and the elevated water levels in the CCS.

Another scenario studied the effectiveness of remedial wells, located at several different locations including at L31, in between ACI and L31, and at ACI. Pumping rates at the wells and combinations of the wells were assessed. The most effective wells for removing contaminant mass were located in between ACI and L31. However, stopping the westward migration towards the ACI property required extraction wells at the boundary of the ACI property. Other factors, however, such as an unacceptable impact of pumping on water levels in the adjacent wetlands, may prevent the implementation of pumping at the optimal locations or at optimal rates.

2. *Analysis of FPL Predictions of Remedial Measures Effectiveness*

As part of our investigations, we reviewed the predictive analyses presented by FPL to demonstrate that their remedial actions would be effective and would halt the westward movement of hypersaline water. Models developed by FPL's consultants prior to 2015 were felt to be inadequate to the task because, among other factors, they did not represent the three-dimensional nature of the aquifer. A separate review of a new FPL three-dimensional model was conducted and found significant limitations, including a poor representation of aquifer properties in the western area between the CCS and C-111. This limits the ability of the FPL-3D model to predict the movement of the hypersaline plume in the area west of the CCS. (The review is included as Attachment 4)

Our opinion is that predicting the behavior of the body of hypersaline water introduced into the Biscayne aquifer by the CCS operations is complex and requires a three-dimensional density-dependent groundwater flow and transport model that adequately represents the hydrogeologic conditions in the area. The analyses that we have reviewed to date did not meet those conditions.

3. Witness Qualifications.

Attachment 1 provides a Curricula Vitae for E.J. Wexler, P.Eng. which includes a description of my educational background and work experience. Also provided is a list of publications that I have authored or co-authored.

PRIOR TESTIMONY

During the past 4 years, I have testified in deposition and at trial in the following case:

In re Florida Power and Light Company Turkey Point Power Plant Unites 3-5 Modification to Conditions of Certification. Case No. 15-1559EPP (Florida Division of Administrative Hearings, December 1-4, 2015).

COMPENSATION

Earthfx Incorporated is being compensated for my work in this matter at $180.00 per hour.

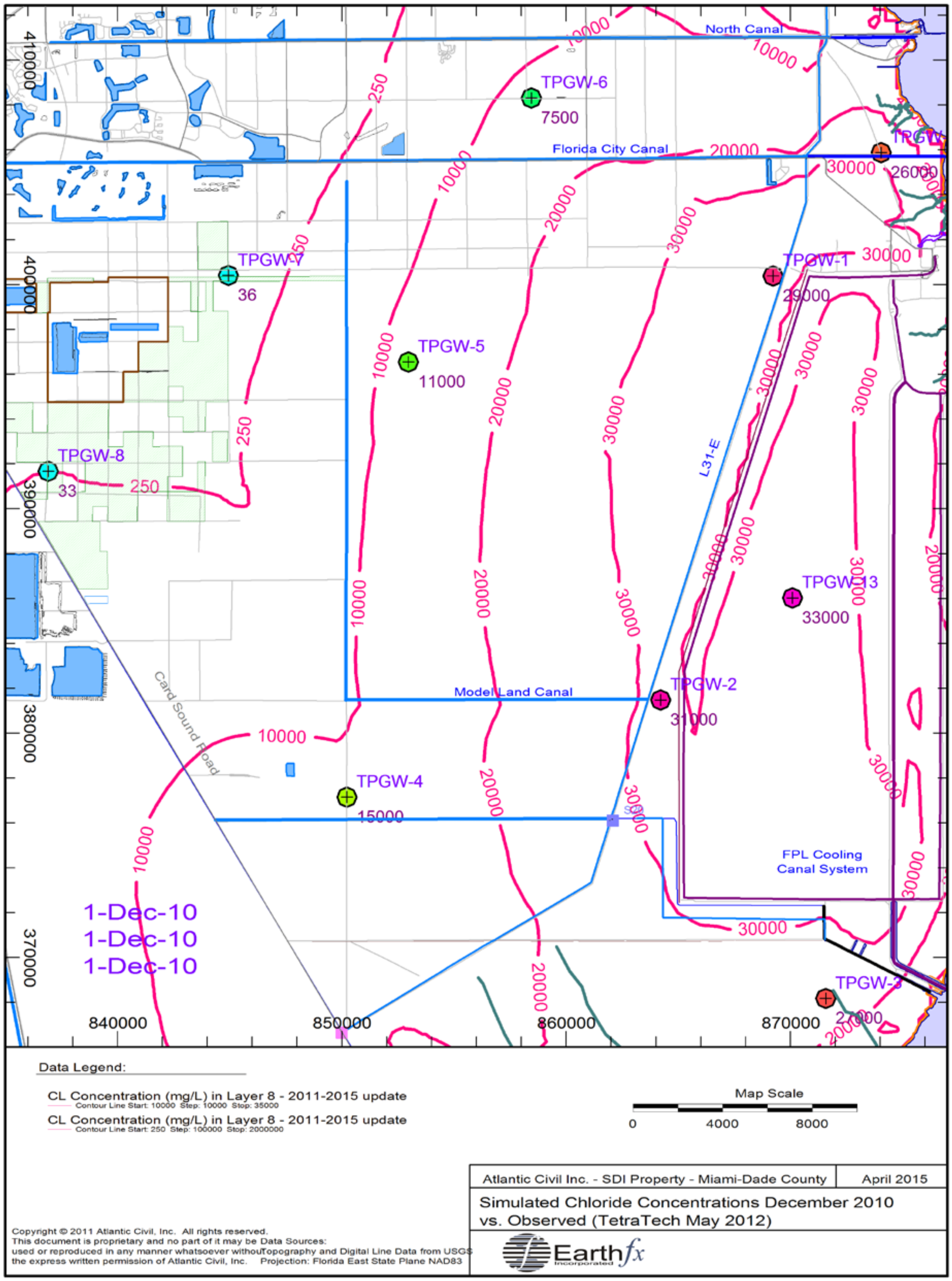
North Canal
Florida City Canal
Model Land Canal
Card Sound Road
L31-E
FPL Cooling Canal System
TPGW-6
7500
TPGW-7
36
TPGW-5
11000
TPGW-8
33
TPGW-1
29000
TPGW-13
33000
TPGW-2
31000
TPGW-4
15000
TPGW-3
27000
26000
1-Dec-10
1-Dec-10
1-Dec-10
410000
400000
390000
380000
370000
840000
850000
860000
870000
Data Legend:
CL Concentration (mg/L) in Layer 8 - 2011-2015 update
Contour Line Start: 10000 Step: 10000 Stop: 35000
CL Concentration (mg/L) in Layer 8 - 2011-2015 update
Contour Line Start: 250 Step: 100000 Stop: 2000000
Map Scale
0
4000
8000
Atlantic Civil Inc. - SDI Property - Miami-Dade County
April 2015
Simulated Chloride Concentrations December 2010 vs. Observed (TetraTech May 2012)
Copyright © 2011 Atlantic Civil, Inc. All rights reserved.
This document is proprietary and no part of it may be used or reproduced in any manner whatsoever without the express written permission of Atlantic Civil, Inc.
Data Sources: Topography and Digital Line Data from USGS
Projection: Florida East State Plane NAD83
Earthfx Incorporated

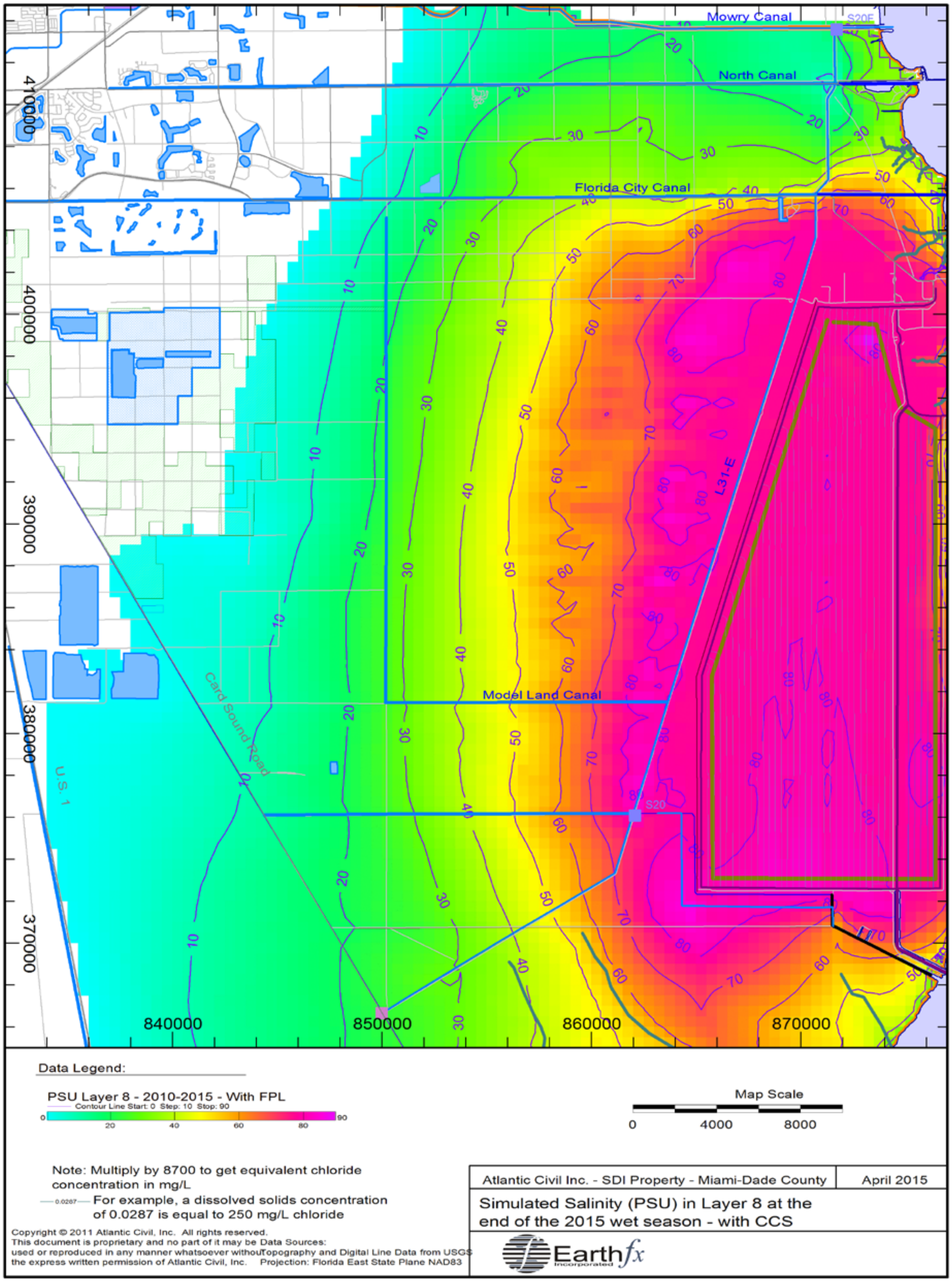
Mowry Canal
S20F
North Canal
Florida City Canal
Model Land Canal
L31-E
Card Sound Road
U.S. 1
S20
410000
400000
390000
380000
370000
840000
850000
860000
870000
Data Legend:
PSU Layer 8 - 2010-2015 - With FPL
Contour Line Start: 0 Step: 10 Stop: 90
Map Scale
0 4000 8000
Note: Multiply by 8700 to get equivalent chloride concentration in mg/L
0.0287
For example, a dissolved solids concentration of 0.0287 is equal to 250 mg/L chloride
Copyright © 2011 Atlantic Civil, Inc. All rights reserved.
This document is proprietary and no part of it may be used or reproduced in any manner whatsoever without the express written permission of Atlantic Civil, Inc.
Data Sources:
Topography and Digital Line Data from USGS
Projection: Florida East State Plane NAD83
Atlantic Civil Inc. - SDI Property - Miami-Dade County
April 2015
Simulated Salinity (PSU) in Layer 8 at the end of the 2015 wet season - with CCS
Earthfx

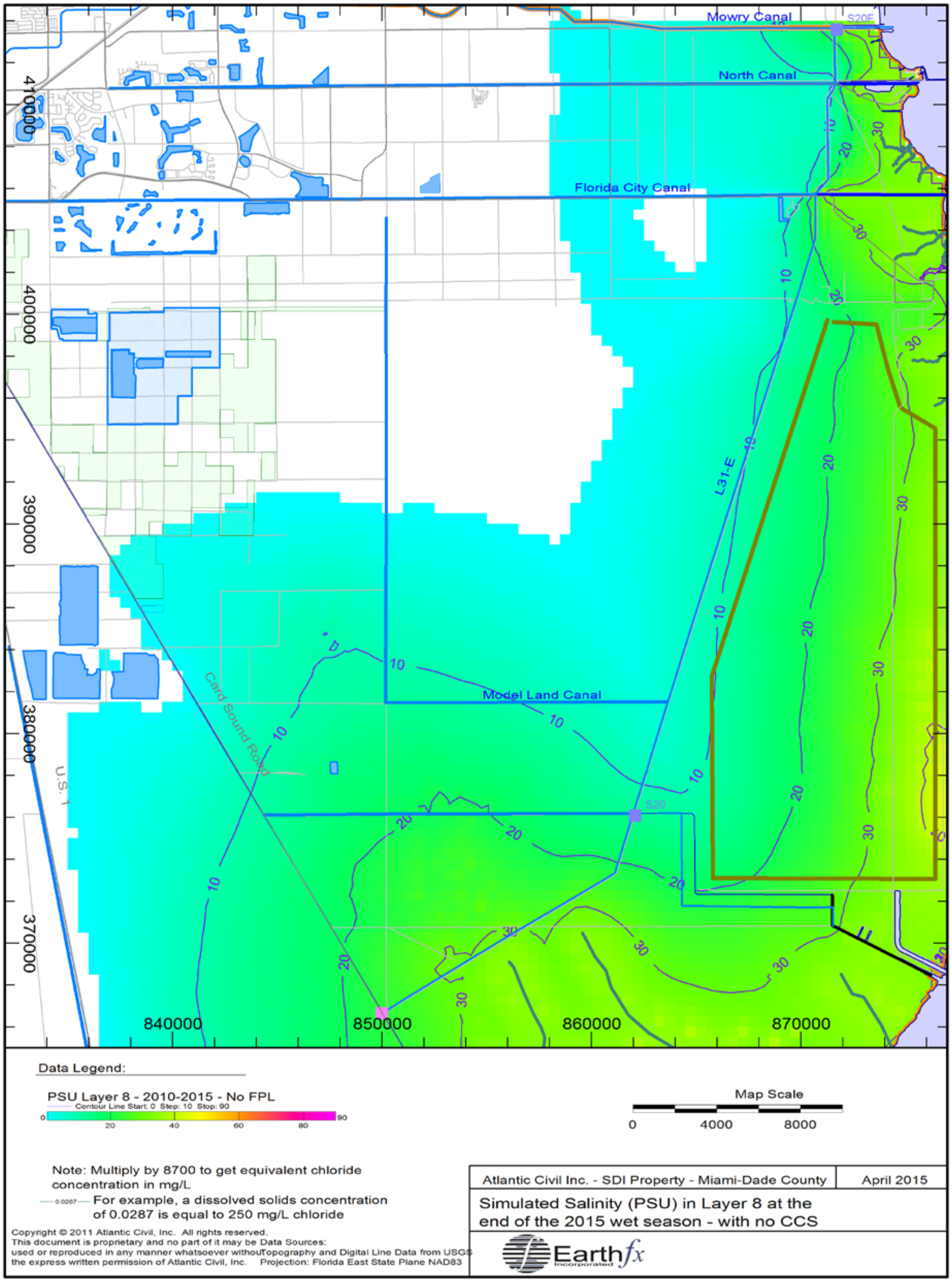
Mowry Canal
S20F
North Canal
Florida City Canal
L31-E
Model Land Canal
Card Sound Road
U.S. 1
S20
410000
400000
390000
380000
370000
840000
850000
860000
870000
Data Legend:
PSU Layer 8 - 2010-2015 - No FPL
Contour Line Start: 0 Step: 10 Stop: 90
0
20
40
60
80
90
Map Scale
0
4000
8000
Note: Multiply by 8700 to get equivalent chloride concentration in mg/L
For example, a dissolved solids concentration of 0.0287 is equal to 250 mg/L chloride
Copyright © 2011 Atlantic Civil, Inc. All rights reserved. This document is proprietary and no part of it may be used or reproduced in any manner whatsoever without the express written permission of Atlantic Civil, Inc.
Data Sources: Topography and Digital Line Data from USGS
Projection: Florida East State Plane NAD83
Atlantic Civil Inc. - SDI Property - Miami-Dade County
April 2015
Simulated Salinity (PSU) in Layer 8 at the end of the 2015 wet season - with no CCS
Earthfx

ATTACHMENT 1: CV for E.J. Wexler, P.Eng.

E. J. Wexler, M.Sc., M.S.E., P.Eng.

Vice-President and Director of Modeling Services

BIOGRAPHY

E.J. Wexler is Vice-President and Director of Modeling Services at Earth*fx* and has over 35 years of experience in groundwater modeling, contaminant hydrogeology, geostatistical analysis, and model code development. He has taught graduate courses in groundwater at universities in Canada, FL, and NY. He worked as a research hydrologist and groundwater modeling specialist for the USGS in Reston, VA, Long Island, NY, and Miami, FL. Mr. Wexler is a licensed engineer in the Province of Ontario, Canada.

EDUCATION

- B.E. Civil Engineering, City University of New York (1977)
- M.S.E. Civil Engineering, Princeton University (1978)
- M.Sc. Earth Science, University of Waterloo (1988)

PROFESSIONAL EXPERIENCE

Director of Modeling Services, Earthfx Inc. ***2002 - Present***

Mr. Wexler is the Director of Modeling Services at Earth*fx* where he leads a team of surface and groundwater modelers. Mr. Wexler's experience at Earth*fx* includes:

- Directing groundwater flow and contaminant transport studies, with an emphasis on integrated groundwater/surface water modeling using GSFLOW.
- Technical Manager for Source Water Protection studies in southern Ontario. This included regional groundwater flow modeling studies for aquifer and wellhead vulnerability assessment and hydrologic modeling for water quality and water quantity risk assessment.
- Technical Manager for Lake Simcoe Protection Plan studies in southern Ontario. These subwatershed studies assessed regional groundwater flow, delineated ecologically significant groundwater recharge areas, and quantified the impact of land development, drought, and climate change on watershed function.
- Project Manager for an Integrated Catchment Management Plan for in Northern Oman.
- Member of Scientific Peer Review team for evaluating the Tampa Bay Water/SWFWMD North Tampa Bay integrated model.
- Conducted integrated GW/SW modeling study for a large-land development in Ft. Meyers, FL and a study of FW/SW interface movement in the Homestead, FL area.
- Project Manager for hydrogeologic data analyses in South Florida related to the Comprehensive Everglades Restoration Program (CERP)

- Developed geostatistical analysis codes (3-D kriging and variogram analysis) for VIEWLOG and advanced water quality analysis modules for SiteFX.

Hydrogeologist/Hydrologist, Gartner Lee Limited ***1990 - 2002***

As a senior hydrogeologist at Gartner Lee, Mr. Wexler directed groundwater modeling, groundwater resources management and contaminant hydrogeology studies in Canada, Florida and the Middle East. Selected projects where he was principal investigator include:

- Development of a groundwater flow and contaminant transport model for a low-level radioactive waste disposal site and evaluation of remedial measures.
- Development of a groundwater flow model for St. Thomas, U.S. Virgin Islands used to investigate the source of volatile organic compounds affecting water supply wells.
- Development of surface water and groundwater models to assess the impact of artificial recharge on the water balance, groundwater flow patterns and salt water intrusion in the arid coastal regions of Northern Oman.
- Co-development of MODNET, a surface water and groundwater model based on the USGS MODFLOW model and the USACE UNET surface water model for SFWMD.

Research Hydrologist, U.S. Geological Survey, Miami, Florida ***1986 - 1990***

Mr. Wexler researched and developed models for simulating groundwater/surface water interaction. He also investigated the effects of density-dependent groundwater flow and solute transport on the feasibility of freshwater storage and recovery in saline aquifers (ASR) at Cape Coral, FL. He developed a coupled, regional-scale/fine-scale flow and transport model for simulating leachate migration at landfills in West Palm Beach, FL. He served as the Groundwater Discipline Specialist and Digital Modeling Specialist and was responsible for technical review and quality control for other surface water and groundwater modeling investigations.

Hydrologist, U.S. Geological Survey, Long Island, New York ***1981 - 1985***

Mr. Wexler was the Project Chief of a groundwater contaminant transport study at a sanitary landfill site. He investigated the local hydrogeology and studied the physical and geochemical controls on the transport of groundwater solutes. He developed flow and transport models for the study area and simulated long-term contaminant migration.

Research Hydrologist, U.S. Geological Survey, Reston Virgina ***1979 - 1981***

Mr. Wexler was responsible for developing and testing finite-element models for simulating groundwater flow, solute transport and parameter estimation. E.J. consulted on field application of these models to sites in Maine, Kansas, and California.

TECHNICAL PAPERS FROM 2008 (FULL BIBLIOGRAPHY AVAILABLE ON REQUEST)

Earthfx Incorporated, 2018, Whitemans Creek Tier Three Local Area Water Budget and Risk Assessment - Risk Assessment Report: prepared for the Grand River Conservation Authority, May 2018, 170 p.

Earthfx Incorporated, 2017, Tier 3 Water Budget and Local Area Risk Assessment for the Greensville Groundwater Municipal System - Updated Risk Assessment Report, : prepared for Conservation Halton, July 2017, 197 p.

Earthfx Incorporated, 2016, Phase 2 Review of potential cumulative effects to surface water and groundwater from in-situ oil sands operations, focusing on the Mackay River Watershed: prepared for the CEMA – Water Working Group, January 2016, 416 p.

Earthfx Incorporated, 2016, Phase 2 Review of potential cumulative effects to surface water and groundwater from in-situ oil sands operations, focusing on the Mackay River Watershed: prepared for the CEMA – Water Working Group, January 2016, 416 p.

Earthfx Incorporated, 2015, Update of Statistics Module in Sitefx: draft report prepared for Environment Programs Department - Ontario Power Generation, January 2015, 42 p.

Earthfx Incorporated, 2014, Additional Groundwater Flow and Saltwater/Freshwater Interface Modeling for the Atlantic Civil Property South Miami-Dade County, FL: prepared for EAS Engineering, Incorporated, March 2014.

Earthfx Incorporated, 2014, Tier 3 Water Budget and Local Area Risk Assessment for the Region of York Municipal Systems – Risk Assessment Report; prepared for the Regional Municipality of York Transportation and Works Department, March 2014.

Earthfx Incorporated, 2014, Tier 3 Water Budget and Local Area Risk Assessment for the Kelso and Campbellville Groundwater Municipal Systems - Phase 2 Risk Assessment Report: prepared for the Halton Region Conservation Authority, February 2014.

Earthfx Incorporated, 2014, Ecologically Significant Groundwater Recharge Area Delineation in the Central Lake Ontario Conservation Authority Area: prepared for the Central Lake Ontario Conservation Authority, May 2014.

Earthfx Incorporated, 2012, Simulation of Groundwater Flow and Saltwater Movement in the vicinity of the Atlantic Civil Property South Miami-Dade County, FL:

Earthfx Incorporated, 2010, Tier 2 water budget analysis and water quantity stress assessment for Lake Ontario Subwatersheds 1 and 3 in the Brighton and Colborne area: prepared for the Trent Conservation Coalition Source Protection Region - Lower Trent Conservation, April 2010.

Earthfx Incorporated, 2008, Appendix L: Simulation of groundwater flow in the vicinity of the proposed Southeast Collector trunk sewer -- Southeast Collector Trunk Sewer Environmental Assessment: Prepared for Conestoga-Rovers and Associates, the Regional Municipality of York, and the Regional Municipality of Durham, March 2008

Earthfx Incorporated, 2008, Simulation of groundwater flow in the vicinity of the New Nuclear-Darlington project -- New Nuclear-Darlington Geology and Hydrogeology Effects Assessment: Prepared for CH2M Hill Canada Limited and Ontario Power Generation Inc., December 2008.

Earthfx Incorporated, Greg Rawl, P.G., and Dean M. Mades (HSW Engineering Inc.), 2012: An integrated surface-water/groundwater modeling analysis of infiltration and stormwater runoff from the Babcock Ranch Community Development, Charlotte and Lee Counties, Florida: Prepared for Babcock Property Holdings, LLC, July 2012.

Fenske, J., Banta, R., Piper, S., Donchyts, G., and Wexler, E.J, 2011: Coupling HEC-RAS and MODFLOW using OpenMI: in Proceedings of the MODFLOW and More 2011 - Integrated Hydrologic Modeling Conference, p. 101-105

Kassenaar, J.D.C., Wexler, E.J., Marchildon, M., Qing Li, 2011, GSFLOW Modeling of Surface Water And Groundwater Flow for Source Water Protection, Regional Municipality of York, Ontario, Canada: presented at MODFLOW and More, June 2011.

Kassenaar, J.D.C., Wexler, E.J., Thompson, P.J., and Takeda, M.G.S., 2017, Assessing the cumulative effects of groundwater withdrawals for oil sands production on a watershed scale: 2017 MODFLOW and More conference, Golden CO, May 2017

Li, Q., Unger, A.J., Sudicky, E.A., Kassenaar, J.D., Wexler, E.J., and Shikaze, S., 2008: Simulating the multi-seasonal response of a large-scale watershed with a 3-D physically-based hydrologic model: J. of Hydrology, v. 357, no. 3-4.

Takeda, M.G.S., Wexler, E.J., Thompson, P.J., and Kassenaar , J.D.C., 2017, Characterization of seasonal thermal plume migration from a below-water-table aggregate extraction operation: 2017 MODFLOW and More conference, Golden CO, May 2017

Thompson, P.J., Wexler, E.J., Takeda, M.G.S., and Kassenaar, D., 2015, Integrated surface water/groundwater modelling to simulate drought and climate change impacts from the reach to the watershed scale: paper presented at the IAH-CNC Conference, Waterloo, Ontario, November 2015.

WEST Consultants Inc. Earthfx Incorporated, and Hydrocomp Incorporated, 2013: Peer Review of the Integrated Northern Tampa Bay Model Application – Final Report prepared for Tampa Bay Water and Southwest Florida Water Management District.

WEST Consultants Inc. Earthfx Incorporated, and Hydrocomp Incorporated, 2013: Peer Review of the Integrated Northern Tampa Bay Model Application – Final Report prepared for Tampa Bay Water and Southwest Florida Water Management District.

WEST Consultants Inc. Earthfx Incorporated, and Hydrocomp Incorporated, 2018: Integrated Hydrologic Model Scientific Review – Final Report prepared for Tampa Bay Water and Southwest Florida Water Management District.

Wexler, E.J., Strakowski, J., Kassenaar, D., Marchildon, M., Thompson, P.J., 2013, Using GSFLOW to Simulate Wellfield/Reservoir Interaction in a Re-Entrant Valley: presented at MODFLOW and More, June 2013

Wexler, E.J., Thompson, P.J., Rawl, G., and Kassenaar, J.D.C., 2015, Analysis of Groundwater/Surface Water Interaction at the Site Scale Babcock Ranch Community Development Lee County, Florida: paper presented at the IAH-CNC Conference, Waterloo, Ontario, November 2015.

Wexler, E.J., Thompson, P.J., Kassenaar, J.D.C., and Takeda, M.G.S., 2016, Applications of integrated models to watershed and sub-watershed scale analysis -- A Canadian context: XXI International Conference Computational Methods in Water Resources, June 2016, Waterloo, Ontario.

Wexler, E.J., Thompson, P.J., Takeda, M.G.S., Howson, K.N., Cuddy, S.E., and Kassenaar, J.D.C., 2014, Simulating climate change and extremes with an integrated surface water-groundwater model to assess hydrologic response in the Lake Simcoe watershed: Canadian Water Resources Association Conference, Hamilton, ON, June 2014.

Wexler, E.J., Thompson, P.J., Takeda, M.G.S., Malott, S., Shifflett, S.J., and Kassenaar , J.D.C., 2017, Development and application of an irrigation demand module for the USGS GSFLOW Model: 2017 MODFLOW and More conference, Golden CO, May 2017

ATTACHMENT 2: Copy of Final Report. Body of report attached as Attachment 2.

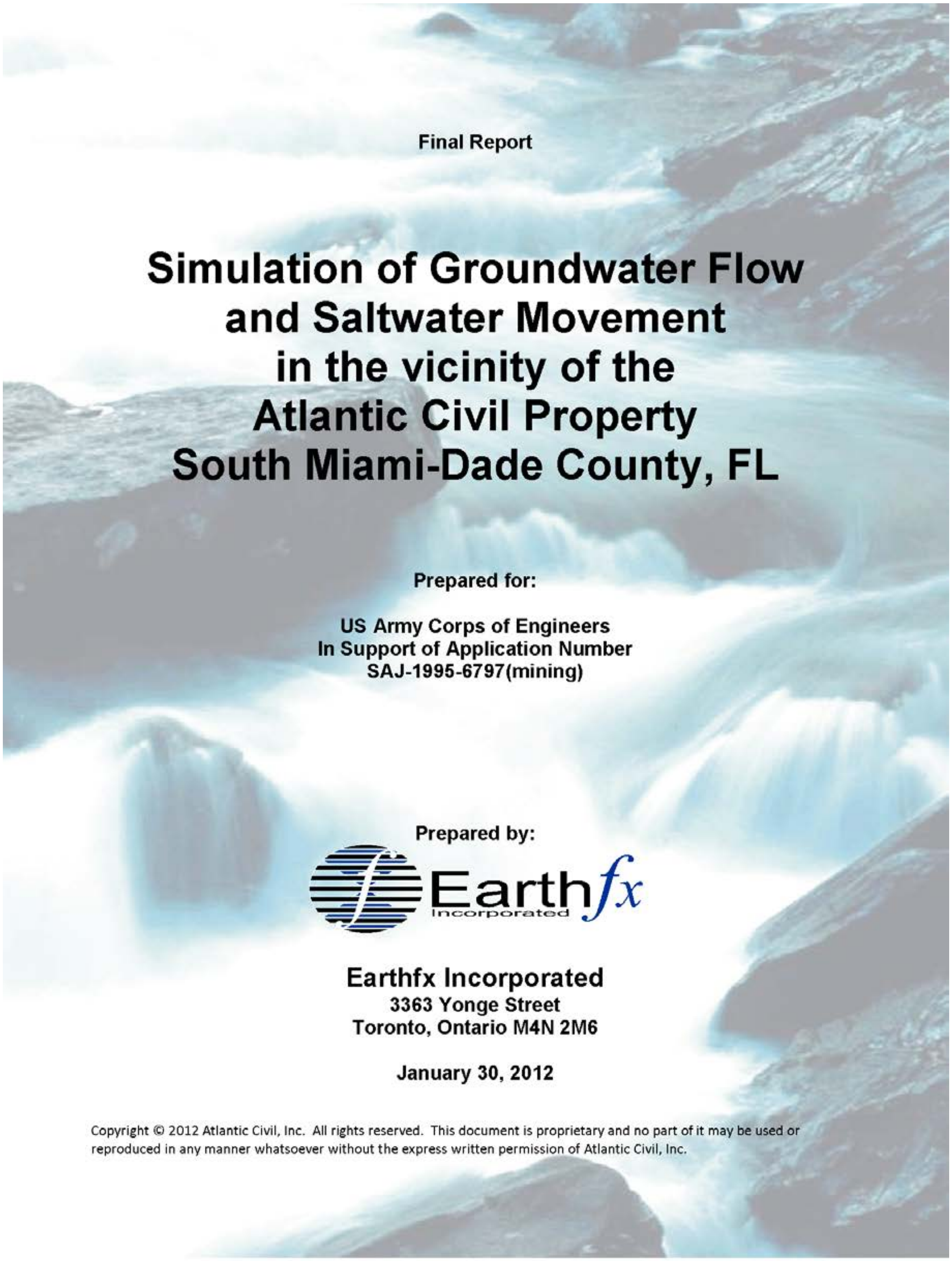

Final Report

Simulation of Groundwater Flow and Saltwater Movement in the vicinity of the Atlantic Civil Property South Miami-Dade County, FL

Prepared for:

US Army Corps of Engineers
In Support of Application Number
SAJ-1995-6797(mining)

Prepared by:

Earthfx Incorporated

Earthfx Incorporated
3363 Yonge Street
Toronto, Ontario M4N 2M6

January 30, 2012

ATTACHMENT 3: Copy of Final Report. Body of report attached as Attachment 3.

Technical Appendix A

Additional Groundwater Flow and Saltwater/Freshwater Interface Modeling for the Atlantic Civil Property South Miami-Dade County, FL

Prepared for:
EAS Engineering, Incorporated

Prepared by:

Earthfx Incorporated

Earthfx Incorporated
3363 Yonge Street
Toronto, Ontario M4N 2M6

March 25, 2014

ATTACHMENT 4: Copy of Final Report. Body of report attached as Attachment 4.

Privileged and Confidential

Review of the FPL Three-Dimensional Groundwater Flow and Saltwater Transport Model

Prepared for:

Lewis, Longman, and Walker, P.A.
EAS Engineering, Incorporated

Prepared by:

Earthfx Incorporated

Earthfx Incorporated
3363 Yonge Street
Toronto, Ontario M4N 2M6

June 5, 2016

Final Report

Simulation of Groundwater Flow and Saltwater Movement in the vicinity of the Atlantic Civil Property South Miami-Dade County, FL

Prepared for:

US Army Corps of Engineers
In Support of Application Number
SAJ-1995-6797(mining)

Prepared by:

Earthfx Incorporated
3363 Yonge Street
Toronto, Ontario M4N 2M6

January 30, 2012

Earth*fx* Incorporated

Earth Science Information Systems

January 30, 2012

Stephen A. Walker, Esquire
Lewis, Longman & Walker, P.A.
515 North Flagler Drive, Suite 1500
West Palm Beach, Florida 33401
Phone: 561-640-0820
Facsimile: 561-640-8202
email: swalker@llw-law.com

RE: Simulation of Groundwater Flow and Saltwater Movement in the vicinity of the Atlantic Civil Property, South Miami-Dade County, FL.

Dear Mr. Walker:

We are pleased to provide the attached summary of our modelling of groundwater flow and saltwater movement in the area surrounding the Atlantic Civil Property in South Miami-Dade County, Florida with specific reference to predicted movement of the saltwater front due to the expansion of the quarry and other changes in the local hydrology. This report addresses review comments by USACE Jacksonville District staff to our earlier draft.

The modeling represents an update to previous work completed for the site in 2004. Key improvements include (1) the simulation of transient (time-dependent) flow to better match observed response to wet and dry periods; (2) the simulation of density-dependent flow and transport to simulate the historic and future migration of the freshwater/saltwater interface; (3) the inclusion of external factors (current and proposed) that affect the site including municipal pumping, changes in canal operation, and operation of the FPL cooling canals, that needed to be assessed as part of the cumulative impact analysis, and (4) improvements to the representation of the local geology and hydrology based on ongoing field data collection and results of other modeling efforts.

We believe that this report will help meet the requirement of the Cumulative Impact Analysis required for the quarry expansion. Should you have any questions, please do not hesitate to call.

Yours truly
Earth*fx* Incorporated

Dirk Kassenaar, M.Sc., P.Eng.

E.J. Wexler, M.Sc., M.S.E., P.Eng.

Table of Contents

List of Figures

List of Tables

Simulation of Groundwater Flow and Saltwater Movement in the Vicinity of the Atlantic Civil Property, South Miami-Dade County, FL

Executive Summary

A numerical model was developed to simulate regional groundwater flow and saltwater movement in the vicinity of the proposed quarry lake on the Atlantic Civil, Inc. (ACI) property in southeast Miami-Dade County. The model used hydraulic properties and recharge rates based on the available field data and the results of previous modeling studies by the U.S. Geological Survey (USGS) and Earthfx. The model was calibrated by matching response in observation wells and the mapped position of the saltwater front.

The primary focus of the modelling effort was to examine the impact of the quarry development on the position of the saltwater front. The updated model included the ability to simulate transient, rather than steady-state flow, could account for density-dependent flow and solute transport, and better represented the history of change to the canal systems that greatly influence groundwater flow and saltwater intrusion in the study area. Results of saltwater intrusion modelling were presented in a series of plan view maps of dissolved solids concentrations. Animations of the results of the continuous simulations are provided on the enclosed DVD. A secondary objective of the modelling effort was to confirm results of earlier Earthfx studies that showed construction of lakes on the ACI property would have no significant impacts on the surrounding wetland mitigation areas.

Model results indicated that groundwater levels in the "With ACI Quarry" simulation were slightly lower on the upgradient (west) side of the lake but slightly higher on the downgradient (east) side. No significant change was seen to the south. A reduction in the number of months in which the simulated dry season water levels dropped below land surface on the east side in the "With ACI Quarry simulations indicated a slight improvement in hydroperiod. The higher water levels in the east also helped to reduce dissolved solids concentrations and prevented landward migration of the saltwater front in the vicinity of the proposed quarry expansion. Similarly, results for the other predictive scenarios for the period from 2010 to 2030, which included the proposed ACI quarry expansion along with the expansion of other nearby quarries and changes in the canal operations, showed that the construction of the ACI quarry will not cause landward movement of the salt front.

1 Introduction

Atlantic Civil Inc. (ACI) is planning to expand an existing rock quarry site located east of Card Sound Road in South Miami-Dade County, Florida. A cumulative impact assessment (CIA) is being done for the site and surrounding area in response to a request by the U.S. Army Corps of Engineers (COE) following their review of the application for a permit (SAJ-1995-06797 Rock Mining) and supplemental data and analysis supplied by the applicant. The scope of the cumulative impact assessment was originally defined as the watershed containing the proposed quarry (primary watershed) and the two adjacent watersheds (secondary watersheds), as shown in Figure 1. Subsequently, the COE expanded the study area, which was the subject of this modeling effort, to the larger area shown in Figure 1. The expanded study area is 2.5 times larger than originally envisioned, resulting in some model grid adjustments.

The assessment of cumulative impacts is supported by the development and application of a comprehensive numerical model to assess likely changes to current conditions in the groundwater and surface water systems induced by the development of the rock quarry. The model incorporates available hydrologic and hydrogeologic data from the study area and builds on earlier efforts by the U.S. Geological Survey (USGS), COE, and previous studies by Earthfx in 2004. Model development and calibration incorporated data collected from the site by ACI along with data from the surrounding area collected by a large number of agencies including the USGS, the South Florida Water Management District (SFWMD), Florida Power and Light (FPL), the Florida Keys Aqueduct Authority (FKAA), and Miami-Dade County. The data included recent information as well as historical data.

The primary focus of the modelling effort is on assessing the likely changes to the position of the freshwater/saltwater (FW/SW) interface in response to expansion of the rock quarry. The assessment considers the cumulative effect of other recent and future changes within the study area including expansion of other quarries and changes to the canal system. Location of the proposed quarry, other quarry expansions, and changes to the canal system are shown in Figure 2 and discussed in more detail further on in the report. The cumulative assessment also addresses likely changes to groundwater levels in the vicinity of the quarry and the possible effects on stage and hydroperiod in surrounding wetlands along with interference effects on existing water supply wells.

Preliminary model simulations indicated that the current position of the freshwater/saltwater (FW/SW) interface is the result of historical climate conditions and, more importantly, the sequence of man-made changes that altered the natural groundwater and surface water flow systems in the study area. These simulations showed that the hydraulic heads along with canal and wetland stage responded quickly to change, but movement of solutes, while quite rapid compared to many other areas in the U.S., is much slower and the FW/SW system is not at equilibrium everywhere in the study area. Therefore, a significant effort was directed to recreating the hydrologic history of the study area starting in 1945 to the present (2010) and on representing the migration of the FW/SW interface over time.

The original model developed by Earthfx in 2004 had been used to assess the potential impacts of mining on the groundwater system caused by local changes in recharge, evapotranspiration (ET), and evaporation. The 2004 model assumed steady-state (i.e., dynamic equilibrium) conditions at the end of an average wet and dry season but did not simulate transient response to the natural range of climate conditions. The 2004 model approximated the position of the saltwater front but did not consider its movement over time. The current model is fully transient and simulates the continuous response of the groundwater and surface water systems. It also simulates migration of solutes in saltwater entering the aquifer from Biscayne Bay and from uncontrolled canals and considers the effect of density variation on groundwater flow. The model utilizes recorded precipitation data for historical simulations and average precipitation values for future simulations.

Potential impacts were assessed by running a series of simulations. As noted, the model was used to simulate historic conditions from pre-development to the current time (2010). These simulations were used to verify the model's ability to simulate potentials and saltwater migration under variable hydrologic conditions. The simulated heads and saltwater concentrations at the end of 2010 served as the starting point for the assessment of future conditions.

A predictive model run was made to simulate conditions from 2011 to 2030 with the proposed quarry lake expansion. This 20-year simulation examined the incremental effects of (1) expanding the ACI quarry lakes, (2) expanding the ACI quarry lakes and along with other proposed quarry expansions, (3) expanding the ACI and other quarries along with other proposed changes to the Card Sound

Road and Florida City canals. Each simulation was compared against a baseline case in which none of the future changes occurred. The incremental effects, such as increases and decreases in simulated potentials, changes in the position of the saltwater interface, and changes in wetland hydroperiod, were quantified by comparing hydrographs and maps of simulated potentials and dissolved solids concentrations. Descriptions of the study area and additional detail on the modelling effort are provided below.

2 Hydrologic Setting

The study area lies in southeastern Miami-Dade County which has a unique and complex hydrologic and hydrogeologic setting that would be impossible to fully describe in detail in this report. The comprehensive study by Parker and others (1955) provides an invaluable snapshot of early post-development conditions in the study area. In addition, their report discusses issues that are still timely, such as saltwater intrusion along the coastline due to drainage canals and municipal pumping, the inland migration of seawater into uncontrolled canals and subsequent leakage to the underlying aquifer, the leakage of hypersaline power plant cooling waters, and the drainage of wetlands. Numerous follow-up studies by the USGS and SFWMD have built a knowledge base regarding the geology and hydrogeology in the study area, in particular, the work by Klein and Hull (1978), Fish and Stewart (1991), and Causaras (1987). Modelling studies, particularly the one by Merritt (1997), provided insight into aquifer properties and recharge rates and documented changes to the canal network and the effect on the flow system.

To the west of the study area is the Everglades, a vast wetland with shallow surface water flow from Lake Okeechobee in the north to Florida Bay in the south. The eastern boundary of the study area is Biscayne Bay. The urbanized area of Homestead, in the northwest corner of the study area, is located on the Atlantic coastal ridge, an area of slightly higher topography (5-10 ft above mean sea level in the study area) that separates the Everglades from the low-lying marl flats, coastal marshes, and mangrove swamps that adjoin Biscayne Bay and make up the bulk of the study area.

The coastal areas, particularly in the northern third of the study area, have been drained by canal networks to allow agriculture and, more recently, urban development. Some of the large agricultural drainage canals (Mowry, North, Florida City, and the Model Land canals), the Card Sound Road canal, and the U.S. 1 borrow canal were constructed in the period between 1912 and 1942 and were open to Biscayne Bay. Additional canals were constructed by the South Florida Water Management District (SFWMD) in the early 1960s and control structures were placed on the older canals with the exception of the Card Sound Road canal. Stage in the larger canals (e.g., C-103, C-110, C-111, L 31-E, North Canal, Florida City Canal, and the Model Land Canal) is controlled by SFWMD to provide drainage and flood-control. High elevations are maintained at the upstream side of the control structures to minimize saltwater encroachment into the underlying aquifer.

A soil map for the study area is shown in Figure 3. Soils in the area are thin and marly (Biscayne Marl, Pennsuco Marl, and Perrine Marl). Soils in the site vicinity have been described as wet to very wet and the site has been farmed to varying levels of intensity. Open areas to the east, west and south of the proposed quarry lakes are being set aside as wetland mitigation to preserve and enhance existing wetlands.

Quarrying of the underlying limestone occurs at several locations in the study area. Crushed limestone is used as raw material for roads, housing developments, and high grade material for local state and federal construction projects. A generalized land use map for the study area is shown in

Figure 4. Most of the area surrounding the site is classified as wetlands with a lesser amount of upland forest and agricultural lands.

Rainfall in the study area averages 55.5 inches per year with about 75% of the rainfall occurring during the May through September wet season (Langevin, 2001). Measured precipitation data for stations in the Homestead area were obtained for the study period from the SFWMD DBHYDRO database. Annual rainfall for the 1945 to 2010 water years along with the long-term average for the period (61.85 inches) is shown in Figure 5. The values were summarized into wet season and dry season daily averages for the simulations of historic conditions. Wet season and dry season rainfall for 1945 to 2010 along with the long-term averages for the period (42.0 and 19.9 inches, respectively) are shown in Figure 6. Long-term average wet season and dry season daily rainfall rates were used in model simulations of future conditions.

Evapotranspiration may be up to 90% of annual rainfall (Merritt, 1997). Parker and others (1955) indicated that ET in South Florida removes a greater amount of water from below the water table compared to that from the soil zone. Accordingly, many models for the study area, including the one developed for this study, have applied precipitation minus runoff as the net recharge term and allowed the model to calculate ET from below the water table. ET from the water table is assumed to occur at a maximum rate when the water surface is exposed, such as in a wetland or quarry lake, and linearly decreases with depth to water. If the water table falls below the “extinction depth”, ET is assumed to fall to zero.

Table 1 lists the daily maximum ET rates on a monthly basis which were used by Merritt (1997) and Langevin (2001). These rates were averaged over the wet season and dry season for historic and future conditions simulations. Langevin (2001) suggested runoff coefficients and extinction depths for different land use types based on earlier studies and model calibration. These values were modified slightly during the model calibration process. Calibrated values are presented in Table 2.

Saltwater Intrusion

Parker and others (1955) indicated that the saltwater front, as defined by the 1000 milligram per liter (mg/L) isochlor, was likely very close to the shoreline prior to development of South Florida. They noted that the dredging of the Miami River and other canals lowered water levels in the Everglades, upset the natural equilibrium, and allowed inland migration of the saltwater front.

Detailed investigation of seawater intrusion in the study area began after salty water destroyed crops during a series of severe droughts in 1943 and 1944 (Parker and others, 1955). They mapped the position of the saltwater front in 1945 and noted that “*The widest zone of saltwater encroachment occurs in the marl flats along the southeastern Dade County coast line where a maze of drainage canals has lowered the water table.*”

Current conditions at wells monitored by the USGS and the FKAA are available at http://www.sflorida.er.usgs.gov. Historic mapping of the position of the saltwater front at various times between 1945 and 2010 is shown in Figure 7. As Langevin (2001) noted, the differences between the lines do not necessarily indicate movement of the saltwater front between the sampling times but may reflect differences in the number of wells sampled, interpretation, and interpolation methods. In general, the lines show reasonable consistency on a regional scale. Localized movement of the front likely occurs in response to climatic variation (wet years and dry years). For example, Klein and Hull (1978) noted that seawater intrusion had been halted as a result of the installation of control structures but a re-advance of saltwater occurred in 1970-1971 in the South Dade area due to a prolonged dry season.

Local features to be noted in these maps include the landward extension of the saltwater front at the end of the Card Sound Road Canal. The extension is assumed to result from the inland migration of saltwater in the uncontrolled canal during dry periods and the subsequent leakage of saltwater through the canal bottom. Parker and others (1955) recorded chloride concentrations in excess of 26,000 mg/L at the northern end of the canal in July 1945. Similar concentrations were noted in the other canals at that time and were felt to be a major contributor to saltwater entry to the aquifer.

Parker and others (1955) conducted some important baseline analyses of salinity values in Biscayne Bay, chloride concentrations, and density measurements. These values were used in the modelling study by Langevin (2001) as well as the current study.

3 Conceptual Hydrogeologic Model

The formulation of a conceptual model was the starting point for the numerical model development. The conceptual model is an interpretation of the hydrogeological setting of the study area and includes an evaluation of the critical factors affecting groundwater flow such as model geometry (hydrostratigraphy), model boundaries, estimates of aquifer properties, and the rates of recharge and discharge from the model area.

The conceptual model was formulated based on our review and analysis of existing data for the project site and for the surrounding area and the review of two key modeling studies (Merritt, 1997 and Langevin, 2001) that included the study area. Maps, reports, and digital data sets that related to southeast Miami-Dade County geology, hydrogeology, land surface topography, and surface water flow were gathered and used to build a modeling database. Data on soil types, local climatic conditions, and depth to groundwater were analyzed to estimate the rates and distribution of groundwater recharge within the site and to formulate a water balance for the study area.

Hydrostratigraphy

The hydrogeology of South Florida has been studied extensively by the USGS (e.g., Parker and others (1955), Causaras (1987), and Fish and Stewart (1991)). This study focuses on the upper part of the surficial aquifer system (SAS) which includes the surficial soils and the Biscayne aquifer. Based on a cross-section through the study area by Fish and Stewart (1991), the Biscayne aquifer consists of the Miami Limestone and the Fort Thompson Formation of Pleistocene age. It is underlain by the Tamiami Formation of Pliocene age. The base of the Biscayne aquifer includes beds of higher permeability Tamiami deposits where these are continuous with the Fort Thompson Formation. An east-west section through the study area is shown in Figure 8. The section line location is shown on Figure 1.

The conceptual model uses five layers to represent the local hydrostratigraphy. These are labelled on the left side of Figure 8 and consist of:

Conceptual Model Layer 1: Surface Flow Layer
Conceptual Model Layer 2: Surficial Soils – Predominantly Marl

Conceptual Model Layer 3: Miami Limestone
Conceptual Model Layer 4: Fort Thompson Formation
Conceptual Model Layer 5: Permeable, contiguous beds of the Tamiami Formation

The three lower layers represent the highly permeable Biscayne aquifer. Fish and Stewart (1991) presented a map of transmissivity for the Biscayne aquifer based on numerous aquifer tests. The map was updated by Merritt (1997). Based on the mapping, it is apparent that hydraulic properties vary significantly within the study area. However, Merritt (1997) and Langevin (2001) assumed a constant, uniform hydraulic conductivity of 30,000 ft/d for their models within the study area. For this study, we assigned a uniform hydraulic conductivity value of 12,000 ft/d for the Miami Limestone and 3,000 ft/d for the included beds of the Tamiami Formation based on model calibration. The hydraulic conductivity of the Fort Thompson Formation, the principal aquifer unit, was then calculated based on the relative thicknesses of the three units and the map of Biscayne aquifer transmissivity. Calculated values for the Fort Thompson Formation ranged from 12,000 to 65,000 ft/d as shown in Figure 9. It should be noted that the lower values in the southwest corner of the study area are based on limited data as will be discussed further on in this report. The anisotropy factor (i.e., the ratio of vertical to horizontal hydraulic conductivity) was assumed to be 0.01 similar to Merritt (1997) and Langevin (2001).

It is recognized that the above discussion of aquifer properties represents a simplification of the complex spatial variability of aquifer porosity and hydraulic conductivity. Cunningham and others (2006), for example, note that the hydraulic conductivity of the Biscayne aquifer is highly heterogeneous and anisotropic. They identify four general classes of flow zones, (1) a low-permeability peat, muck, and marl zone near the top of the Biscayne aquifer where it contacts Holocene sediments, (2) a horizontal conduit flow class with high hydraulic conductivity allowing flow between "touching" vugs and solution enlarged bedding planes fractures and cracks, (3) a leaky low-permeability class (e.g., near the contact between the Miami Limestone and the Fort Thompson Formation) where substantial flow occurs through near-vertical pores and (4) a "diffuse -carbonate class where the flow is principally through a small-scale network of vug-to-matrix-to-vug connections.

The bottom of Conceptual Model Layer 5 was interpolated from the contour map of the base of the Biscayne aquifer in Fish and Stewart (1991) and is shown in Figure 10. The tops of the Tamiami Formation, Fort Thompson Formation, and the Miami Limestone (top of bedrock), are shown in Figure 11 through Figure 13 and were interpolated from cross-sections through the study area by Fish and Stewart (1991) and a top of bedrock surface by Parker and others (1955).

Conceptual Model Layer 2 represents the thin surficial soils. The top of Layer 2 was defined by land surface topography which was interpolated to the model grid from LIDAR data, as shown in Figure 14. (The LIDAR data had to be adjusted where it incorrectly mapped man-made structures such as highway ramps and stadiums as part of the natural topography). The layer thickness was calculated by subtracting the interpolated top-of-bedrock surface from the interpolated topography. A minimum thickness of one foot was assumed in areas where bedrock is very near or at surface. A uniform hydraulic conductivity of 10 ft/d was assigned to Layer 2 as in Merritt (1997) and Langevin (2001) based on the predominance of relatively low permeability soils in the study area.

The low lying, non-urbanized areas away from the coastal ridge are often flooded during the wet season. Conceptual Model Layer 1 was used to represent a free-surface where sheet-flow could occur. A similar approach was used by Merritt (1997). The base of Layer 1 was set equal to land surface topography. A high hydraulic conductivity (3,000,000 ft/d) was assigned to Layer 1 over most of the study area. Lakes were assigned a hydraulic conductivity of 30,000,000 ft/d, a value consistent with Merritt (1997).

FW/SW Interface

The freshwater/saltwater (FW/SW) interface behaves to a large-extent as a boundary to freshwater flow within the aquifer system. This boundary was not implemented in the work by Merritt (1997) but in previous modelling by Earthfx, the position of the interface was approximated by the Ghyben-Herzberg relationship which states that the FW/SW interface is located at a depth equal to about 40 times the water-table elevation (assuming a density of saltwater of 64.0 lb/ft^3 (1025 kg/m^3)). For this study, we simulated the position of the saltwater interface by numerically modelling density-dependent flow and transport of salt-water in the Biscayne aquifer using the USGS SEAWAT code (Weixing and Langevin, 2002).

The implementation of the SEAWAT code for the study area was consistent with the work of Langevin (2001). Langevin (2001) applied the code to calculate freshwater discharge to Biscayne Bay. He calculated the current position of the FW/SW interface by starting model simulations in 1989, when conditions were generally similar to the present, and concluded that the saltwater front is close to equilibrium conditions over most of southeast Miami-Dade County. Preliminary SEAWAT simulations for the current study indicated that the current position of the interface still reflected the history of changes to the hydraulic system such as the digging of drainage canals, the construction of control structures, the creation of the FPL cooling system canals and the recirculation of hyper-saline cooling water. This study, therefore, combined the approach of Merritt (1997) in representing the historic changes to the flow system with that of Langevin (2001) simulating the migration of the FW/SW interface to arrive at a better representation of the transient behavior of the groundwater flow system.

Model Extent

The model extent was selected to include natural hydrologic boundaries, where possible. These include a combination of shoreline boundaries to the east, major SFWMD canals to the north and west, and flow-line boundaries (for pre-canal conditions). Methods for representing these boundaries in the numerical model are discussed further on. The northwest boundary, prior to canal construction, is not a natural boundary because groundwater inflow can occur from areas of higher water table elevation to the northwest. Even with the C-111 and C-103 canals in place, it is possible that some inflow still occurs from the northwest. Inflow across this area was estimated as described further on in the section on numerical model development.

Factors Affecting the Water Balance

Recharge to the groundwater system results primarily from infiltrating rainfall and to a lesser extent from leakage beneath the canals and from inflow across the northwest boundary. Discharge from the study area is mainly through ET losses from shallow groundwater and to a lesser extent as leakage back to the canal system. Langevin (2001) concluded that there is very little freshwater discharge to Biscayne Bay or Card Sound from the low-lying areas of Southeast Miami-Dade County although the volume of discharge is hard to measure directly.

There are a number of wellfields in the study area. Monthly pumping rates for the larger water takings were supplied by SFWMD. Permit rates were assumed for the other takings. Pumping rates for 2010 are presented in Table 3. Well locations are shown in Figure 15. Rates used in the historic simulations were based on the reported rates for the simulation period where available and extrapolated from the reported rates where data were not available. Several smaller takings were identified as recovery wells which were assumed to be taking water from shallow depths and returning the treated water to the aquifer.

An additional issue addressed by the model is whether development of the proposed quarry lake might locally affect the water-balance. Changes would likely include the lowering of water levels on the upgradient (west) side of the lake and increasing water levels on the downgradient side. Changes in the water levels would, in turn, have offsetting effects on groundwater ET rates, decreasing ET where the water table is lowered and increasing ET where the water-table is raised. Recharge to the quarry lakes could increase in areas because the land use classification is changed from agriculture to open water and the runoff is changed from 0.25 (see Table 1) to 0.0. ET rates for the open water surface would be set to the maximum rate, similar to the existing lakes and wetlands. The combination of these processes and their net effect on the groundwater levels and the position of the FW/SW interface were analyzed using the numerical model, as described in the next section.

4 Numerical Model Development

Previous modelling of the study area by Earthfx was conducted using the USGS MODFLOW code (McDonald and Harbaugh (1988) and Harbaugh and McDonald (1996)). MODFLOW is a three-dimensional, finite-difference code capable of simulating transient and steady-state flow in multi-layered, confined and unconfined aquifer systems. The computer code (updated recently as MODFLOW 2005 V1.8) is recognized worldwide and has been extensively tested and verified. A second code, MT3D (Zheng and Wang, 1998), has often been used in conjunction with MODFLOW to simulate the advective-dispersive migration of solutes within the groundwater system.

Some models approximate the FW/SW interface as a sharp front and assume that no mixing between the fluids occurs. Because the fluids are miscible, dispersive mixing can occur along the front. The alternating wet season/dry season fluctuations in water levels cause small oscillations in the FW/SW interface. The occurrence of a series of generally wet years or a series of generally dry years causes larger-scale movements of the FW/SW interface. These movements lead to additional, larger-scale mixing and affect both solute concentrations and fluid density. Density gradients, in turn, can induce additional fluid flow and additional mixing. To properly simulate these complex interactions, a model must simultaneously solve the density-dependent fluid flow equations as well as the solute transport equations.

Variable density flow can be described by the following form of the continuity equation:

$$\frac{\partial}{\partial x}\left(\rho K_x \frac{\partial h_f}{\partial x}\right) + \frac{\partial}{\partial y}\left(\rho K_y \frac{\partial h_f}{\partial y}\right) + \frac{\partial}{\partial z}\left(\rho K_z \left(\frac{\partial h_f}{\partial x} + \left[\frac{(\rho - \rho_f)}{\rho_f}\right]\right)\right) = \rho S \frac{\partial h_f}{\partial t} + \left[n \frac{\partial \rho}{\partial C}\frac{\partial C}{\partial t}\right]$$

where K_X, K_Y, and K_Z are the hydraulic conductivities (measured with low solute water) in the x, y, z directions, ρ is the fluid density, ρ_f is the density of freshwater, h_f is the equivalent freshwater head at that point in the aquifer, S_f is the specific storage of the aquifer (assuming freshwater density), C is the fluid concentration. The terms in the square brackets are the additional terms added to the standard (non-density-dependent) equation for groundwater flow. Temperature effects on fluid density and viscosity are not considered in this form of the equation. The fluid concentration, in turn, is governed by the advective dispersive solute transport equation:

$$\frac{\partial C}{\partial t} = \nabla \cdot \mathbf{D} \nabla C - \nabla \cdot \left(\frac{qC}{n} \right) - \frac{q_s C_s}{n}$$

where D is the dispersion tensor, q is the specific discharge (Darcy velocity), n is the effective porosity, q_s is the flux rate associated with a source or sink (e.g., a boundary flow, recharge, or a well) and C_s is the fluid concentration in the source or sink.

The USGS SEAWAT model was developed specifically to simulate these processes. It combines the MODFLOW code, which was modified to include the extra density-dependent flow terms in Equation 1, with the MT3D code used to solve the solute-transport equation. The two equations are solved in an iterative manner with C and ρ updated based on the latest solution of the solute transport equation, and q and the velocity-dependent dispersion coefficients in the solute transport equation updated with the latest velocities determined from the heads and Darcy's Law.

The application of the SEAWAT code to the study area closely follows that of Langevin (2001) for Miami-Dade County. The current model focuses on a smaller region than that of Langevin (2001), has finer spatial resolution, and accounts for other factors, such as the FPL cooling canals, that can influence local flow and solute transport conditions. As noted earlier, the model starts with simulating the hydrologic history of the study area from pre-development conditions as opposed to Langevin (2001) which started with current conditions.

Model data management was conducted using VIEWLOG, a hydrogeologic data analysis and management system, that also serves as a highly efficient pre- and post-processor for MODFLOW, MT3D and SEAWAT. The available maps and hydrogeologic data were entered into the VIEWLOG system. Information from wells and test holes related to stratigraphy, formation properties, and observed water levels and water quality data were maintained in an MS-Access database linked to VIEWLOG for graphical display and analysis. Model development was made easier through special geostatistical analysis functions used to interpolate hydrogeologic data to the model grids. VIEWLOG was used to generate the input data sets for the MODFLOW model and post-process the extensive model output generated in the transient simulations.

Model Grid

A finite-difference grid was designed to represent the study area and consisted of square cells, 500 ft on a side. Initial model runs indicated that using larger cell sizes tended to smear the saltwater front while using smaller cell sizes required very large computational times. The cell size selected balanced the two constraints and yielded accurate results and is significantly smaller than the 3048 ft square cells used by Langevin (2001) and the 5000 to 14,000 ft variable-sized cells used by Merritt (1997). The grid dimensions are 188 rows by 170 columns in each model layer.

The grid is oriented north-south with the origin of the grid (lower left corner) located at 800,000 ft East and 337,000 ft North in the NAD-83 Florida East state plane coordinate system. Figure 16 shows the active portion of the model grid covering the study area.

The numerical model uses 13 layers. The first two represent the surface flow layer and surficial soils, similar to the Conceptual Model. The base of model Layer 1 was set at land surface and the base of Layer 2 coincides with the base of the surficial soil layer with a minimum thickness of one foot. For better accuracy, the Biscayne aquifer (Conceptual Model Layers 3 through 5) was subdivided into 11 sublayers. As before, initial simulations indicated that some smearing occurred with fewer layers while using 11 layers do not require excessive computational times. The base of Layer 3 is at 10 ft below land surface and the thickness of the layer varied based on the interpolated top of bedrock surface. Lower model layers are all 10 feet thick. By comparison, Langevin (2001) used 16.4 ft (5 meter) thick layers. Model layer configuration is shown on the right side of Figure 5.

Time Steps

The model simulations were broken down into a series of historical periods which are discussed, further on, in the section on Model Calibration. The historic periods ranged in length from 4 to 32 years. Each year was subdivided into a wet season and dry season. Wet and dry seasons were further subdivided into a series of time steps. The wet season had an initial time step size of 3.875 days which increased by a factor of 1.2 each time step until a maximum of 15.5 days. For stability reasons, the dry season simulations required a smaller initial time step of 0.5 days with a maximum of 7.75 days. Convergence problems occurred in particularly dry years. In these cases, the time step sizes were reduced and the simulations were repeated until stable solutions were achieved.

Model Boundaries

Constant head boundaries were applied along the shores of Biscayne Bay and Card Sound (Figure 16). Average water level in Biscayne Bay was set to 0.9 ft above mean sea level based on the average monthly value on the tidal side of S20F and about 0.2 feet above the Mean Tide Elevation published for the Turkey Point tidal bench mark. Constant concentration boundaries were also applied at the shoreline and set equal to a dissolved solids concentration of 2.184 lb/ft3 (35 kg/m^3). These values were used to translate the saltwater head at the boundary to an equivalent freshwater head, h_f, in the underlying layers using:

$$h_f = \frac{\rho_{sw}}{\rho_f} h - \frac{(\rho_{sw} - \rho_f)}{\rho_f} Z$$

where ρ_{sw} is the density of seawater and Z is the elevation above sea level. Thus, the equivalent freshwater head at the shore in Layer 8 (at a mid-layer depth of 55 ft below sea level) would be 2.30 ft assuming a freshwater density of 62.43 lb/ft^3 (1000 kg/m^3) for freshwater and 64.0 lb/ft^3 (1025 kg/m^3) for saltwater in Biscayne Bay. Chloride concentrations were related to the solids concentration by assuming that seawater with a dissolved solid content of 2.184 lb/ft^3 (35 kg/m^3) had a chloride concentration of 1.186 lb/ft^3 (19 kg/m^3).

Cells outside the model boundaries are considered inactive and do not contribute flow to the model (Figure 16). In post-1968 simulations, (i.e., after the SFWMD canals were constructed), the canals along the west and north boundaries are assumed to create flow divides and do not allow lateral flow into the study area. In the pre-1968 simulations, the western and southern boundaries nearer the shoreline were presumed to be aligned with natural flow lines and therefore also represent areas where little lateral flow crosses the boundary. The northwest corner, however, is a location where significant cross boundary flow could occur. This boundary was represented as a MODFLOW general head boundary, with flow across the boundary dependent on the head at the regional groundwater divide beneath the coastal ridge. The head at the divide was assumed to be about 6.5 ft above sea level in pre-development simulations and 4.5 ft in post-development simulations to reflect changes induced by drainage north of the current study area. Flow across the northwest boundary past the C103 canal in post-development simulations is relatively minor.

All lateral model boundaries were located at a sufficient distance from the ACI property such that small changes induced by development of the site would not propagate to the model boundaries. Similarly, the simplifying assumptions employed in representing the model boundaries discussed above should not affect flow in the vicinity of the site.

The bottom boundary of the model is defined by the eastward sloping base of the Biscayne aquifer. Cells in the portion of the lower model layers that fell below the interpolated base of the Biscayne aquifer were set as inactive. Thus only a small portion of Layer 13 representing the deepest part of the Biscayne aquifer is active. Increasing portions of Layers 7 through 12 are active. Figure 17 shows the boundary conditions for Layer 9 as an example. The western portion of the model area is truncated in this layer by the rise of the top of the Tamiami Formation. Layers 6 and above were fully active.

Groundwater/Surface Water Interaction

Quarry lakes excavated into the Biscayne aquifer were treated as zones of extremely high hydraulic conductivity. This allowed lake levels to be affected by the groundwater system, and for the lakes, in turn, to affect groundwater flow by inducing flow into the upgradient end of the lake and discharge out the downgradient end. We did not constrain the model by setting the head in the lake to a fixed value. Hydraulic conductivities and anisotropy values were adjusted in each model layer penetrated by the lake. The growth of quarry lakes over time was represented by changing the lake footprints in each historical simulation period.

The larger SFWMD canals along the boundary of the model were simulated using the MODFLOW RIVER module. Model "rivers" can gain water when simulated aquifer heads are above a specified controlling “river elevation” and lose water to the aquifer when aquifer heads are below the controlling elevation. Stage data for measuring points above and below structures were obtained from the SFWMD DBHYDRO database and were used to set average controlling elevations for the wet season and dry season. Stage values assigned for the wet season and dry season simulations are shown in Figure 18.

Internal canals that were connected to the controlled canals, such as the North, Florida City, and Model Land canals (post-1968) were treated as zones of high hydraulic conductivity. These canals were assumed to have a moderate effect on the groundwater system (compared to the boundary canal) because they are indirectly connected to the controlled canals, are generally narrower, and not excavated as deeply into the bedrock. Hydraulic conductivities and anisotropy values were adjusted in model Layers 2 and 3 only. Natural drainage features and canals that had no control structures, such as the Card Sound Road (pre-2011) and the North, Florida City, and Model Land canals, and the borrow canal along U.S. 1 (pre-1968) were also treated as zones of high hydraulic conductivity. The levels in these canals are affected by the groundwater system and they, indirectly, affect groundwater levels to a limited degree. Dissolved solids concentrations in the uncontrolled canals were set with levels decreasing with distance from the shoreline. The leakage of hyper-saline water from the uncontrolled canals was noted as a key factor in the inland migration of saltwater in the study area away from the coastline (Parker and others, 1955).

The interceptor canal along the western edge of the FPL cooling water canal system for the Turkey Point nuclear power generating facility was simulated as a MODFLOW "drain" which can gain water when simulated aquifer heads are above a specified controlling drain elevation but cannot lose water to the aquifer if heads are lower. The drain elevations were inferred from the DEM. Dissolved solids concentrations in the seepage in to the canal is determined by the model and was not specified.

Finally, the FPL cooling water canal system was represented in post-1972 simulations using specified head and concentration cells. The assigned heads were adjusted to represent the southward flow of water in the western canals with levels interpolated from 2.1 ft above sea level at the north end to 0.8 ft at the south. Heads on the east side were varied from 0.8 ft in the south to -0.8 ft in the north to represent the northward flow of water. Assigned concentrations were adjusted over the simulation period based on historic average wet season and dry season concentrations reported quarterly to DERM by FPL. Temperature effects were evaluated by Hughes and others (2009) and were found to be much less significant when compared to salinity-induced density-driven vertical flow, and were, therefore, not simulated here. Concentrations assigned in the future (post-2010) simulations were calculated by projecting the observed linearly increasing concentration trends forward in time. Leakage of hyper-saline water beneath the FPL canals can be inferred from the reported specific conductance values in the three deep boreholes beneath the cooling canals which ranged from 71,082 to 82,425 μS/cm (data from JLA Geosciences, Inc. (2010)) whereas seawater is about 50,000 μS/cm.

Model Calibration Approach

Model calibration was conducted by refining the initial estimates of aquifer properties, concentrations, controlling heads, and ET rates until a close match with observed water levels and the saltwater front position was obtained. Initial results using model parameters obtained from earlier USGS and Earthfx modelling produced improved responses when used in the updated model and, therefore, the range of adjustments needed for the flow modelling was minimal. This also helped to maintain consistency with the previous work. Model calibration was checked by matching observed historic fluctuations in water levels averaged over the wet season and dry season period. Most of the remaining effort was then spent on properly representing the historic changes to the flow system.

Several historic periods were simulated, primarily to match the time-dependent development of the saltwater front in response to changes in the controlling stage or configuration of the canals and to concentrations in the FPL cooling canals. The runs are described briefly in the table below.

The amount of data available regarding hydrologic conditions differed in the various historic periods. For example, rainfall data are available for the entire simulation period and were used. Continuous data on the controlled stage in the SFWMD canals are available from about 1990. An evaluation of the stage data indicated that the fluctuations were small. In addition, it was recognized that detailed data would not be available for the predictive simulations.

Because one of the primary goals of the modeling effort was to assess the potential impact of the ACI lake excavation on the future position of the salt front, where detailed data would not be available, it was decided that the model simulations would use average wet season/dry season data for a number of parameters primarily as a means of determining whether the simulations could obtain a reasonable match to heads and interface position without using detailed (e.g., daily or monthly) data. For example, canal stage and maximum potential ET were specified using long-term average values. Rainfall, however, was specified based on the observed average wet season and dry season values for each year in the simulation. The results discussed below showed that a reasonable match could be obtained. This provided a level of confidence that projecting into the future with similar average values would give reasonable predictions of the heads and saltwater front position in the future.

Scenario	Key Features
Pre-development	No canals, only near-shore drainage. Higher head (6.5 ft) at northwest GHB boundary (see "Model Boundaries"). No Pumping.
1945-1968	Uncontrolled drainage canals (Mowry, Florida City, Model Land, U.S.1, and Card Sound Road. Near shore drainage modified in vicinity of the canals. Reduced head (4.5 ft) at northwest GHB boundary. No pumping.
1968-1972	SFWMD canals added. Wet Season/dry season stages shown in Figure 18. Changes in configuration of Mowry, Florida City, Model Land, and US 1 canals Otherwise, same as above.
1973-1985	FPL Cooling Canal System added. Assigned stage shown in Figure 18. Municipal water supply and other pumping added. First of quarry lakes added between Card Sound Road and U.S. 1 Otherwise, same as above.
1986-1995	Additional quarry lakes added between Card Sound Rd. and U.S. 1. Pumping rates adjusted to reflect historical increases. Otherwise, same as above.
1996-2010	Additional quarry lakes added Otherwise, same as above.

5 Results of Historical Simulations

Results of historical modelling are presented as a series of figures showing water levels and saltwater concentrations at various depths and at critical times. Dissolved solid concentrations are presented in units of lb/ft^3 and can be converted to equivalent chloride concentrations in mg/L by multiplying by 8700. For example, the 0.115 lb/ft^3 concentration is equivalent to 1000 mg/L of chloride which has been used by the USGS in defining the extent of the saltwater front. The 1000 mg/L isochlor has been used by the USGS for mapping of the edge of the saltwater front. This line has been used to define the position of the saltwater front on the figures discussed below.

Pre-development Conditions

Figure 19 shows the dissolved concentrations in Layer 7 (at a depth of about 55 ft below sea level) at the start of the predevelopment simulations. Initial water levels, also shown in Figure 19, were determined by running a steady-state MODFLOW-only simulation for the study area with average annual recharge and ET values. Dissolved solid concentrations of 2.184 lb/ft^3 were set along the shoreline and the south model boundary. Near-shore natural drainage features, shown in Figure 19, allow inland saltwater movement in Layers 2 and 3. Average wet season precipitation was assumed to be 0.0231 ft/day or 41.6 inches over a 5-month wet season and 0.0076 ft/day (19.1 inches) over a 7 month dry season. Average wet season maximum ET was assumed to be 0.0175 ft/day (31.5 in) and 0.01085 ft/day (27.3 inches) during the dry season. As noted, actual ET losses depend on the depth to the water table in each model cell. Concentrations in recharge to the groundwater system were assumed to be equal to zero. ET is treated differently than other sinks because the solute is left behind as the water evaporates while other sinks (such as wells) remove both water and solute.

The model was run from the starting conditions, shown in Figure 19, until reasonably stable conditions were achieved. Although the potentials vary during the wet and dry cycles and the salt-water interface moves back and forth in response, the overall landward migration of the interface reaches a maximum within 16 years. Langevin (2001) observed an even shorter (10-year) approach to equilibrium, although he started with an interpolated dissolved solid concentration distribution in the area between the mapped saltwater front and Biscayne Bay. The rapid movement to equilibrium in the models is due to the extremely high hydraulic conductivity of the Biscayne aquifer.

Simulated equivalent freshwater heads at the end of the wet season under predevelopment conditions are shown in Figure 20. Simulated dissolved solids concentrations in Layer 7 at the end of the wet season under predevelopment conditions are shown in Figure 21. Layer 7, which is between 40 and 50 ft below sea level, was selected for display because it is the deepest layer that is mostly active and is also within the Fort Thompson Formation. Simulated dissolved solids concentrations in Layer 9 at the end of the wet season under predevelopment conditions are shown in Figure 22. Layer 9, which is between 60 and 70 ft below sea level, was selected for display because it is at the same depth as the proposed lake (67.2 ft below sea level). The simulated concentrations are similar to those in Layer 7 but the contours are displaced further to the west. The simulated concentrations are truncated west of US 1 because of the model boundary (see Figure 17).

The figures show the influence of the natural drainage on the heads and inland movement of the saltwater front. Although there are no predevelopment data to compare with, it is reasonable to assume that the natural streams behave in a similar manner to the uncontrolled canals and that, over time, saltwater moving upstream during dry periods could leak into the underlying groundwater system and move downward to the base of the aquifer.

Figure 23 shows the simulated dissolved solids concentrations within each model layer along a west-east section line east of the ACI property (section line is shown in Figure 21). The figure illustrates that density effects have moved the toe of the saltwater front about 1000 ft further west at the base of the aquifer than near the top. The westward displacement increases with solute concentration and density.

1945 to 1967 Conditions

The simulation period from 1945 to 1967 is meant to represent a time with mostly uncontrolled drainage canals affecting the groundwater and surface water flow systems. Even though construction of these canals took place from 1912 to about 1942, Merritt (1997) selected 1945 as the starting period for the historic simulations, likely due to the paucity of observation data in the earlier time period. The main drainage canals included Mowry, North (formerly known as the Homestead canal), Florida City, Model Land, and Card Sound Road canals and the borrow canal for US 1. The Florida City canal was constructed in 1912, the Model Land and North canals were constructed in the early 1920's, and the Card Sound road canal was constructed in the late 1920's (Merritt, 1997). The US 1 canal was likely completed about 1942. The numerous drainage ditches and smaller canals in the study area were not simulated.

These tidal canals were assumed to allow salt water movement along the full length of the canal during dry periods. Parker and others (1955) note that:

> *During the [1945] drought, each canal acted as an artery for inland movement of saltwater. Samples of canal water, taken during the drought of 1945 at the inland limits of tidal canals near Florida City and Homestead, contained chloride in excess of 26,000 mg/L (as compared to about 19,800 mg/L for normal sea water)....The concentrated saltwater seeped outward and downward from the sides and bottoms of each canal and was the cause of the disastrous crop failure in this area.*

There is some question regarding the effectiveness of controls on the North and Florida City canals at that time. Parker and others (1955) note that these canals had controls but saltwater was detected along the full length of the canal. Merritt (1997) noted that the structures were still present in 1995 and had flapper gates, which allow freshwater discharge during the wet season and are supposed to close during dry periods to prevent seawater intrusion. These were not operational at the time of his report. It is likely that these gates were not very effective even in the earlier period. The tidal reaches of the North and Florida City canals were blocked in the mid 1960's by earth plugs and the canals were connected to the SFWMD L31-E canal.

The simulations for this period used reported average wet season and dry season precipitation for each individual year. Average wet season maximum ET and average dry season maximum ET were set based on long-term average values. Actual ET losses for each wet and dry season depend on the precipitation rate and the depth to the water table in each model cell. The general head boundary at the northwest corner of the model area was reduced to 4.5 ft above sea level to adjust for the drainage of the Everglades by the Miami River and canals north of the study area. Starting conditions for the simulation were the end of wet season heads and dissolved solids concentrations obtained from the predevelopment simulations. As expected, nearly stable conditions were obtained within a relatively short time period.

Figure 24 and Figure 25 show the simulated dissolved solids concentration in Layers 7 and 9, respectively, at the end of the 22 year simulation period. The approximate location of the saltwater interface, as mapped by Parker and others (1955) is shown for comparison. In general, the match to the inferred saltwater interface location is good although the model predicts a greater westward extent of saltwater migration in the vicinity of the northern canals. The position of the interface by Parker and others (1955) was inferred based on limited data and it is likely that it was approximated as being located midway between the available observation wells. It is also possible that the controls on the North and Florida City Canal were more effective than we have assumed, although the current position of the interface is best matched by assuming that saltwater could infiltrate the canals over this period.

1968 to 1972 Conditions

The simulated end of wet season heads and dissolved solids concentrations for 1967 were used as starting conditions for the 1968 to 1972 simulations. This period is meant to represent the construction and initial operating period of the SFWMD drainage and flood control system which regulates the surface water and groundwater flow systems in the study area. The start of this period corresponds to the start of the fourth historic period in Merritt (1997); no significant changes to the canal systems in the study area occurred during Merritt's second and third periods. The model represents SFWMD canals including C-103 which runs west to east along the north boundary of the study area and links with the Mowry canal, C-113, C-111 to the west and south where it replaced the lower reaches of the US 1 borrow canal, and L31-E in the east. The Model Land, Florida City, and North canals are linked into the L31-E system. Also represented are the control structures which regulate stage and prevent inland migration of saltwater. Locations of the canals and structures are shown in Figure 26. To simplify the model, it was assumed that the entire system was operational in October 1967 although S-197 and the southern extension of C-111 were not opened until 1969.

Due to lack of specific year-to-year data for all the canals, long-term average wet season and dry season stage recorded by SFWMD upstream and downstream of each structure were used to set controlling water elevations in the model for this period. Wet season and dry season stage values assigned to the canals are shown in Figure 18. As in the previous simulations, the model used reported average wet season and dry season precipitation for each individual year along with long-term estimates of average wet season and dry season maximum ET. Actual ET losses for each wet and dry season depend on the precipitation rate and the depth to the water table in each model cell.

Figure 26 and Figure 27 show the simulated dissolved solids concentration in Layer 7 and Layer 9, respectively, at the end of the five-year simulation period. A comparison with Figure 24 shows that the simulated saltwater front has been pushed back across the study area except in the vicinity of the Card Sound Road canal which remained uncontrolled. This is due to the generally higher stage maintained in the canals that allows infiltration of freshwater and the control of saltwater encroachment into the canals.

1973 to 1984 Conditions

The simulated end of wet season heads and dissolved solids concentrations for 1972 were used as starting conditions for the 1973 to 1984 simulations. The principal change represented in this period was the construction of the FPL cooling canal system and interceptor canal. To simplify the model, it was assumed that the entire system was operational at the start of 1973. As noted earlier, specified head cells were used to represent the canals with elevations assigned to create southward flow of water in the western canals (from 2.1 ft above sea level at the north to 0.8 ft at the south) and northward flow of water in the eastern canals (from 0.8 ft in the south to -0.8 ft in the north) as shown in Figure 18. Specific information on canal stage and depth was obtained from a report by Lyerly (1998). Time-varying concentrations were adjusted over the simulation period based on historic average wet season and dry season salinity values estimated from quarterly data reported by FPL to DERM (Figure 28).

The simulations also include pumping by the Florida Keys Aqueduct Authority (FKAA), Florida City, City of Homestead Wittkop Park and Harris Field wellfields, and the South Dade Water System Everglades, Newton, and Redavo wellfields, along with several smaller users. Average rates for each year were estimated from data provided by SFWMD. Pumping data for the 1970s and 1980s were not complete for some of the wellfields. Where information on earlier usage was not available, rates were estimated by back-projecting the generally linear increasing trends in water use. Table 4 through Table 6 provide information on the annual pumping rates used in the different simulation periods.

Figure 29 and Figure 30 show the simulated dissolved solids concentration in Layer 7 and Layer 9, respectively, at the end of the 12-year simulation period. A comparison with Figure 26 shows that simulated saltwater front has been pushed further back across most of the study area. Some inland migration occurs in the area between the Model Land canal and L31-E west of the FPL cooling canals and a small westward movement was noted in the vicinity of the expanded quarry lake between Card Sound Road and US 1. The pushback is due to the continued infiltration of freshwater from the SFWMD canals, the control of saltwater encroachment into the tidal reaches of these canals and a series of wetter than average years between 1973 and the 1985 drought (see Figure 5).

Figure 29 and Figure 30 also show the 1985 saltwater front position as mapped by Klein and Waller (1985). The map is probably generalized but the match with the simulated extent is good except in the area west of US 1. The model by Langevin (2001) also showed the saltwater front south of the C-111 canal. It is also interesting to note that Fitterman and Deszcz-Pan (1998) mapped the interface as being south of C-111 but chloride data (Peters and Reynolds, 2008) show that saltwater has contaminated wells north of C-111 in the vicinity of the FKAA wellfield.

A number of factors need to be considered here including the sparsity of data and the interpolation methods used in the mapping. One likely explanation is that the transmissivity mapping by Fish and Stewart (1991) in this area is based on extremely limited data and is biased downward by one estimate of hydraulic conductivity derived from an analysis of leakage from the C-111 canal. Without this data point, it is likely that the area of very high transmissivity would have been interpreted to extend from the Florida City area southward and model results would likely show more extensive inland migration. Another possible explanation is that the model assumes a gently sloping contact between the Fort Thompson Formation and the Tamiami Formation. In reality, the configuration of contact and, in particular, the location, thickness, and extent of the permeable beds within the Tamiami Formation, is very complex. In some areas, trapping of the denser saltwater in relatively stagnant zones may occur and the flushing of saltwater would take a much greater period of time than predicted by the model.

1985 to 1996 Conditions

The simulated end of wet season heads and dissolved solids concentrations for 1984 were used as starting conditions for the 1985 to 1996 simulations. The principal change represented in this period was the expansion of the quarry lakes between Card Sound Road and US 1. Pumping of groundwater for cooling the City of Homestead Power Plant was added to the list of wells. Otherwise, the methods used to represent the canal systems, precipitation, and increased pumping was similar to previous simulations.

Starting with this time period, there were sufficient monitoring data to compare the simulated heads with the observed results. Locations of wells with water level data are shown in Figure 31. As an example, Figure 32 shows the simulated equivalent freshwater heads at well G-3356 (located just east of the ACI property) compared with the observed daily average potentials. As noted earlier, the simulations used average observed wet season and dry season precipitation and average maximum ET values. As a result, the recorded daily and average values of aquifer heads show much more variation than the simulated results. Figure 33, on the other hand, shows model results compared with monthly average potentials. While the monthly average values still show more variability, it can be seen that the model has produced a good match to these values and is sensitive to climatic variation (i.e., to dry, wet, and average dry seasons, and dry, wet, and average wet seasons). Figure 34 shows results for well G-3355 located southwest of the ACI property and Figure 35 shows results for well F-358 located northeast of the property. Both results show a good match to the observed values and trends.

While matching response at individual wells is important, the model must also match the spatial pattern in the potentials so that the predicted solute movement, which depends on the groundwater velocities (as determined by the gradients in potentials), should match the observed. As an example, Figure 36 shows the simulated heads in Layer 3 in November 1993 and the November 1993 water-table map by Sonenshein and Koszalka (1996). The freshwater heads computed by the model have been corrected to aquifer heads based on the simulated dissolved solids concentrations. The match is very good in the vicinity of the ACI property but some discrepancies are noted in the northwest and southwest parts of the model area. The largest differences are primarily related to differences in the stage assumed or observed at the SFWMD structures. The model used average stage elevations for the period of record while daily and month-to-month variations are likely. For example, the average upstream dry season stage at S167 (on C-103) is 3.2 ft and 2.3 ft downstream, putting the 3.0 ft contour at the structure. Data are not available for November 1993, but upstream stage at S167 varied from 1.9 to 4.6 ft between 1995 and 2010. Similarly, average dry season stage at S197 (on C-111) was 1.7 ft upstream and 0.9 ft downstream, putting the 1.0 ft contour at the structure. Observed stage upstream varied from 0.8 ft to 2.6 ft between 1998 and 2010.

Figure 37 and Figure 38 show the simulated dissolved solids concentration in Layer 7 and Layer 9, respectively, at the end of the 14-year simulation period. Careful comparison with the previous simulation (Figure 29) shows that the simulated saltwater front has stabilized and receded slightly across the study area mainly due to some extremely wet years during the period after the 1985 and 1989 droughts (see Figure 5). A minor westward movement was noted in the vicinity of the expanded quarry lakes between Card Sound Road and US 1 primarily because of continued saltwater leakage from the uncontrolled Card Sound Road Canal.

Figure 37 and Figure 38 also show the 1995 saltwater front position as mapped by Sonenshein (1996). This map has the front about 4000 to 5000 feet closer to the shore compared to Klein and Waller (1985). The match with the simulated extent is good except in the area west of US 1. Possible explanations for the discrepancy are provided in the Discussion section below. Differences in the area southeast of the ACI property are possibly due to lack of observation data in the area.

1997 to 2010 Conditions

The simulated end of wet season heads and dissolved solids concentrations for 1996 were used as starting conditions for the 1997 to 2010 simulations. The principal change represented in this period was the construction of the quarry lake on the ACI property. All other lakes in the study area were also represented in these simulations. Otherwise, the methods used to represent the canal systems, precipitation, and increased pumping were similar to previous simulations. Dissolved solids concentrations in the FPL canals increased noticeably during the simulation period as compared to the previous period in which concentrations were relatively stable (see Figure 28).

A more detailed comparison of simulated and observed heads was conducted for this and the preceding period. As an example, Figure 39 shows a scatter plot comparing monthly average observed and simulated heads at well G-3356 (located just east of the ACI property). Most of the values fall within the band of ±0.33 ft. Some error may be due to the simulated values being output at the end of the month while the observed values were obtained from the mean of the daily values for the month.

Several calibration statistics were used to assess and demonstrate model accuracy: the mean error (ME), mean absolute error (MAE), and root mean squared error (RMSE), correlation coefficient (r^2), Nash-Sutcliffe efficiency (NSE), and the index of agreement (d). The first three are given by Anderson and Woessner (1992) as:

$$\text{Mean Error} = \frac{1}{n}\sum_{1}^{n}(h_o - h_s)$$

$$\text{Mean Absolute Error} = \frac{1}{n}\sum_{1}^{n}\left|(h_o - h_s)\right|$$

$$\text{Root Mean Square Error} = \sqrt{\frac{1}{n}\sum_{1}^{n}(h_o - h_s)^2} \qquad \text{(Eq. 12)}$$

The others are given by:

$$r^2 = \frac{n\sum h_o h_s - \sum h_o \sum h_s}{\sqrt{n\sum h_o^{\,2} - \left(\sum h_o\right)^2}\sqrt{n\sum h_s^{\,2} - \left(\sum h_s\right)^2}}$$

$$\text{NSE} = 1 - \frac{\sum_{1}^{n}(Q_o - Q_s)^2}{\sum_{1}^{n}(Q_o - \overline{Q}_o)^2} \qquad \text{(Eq. 14)}$$

$$d = 1 - \frac{\sum_{1}^{n}(h_o - h_s)^2}{\sum_{1}^{n}\left(\left|h_s - \overline{h}_o\right| + \left|h_o - \overline{h}_o\right|\right)^2} \qquad \text{(Eq. 15)}$$

where: h_o = Observed head;
h_s = Simulated head; and,
n = Number of monthly observations.

Calibration statistics for the simulated head at G-3356 are presented in the table below. The magnitudes of the absolute error, in ft, are relatively small and the positive sign indicates that, on average, simulated values are generally lower than the observed values. The ME and MAE are estimates of the average magnitude of the difference between the observed and simulated values. The RMSE is a measure of the variability of the differences. If the differences are normally (or near-normally) distributed, approximately two-thirds of the simulated heads will fall within one RMSE deviation from the observed heads as can be seen in Figure 39.

Simulation	No. of Obser-vations	ME	MAE	RMSE	r^2	NSE	d
Well G-3566	300	0.073	0.26	0.33	0.69	0.404	0.82

The value of NSE can range from 1 to minus infinity with 1 being a perfect fit. An E value less than 0 indicates that the mean value of the observed time series would have been a better predictor than the model (Krause and others, 2005). Values for d range between 0 (no correlation) and 1 (perfect fit) similar to r^2. Krause and others note that d values as high as 0.65 may be obtained with poorly fitted models and that d is not sensitive to model bias (i.e., systematic over- or under-prediction). These calibration statistics indicate that good matches were achieved and confirm the visual match.

Figure 40 and Figure 41 show the simulated dissolved solids concentration in Layer 7 and Layer 9, respectively, at the end of the 14-year simulation period. Comparison with the previous simulation (see Figure 37) shows that the simulated saltwater front has advanced across the vicinity of C-111 and US 1 and in the area east of the ACI property. The movement is mainly in response to the lower than average rainfall over the period (see Figure 5). Additional westward movement of the simulated salt front in the vicinity of the ACI property is also due, in part, to the higher concentrations in the FPL cooling canals. Landward migration of saltwater from the cooling canal system was noted in a two-dimensional modelling analysis of the FPL canals by Hughes and others (2009).

Figure 40 and Figure 41 also show the latest estimate of the 2010 saltwater front position as mapped by (map data provided by Scott Prinos, USGS, April 07, 2011). Again, the match with the simulated extent is good except in the area west of US 1 (discussed below). The simulated end of wet season heads (shown in Figure 42) and dissolved solids concentrations for 2010 were used as starting conditions for the future condition simulations which are described further on in this report.

Discussion

The numerical model was developed using the USGS SEAWAT code to simulate density-dependent groundwater flow and saltwater movement in the study area. The model was applied in a continuous manner to simulate a number of historical periods starting with predevelopment conditions and extending to the present (2010). As in all model applications, a degree of simplification was assumed in the development of this model. The model, however, was able to produce good matches to observed potentials and to the position of the saltwater front in the vicinity of the ACI property.

A number of general observations can be made based on the results of the simulations presented here and based on the results of numerous simulations done during the process of model calibration and testing.

The simulated heads and gradients under pre-development conditions are primarily a function of the high transmissivity of the aquifer, net recharge rates, and the boundary conditions, in particular, the heads assigned to the general head boundary applied in the northwest. These heads were represented as being constant in time, but actually vary in response to climatic conditions. The boundaries are located relatively distant from the ACI property and errors introduced appear not to adversely affect model results in the ACI area.

The pre-development simulations of saltwater movement confirmed that the system tends to move relatively quickly to equilibrium due to the extremely high transmissivity and unconfined conditions in the Biscayne aquifer. The time to equilibrium appears to be about 16 years. In contrast, some confined systems on the Atlantic coast are still responding to sea level change since the Pleistocene era (see Heywood, 2003, for example). The simulated interface is located near the coast. Initial simulations (not shown) had the interface located within 0.5 to 1.0 miles of the coast. Inclusion of leakage of salty water from natural drainage moved the simulated interface further inland and was felt to be more realistic.

Changes in the canal systems, as represented in the post-1945 simulations, have a significant effect on water levels and gradients in the study area. Water levels were generally lower in the study area with uncontrolled drainage (pre-1967) and have risen after construction of the tidal control structures and with generally higher stage maintained during the dry season. Only the major canals were represented in the model so some local variance between observed and simulated water levels can be expected due to local drainage.

As noted, the model used average values for the stage maintained in the canals. Actual stage can vary significantly based on canal losses and the delivery of water to this portion of the SFWMD canal system. For example, during the very arid dry season of 2001-2002, SFWMD had to modify the deliveries of water to the canals thereby exacerbating the effect of the drought on local conditions (Wossenu and others (2002) cited in Peters and Reynolds (2008)). Differences between the simulated and observed water levels can be attributed, in part, to the differences in actual and assumed canal stage. However, data were not available in the DBHYDRO database for much of the period before 1995 to allow any better refinement.

Inland migration of saltwater can be attributed, in part, to the lowered potentials caused by drainage to the canals. As noted early on by Parker and others (1955), leakage of dense, saline water from the canals was a significant contributor to salt water encroachment. The model indicates that imposing the tidal controls has helped to push back the saltwater front since 1967. The model was able to match the observed location of the saltwater front, as mapped by various studies at different times and with different methods of analysis. The match was very good in the ACI vicinity but the match to the inland migration of the saltwater front in the southwest part of the model area was poorer. As mentioned earlier, a likely explanation is that the transmissivity mapping (Fish and Stewart, 1991 and Merritt, 1997) which implied a reduction in hydraulic conductivity in this area was based on limited data and the trend was inferred from one data point. Langevin and others (2005) used a uniform hydraulic conductivity of about 16,400 ft/d for their simulations of the Florida Bay area which included this part of our study area whereas our model had values that decreased in the southerly direction (see Figure 9).

Simulated heads respond to the wet season and dry season cycles. They were also responsive to year-to-year variations such as a sequence of particularly wet years or droughts. The model response was constrained because some model parameters were fixed such as the general head boundary, maximum ET rates, and canal stage. However, the historical data needed were not always available, particularly for the early years of the simulations.

Although the saltwater front can reach equilibrium in a short time, because of climatic variation on the seasonal and annual scales, the saltwater front is constantly in motion. The short term oscillations in the position of the front are not always observable due to the distances between observation wells although Peters and Reynolds (2008) were able to map the response to annual variation by interpolation of data from closely spaced wells in the vicinity of the FKAA wellfield.

The effect of pumping for municipal supply and other water use on potentials in the study is fairly minor and localized due to the high transmissivity of the aquifer. This is consistent with the findings of Merritt (1997). Early simulations done without pumping did not show great differences in the position of the saltwater interface. Peters and Reynolds (2008) noted that the inland migration of the saltwater front in the vicinity of the FKAA wellfield was due to the reduced recharge, decreased canal stage, and increase in pumping over the period. The effect of the quarry lakes on the results of the historic simulations was minor.

As noted earlier, the primary purpose of the model development was to be able to predict the changes in saltwater migration and water levels in the vicinity of wetlands due to the expansion of the quarry lakes in conjunction with other planned changes in the area. As such, detailed hydrologic data are unavailable and the predictive simulations must be done by assuming reasonable average values for important factors such as rainfall, canal stage, and model boundary heads. The model, which was developed and calibrated using average values for the historic periods, was able to obtain good matches with observed water levels and the position of the saltwater front in the vicinity of the ACI property. Therefore, the model, as constructed, is a suitable tool for examining the effects of quarry development by simulating and comparing results of "with" and "without" quarry scenarios.

6 Water Level and Saltwater Front Response to Quarry Lake Development

Results of the model calibration process and historic simulations were taken as starting conditions for determining the impact of the quarry lake development. The model was used to analyze several scenarios with and without the proposed 565-acre quarry lake. Recent changes to the hydrologic system, such as the control structure constructed by FPL in the Card Sound Road canal, and other future projects, such as wetland mitigation, expansion of nearby quarries, and other planned modifications to the canal system were represented in some of the future scenarios, as shown below.

Scenario	Key Features
Baseline-No Changes	Construction of structure on Card Sound Road. Long-term average wet season/dry season precipitation. Constant pumping rates No expansion of quarries Concentrations in FPL canals based on linear projection. Otherwise same as 1996-2010 simulations.
ACI Quarry Lakes Only	Expanded ACI Quarry lakes (East and West) added. Otherwise same as Baseline-No Changes conditions.
ACI and Other Quarry Lakes	Expanded ACI Quarry lakes (East and West) added Expansion of other licensed quarries added. Otherwise, same as No Changes -Without Quarry conditions
All Changes	Expanded ACI Quarry lakes (East and West) added Expansion of other licensed quarries added. Construction of earth plug in lower reaches of Card Sound Rd. Canal. Changes to Florida City canal operations. Otherwise, same as No Changes-Without Quarry conditions

The "Baseline-No Changes" scenario only considered the existing lakes and quarries. The only modification was the addition of the control structure on the Card Sound Road canal built in 2010 (Figure 43). For the "ACI Quarry Lakes Only" scenario, the lakes were assumed to be excavated deeply into the Biscayne aquifer. Hydraulic conductivity and anisotropy factors for Layers 2 through 8 were modified in the expanded footprint of the proposed lake. Similar modifications were made for the other expanded quarries in the "ACI and Other Lakes" and "All Changes" scenarios. Extinction depths for the lake footprints were also changed to reflect that evaporation occurs at the maximum rate over the quarry lakes.

Simulated heads and concentrations at the end of the 1996-2010 model run were used as starting conditions for all future simulations. Other assumptions included constant pumping rates at the existing wells and the use of long-term average (rather than observed) wet season and dry season precipitation. Concentrations in the FPL canals were assumed to increase linearly with time based on projections from the available data (see Figure 28). Chloride concentrations and the position of the saltwater front (i.e., the 1000 mg/L chloride contour) were analyzed by comparing the gridded values used to generate the plan-view maps of predicted concentrations. Results of the three saltwater movement simulations with quarry lakes were compared against the results of the Baseline-No Changes simulation. The 250 mg/L contour is also shown on these figures (the green line west of the color–contoured zone). This concentration can serve as an “early warning” threshold for increasing salinity in monitoring wells. The differences between the simulated position of the 250 mg/L isochlor and the simulated position of the 1000 mg/L isochlor tended to be relatively small, however (about 1000 ft).

Dissolved Solids Concentrations and the Saltwater Front

Figure 47 and Figure 48 show the simulated dissolved solids concentration in Layer 7 and Layer 9, respectively, at the end of the 22-year baseline simulation period with no changes except the structure on Card Sound Road. Comparison with the starting conditions (see Figure 40) shows that the simulated saltwater front has receded in the center of the study area due to the prevention of saltwater migration up the Card Sound Road canal and to increased potentials. The front has advanced westward in the vicinity of the ACI site, however, this is primarily due to the assumed linear increase in solute concentrations in the FPL canals and the continued leakage of hypersaline water and not a result of the existing quarries, the proposed expanded ACI quarry or other potential quarry expansion in the study area. Preliminary simulations of scenarios, including where the FPL canals had (1) a constant concentration at 2010 levels, (2) a constant concentration equal to Biscayne Bay water, and (3) freshwater concentrations, were conducted to test model sensitivity to this assumption but are not presented here.

Figure 49 and Figure 50 show the simulated dissolved solids concentration in Layer 7 and Layer 9 at the end of the 22-year "ACI Lakes Only" simulation period with no additional changes except the expansion of the ACI east and west quarry lake footprints. Visual comparison with the previous simulation shows only minor change. To better quantify the simulated changes, the gridded concentration values at the end of the "ACI Quarry Lakes Only" simulation were subtracted from the gridded concentration values at the end of the ""Baseline-No Changes"" simulation. Results for Layer 9, presented in Figure 51, showed no increases and only a minor decrease in dissolved solids concentration (maximum value of 0.104 lb/ft^3 or about 900 mg/L chloride) in the area east of the ACI property where concentrations were projected to reach 15,890 without the quarry. Results for Layer 7 (not shown) were very similar. The simulated decrease is due to slightly higher heads on the downgradient (east) side of the quarry lake (discussed further in the next section) that help to hold back the advance of the saltwater front.

Figure 52 and Figure 53 show the simulated dissolved solids concentration in Layer 7 and Layer 9, respectively, at the end of the 22-year "ACI and Other Quarry Lakes" simulation period with expansion of the east and west quarry lakes and the addition of all other future quarry expansions in the study area. Again, visual comparison of this simulation with the baseline simulation shows only minor change. Subtracting the two results (Figure 54) shows a further decrease in dissolved solids concentration in Layer 9 (maximum value of 0.17 lb/ft^3 or about 1480 mg/L chloride) in the area east of the ACI property where concentrations were simulated to reach 15,090 without the quarry. The decrease is still due primarily to the slightly higher heads on the downgradient (east) side of the quarry lake that help to hold back the advance of the saltwater front.

Figure 55 and Figure 56 show the simulated dissolved solids concentration in Layer 7 and Layer 9, respectively, at the end of the 22-year "All Changes" simulation period with the expansion of the east and west quarry lakes, the addition of all other future quarry expansions in the study area, the addition of the earth plug in the lower reaches of the Card Sound Road canal, and changes to operations of the Florida City canal. The most noticeable change is the reduction of dissolved solids concentrations in the area between the earth plug and the new control structure (see Figure 43 for locations). Subtracting the two results for Layer 9 confirms the change in the vicinity of the plug (maximum value of 2.0 lb/ft^3 or about 17,500 mg/L chloride), shows a slight decrease in the vicinity of the Florida City canal (maximum value of 0.31 lb/ft^3 or about 2700 mg/L chloride), and shows the minor decrease in dissolved solids concentration (maximum value of 0.15 lb/ft^3 or about 1300 mg/L chloride) in the area east of the ACI property where concentrations were simulated to reach 8,300 without the quarry (Figure 58). It is important to note the scale change on the color-contouring in Figure 58 which goes from 0.1 to 3.0 lb/ft^3 rather than from 0.1 to 0.3 as on Figure 51 and Figure 54.

As in all models, a number of simplifying assumptions were necessary to conduct these simulations but they are not likely to significantly affect final results. They include the simplification of the recharge and ET processes mentioned above as well as all the previously discussed assumptions used in representing the lakes, the SFWMD canals and other drainage canals, the FPL cooling canals, and the aquifer properties and boundaries. The procedures followed were similar to those employed in previous modeling studies of groundwater flow and saltwater encroachment (e.g., Merritt (1997) and Langevin (2001)) and built on a significant amount of data collected over the years. While the model indicates that small decreases in concentrations will occur east of the ACI property in all scenarios, the magnitude of these decreases should be taken as approximations. It is reasonable, however, to assume that any changes in the position of the saltwater front induced by the quarry lake will be insignificant when compared to the impacts caused by drought or changes in canal operations. The model results for all scenarios evaluated for the period from 2010 to 2030, including the proposed ACI quarry lake expansion, expansion of other quarries in the study area, and other possible future changes to canal operations, showed no increase in the salt front movement.

Wetland Stage

Model simulations with and without the ACI quarry were examined to quantify the effects of the expanded ACI east quarry lake on wetland stage and hydroperiod. As noted earlier, Model Layer 1 was used to represent a free-surface where sheet-flow could occur. A similar approach was used by Merritt (1997). While not the best method for simulating sheet flow, we are not aware of an alternative open-source model with sheet flow that can also simulate density-dependent flow. The approach to simulating overland flow was used first in this area by Merritt (1997) and by Langevin (2005) using the SEAWAT model.

The "without quarry" scenario considered all changes except the expansion of the east quarry lake. The "with quarry" scenario was identical to the All Changes scenario discussed above. Predicted water levels at selected points in the wetland mitigation areas on the east, west, and south side of the proposed quarry lake (Figure 43) were examined using hydrographs and plan-view potentiometric surface maps.

Figure 59 through Figure 61 show hydrographs for the simulated wetland stage based on heads in Layer 1 on the west, south, and east sides of the quarry lake, respectively, for the With Quarry (All Changes) and the Without Quarry simulations. The hydrographs show little difference in overall response. Water levels in the With Quarry simulation are slightly lower on the upgradient (west) side of the lake but slightly higher on the downgradient (east) side. No significant change was shown to the south. Model simulations indicated that dry season water levels dropped below land surface on the east side in all years in both simulations. The number of months with water levels below land surface was lower in the With Quarry simulations, however, indicating a slight improvement in hydroperiod with the east quarry lake.

Figure 62 shows the simulated groundwater levels at the end of the 2030 wet season for the two simulations. Gaps in the contour lines indicate areas where simulated heads in Layer 1 were below land surface. Figure 63 shows the simulated groundwater levels at the end of the 2030 dry season. Only small differences in water levels are noted. These changes can be seen better by presenting maps of drawdowns, that is, the changes in water levels calculated by subtracting the results of the two scenarios. The resulting maps for Layer 1 were quite noisy because of slight differences in the number and locations of cells that went dry in the model. Instead, results are presented here for Layer 3 which had similar but continuous heads. Figure 64 presents the change in Layer 3 potentials for the wet season. The two maps also show that change is minor offsite. The maximum increase in wet season water levels is about 0.08 ft adjacent to the east end of the quarry and the maximum decrease is about 0.05 ft at the northwest corner of the quarry lake. Dry season changes are smaller, with increases of 0.02 ft at the east edge of the lake and in the area between the site and the FPL canals. Maximum decreases are less than 0.05 ft at the northern end of the quarry.

As stated above (regarding the previous analyses), a number of simplifying assumptions were necessary to conduct these analyses. Foremost was the simplification of the recharge and ET processes, however, the methods used were similar to those employed in previous modeling studies of southeast Dade County. The model indicates that the water level changes in the adjacent wetlands from the expansion of the ACI quarry will be small and will likely have no significant impact on the wetland mitigation program or on neighboring properties.

7 Summary and Conclusions

A model was developed to simulate regional groundwater flow and saltwater movement in the vicinity of the proposed quarry lake on the ACI property in southeast Miami-Dade County. The model used hydraulic properties and recharge rates based on the available field data and the results of previous modeling studies by the USGS and Earthfx. The model was calibrated by matching response in observation wells and the position of the saltwater front.

The primary focus of the modelling effort was to examine the impact of the quarry development on the position of the saltwater front. The updated model included the ability to simulate transient, rather than steady-state flow, could account for density-dependent flow and solute transport, and better represented the history of change to the canal systems that greatly influence groundwater flow and saltwater intrusion in the study area. Results of saltwater intrusion modelling were presented in a series of plan view maps of dissolved solids concentrations. Animations of the results of the continuous simulations are provided on the enclosed DVD. A secondary objective of the modelling effort was to confirm results of earlier Earthfx studies that showed construction of lakes on the ACI property would have no significant impact on the surrounding wetland mitigation areas.

While the model indicates that small decreases in concentrations will occur east of the ACI property in all scenarios, the magnitude of these decreases should be taken as approximations. It is reasonable, however, to assume that any changes in the position of the saltwater front induced by the quarry lake will be insignificant when compared to the impacts caused by drought or changes in canal operations. The model results, in all scenarios evaluated for the period from 2010 to 2030, including the proposed ACI quarry lake expansion, expansion of other quarries in the study area, and other possible future changes to canal operations, showed no increase in the salt front movement.

8 Limitations

Services performed by Earth*fx* Inc. were conducted in a manner consistent with that level of care and skill ordinarily exercised by members of the environmental engineering and consulting profession.

This report presents the results of data compilation and computer simulations of a complex geologic setting. Models constructed from this data are limited by the quality and completeness of the information available at the time the work was performed. The applicability of the simplifying assumptions may or may not be applicable to a variety of applications.

It should be recognized that the passage of time affects the information provided in this report. Environmental conditions and the amount of data available can change. Discussions relating to the conditions are based upon information that existed at the time the conclusions were formulated. Consistent with the foregoing, Earthfx Inc. used its best professional efforts to consider and evaluate all reasonably relevant and accessible data during its efforts to prepare this report. Data reviewed for this report was evaluated in its reported state; it was beyond the scope of this project to review each data measurement or to audit the reported data.

All of which is respectively submitted,

EARTHFX INC.

Report prepared by:

E.J. Wexler, M.Sc., M.S.E., P.Eng.
Director of Modelling Services
Earthfx Incorporated

9 REFERENCES

Causaras, C.R., 1987, Geology of the surficial aquifer system, Dade County, Florida: U.S. Geological Survey Water-Resources Investigations Report 86-4126, 240 p., 3 sheets.

Cunningham, K.J., Wacker, M.A., Robinson, E., Dixon, J.F., and Wingard, G.L., 2006, Application of cyclostratigraphic and borehole geophysics to delineate porosity and preferential flow in the karst limestone of the Biscayne aquifer, SE Florida: in Harmon, R.S., and Wicks, C., eds., Perspectives on karst geomorphology, hydrology, and geochemistry—A tribute volume to Derek C. Ford and William B. White: Geological Society of America Special Paper 404, p. 191-208,

Fish, J.E., and Stewart, Mark, 1991, Hydrogeology of the surficial aquifer system, Dade County, Florida: U.S. Geological Survey Water-Resources Investigations Report 90-4108, 50 p.

Fitterman and Deszcz-Pan (1998), Fitterman, D.V., and Deszcz-Pan, M., 1998, Helicopter EM mapping of saltwater intrusion in Everglades National Park, Florida: Exploration Geophysics, v. 29, p. 240-243.

Harbaugh, A.W. and McDonald, M.G., 1996, User's documentation for MODFLOW-96, an update to the U.S. Geological Survey Modular Finite-Difference Ground-Water Flow Model: U.S. Geological Survey Open-File Report 96-485, 56 p.

Heywood, C.E., 2003, Influence of the Chesapeake Bay impact structure on ground-water flow and salinity in the Atlantic Coastal Plain aquifer system of Virginia in MODFLOW and More 2003: Understanding through Modeling, International Ground Water Modeling Center, p. 871-875

Hughes, J., Langevin, C.D., and Brakefield-Goswami, L., 2009, Effect of hypersaline cooling water on aquifer salination: Hydrogeology Journal, published online August 12, 2009.

JLA Geosciences, Inc., 2010, Geology & hydrogeology report for FPL Turkey Point Plant - Groundwater, surface water, & ecological monitoring plan, FPL, Turkey Point Plant, Homestead, Florida: prepared for Florida Power and Light, October 2010.

Klein, H. and Hull, J.E., 1978, Biscayne aquifer, southeast Florida: U.S. Geological Survey Water-Resources Investigations 78-107, 52 p.

Klein, H. and Waller, B.G., 1985, Synopsis of saltwater intrusion in Dade County, Florida, through 1984: U.S. Geological Survey (USGS) Water-Resources Investigations Report 85-4104.

Langevin, C.D., 2001, Simulation of ground-water discharge to Biscayne Bay, southeastern Florida: U.S. Geological Survey Water-Resources Investigations Report 00-4251, 127 p.

Langevin, C.D., Shoemaker, W.B., and Guo, W., 2003, MODFLOW-2000, The U.S. Geological Survey modular ground-water model - documentation of the SEAWAT-2000 version with the variable density flow process (VDF), and the integrated MT3DMS transport process (IMT); U.S. Geological Survey Open File Report 03-426, 43 p.

Lyerly, R.L., 1998, Thermal performance of the Turkey Point cooling canal system in 1998: prepared for Turkey Point Plant Florida Power and Light, Miami, FL.

Merritt, Michael L., 1997, Simulation of the water-table altitude in the Biscayne aquifer, southern Dade County, Florida, water years 1945-89: U.S. Geological Survey Water-Supply Paper 2458, prepared in cooperation with the Metro-Dade Department of Environmental Resources Management, 148 p.

McDonald, M.G., and Harbaugh, A.W., 1988, A modular three-dimensional finite-difference ground-water flow model: U.S. Geological Survey Techniques of Water Resources Investigations, book 6, chapter A1, 586 p.

Parker, G.G., Ferguson, G.E., Love, S.K., and others, 1955, Water resources of southeastern Florida: U.S. Geological Survey Water-Supply Paper 1255, 965 p.

Peters, C.J. and Reynolds, J., 2008, Saltwater Intrusion Monitoring in the Biscayne Aquifer near Florida City, Miami-Dade County, Florida: 1996-2007

Sonenshein, R.S. 1996. Delineation of saltwater intrusion in the Biscayne Aquifer, Eastern Dade County, Florida, 1995. USGS Water Resources Investigation Report 96-4285.

Sonenshein, R.S. and Koszalka, E.J., 1996, Trends in water-table altitude (1984-93) and saltwater intrusion (1974-93) in the Biscayne aquifer, Dade County, Florida: U.S. Geological Survey Open-File Report 95-705, 2 sheets.

Weixing Guo, W. and Langevin, C.D, 2002, User's guide to SEAWAT: a computer program for simulation of three-dimensional variable-density ground-water flow: U.S. Geological Survey Techniques of Water-Resources Investigations 6-A7, 77 p.

Wossenu A., Huebner, R.S., Sunderland, S., 2002, 2006, The 2000-2001 drought in South Florida: SFWMD, West Palm Beach, FL.

Zheng, C., and Wang, P.P., 1998, MT3DMS, A modular three-dimensional multispecies transport model for simulation of advection, dispersion and chemical reactions of contaminants in groundwater systems; Documentation and User's Guide: prepared for U.S. Army Corps of Engineers; monitored by U.S. Army Engineer Research and Development Center, Vicksburg, MS., 220 p.

TABLES

Table 1: Daily maximum ET rates by month (after Merritt (1997) and Langevin (2001)).

Month	Maximum ET (in/d)	Season
January	0.08	Dry
February	0.11	
March	0.14	
April	0.17	
May	0.18	Wet
June	0.21	
July	0.21	
August	0.21	
September	0.21	
October	0.21	Dry
November	0.12	
December	0.11	

Table 2: Runoff coefficients and extinction depths (after Langevin (2001)).

Land Use Category	Runoff Coefficient	Extinction Depth (ft)
Urban/Paved	0.50	1.0
Agriculture	0.25	1.0
Rangeland	0.2	2.0
Upland Forest	0.2	2.3
Open Water	0.0	20*
Wetlands	0.0	2.3
Barren Land	0.0	0.5
Transportation	0.5	1.0
* The number 20 (an arbitrary large value) was assigned to ensure that ET from the water surface always occurred at the maximum rate.		

Table 3: Simulated pumping rates (data from SFWMD).

Wellfield	No. of Wells	Assigned Pumping 2010* (ft^3/d)
Florida Keys Aqueduct Authority	9	1897863
City of Homestead Water Division - Wittkop Park	4	792811
City of Homestead Water Division - Harris Field	2	587754
City of Homestead Power Plant	10	306099
South Dade Water System - Everglades	3	397059
South Dade Water System - Newton	2	462032
South Dade Water System - Redavo	2	61364
Florida City Water Treatment Plant	4	237566
Everglades Academy	1	14439
Kingdom Hall of Jehovah's Witness	1	7701
Homestead Field Station	1	4332
Last Chance Saloon	1	481

*Note: Simulated rates used in historic simulations were adjusted to represent reported usage rates. Well locations shown in Figure 15.

Table 4: Pumping rates used in the 1973 to 1984 simulations.

Well Name	Easting	Northing	Layer	Row	Col	Pumping Rates used in 1973-1984 Simulation Period (ft^3/d)											
						1973	1974	1975	1976	1977	1978	1979	1980	1981	1982	1983	1984
Florida Keys Aqueduct Authority 4	818336	402079	9	58	37	0	9431	21692	33324	44641	55330	69603	70850	67942	80078	114768	111842
Florida Keys Aqueduct Authority 7	818679	402196	8	58	38	0	14147	32538	49986	66962	82995	104404	106274	101914	120116	172153	167763
Florida Keys Aqueduct Authority 8	818541	402123	9	58	38	0	9431	21692	33324	44641	55330	69603	70850	67942	80078	114768	111842
Florida Keys Aqueduct Authority 9	818548	402275	9	58	38	0	9431	21692	33324	44641	55330	69603	70850	67942	80078	114768	111842
Florida Keys Aqueduct Authority 10	818270	402137	8	58	37	0	13473	30988	47605	63773	79043	99432	101214	97061	114397	163955	159774
Florida Keys Aqueduct Authority 11	818167	402138	8	58	37	0	13473	30988	47605	63773	79043	99432	101214	97061	114397	163955	159774
Florida Keys Aqueduct Authority 12	818113	402315	8	58	37	0	13473	30988	47605	63773	79043	99432	101214	97061	114397	163955	159774
Florida Keys Aqueduct Authority 13	818311	402308	8	58	37	0	13473	30988	47605	63773	79043	99432	101214	97061	114397	163955	159774
Florida Keys Aqueduct Authority 14	818685	402302	8	58	38	0	13473	30988	47605	63773	79043	99432	101214	97061	114397	163955	159774
Florida City Water Treatment Plant 1	826168	407277	9	48	53	0	0	0	0	0	0	0	0	0	0	0	0
Florida City Water Treatment Plant 2	825984	407377	9	48	52	0	0	563	6489	12095	17392	27953	27953	27663	30229	38886	43732
Florida City Water Treatment Plant 3	825983	407579	9	47	52	0	0	563	6489	12095	17392	27953	27953	27663	30229	38886	43732
Florida City Water Treatment Plant 4	826348	408186	9	46	53	0	0	1433	16518	30789	44270	71154	71154	70417	76948	98983	111318
City of Homestead Water Division - Wittkop Park - W1	826388	416391	5	30	53	56938	103695	144516	179784	209883	235198	256619	256619	221610	299978	380347	271227
City of Homestead Water Division - Wittkop Park - W2	826393	416577	5	29	53	43924	79993	111484	138690	161910	181439	197963	197963	170956	231411	293410	209232
City of Homestead Water Division - Wittkop Park - W3	826131	416586	5	29	53	39043	71105	99096	123280	143920	161279	175967	175967	151961	205699	260809	185984
City of Homestead Water Division - Wittkop Park - W4	826068	416410	5	30	53	22775	41478	57806	71913	83953	94079	102647	102647	88644	119991	152139	108491
City of Homestead Water Division - Harris Field - W5	833850	415084	5	32	68	0	0	0	0	0	0	0	0	0	0	0	0
City of Homestead Water Division - Harris Field - W6	832186	414797	5	33	65	0	0	0	0	0	0	0	0	0	0	0	305823
Kingdom Hall of Jehovah's Witness 1	823536	424210	4	73	36	7701	7701	7701	7701	7701	7701	7701	7701	7701	7701	7701	7701
Last Chance Saloon 1	829195	401249	4	60	59	481	481	481	481	481	481	481	481	481	481	481	481
Everglades Academy 1	827221	378160	4	96	71	14439	14439	14439	14439	14439	14439	14439	14439	14439	14439	14439	14439
Homestead Field Station 1/2	838425	416489	4	30	77	4332	4332	4332	4332	4332	4332	4332	4332	4332	4332	4332	4332
South Dade Water Supply - Everglades 1	820031	394560	6	73	41	50535	50535	50535	50535	50535	50535	50535	50535	50535	50535	50535	50535
South Dade Water Supply - Everglades 2	820031	394560	5	73	41	231016	231016	231016	231016	231016	231016	231016	231016	231016	231016	231016	231016
South Dade Water Supply - Everglades 3	820031	394560	5	73	41	115508	115508	115508	115508	115508	115508	115508	115508	115508	115508	115508	115508
South Dade Water Supply - Newton 1	838313	408582	5	45	77	231016	231016	231016	231016	231016	231016	231016	231016	231016	231016	231016	231016
South Dade Water Supply - Newton 2	839313	408582	5	45	79	231016	231016	231016	231016	231016	231016	231016	231016	231016	231016	231016	231016
South Dade Water Supply - Redavo 1	823506	422541	5	17	48	28877	28877	28877	28877	28877	28877	28877	28877	28877	28877	28877	28877
South Dade Water Supply - Redavo 2	823506	422541	5	17	48	32487	32487	32487	32487	32487	32487	32487	32487	32487	32487	32487	32487

Table 5: Pumping rates used in the 1985 to 1996 simulations.

Well Name	Easting	Northing	Layer	Row	Col	Pumping Rates used in 1985-1996 Simulation Period (ft^3/d)											
						1985	1986	1987	1988	1989	1990	1991	1992	1993	1994	1995	1996
Florida Keys Aqueduct Authority 4	818336	402079	9	58	37	123498	138090	151772	148690	155575	148220	135999	145473	156711	163090	160769	163950
Florida Keys Aqueduct Authority 7	818679	402196	8	58	38	185246	207135	227658	223035	233363	222329	203998	218209	235066	244635	241153	245925
Florida Keys Aqueduct Authority 8	818541	402123	9	58	38	123498	138090	151772	148690	155575	148220	135999	145473	156711	163090	160769	163950
Florida Keys Aqueduct Authority 9	818548	402275	9	58	38	123498	138090	151772	148690	155575	148220	135999	145473	156711	163090	160769	163950
Florida Keys Aqueduct Authority 10	818270	402137	8	58	37	176425	197271	216817	212414	222250	211742	194284	207819	223873	232986	229670	234214
Florida Keys Aqueduct Authority 11	818167	402138	8	58	37	176425	197271	216817	212414	222250	211742	194284	207819	223873	232986	229670	234214
Florida Keys Aqueduct Authority 12	818113	402315	8	58	37	176425	197271	216817	212414	222250	211742	194284	207819	223873	232986	229670	234214
Florida Keys Aqueduct Authority 13	818311	402308	8	58	37	176425	197271	216817	212414	222250	211742	194284	207819	223873	232986	229670	234214
Florida Keys Aqueduct Authority 14	818685	402302	8	58	38	176425	197271	216817	212414	222250	211742	194284	207819	223873	232986	229670	234214
Florida City Water Treatment Plant 1	826168	407277	9	48	53	0	0	0	0	0	0	0	0	0	0	0	0
Florida City Water Treatment Plant 2	825984	407377	9	48	52	53519	42696	63416	64722	58017	57332	58017	58017	58868	56532	62224	76104
Florida City Water Treatment Plant 3	825983	407579	9	47	52	53519	42696	63416	64722	58017	57332	58017	58017	58868	56532	62224	76104
Florida City Water Treatment Plant 4	826348	408186	9	46	53	136231	108683	161422	164748	147681	145938	147681	147681	149847	143900	158390	193721
City of Homestead Water Division - Wittkop Park - W1	826388	416391	5	30	53	211778	173836	205013	115874	171053	177531	145031	119724	108285	131647	122725	213278
City of Homestead Water Division - Wittkop Park - W2	826393	416577	5	29	53	163372	134102	158153	89389	131955	136952	111881	92358	83534	101556	94673	164529
City of Homestead Water Division - Wittkop Park - W3	826131	416586	5	29	53	145219	119201	140580	79456	117293	121735	99450	82096	74252	90272	84154	146248
City of Homestead Water Division - Wittkop Park - W4	826068	416410	5	30	53	84711	69534	82005	46349	68421	71012	58012	47889	43314	52658	49090	85311
City of Homestead Water Division - Harris Field - W5	833850	415084	5	32	68	0	0	0	0	0	0	0	0	0	0	0	0
City of Homestead Water Division - Harris Field - W6	832186	414797	5	33	65	341627	294531	323544	331070	281177	297611	482606	466857	433630	356157	511596	386194
Kingdom Hall of Jehovah's Witness 1	823536	424210	4	73	36	7701	7701	7701	7701	7701	7701	7701	7701	7701	7701	7701	7701
Last Chance Saloon 1	829195	401249	4	60	59	481	481	481	481	481	481	481	481	481	481	481	481
Everglades Academy 1	827221	378160	4	96	71	14439	14439	14439	14439	14439	14439	14439	14439	14439	14439	14439	14439
Homestead Field Station 1/2	838425	416489	4	30	77	4332	4332	4332	4332	4332	4332	4332	4332	4332	4332	4332	4332
South Dade Water Supply - Everglades 1	820031	394560	6	73	41	50535	50535	50535	50535	50535	50535	50535	50535	50535	50535	50535	50535
South Dade Water Supply - Everglades 2	820031	394560	5	73	41	231016	231016	231016	231016	231016	231016	231016	231016	231016	231016	231016	231016
South Dade Water Supply - Everglades 3	820031	394560	5	73	41	115508	115508	115508	115508	115508	115508	115508	115508	115508	115508	115508	115508
South Dade Water Supply - Newton 1	838313	408582	5	45	77	231016	231016	231016	231016	231016	231016	231016	231016	231016	231016	231016	231016
South Dade Water Supply - Newton 2	839313	408582	5	45	79	231016	231016	231016	231016	231016	231016	231016	231016	231016	231016	231016	231016
South Dade Water Supply - Redavo 1	823506	422541	5	17	48	28877	28877	28877	28877	28877	28877	28877	28877	28877	28877	28877	28877
South Dade Water Supply - Redavo 2	823506	422541	5	17	48	32487	32487	32487	32487	32487	32487	32487	32487	32487	32487	32487	32487
City of Homestead Power Plant A	831089	415405	7	32	63	38503	38503	38503	38503	38503	38503	38503	38503	38503	38503	38503	38503
City of Homestead Power Plant B	831070	415418	7	32	63	38503	38503	38503	38503	38503	38503	38503	38503	38503	38503	38503	38503
City of Homestead Power Plant C	831051	415430	7	32	63	38503	38503	38503	38503	38503	38503	38503	38503	38503	38503	38503	38503
City of Homestead Power Plant D	831021	415462	7	31	63	28877	28877	28877	28877	28877	28877	28877	28877	28877	28877	28877	28877
City of Homestead Power Plant E	831000	415468	7	31	63	38503	38503	38503	38503	38503	38503	38503	38503	38503	38503	38503	38503
City of Homestead Power Plant F	830892	415335	7	32	62	23102	23102	23102	23102	23102	23102	23102	23102	23102	23102	23102	23102
City of Homestead Power Plant G	830924	415322	7	32	62	23102	23102	23102	23102	23102	23102	23102	23102	23102	23102	23102	23102
City of Homestead Power Plant H	830943	415303	7	32	62	30802	30802	30802	30802	30802	30802	30802	30802	30802	30802	30802	30802
City of Homestead Power Plant K	831070	415297	7	32	63	23102	23102	23102	23102	23102	23102	23102	23102	23102	23102	23102	23102
City of Homestead Power Plant L	831089	415316	7	32	63	23102	23102	23102	23102	23102	23102	23102	23102	23102	23102	23102	23102

Table 6: Pumping rates used in the 1997 to 2010 simulations.

Well Name	Easting	Northing	Layer	Row	Col	Pumping Rates used in 1985-1996 Simulation Period (ft^3/d)													
						1997	1998	1999	2000	2001	2002	2003	2004	2005	2006	2007	2008	2009	2010
Florida Keys Aqueduct Authority 4	818336	402079	9	58	37	169143	168036	187000	191891	187293	193014	0	0	0	0	0	0	0	0
Florida Keys Aqueduct Authority 7	818679	402196	8	58	38	253715	252054	280500	287836	280939	289520	285180	251328	308259	269342	248122	306498	188424	247159
Florida Keys Aqueduct Authority 8	818541	402123	9	58	38	169143	168036	187000	191891	187293	193014	170733	207762	196985	136161	162462	128950	136828	139093
Florida Keys Aqueduct Authority 9	818548	402275	9	58	38	169143	168036	187000	191891	187293	193014	198225	136714	168270	102541	166897	137462	168274	162522
Florida Keys Aqueduct Authority 10	818270	402137	8	58	37	241633	240051	267143	274130	267562	275734	184925	195360	185660	162589	185686	242423	227396	222635
Florida Keys Aqueduct Authority 11	818167	402138	8	58	37	241633	240051	267143	274130	267562	275734	232440	351583	266444	357183	246286	307554	308662	396610
Florida Keys Aqueduct Authority 12	818113	402315	8	58	37	241633	240051	267143	274130	267562	275734	302478	344288	291926	363688	185914	280042	347218	362496
Florida Keys Aqueduct Authority 13	818311	402308	8	58	37	241633	240051	267143	274130	267562	275734	286753	293172	390329	318293	236086	420136	249690	37053
Florida Keys Aqueduct Authority 14	818685	402302	8	58	38	241633	240051	267143	274130	267562	275734	273409	199201	249368	236244	204832	381280	298719	330295
Florida City Water Treatment Plant 1	826168	407277	9	48	53	0	0	0	0	0	0	0	0	36	4573	114537	86082	68022	58867
Florida City Water Treatment Plant 2	825984	407377	9	48	52	69164	66455	74546	75215	69065	75611	90243	57293	99359	133626	77277	72596	45715	44136
Florida City Water Treatment Plant 3	825983	407579	9	47	52	69164	66455	74546	75215	69065	75611	90243	60065	95433	55276	101188	70318	60558	71416
Florida City Water Treatment Plant 4	826348	408186	9	46	53	-176054	169158	189755	191456	175803	192465	229711	159104	134594	135821	53342	68562	64190	63147
City of Homestead Water Division - Wittkop Park - W1	826388	416391	5	30	53	-118166	154809	237591	258864	261579	267066	268673	241769	290800	252923	187598	141162	207281	294369
City of Homestead Water Division - Wittkop Park - W2	826393	416577	5	29	53	91157	119424	183285	199695	201790	206022	207262	188637	207403	155985	96792	215141	250083	189976
City of Homestead Water Division - Wittkop Park - W3	826131	416586	5	29	53	81028	106155	162920	177507	179369	183131	184232	167614	158063	238661	326923	313318	198029	238104
City of Homestead Water Division - Wittkop Park - W4	826068	416410	5	30	53	47266	61923	95036	103545	104631	106826	107469	90947	94652	139192	245063	223153	237705	70362
City of Homestead Water Division - Harris Field - W5	833850	415084	5	32	68	0	0	0	18040	2020	24756	5761	204671	356851	416068	367578	368793	294483	289160
City of Homestead Water Division - Harris Field - W6	832186	414797	5	33	65	618471	555721	360810	369646	383895	352722	337467	333583	330703	324473	327926	328680	303424	298594
Kingdom Hall of Jehovah's Witness 1	823536	424210	4	73	36	7701	7701	7701	7701	7701	7701	7701	7701	7701	7701	7701	7701	7701	7701
Last Chance Saloon 1	829195	401249	4	60	59	481	481	481	481	481	481	481	481	481	481	481	481	481	481
Everglades Academy 1	827221	378160	4	96	71	14439	14439	14439	14439	14439	14439	14439	14439	14439	14439	14439	14439	14439	14439
Homestead Field Station 1/2	838425	416489	4	30	77	4332	4332	4332	4332	4332	4332	4332	4332	4332	4332	4332	4332	4332	4332
South Dade Water Supply - Everglades 1	820031	394560	6	73	41	50535	50535	50535	50535	50535	50535	50535	50535	50535	50535	50535	50535	50535	50535
South Dade Water Supply - Everglades 2	820031	394560	5	73	41	231016	231016	231016	231016	231016	231016	231016	231016	231016	231016	231016	231016	231016	231016
South Dade Water Supply - Everglades 3	820031	394560	5	73	41	115508	115508	115508	115508	115508	115508	115508	115508	115508	115508	115508	115508	115508	115508
South Dade Water Supply - Newton 1	838313	408582	5	45	77	231016	231016	231016	231016	231016	231016	231016	231016	231016	231016	231016	231016	231016	231016
South Dade Water Supply - Newton 2	839313	408582	5	45	79	231016	231016	231016	231016	231016	231016	231016	231016	231016	231016	231016	231016	231016	231016
South Dade Water Supply - Redavo 1	823506	422541	5	17	48	28877	28877	28877	28877	28877	28877	28877	28877	28877	28877	28877	28877	28877	28877
South Dade Water Supply - Redavo 2	823506	422541	5	17	48	32487	32487	32487	32487	32487	32487	32487	32487	32487	32487	32487	32487	32487	32487
City of Homestead Power Plant A	831089	415405	7	32	63	38503	38503	38503	38503	38503	38503	38503	38503	38503	38503	38503	38503	38503	38503
City of Homestead Power Plant B	831070	415418	7	32	63	38503	38503	38503	38503	38503	38503	38503	38503	38503	38503	38503	38503	38503	38503
City of Homestead Power Plant C	831051	415430	7	32	63	38503	38503	38503	38503	38503	38503	38503	38503	38503	38503	38503	38503	38503	38503
City of Homestead Power Plant D	831021	415462	7	31	63	28877	28877	28877	28877	28877	28877	28877	28877	28877	28877	28877	28877	28877	28877
City of Homestead Power Plant E	831000	415468	7	31	63	38503	38503	38503	38503	38503	38503	38503	38503	38503	38503	38503	38503	38503	38503
City of Homestead Power Plant F	830892	415335	7	32	62	23102	23102	23102	23102	23102	23102	23102	23102	23102	23102	23102	23102	23102	23102
City of Homestead Power Plant G	830924	415322	7	32	62	23102	23102	23102	23102	23102	23102	23102	23102	23102	23102	23102	23102	23102	23102
City of Homestead Power Plant H	830943	415303	7	32	62	30802	30802	30802	30802	30802	30802	30802	30802	30802	30802	30802	30802	30802	30802
City of Homestead Power Plant K	831070	415297	7	32	63	23102	23102	23102	23102	23102	23102	23102	23102	23102	23102	23102	23102	23102	23102
City of Homestead Power Plant L	831089	415316	7	32	63	23102	23102	23102	23102	23102	23102	23102	23102	23102	23102	23102	23102	23102	23102

FIGURES

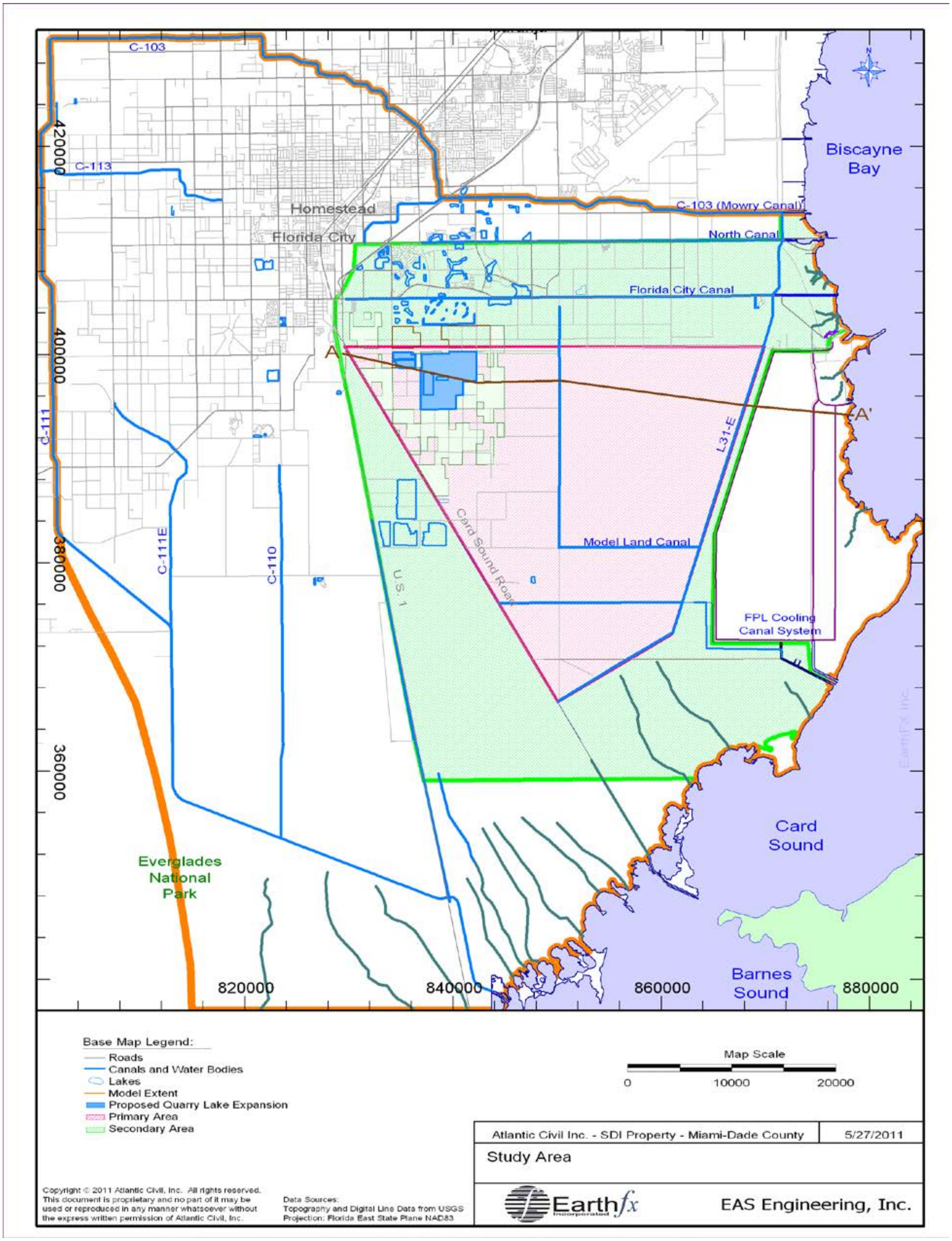

Figure 1: Primary (red) and secondary (green) watersheds for the cumulative impact assessment.

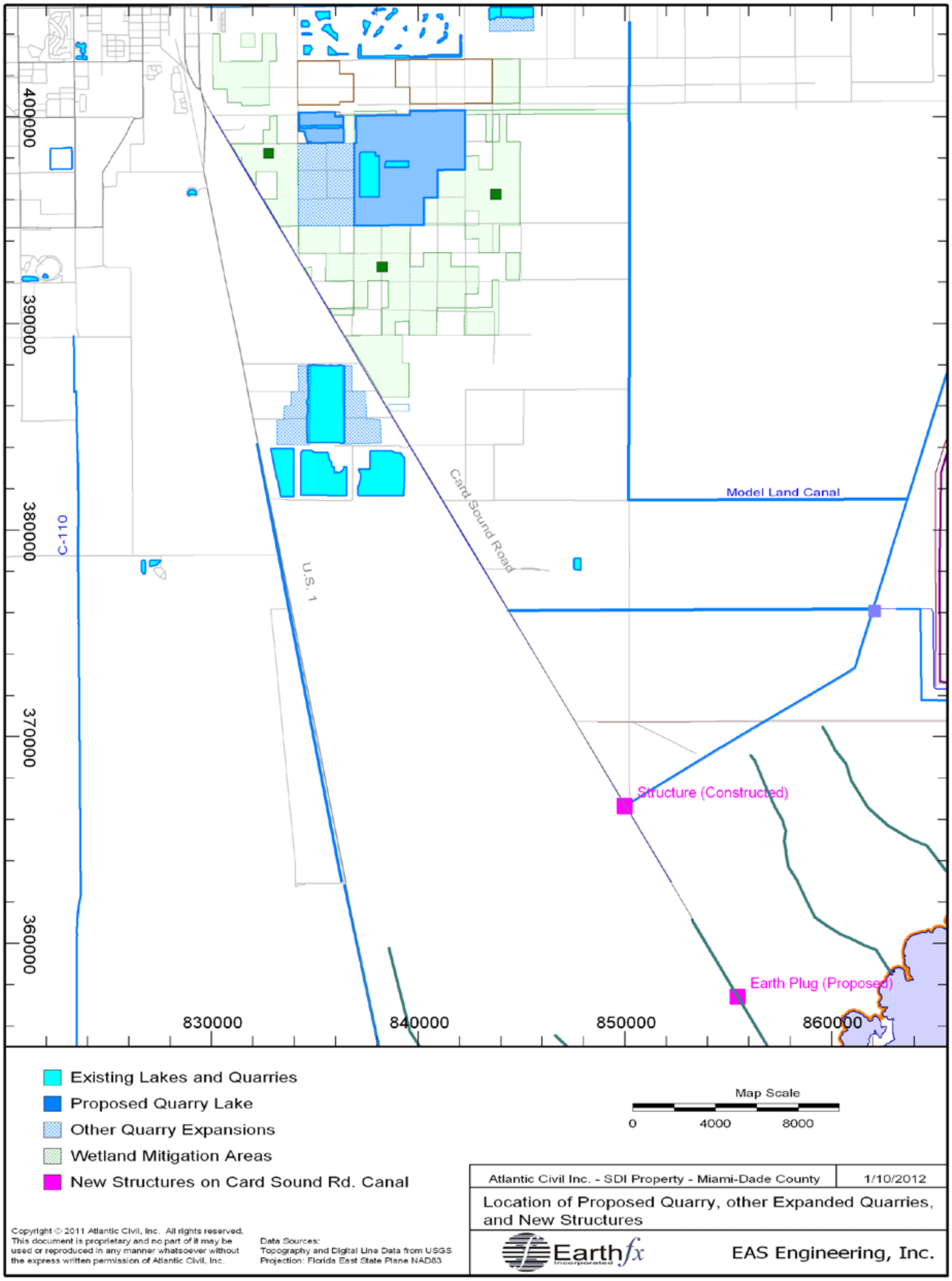

Figure 2: Proposed quarry, other quarry expansions, new structures, and cells selected for hydrograph comparison.

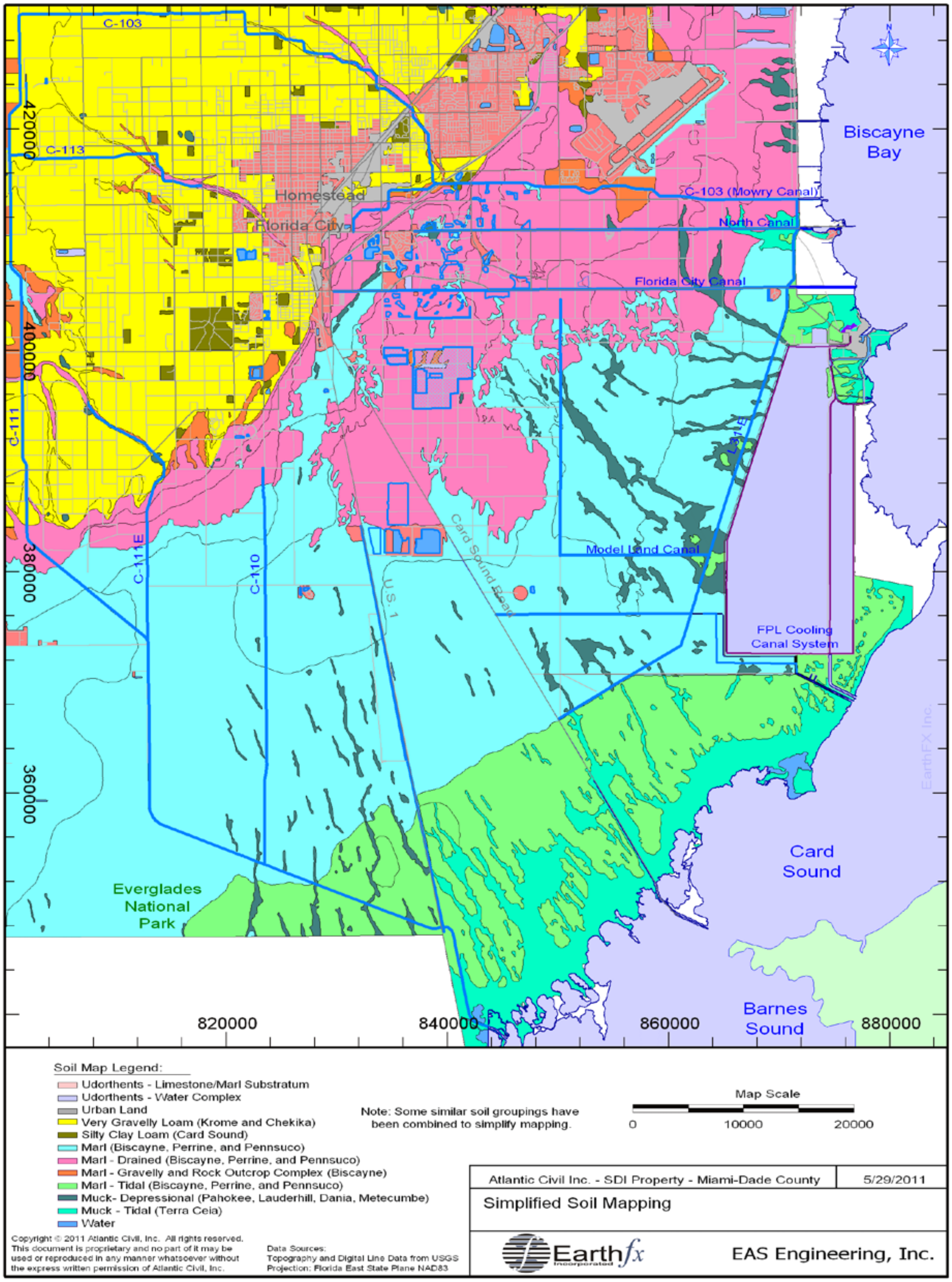

Figure 3: Simplified soils map for the study area.

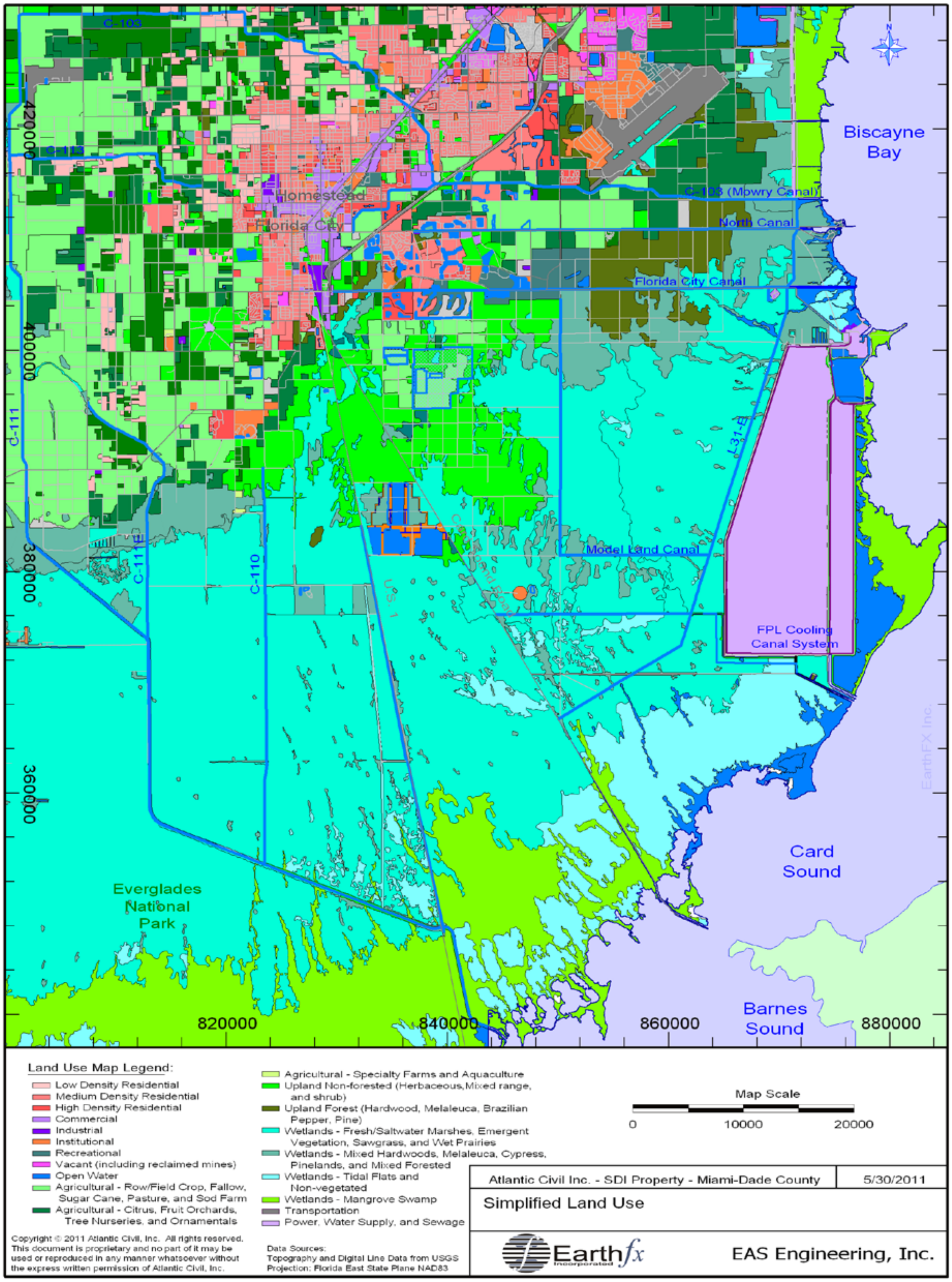

Figure 4: Simplified land use mapping based on the Florida Land Use Classification System.

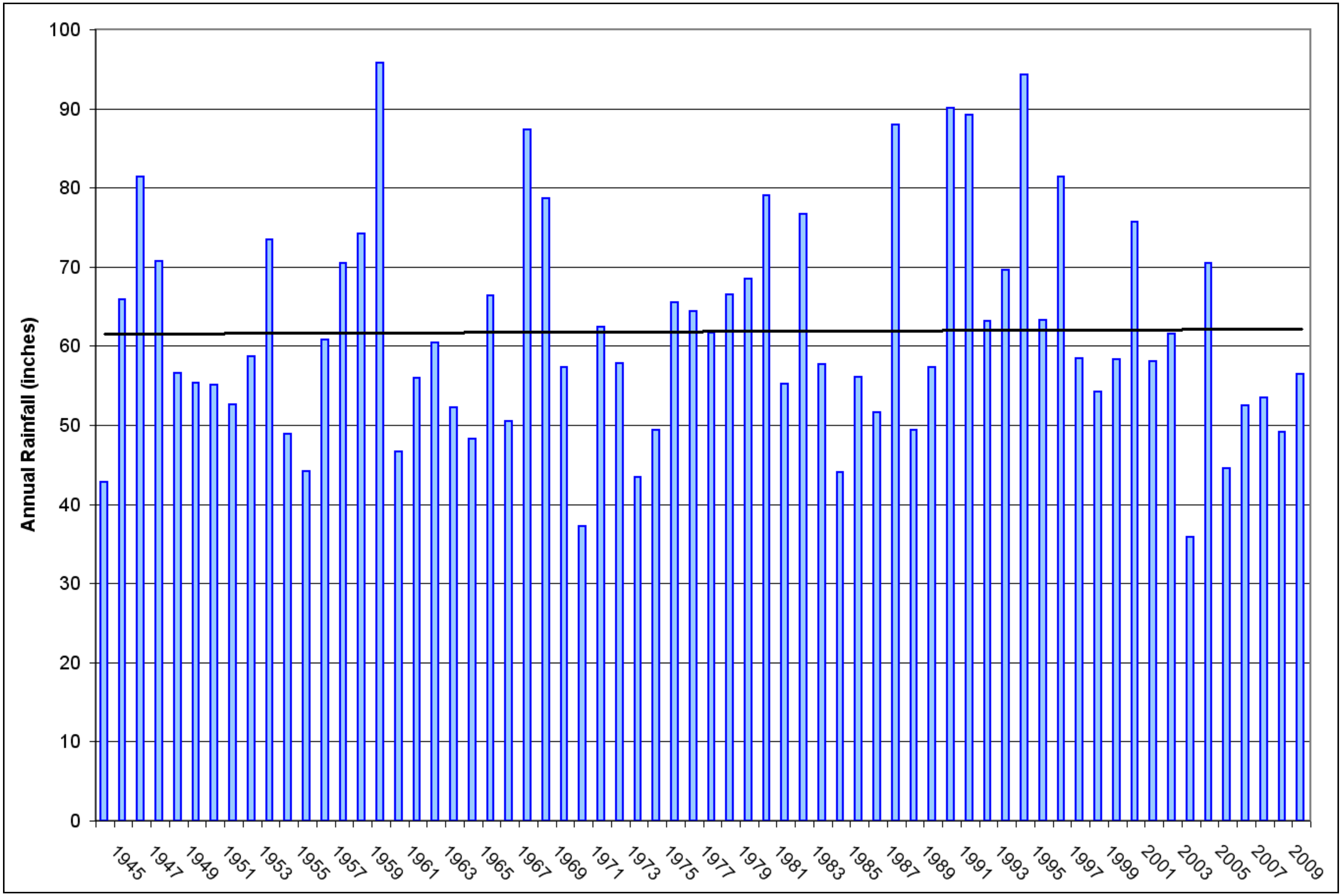

Figure 5: Annual rainfall for 1945 to 2010 at Homestead, FL.

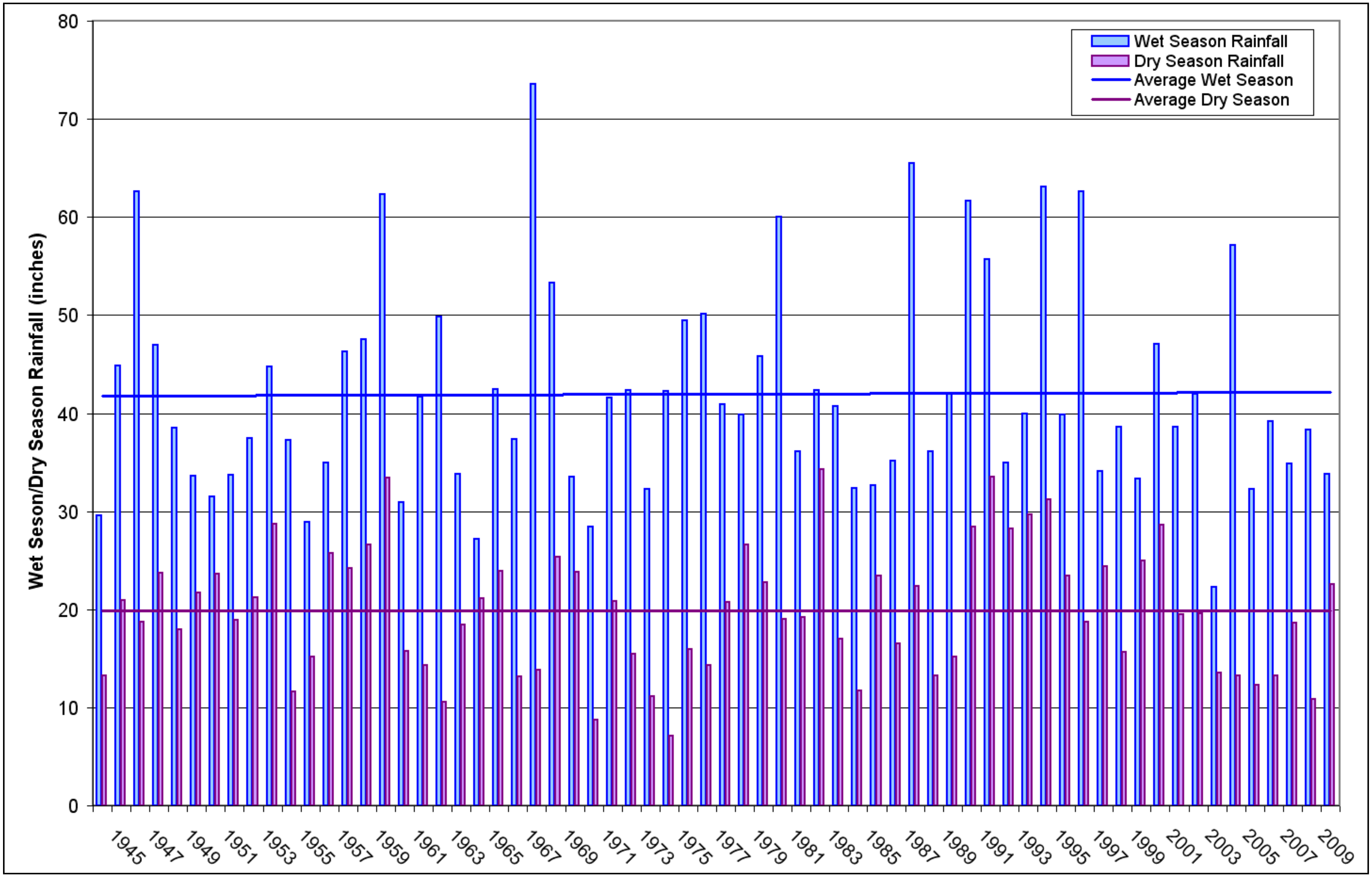

Figure 6: Wet and dry season rainfall for 1945 to 2010 at Homestead.

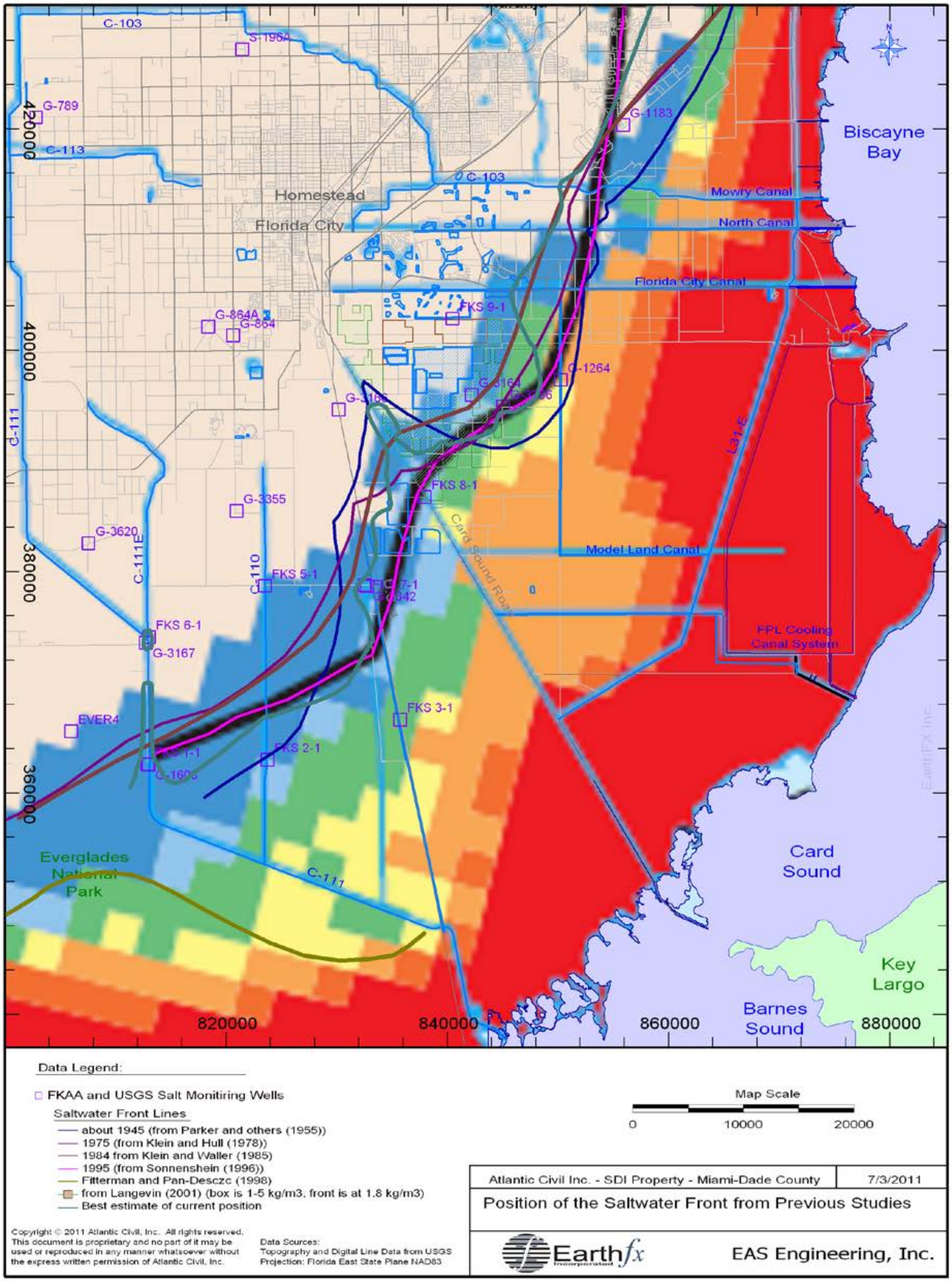

Figure 7: Estimated position of the saltwater front at various times from previous studies including model results from Langevin (2001).

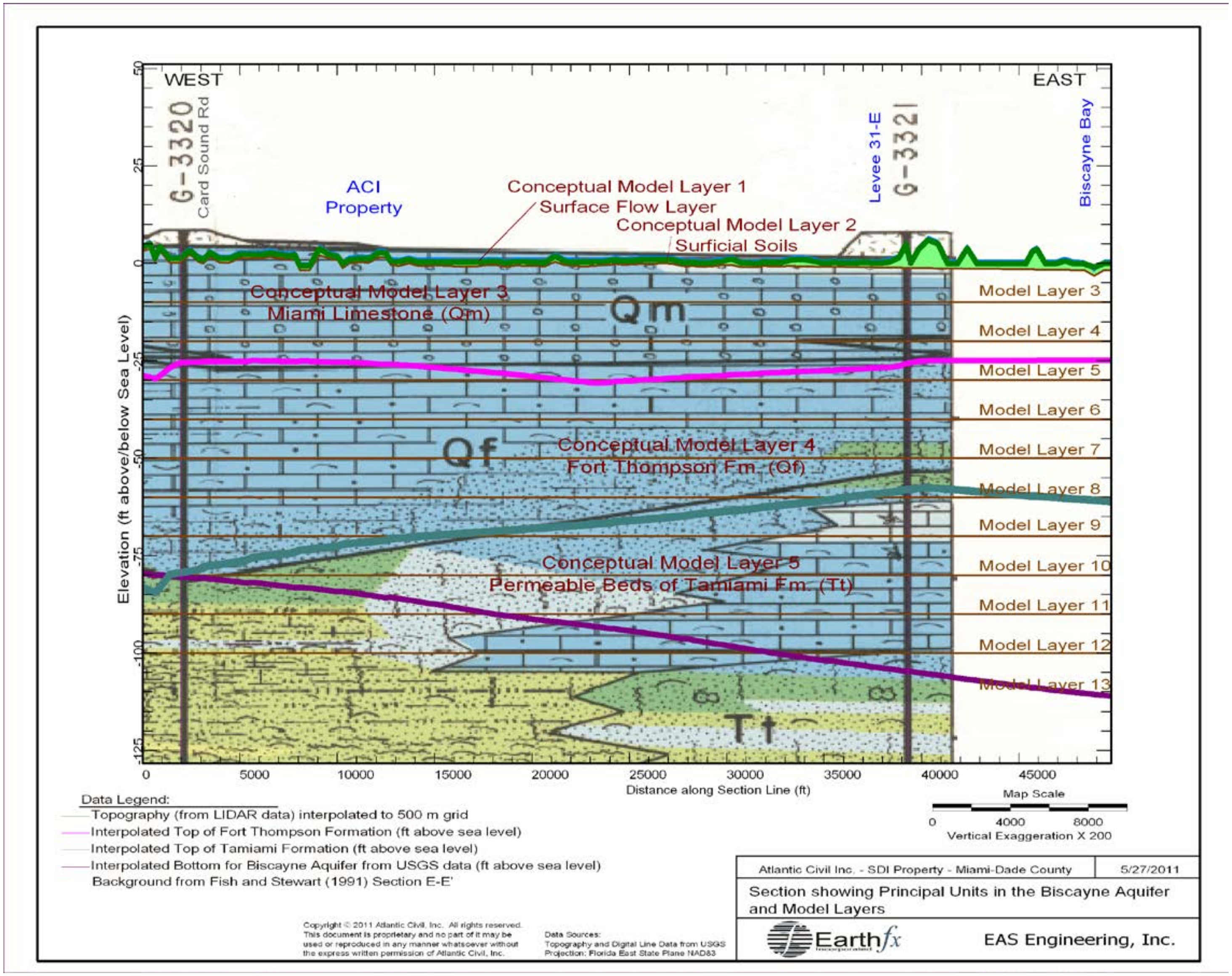

Figure 8: Cross section showing principal units in the Biscayne aquifer and model layering.

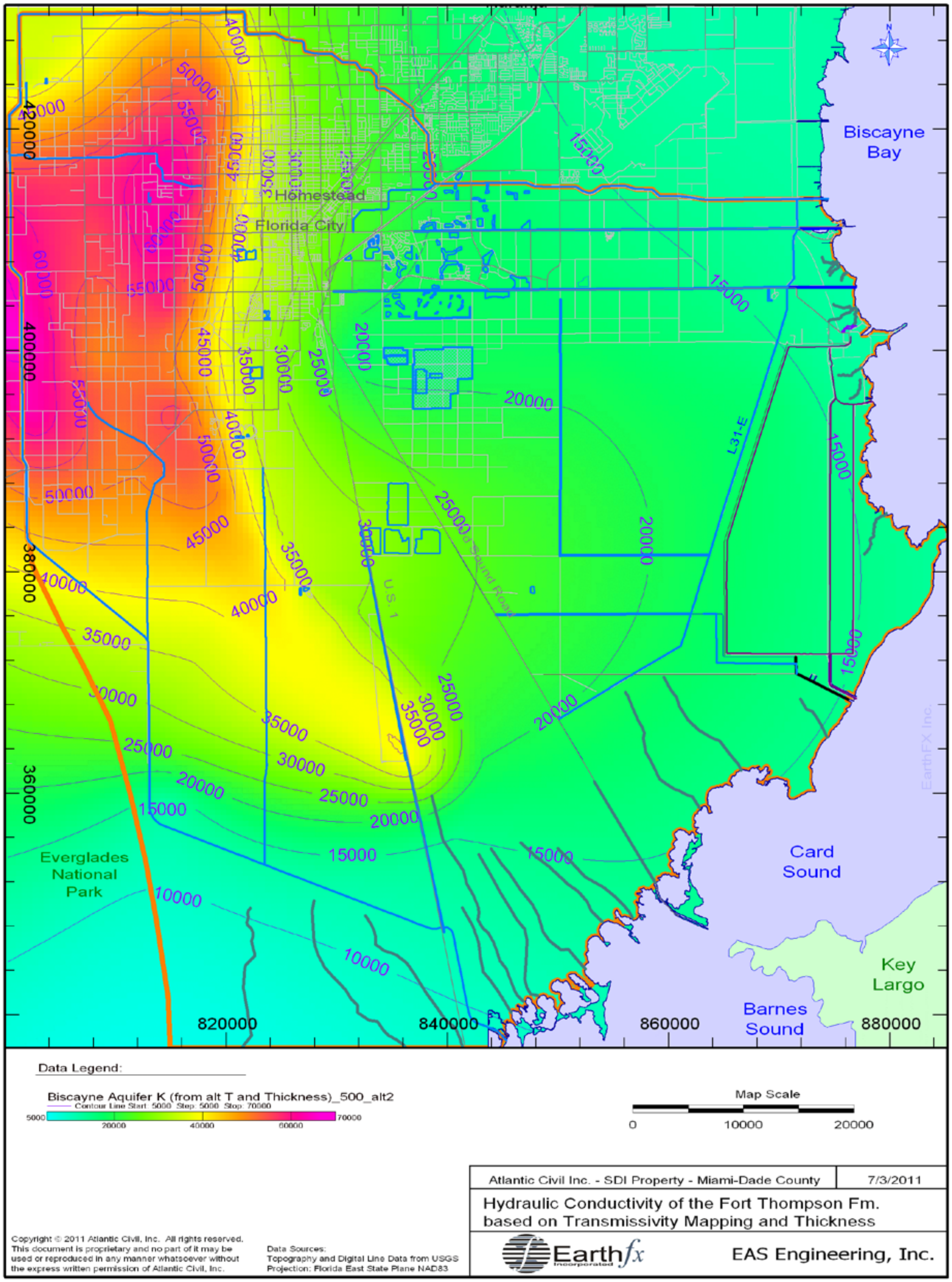

Figure 9: Calculated hydraulic conductivity for the Fort Thompson Formation based on transmissivity mapping (Merritt, 1997) and interpolated thickness of the formation.

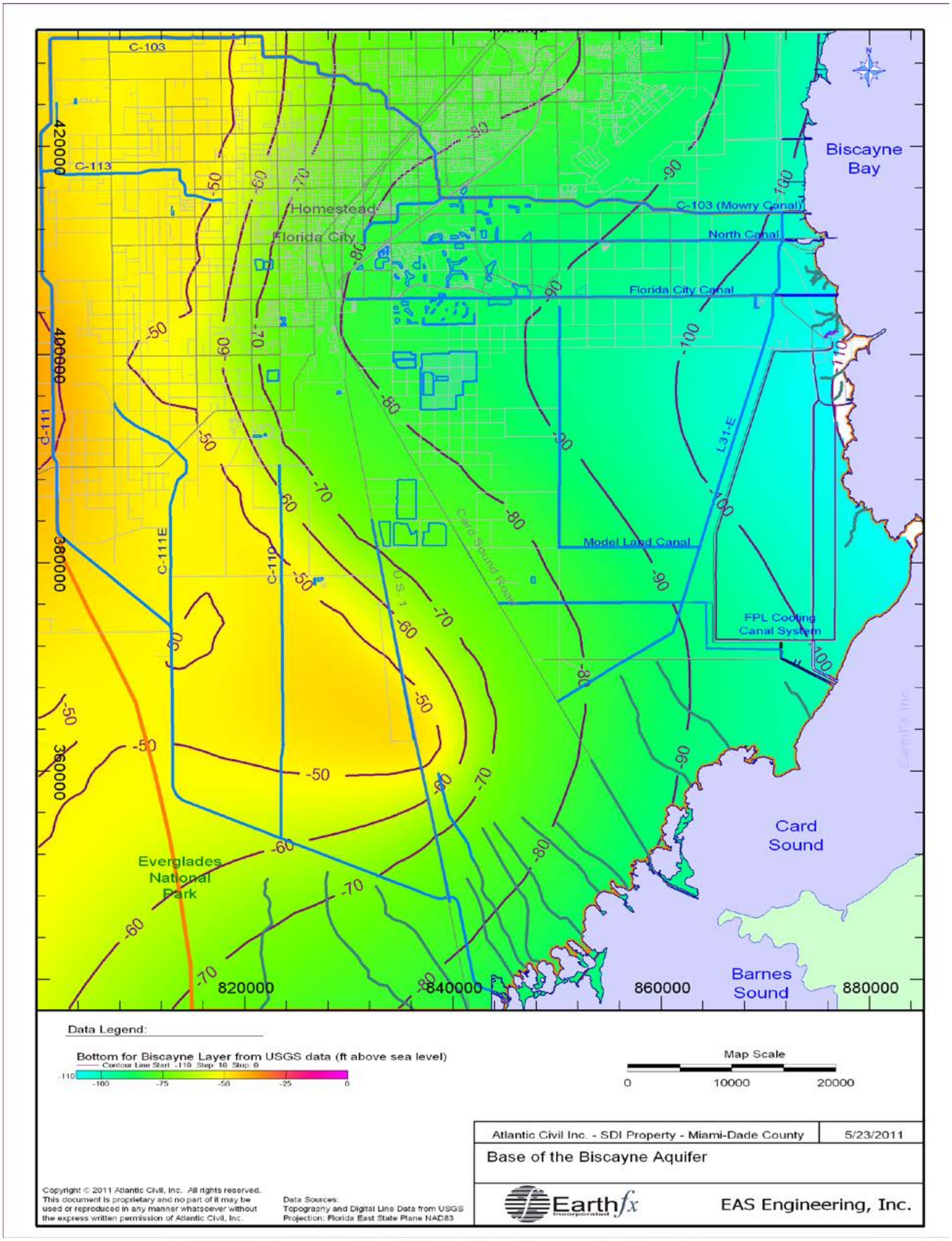

Figure 10: Base of the Biscayne aquifer (from Fish and Stewart, 1991).

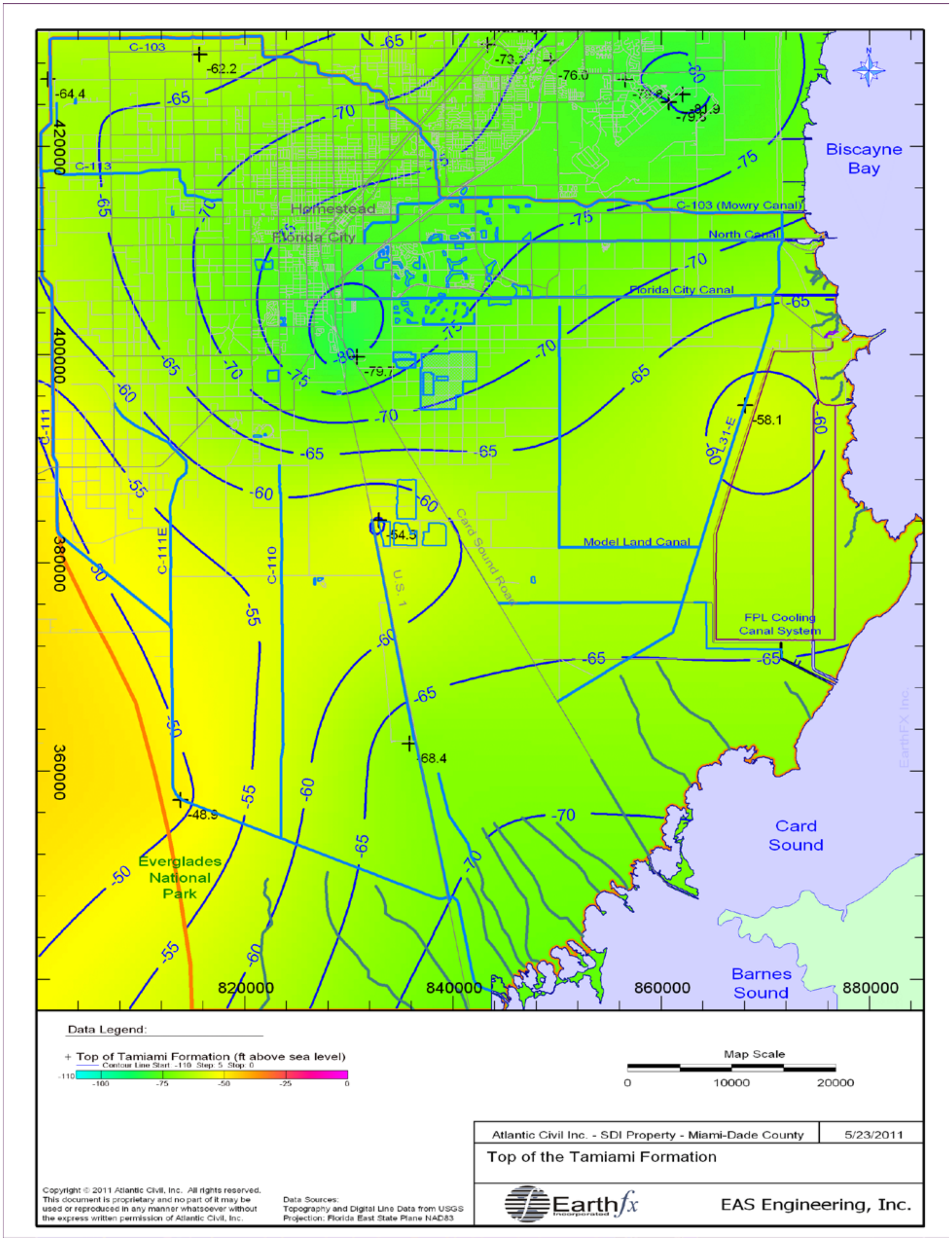

Figure 11: Top of the Tamiami Formation (data from Fish and Stewart, 1991).

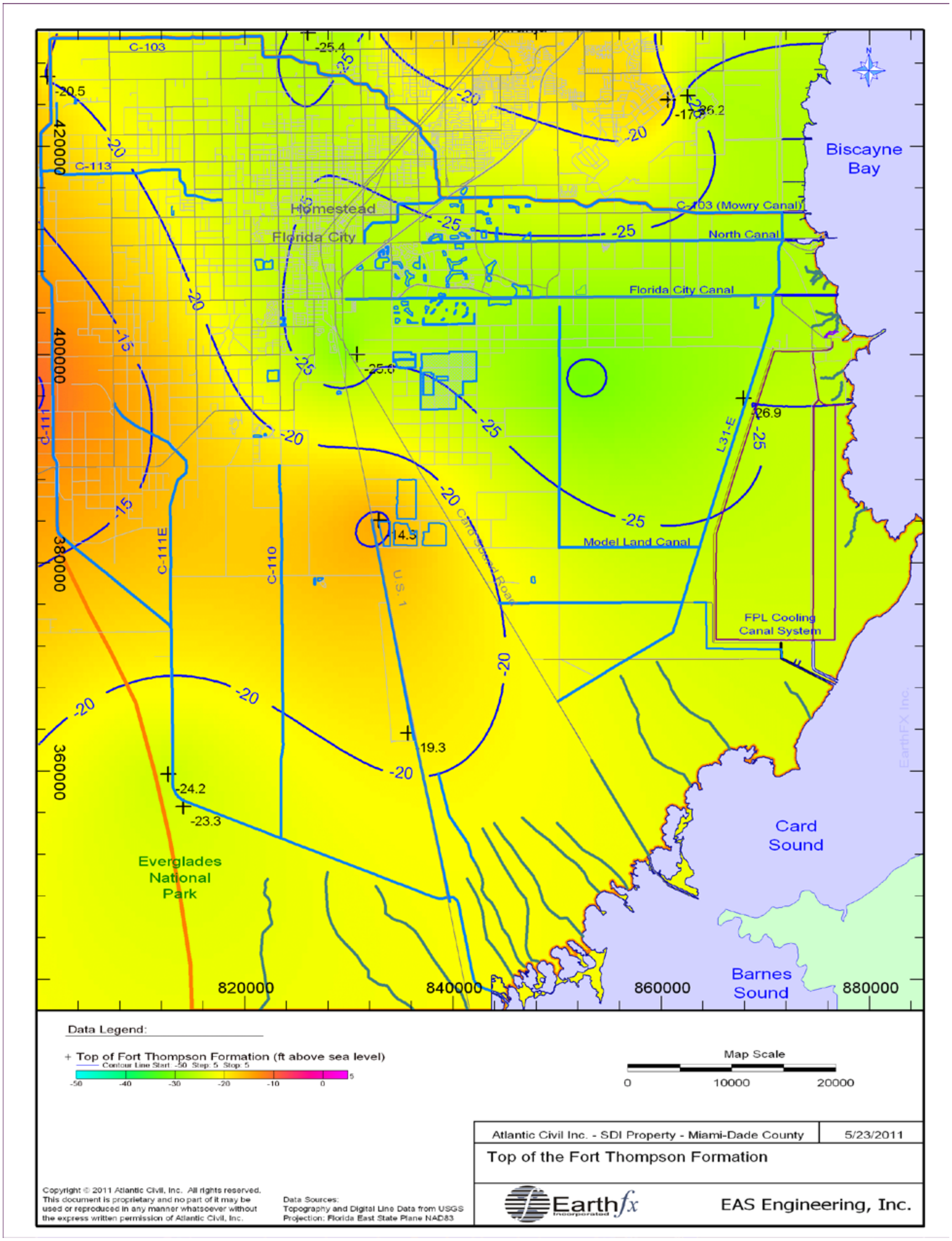

Figure 12: Top of the Fort Thompson Formation (data from Fish and Stewart, 1991).

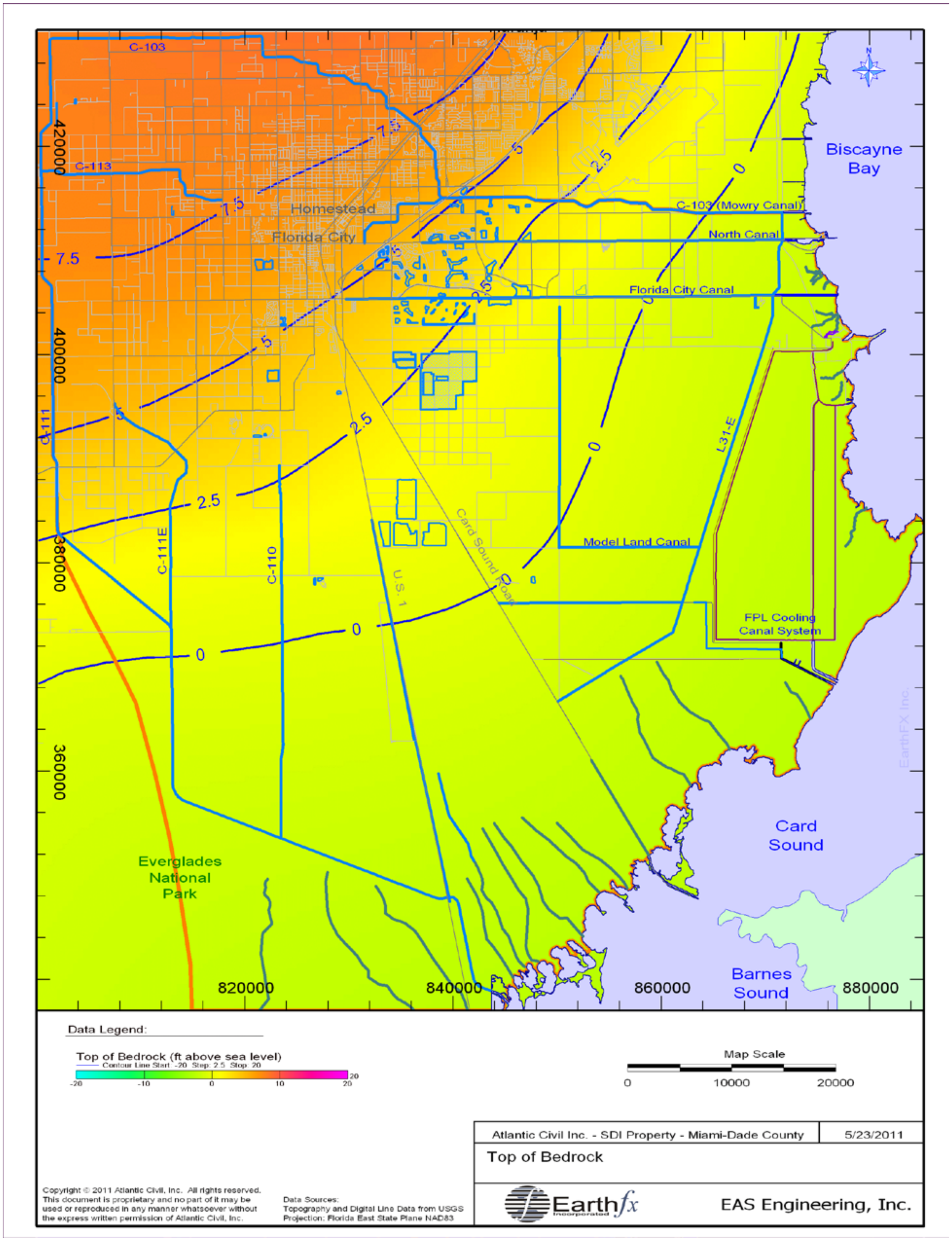

Figure 13: Top of Bedrock (data from Parker and others, 1955).

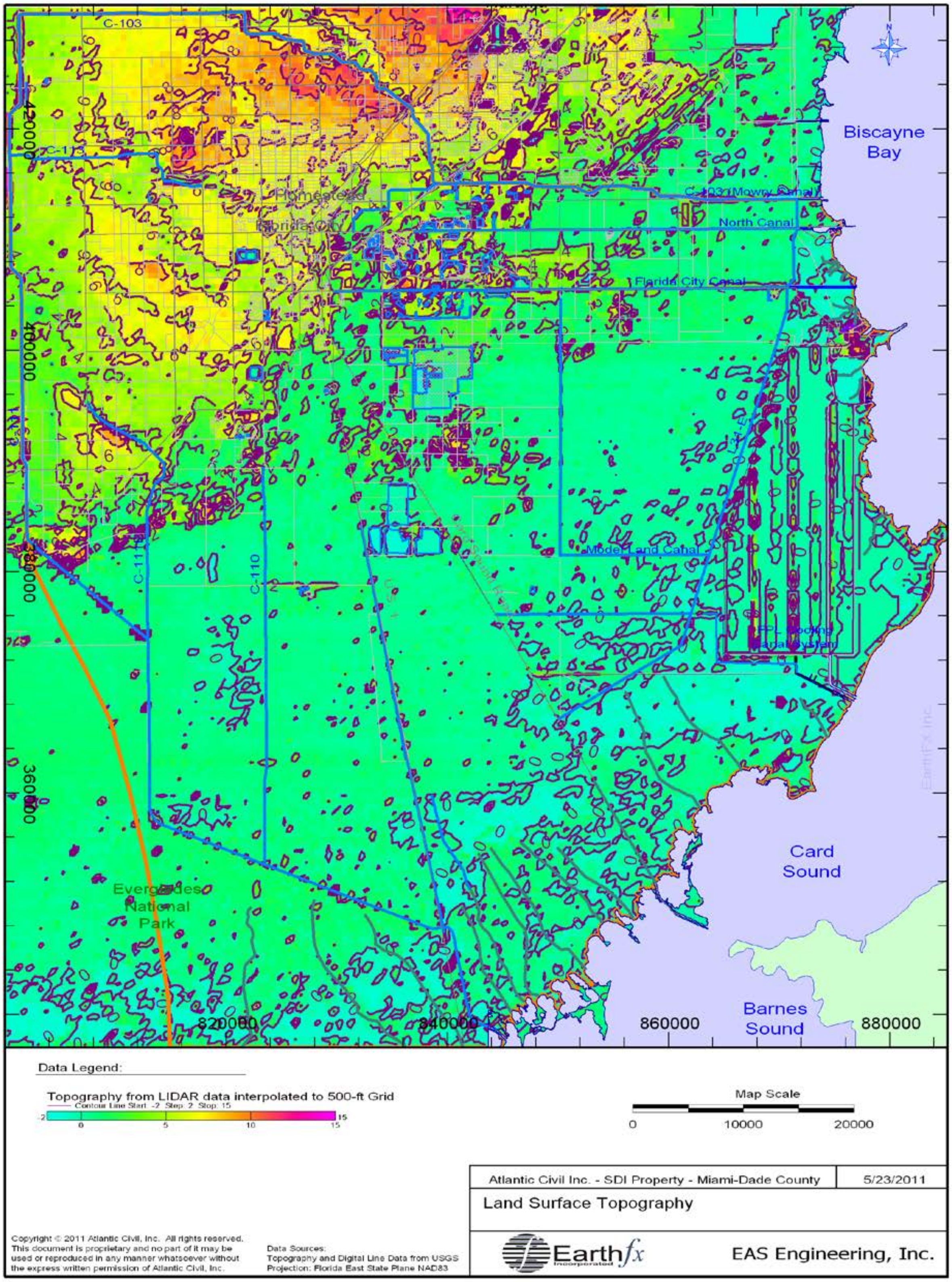

Figure 14: Land surface topography interpolated to model grid from LIDAR data.

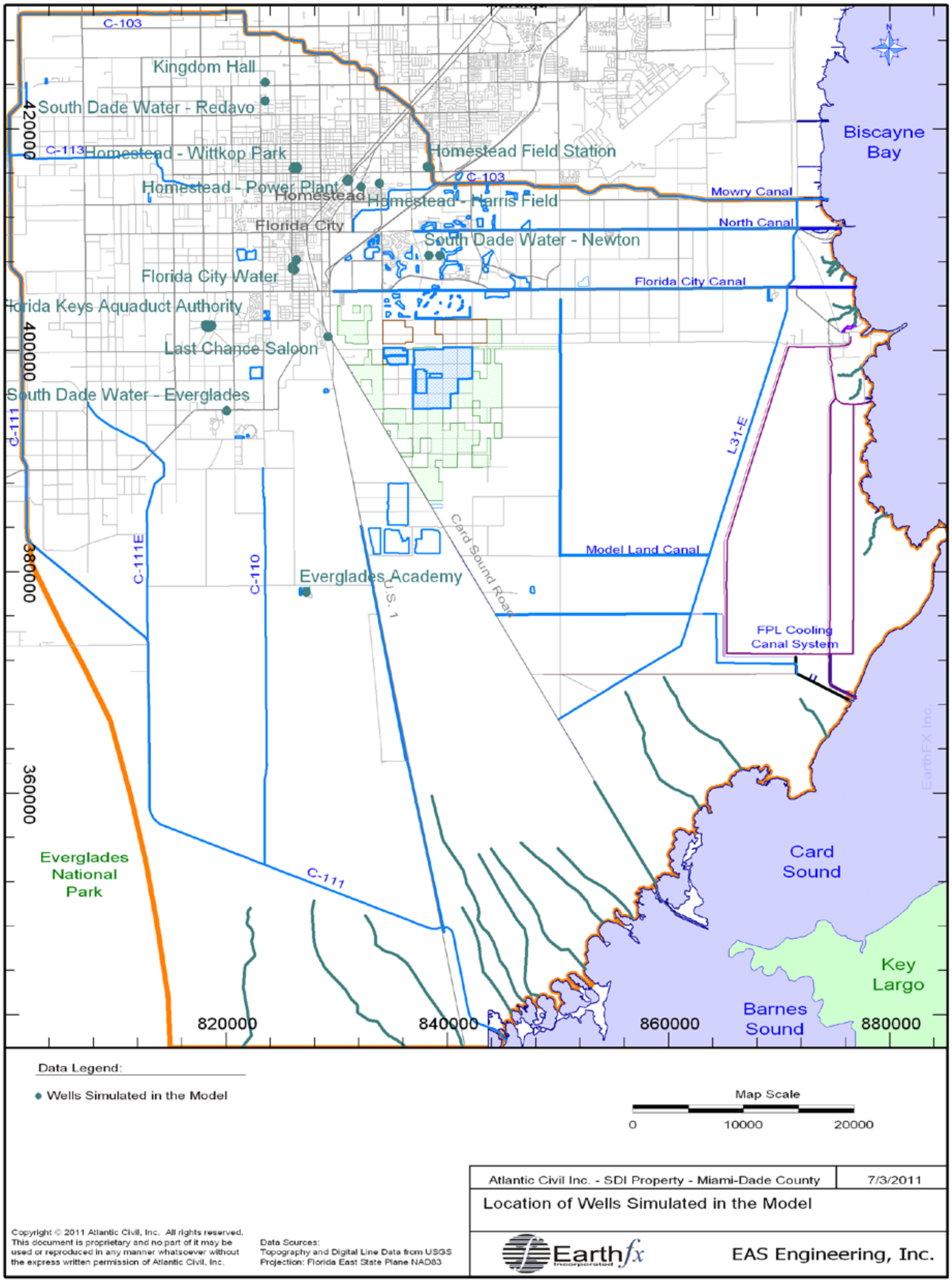

Figure 15: Location of wells simulated in the model.

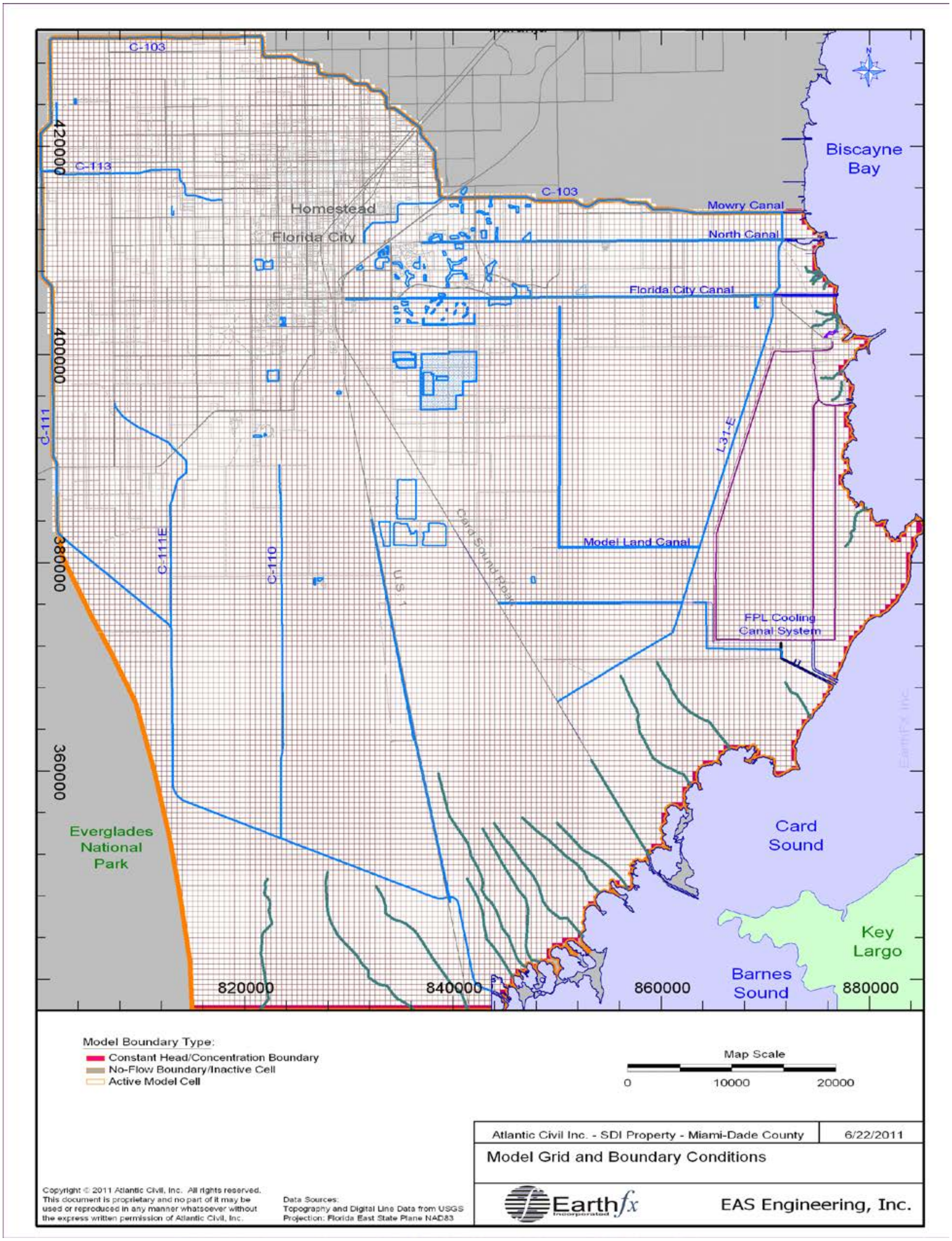

Figure 16: Model grid and boundary conditions.

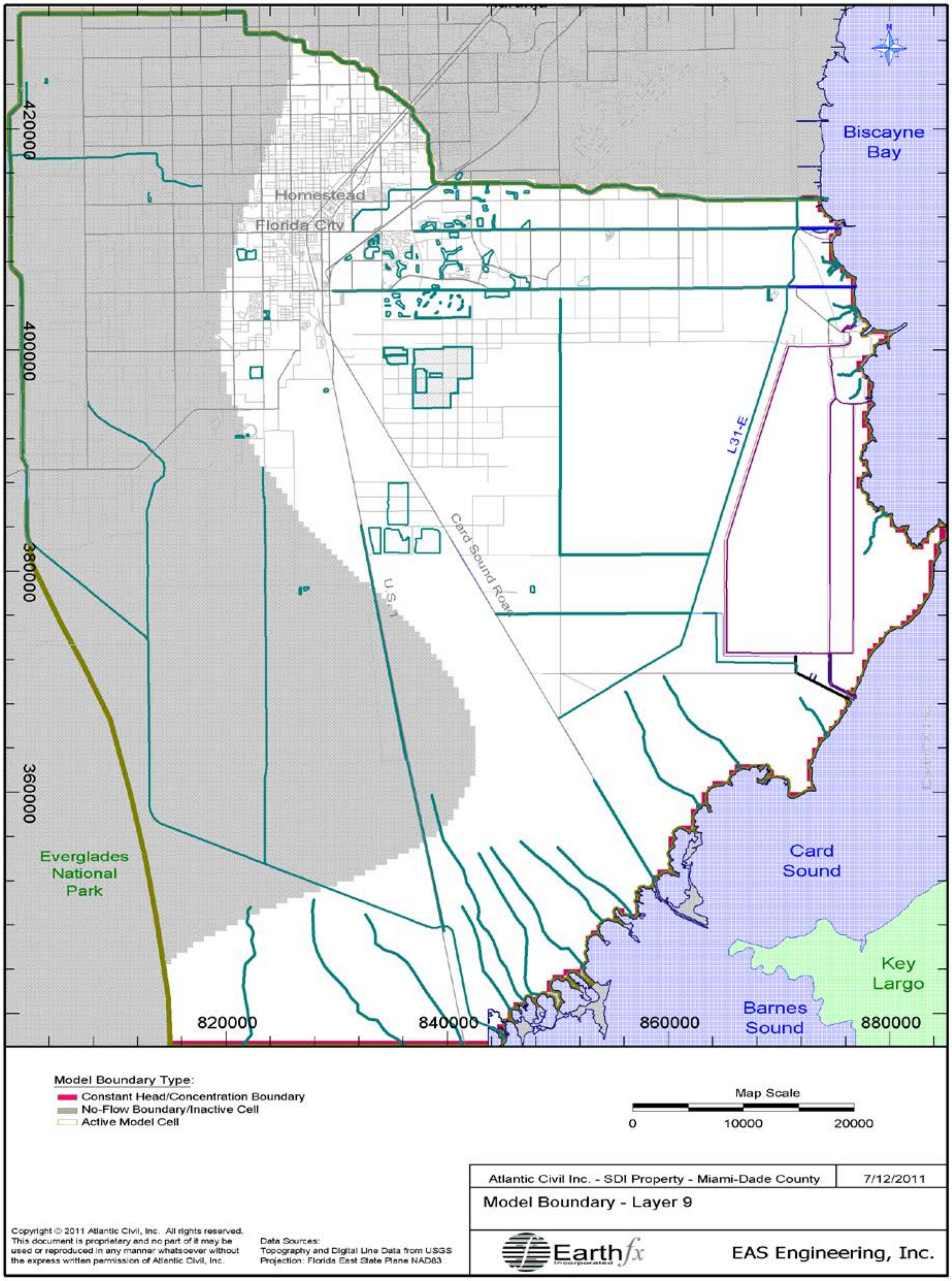

Figure 17: Boundary conditions in model Layer 9.

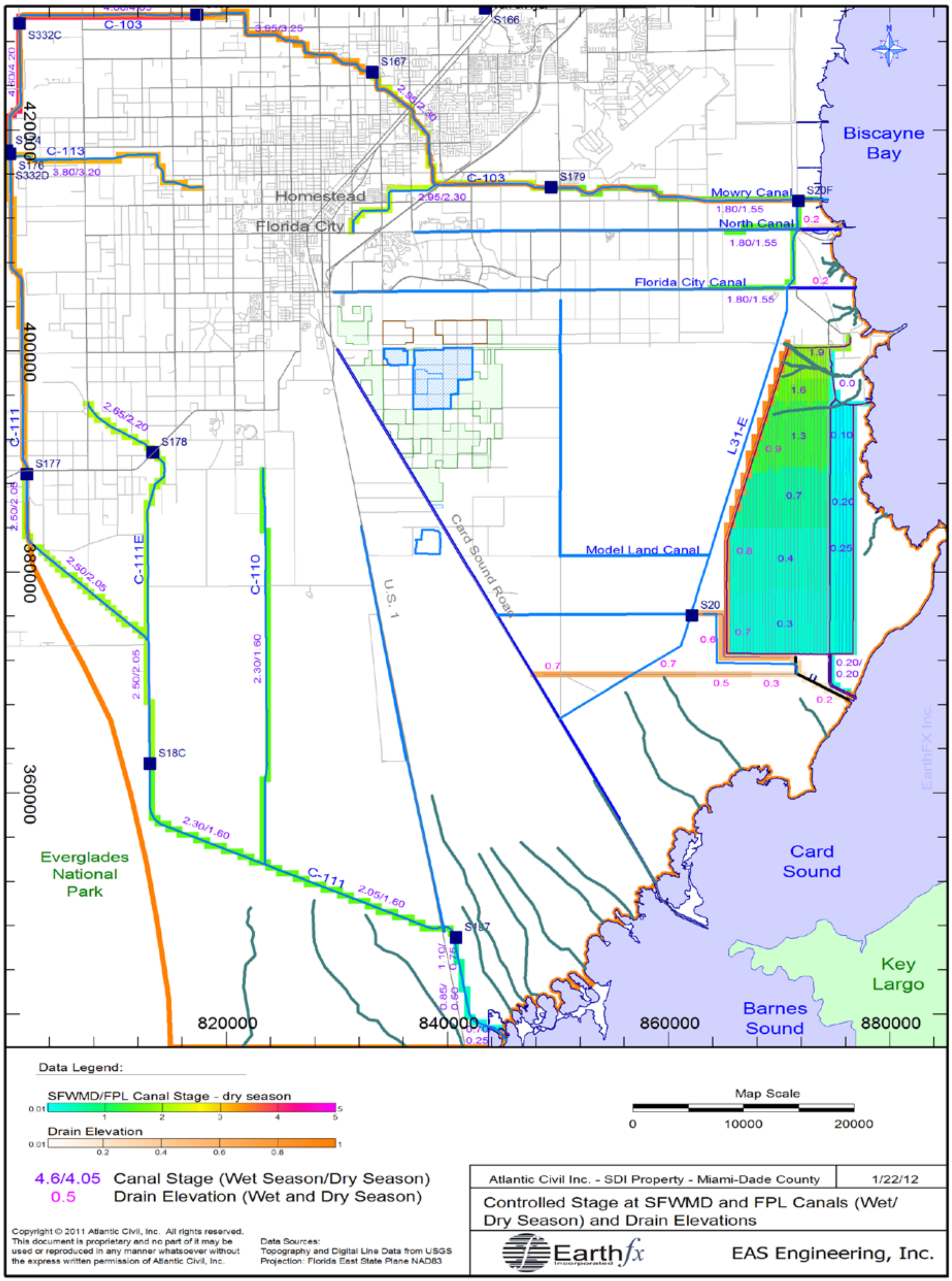

Figure 18: Wet season and dry season stage specified at SFWMD and FPL canals and controlling elevations for drains.

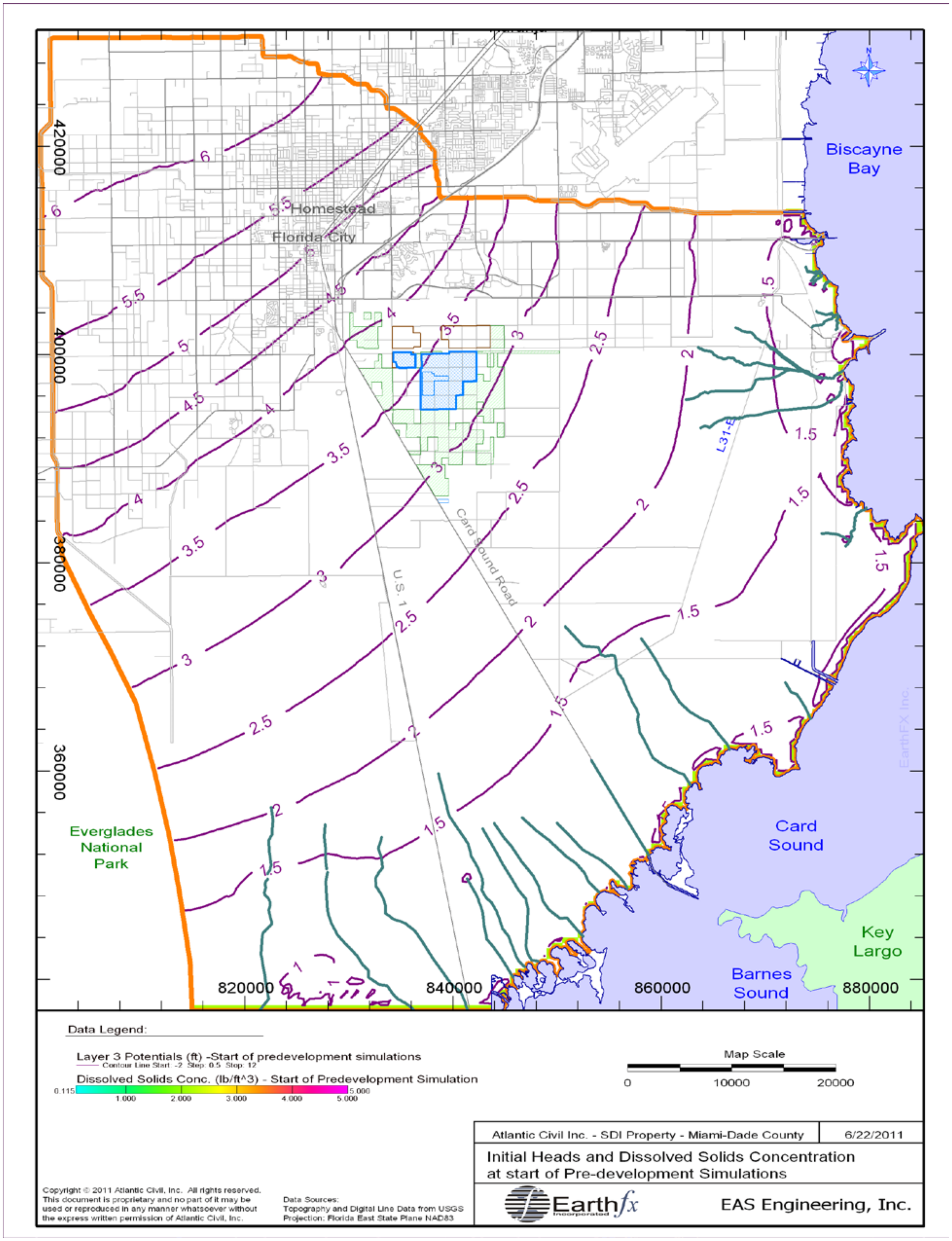

Figure 19: Initial heads and dissolved solids concentrations at start of model simulation of pre-development conditions.

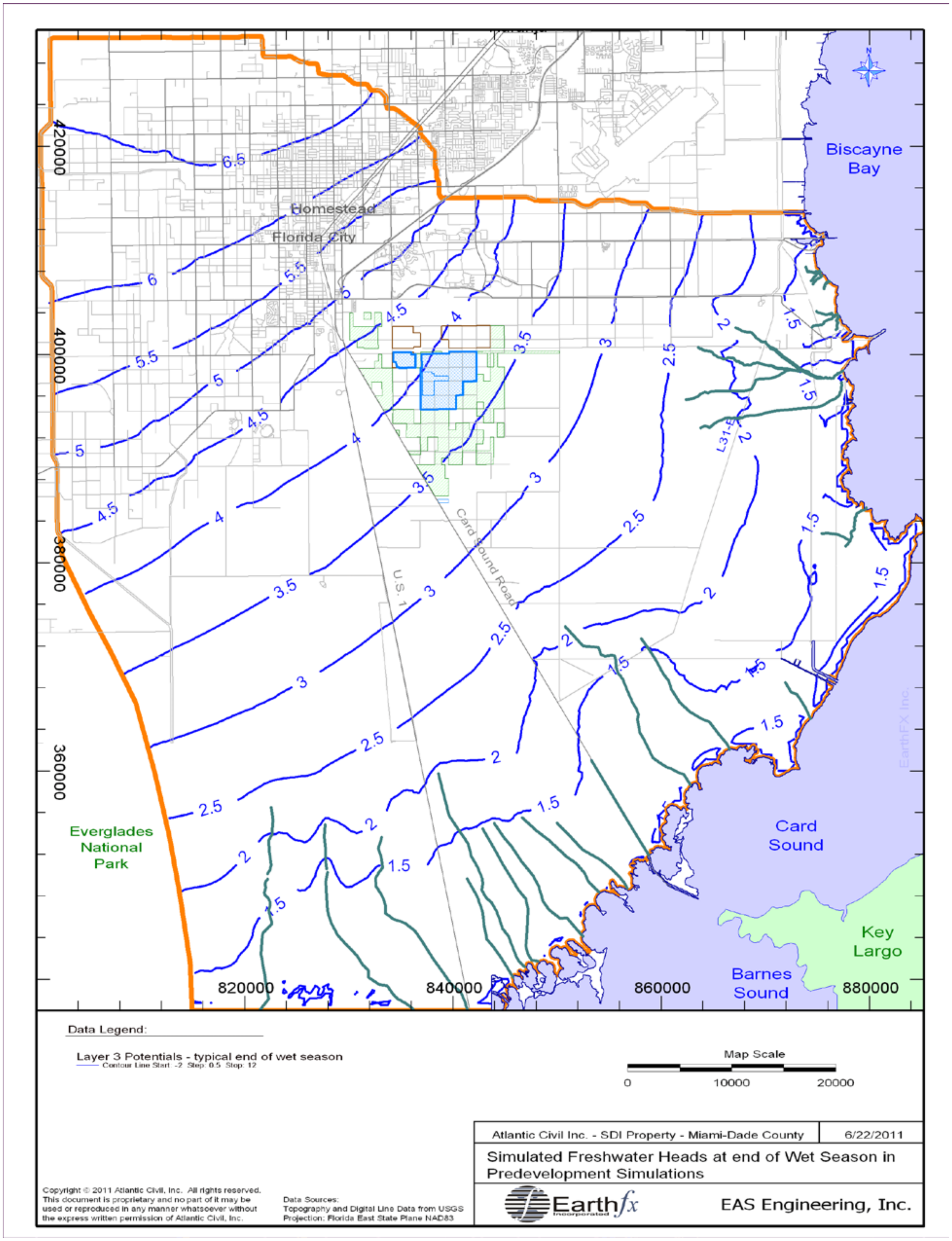

Figure 20: Simulated end of wet season equivalent freshwater heads (Layer 3) under predevelopment conditions.

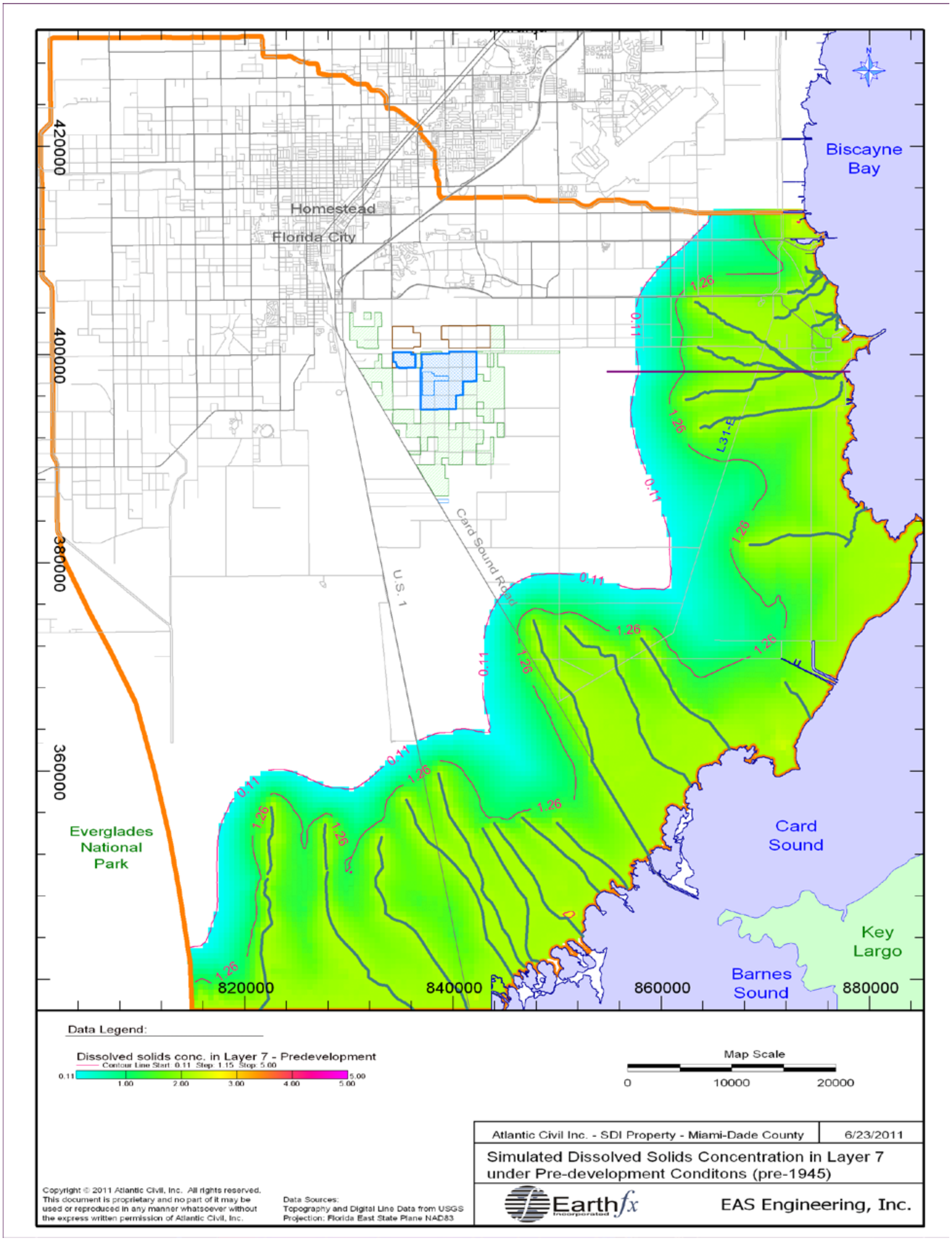

Figure 21: Simulated dissolved solids concentration in Layer 7 at the end of the wet season under predevelopment conditions.

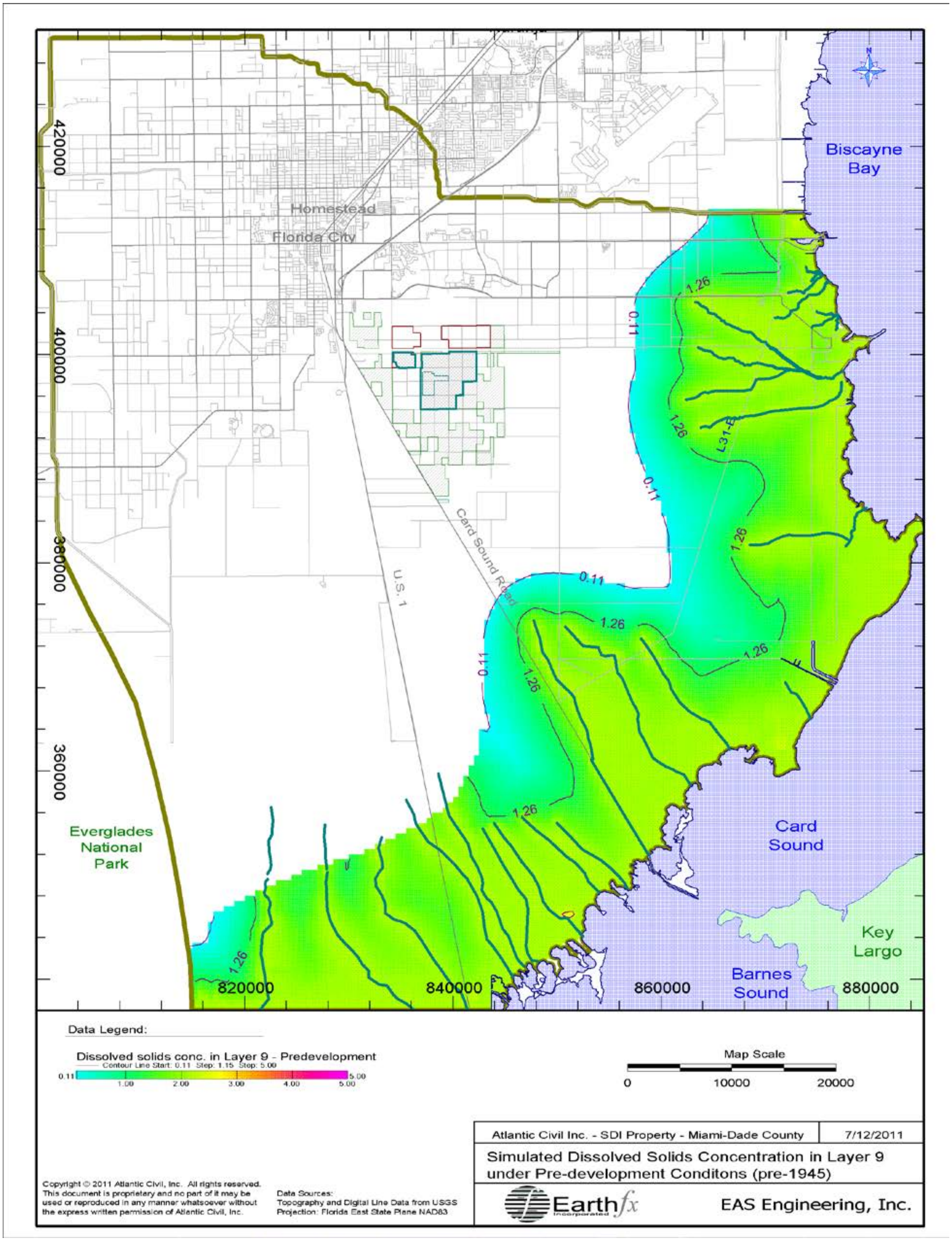

Figure 22: Simulated dissolved solids concentration in Layer 9 at the end of the wet season under predevelopment conditions.

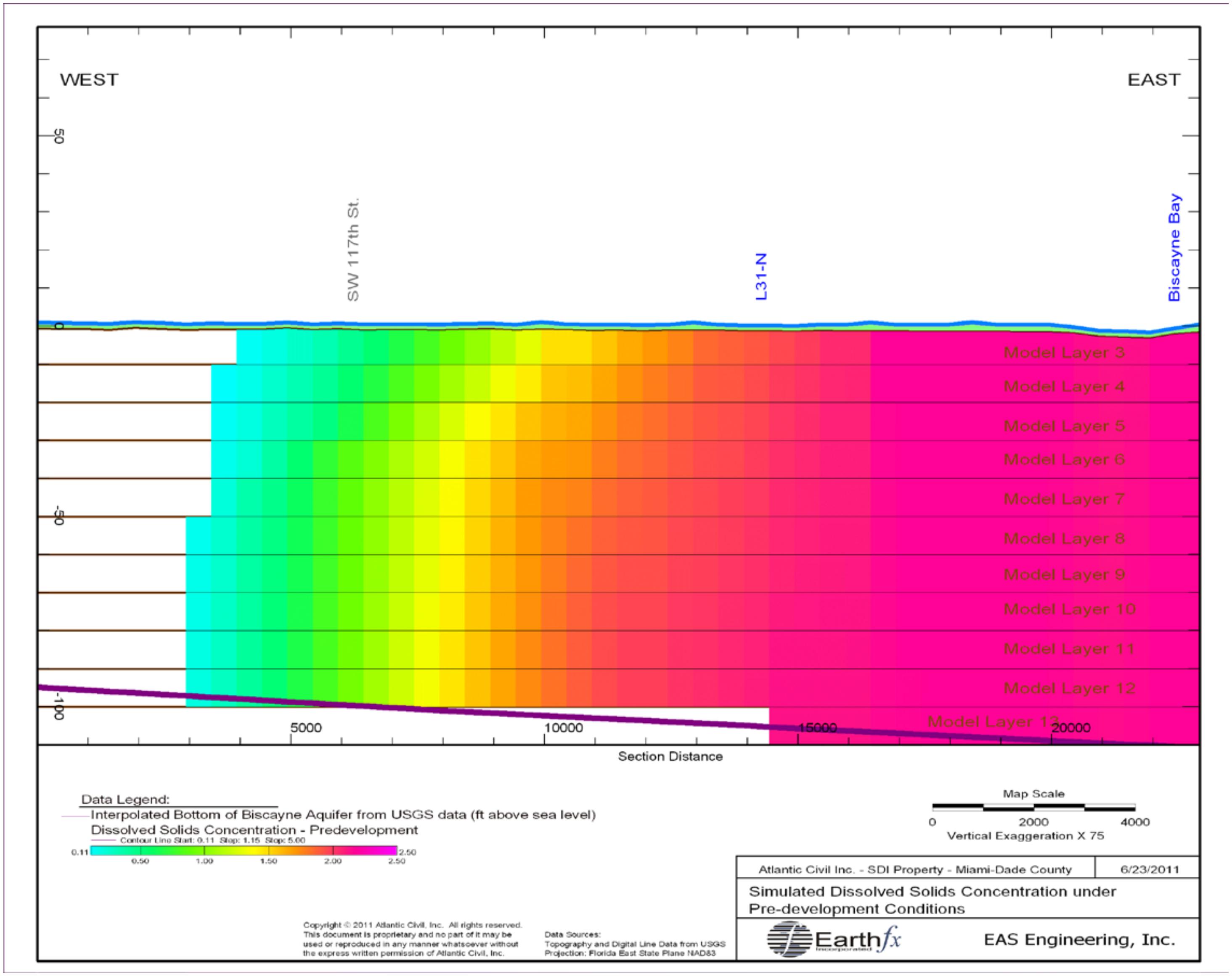

Figure 23: Simulated dissolved solids concentration with depth - predevelopment conditions (Section line shown on Figure 20).

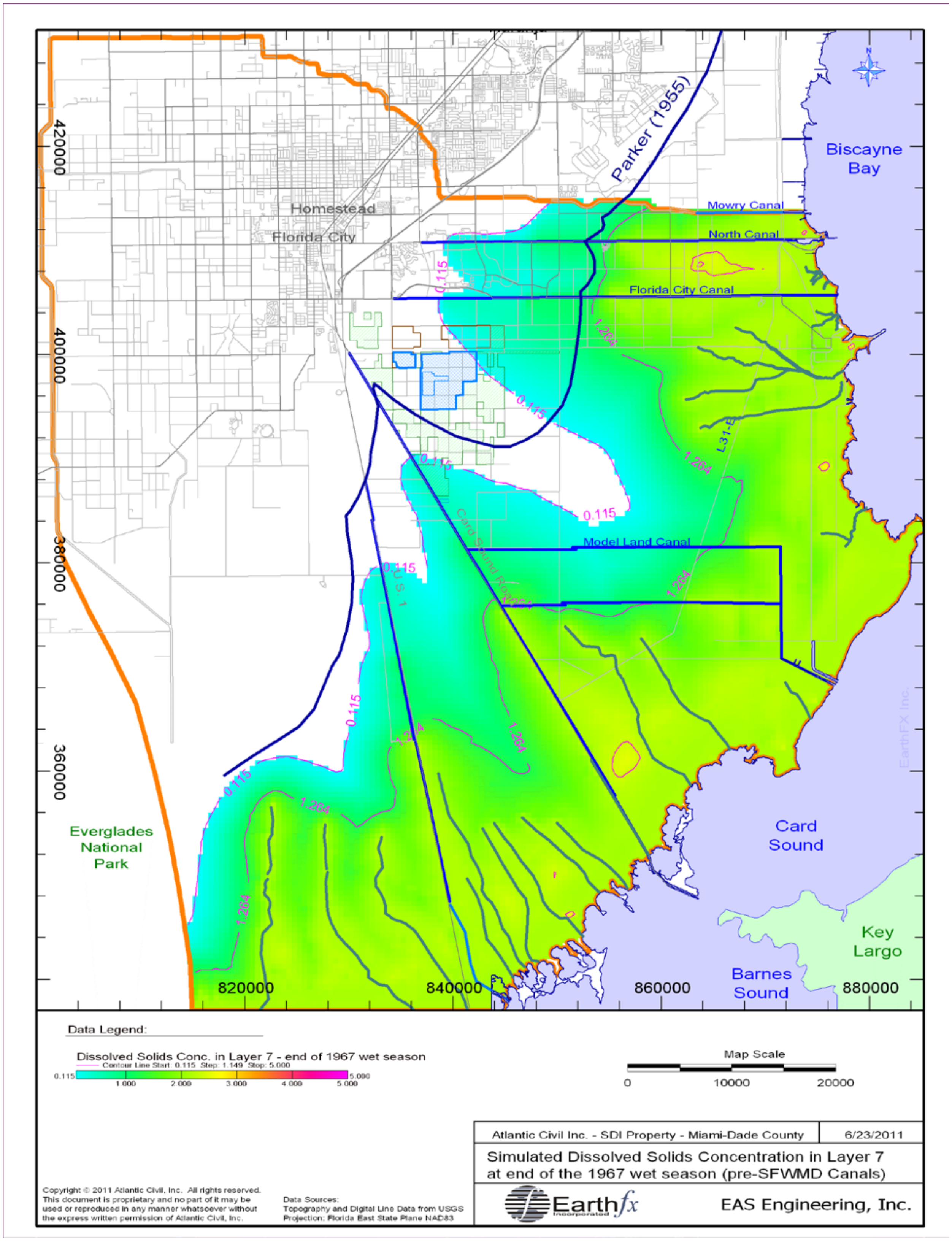

Figure 24: Dissolved solids concentration in Layer 7 at end of 1945 to 1967 simulations.

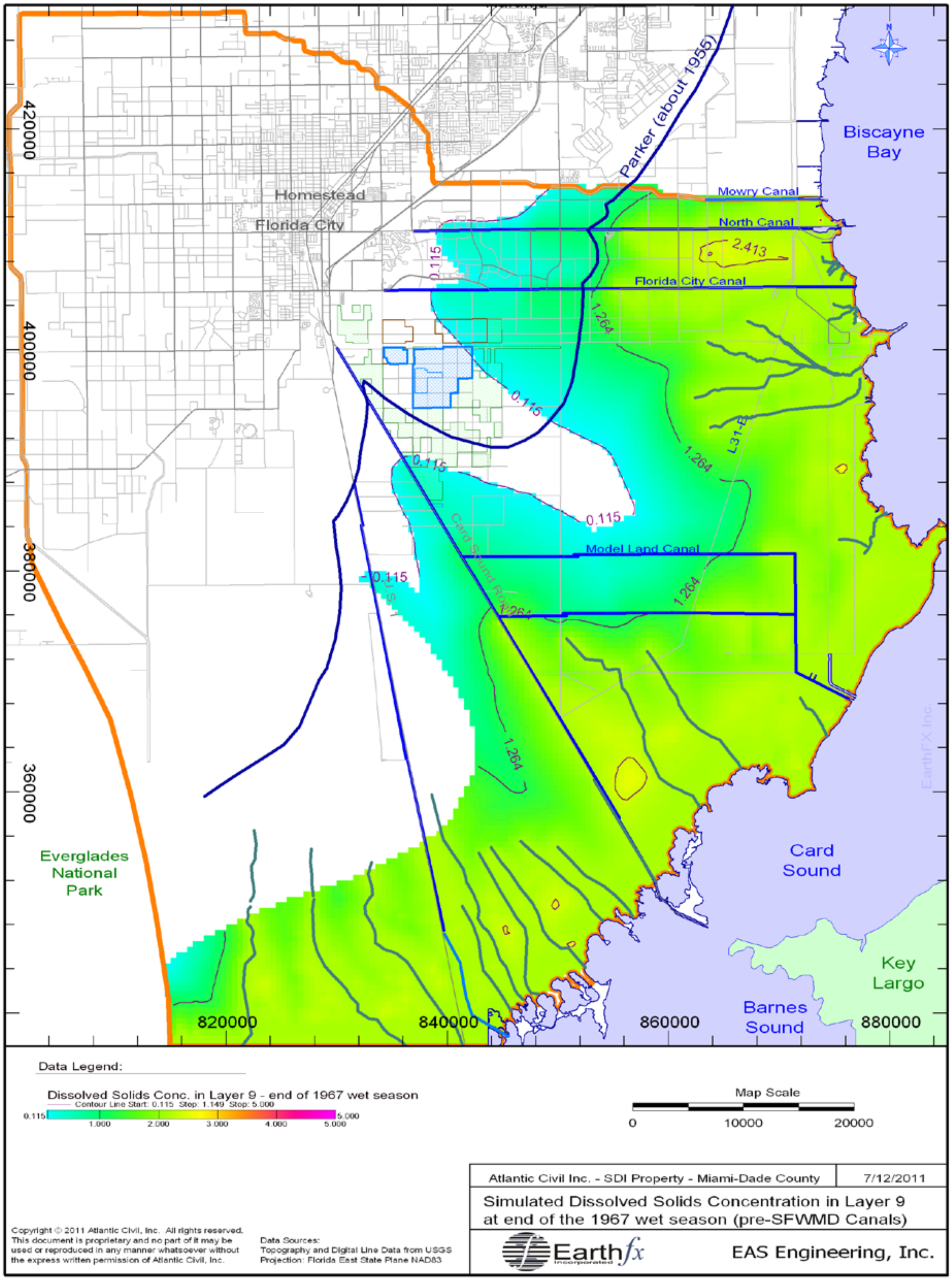

Figure 25: Dissolved solids concentration in Layer 9 at end of 1945 to 1967 simulations.

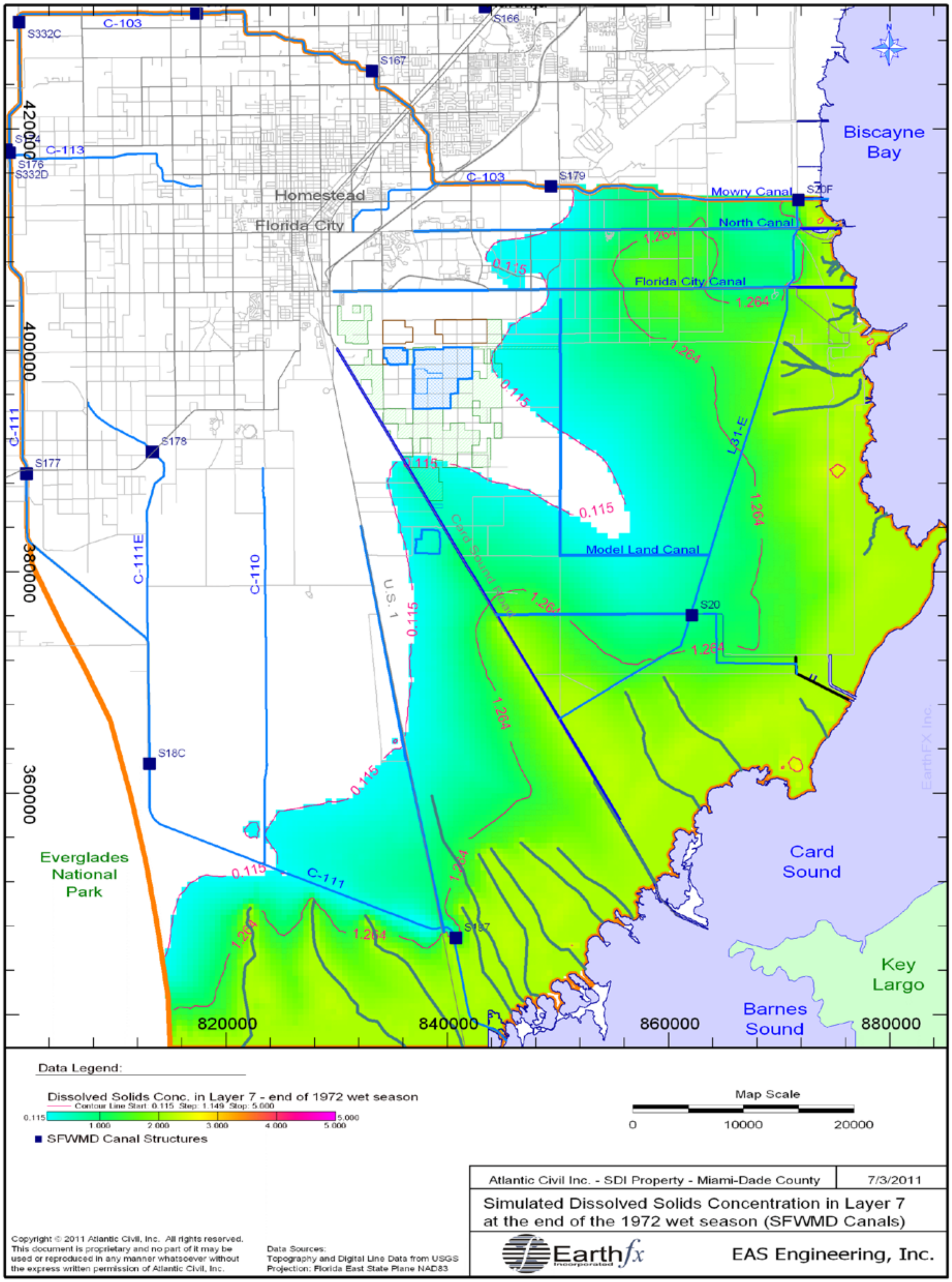

Figure 26: Dissolved solids concentration in Layer 7 at end of 1968 to 1972 simulations.

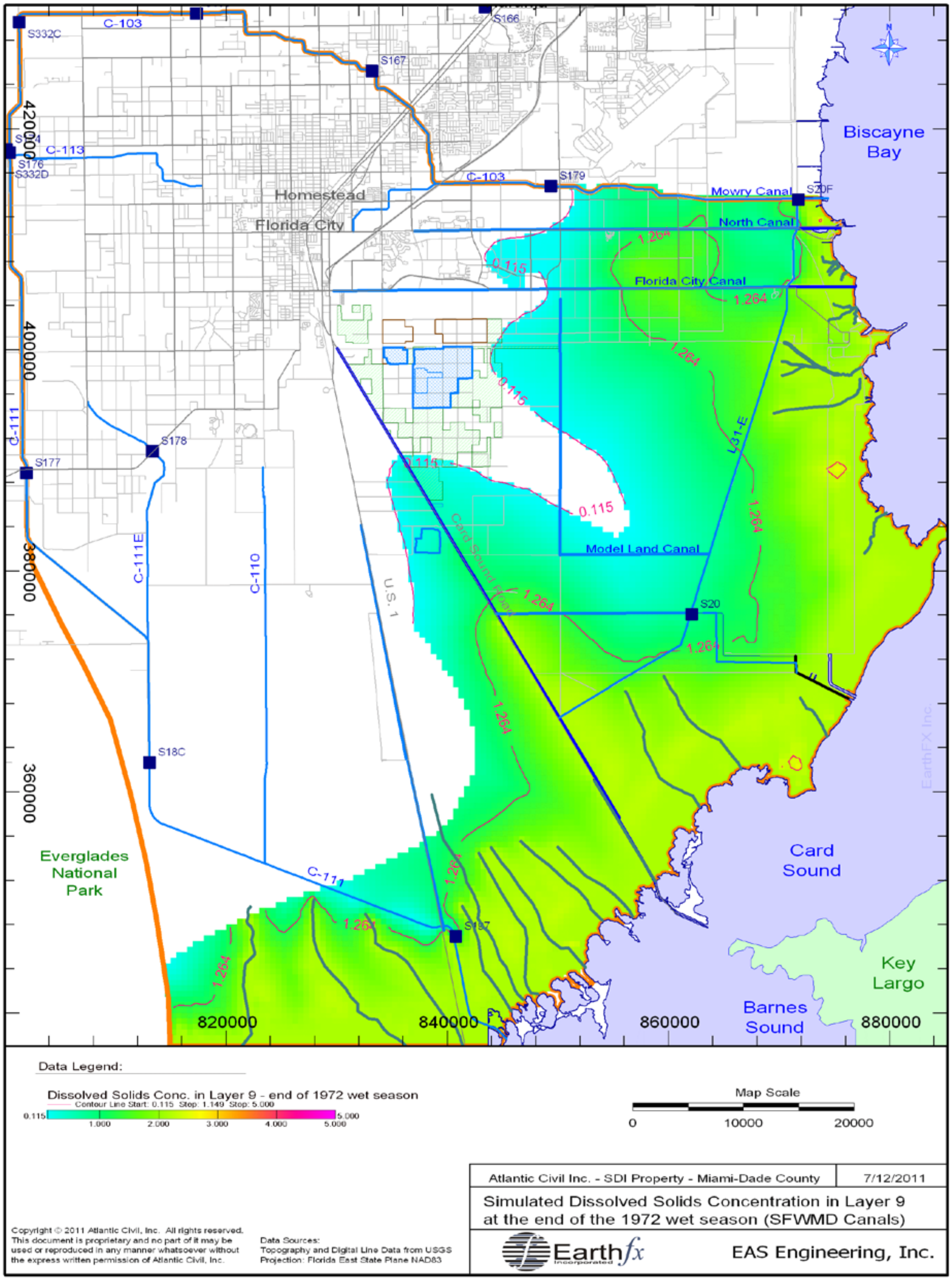

Figure 27: Dissolved solids concentration in Layer 9 at end of 1968 to 1972 simulations.

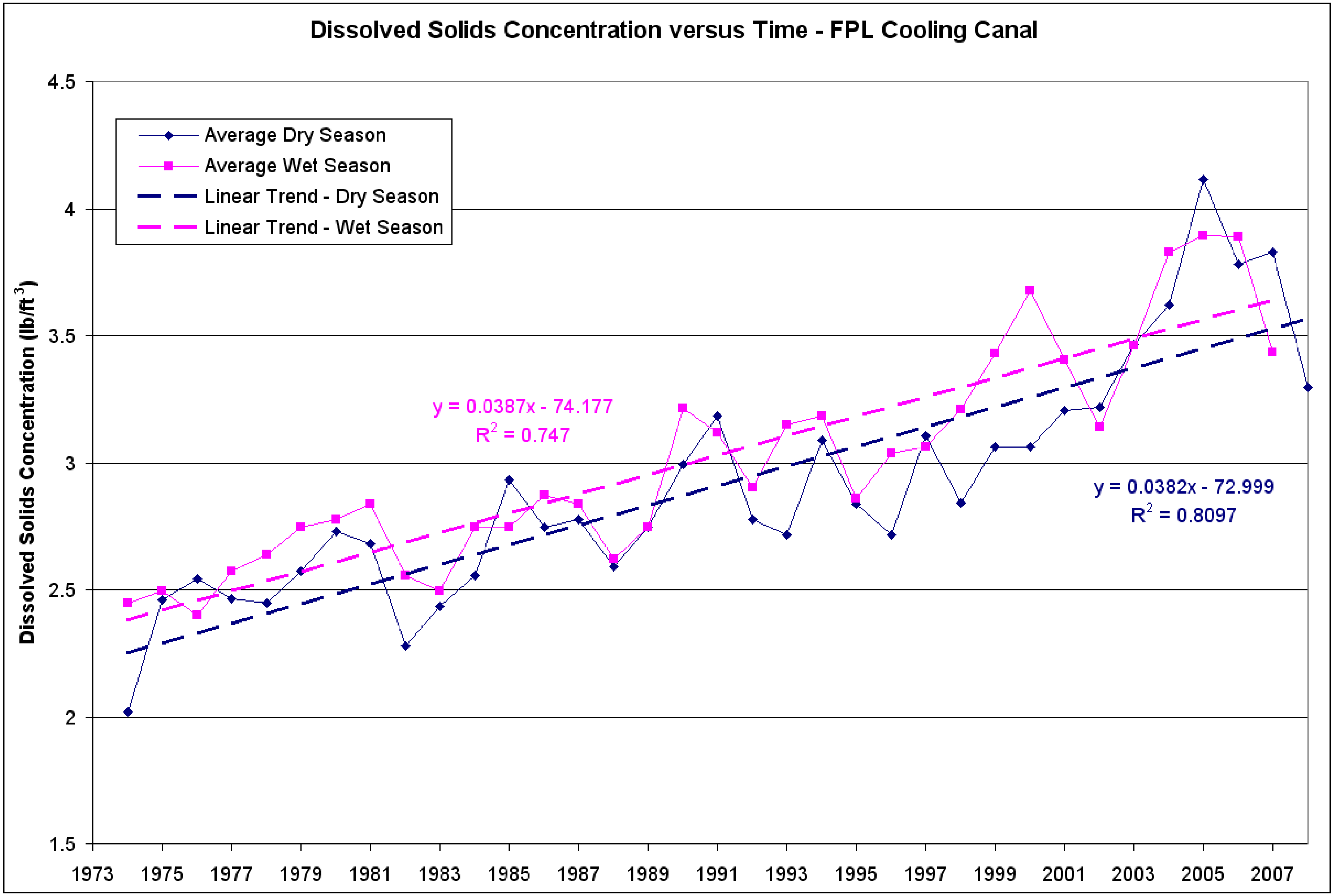

Figure 28: Observed average wet season and average dry season dissolved solids concentration in FPL cooling canals and trends.

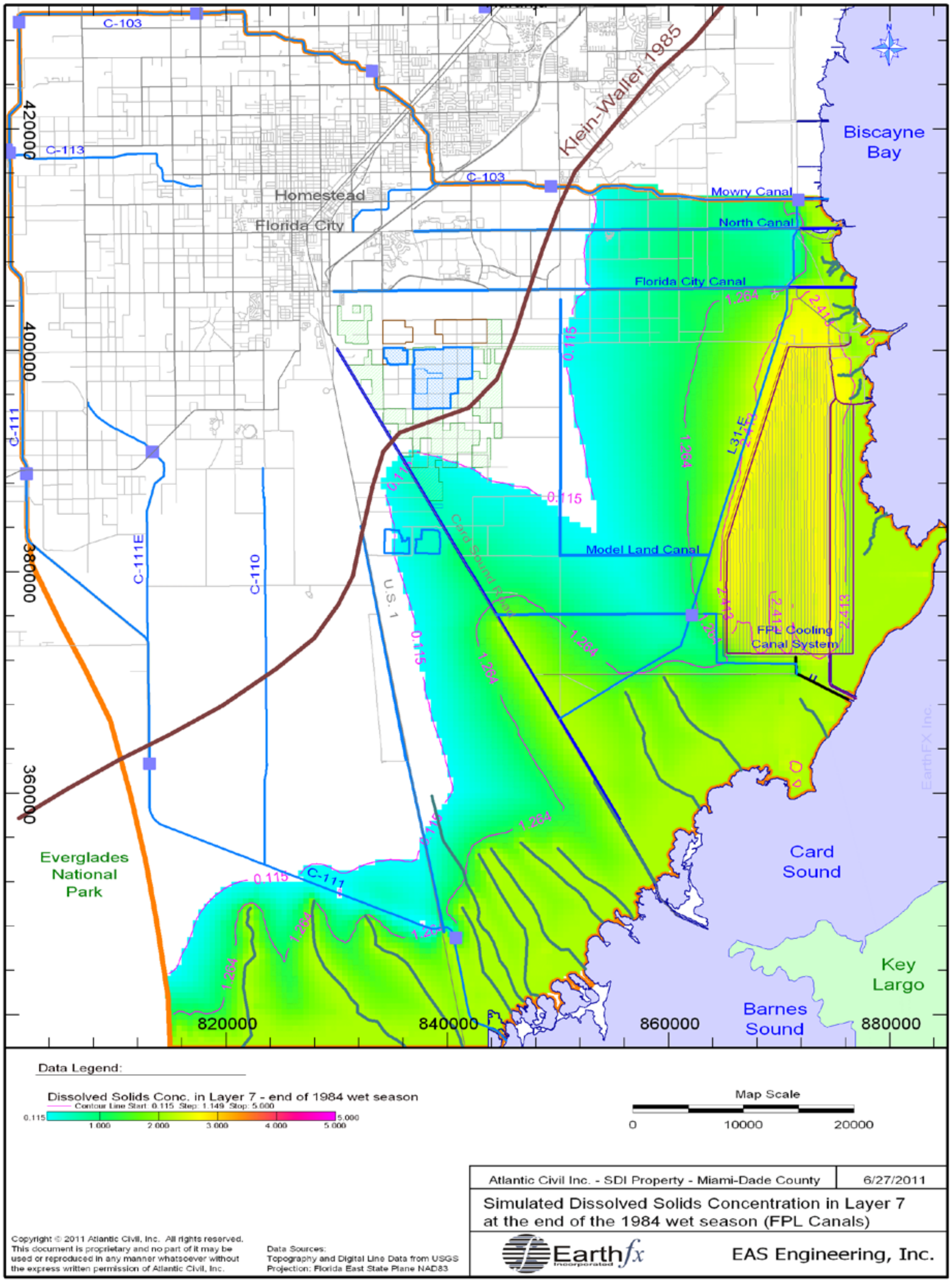

Figure 29: Dissolved solids concentration in Layer 7 at end of 1973 to 1984 simulations.

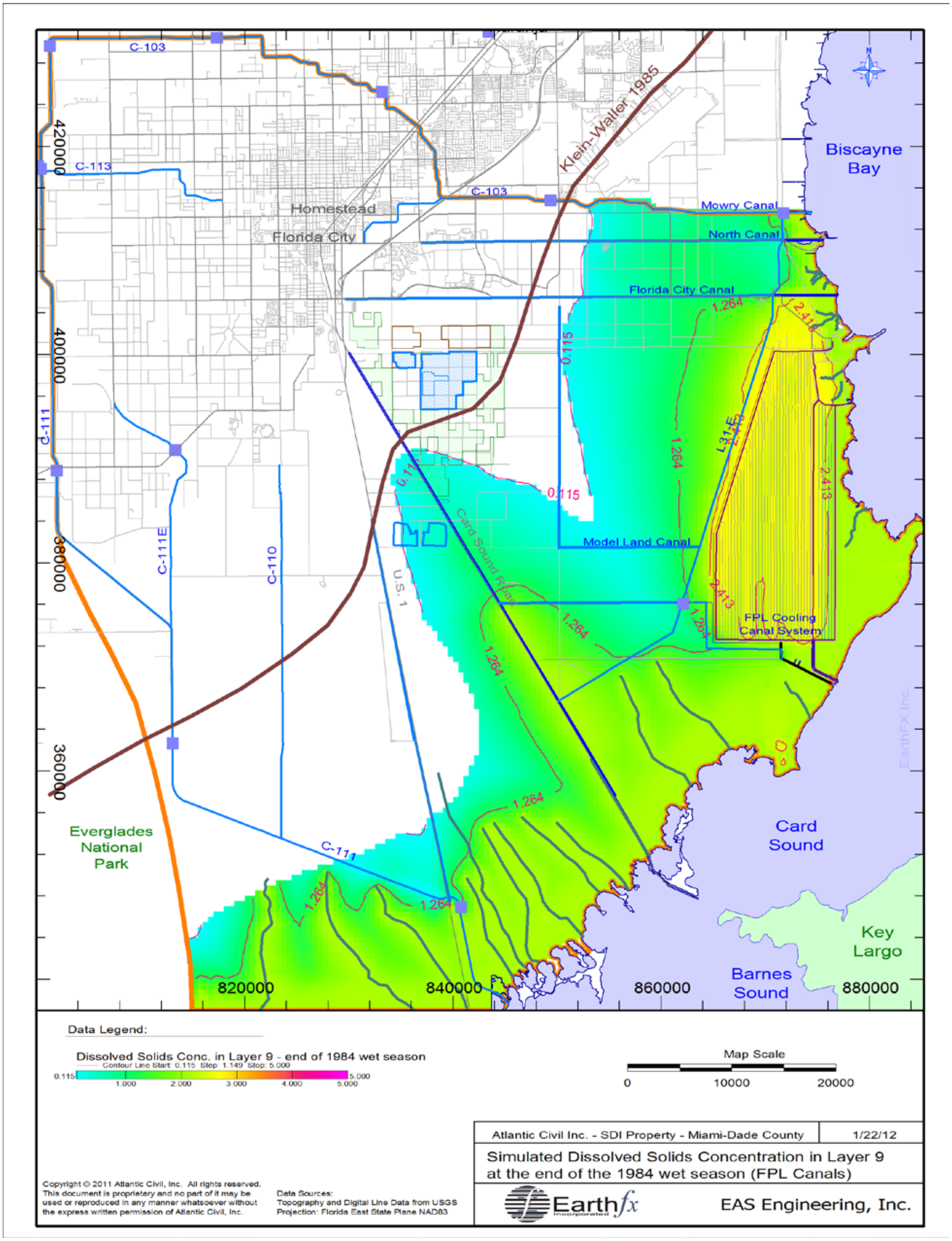

Figure 30: Dissolved solids concentration in Layer 9 at end of 1973 to 1984 simulations.

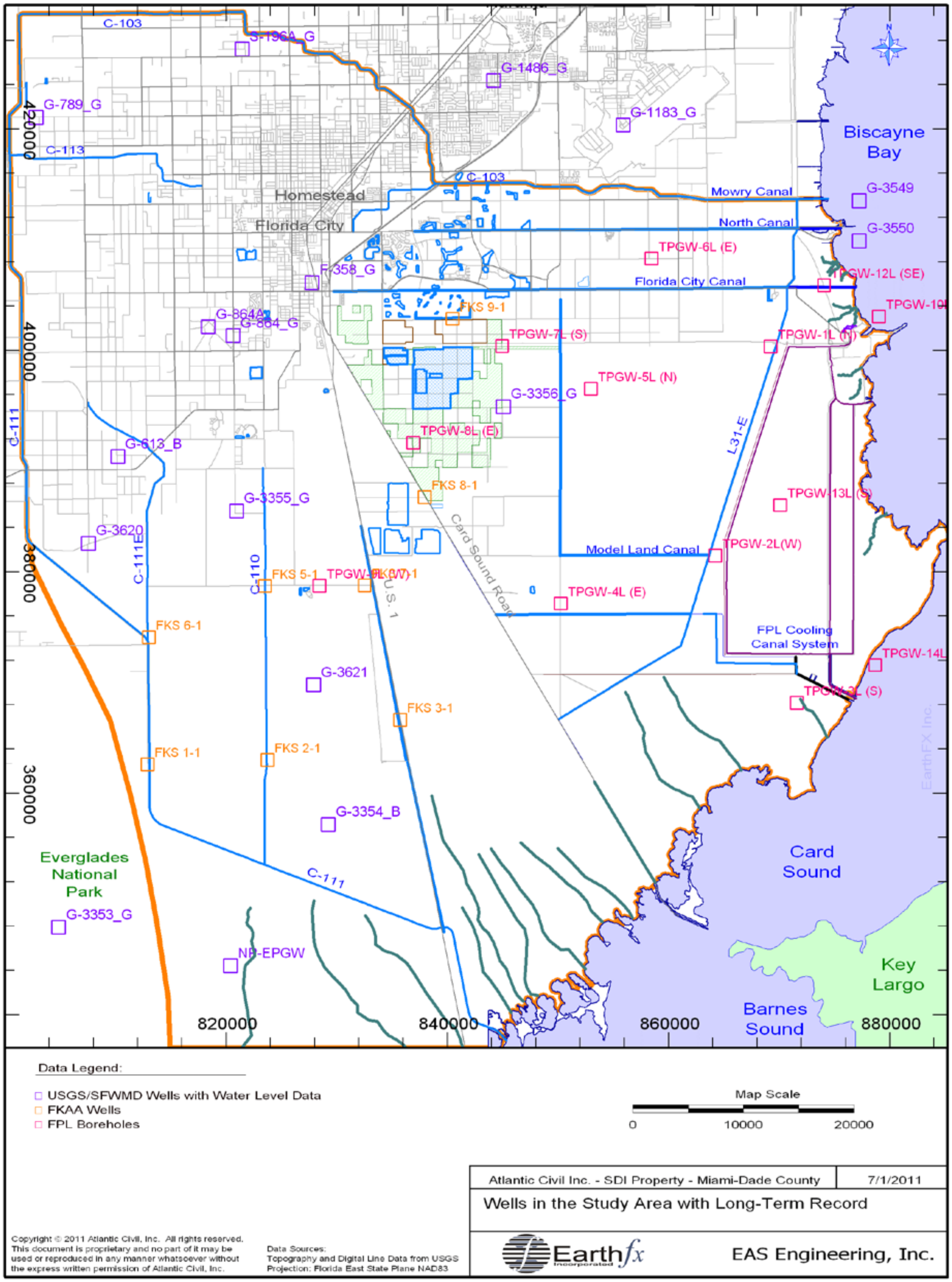

Figure 31: Wells in the study area with continuous record.

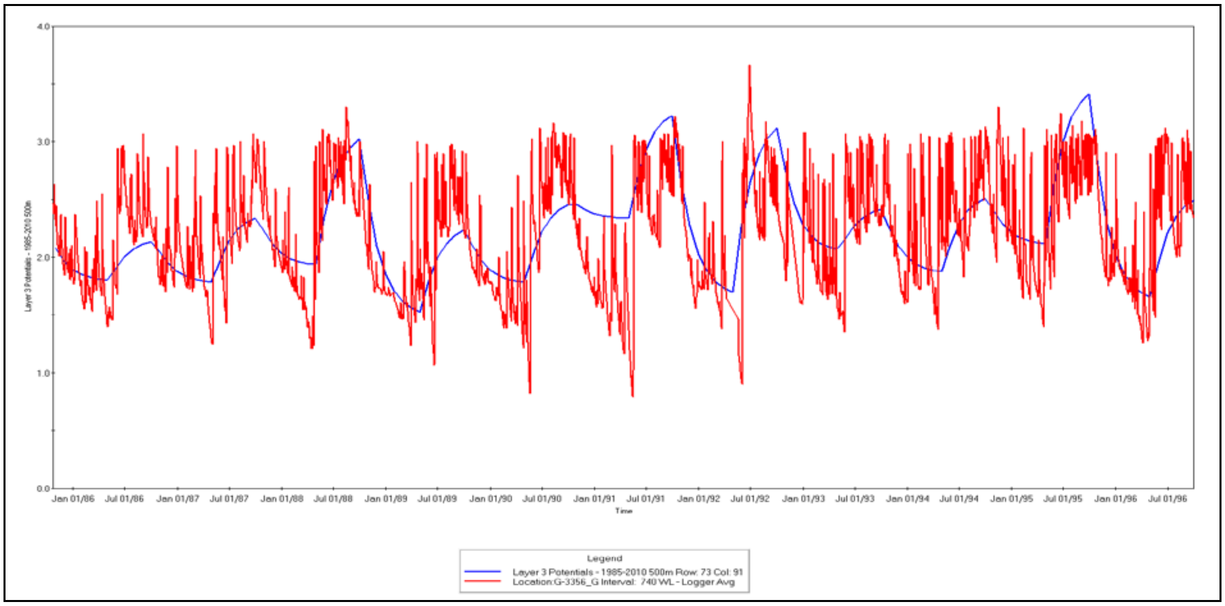

Figure 32: Simulated heads and observed daily average heads at well G-3356.

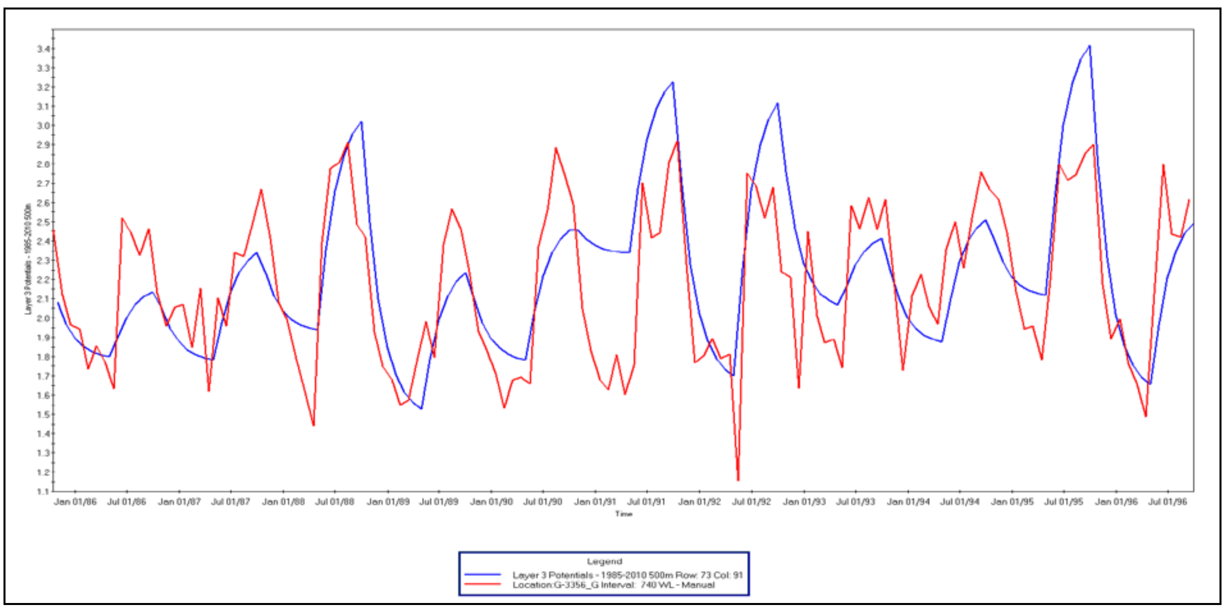

Figure 33: Simulated heads and observed monthly average heads at well G-3356.

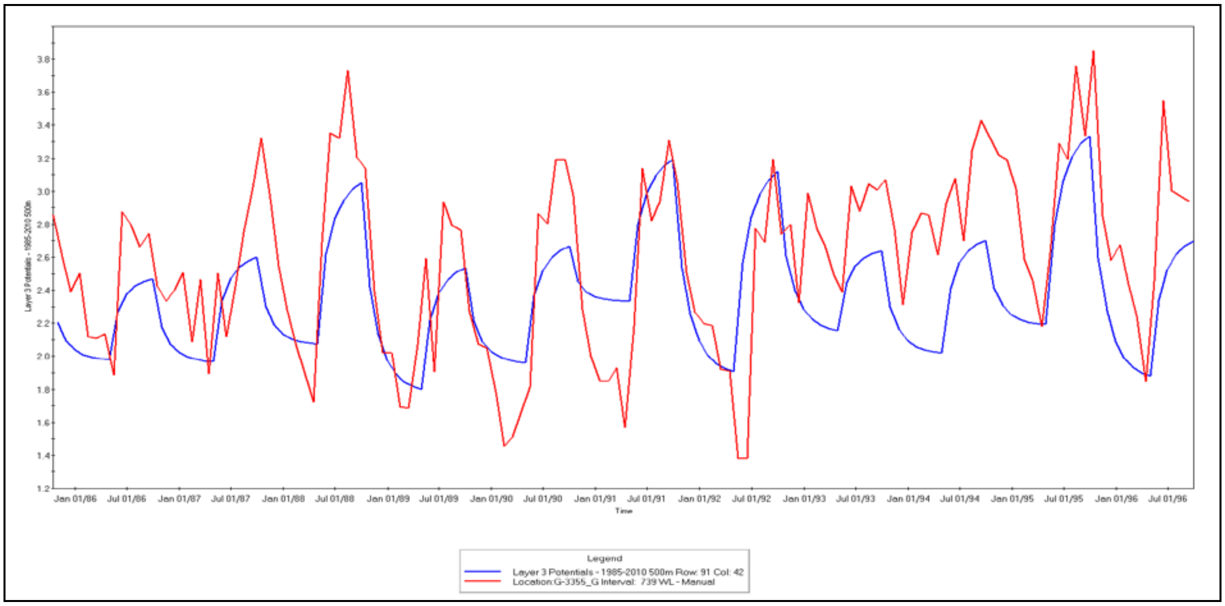

Figure 34: Simulated heads and observed monthly average heads at well G-3355.

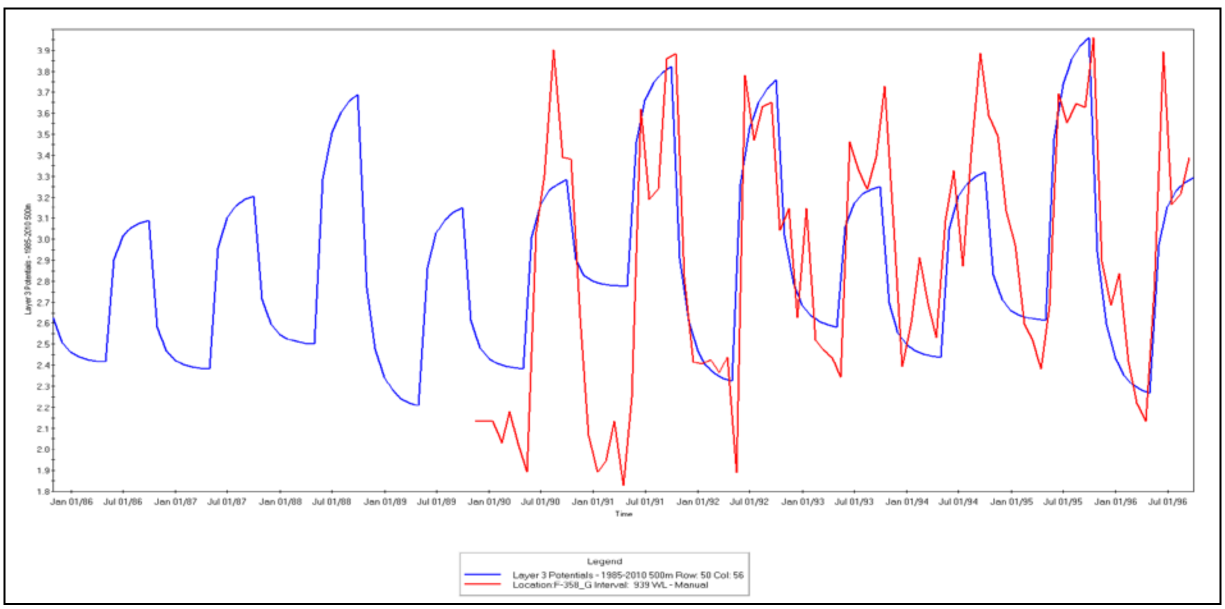

Figure 35: Simulated heads and observed monthly average heads at well F-358.

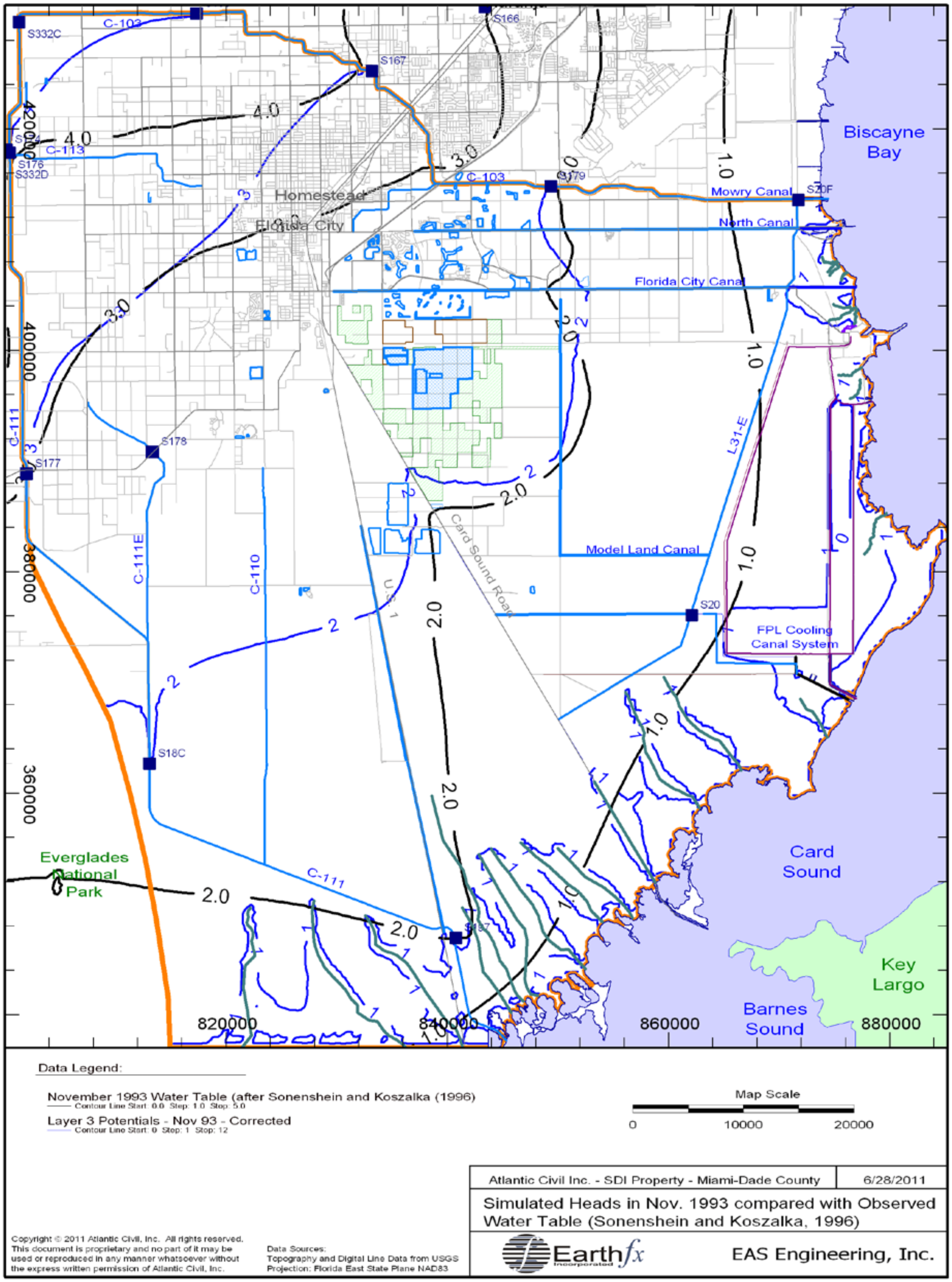

Figure 36: Simulated heads versus November 1993 water table (Sonenshein and Koszalka, 1996).

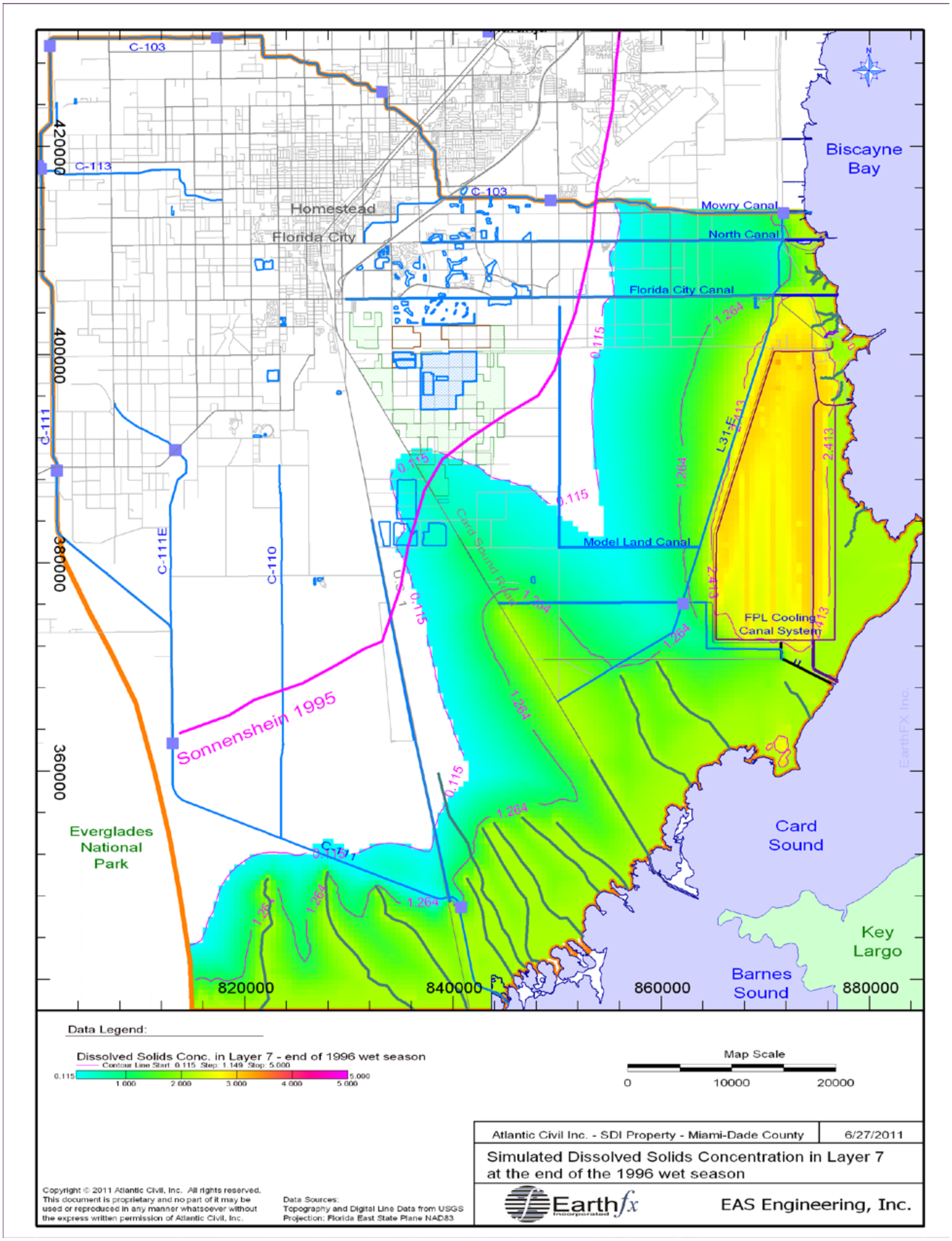

Figure 37: Dissolved solids concentration in Layer 7 at end of 1985 to 1996 simulations.

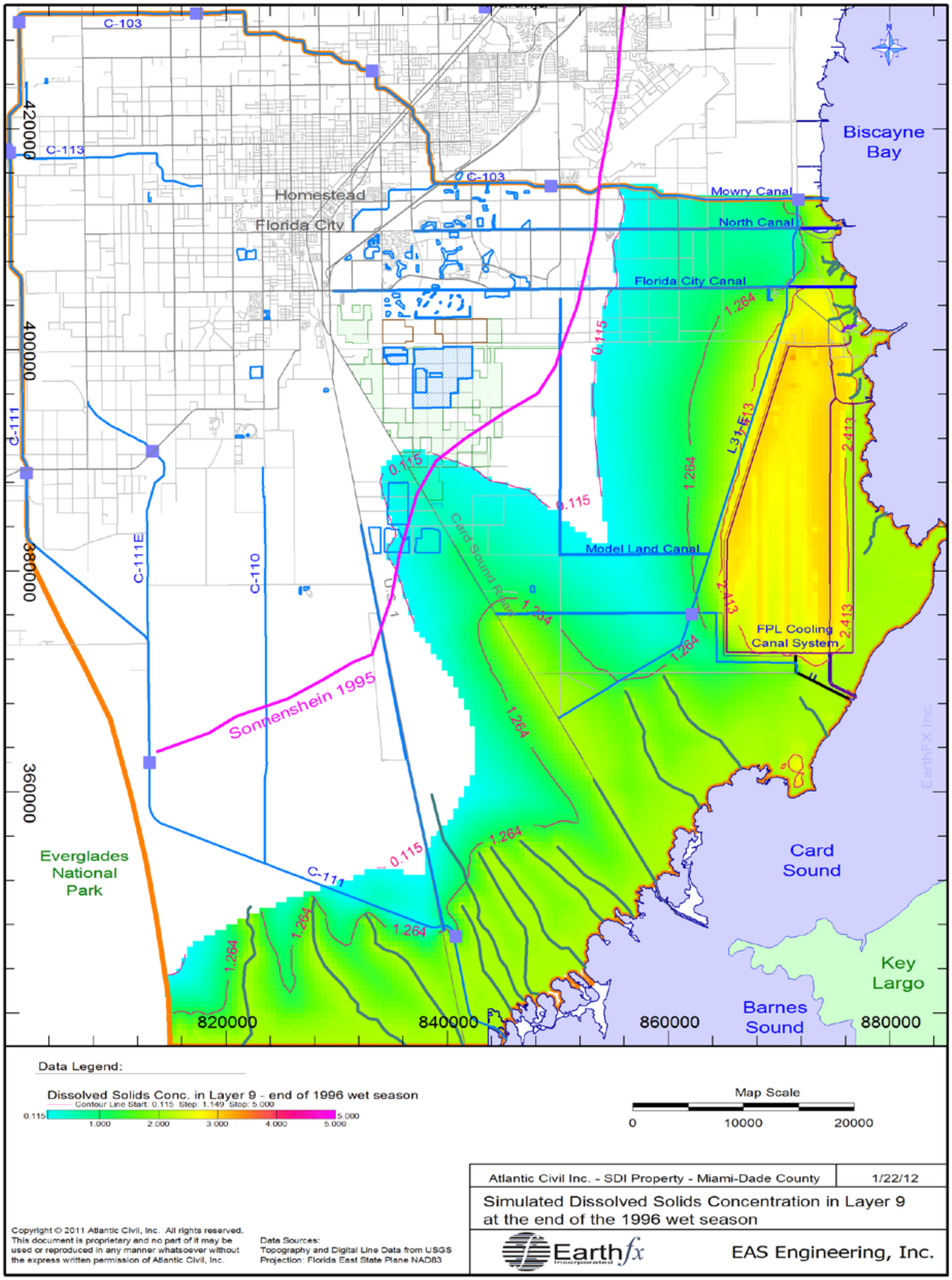

Figure 38: Dissolved solids concentration in Layer 9 at end of 1985 to 1996 simulations.

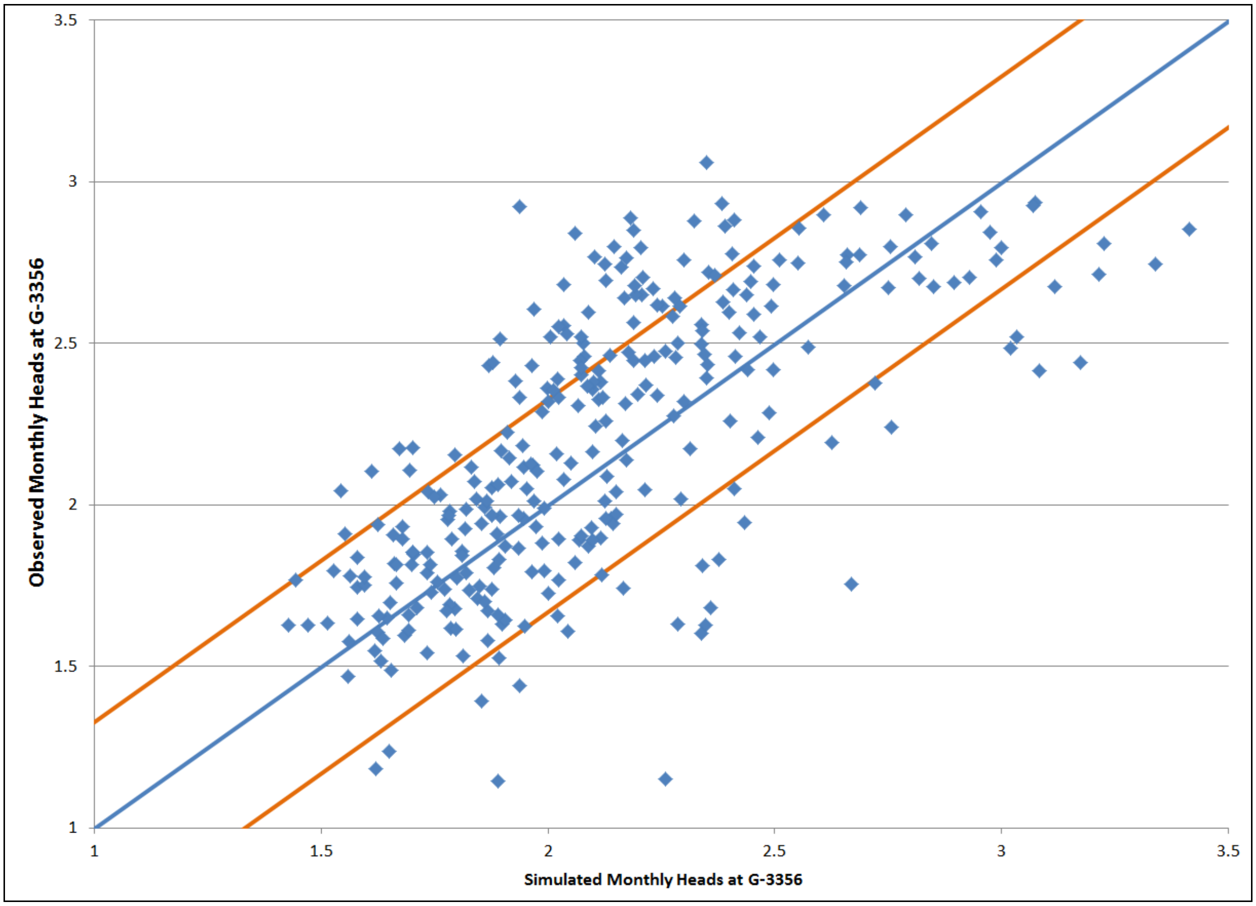

Figure 39: Scatterplot of monthly simulated and observed heads at well G-3356.

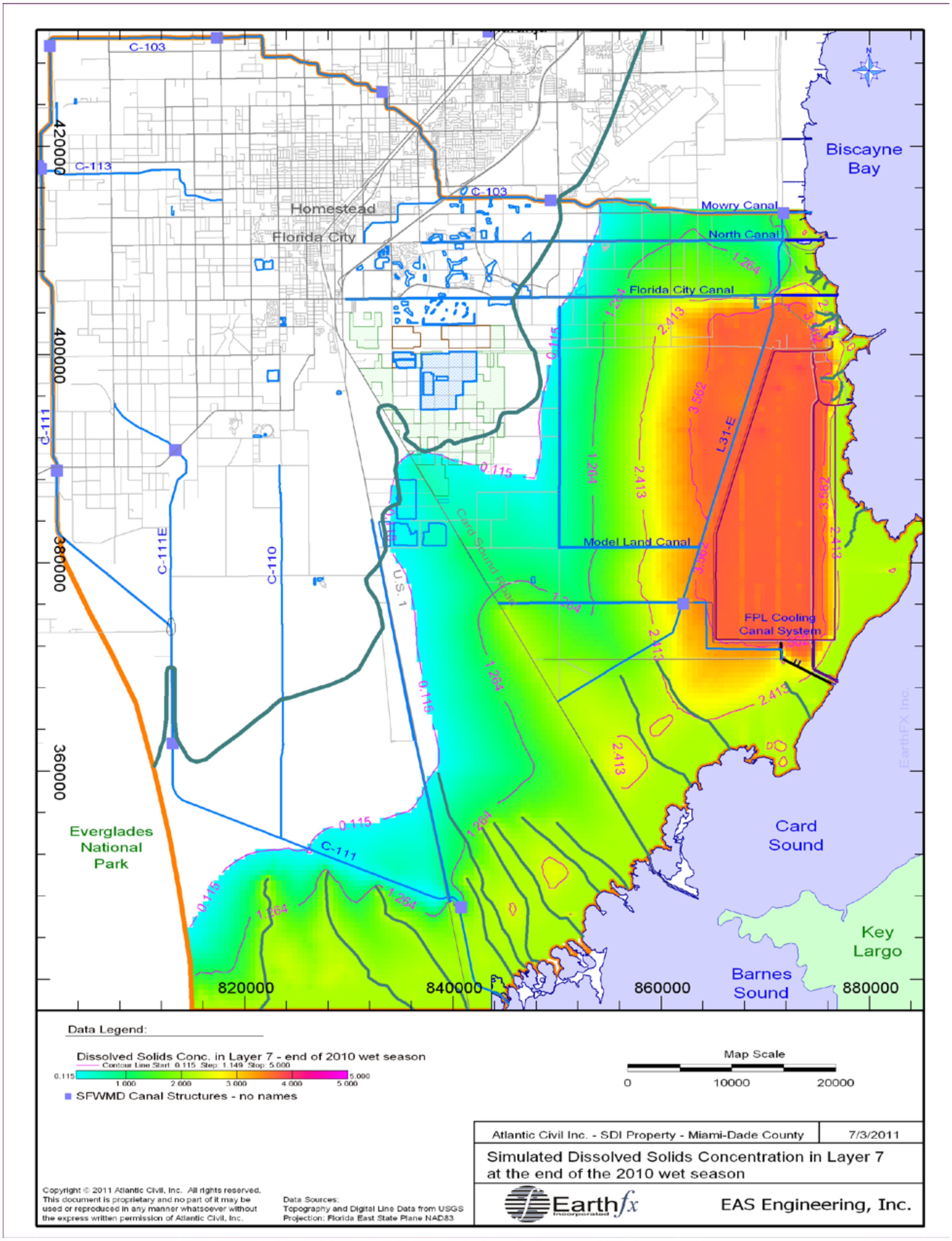

Figure 40: Dissolved solids concentration in Layer 7 at end of 1997 to 2010 simulations.

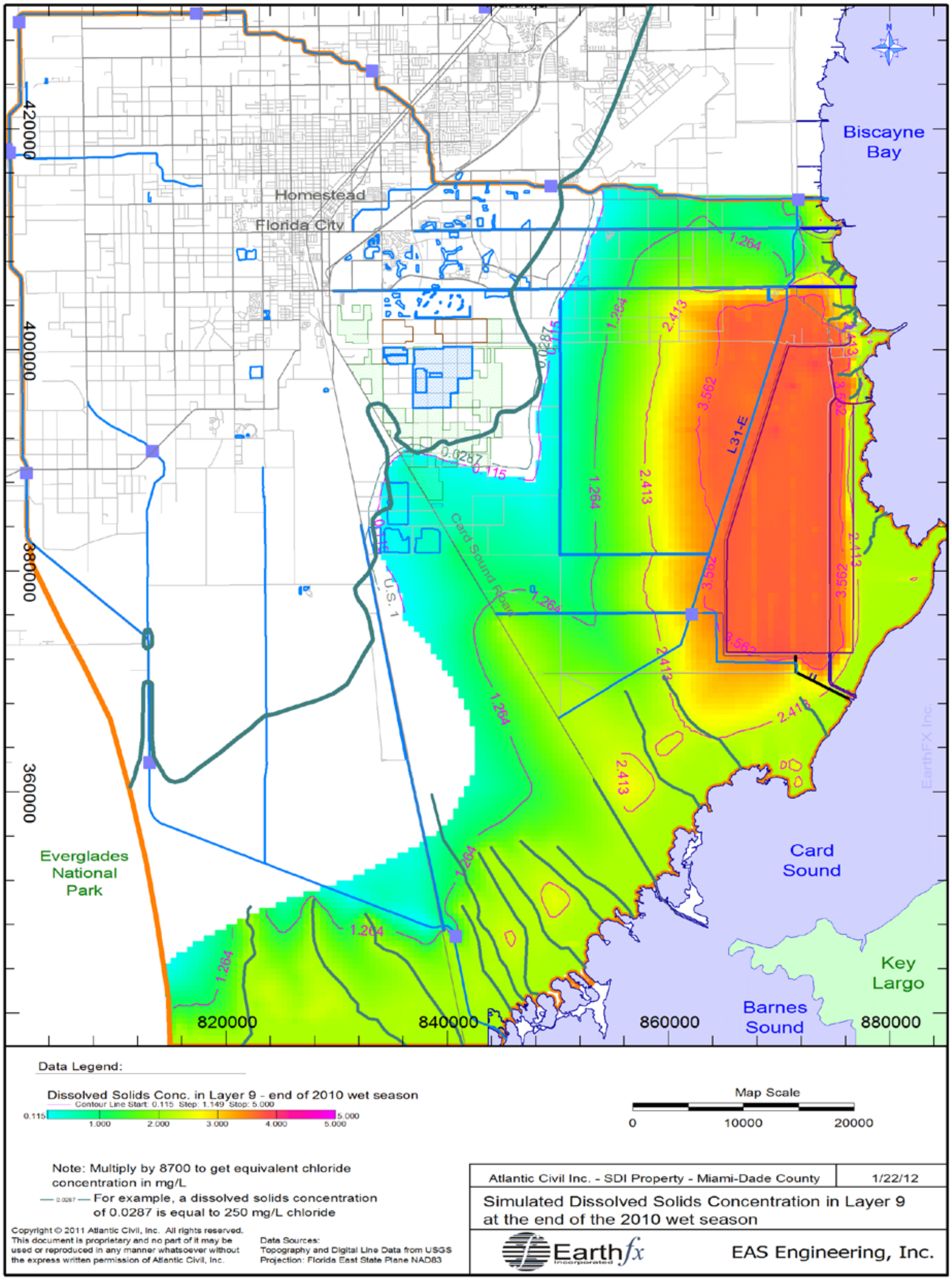

Figure 41: Dissolved solids concentration in Layer 9 at end of 1997 to 2010 simulations.

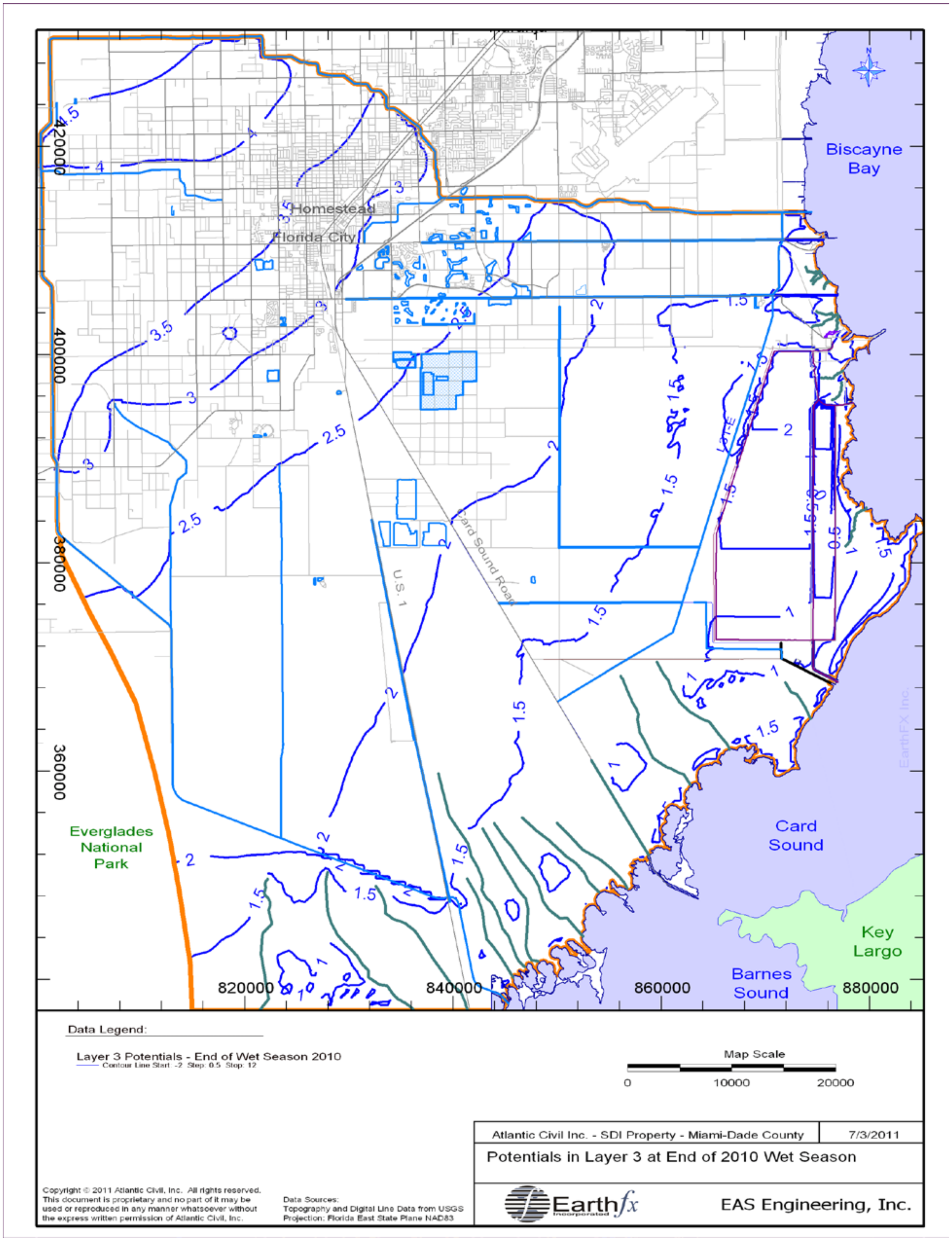

Figure 42: Simulated potentials in Layer 3 (in ft above sea level) at the end of the 2010 wet season.

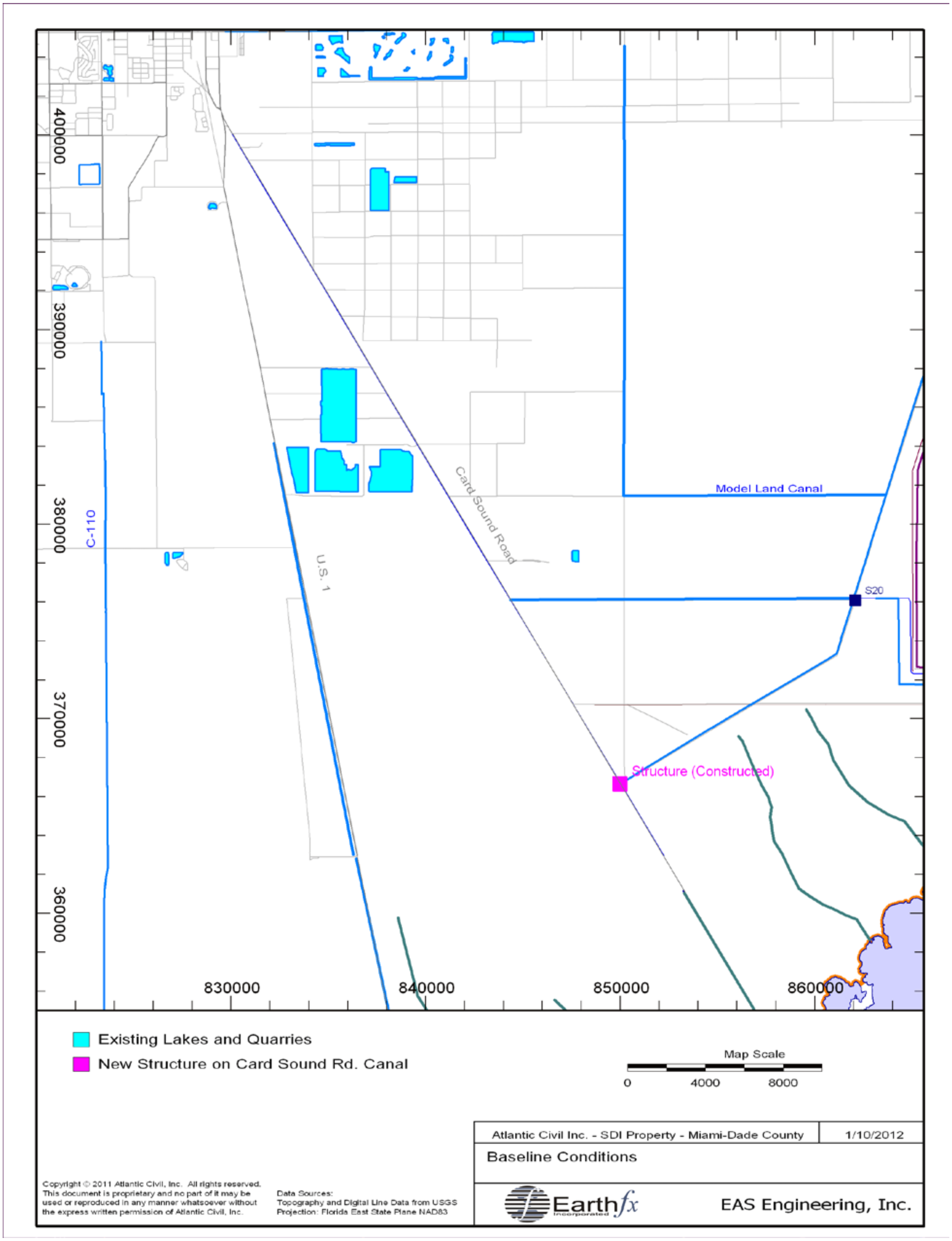

Figure 43: Baseline conditions with existing lakes and new structure on Card Sound Rd.

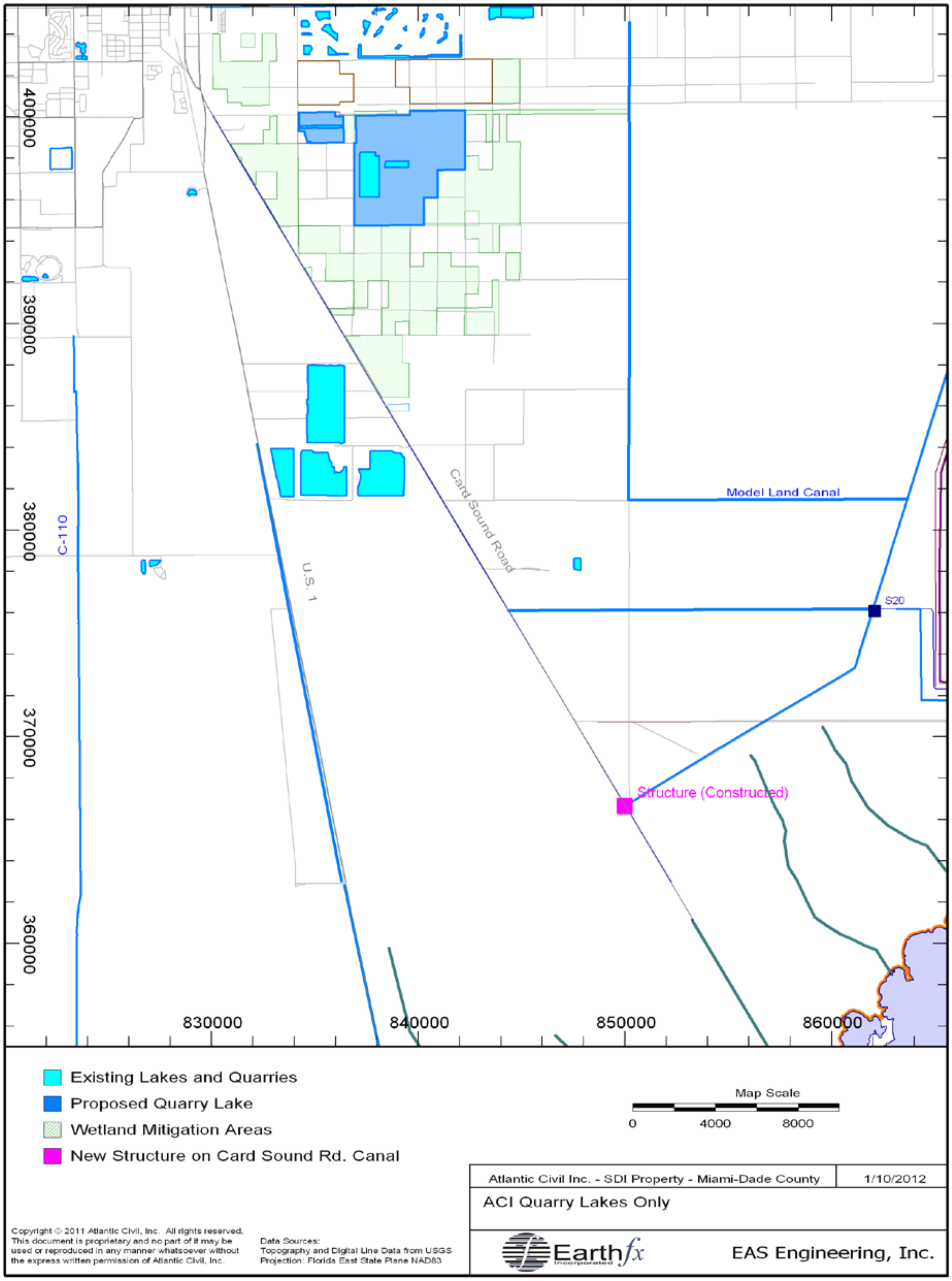

Figure 44: Conditions for "ACI Quarry Lakes Only" with proposed quarry lakes and wetland mitigation areas.

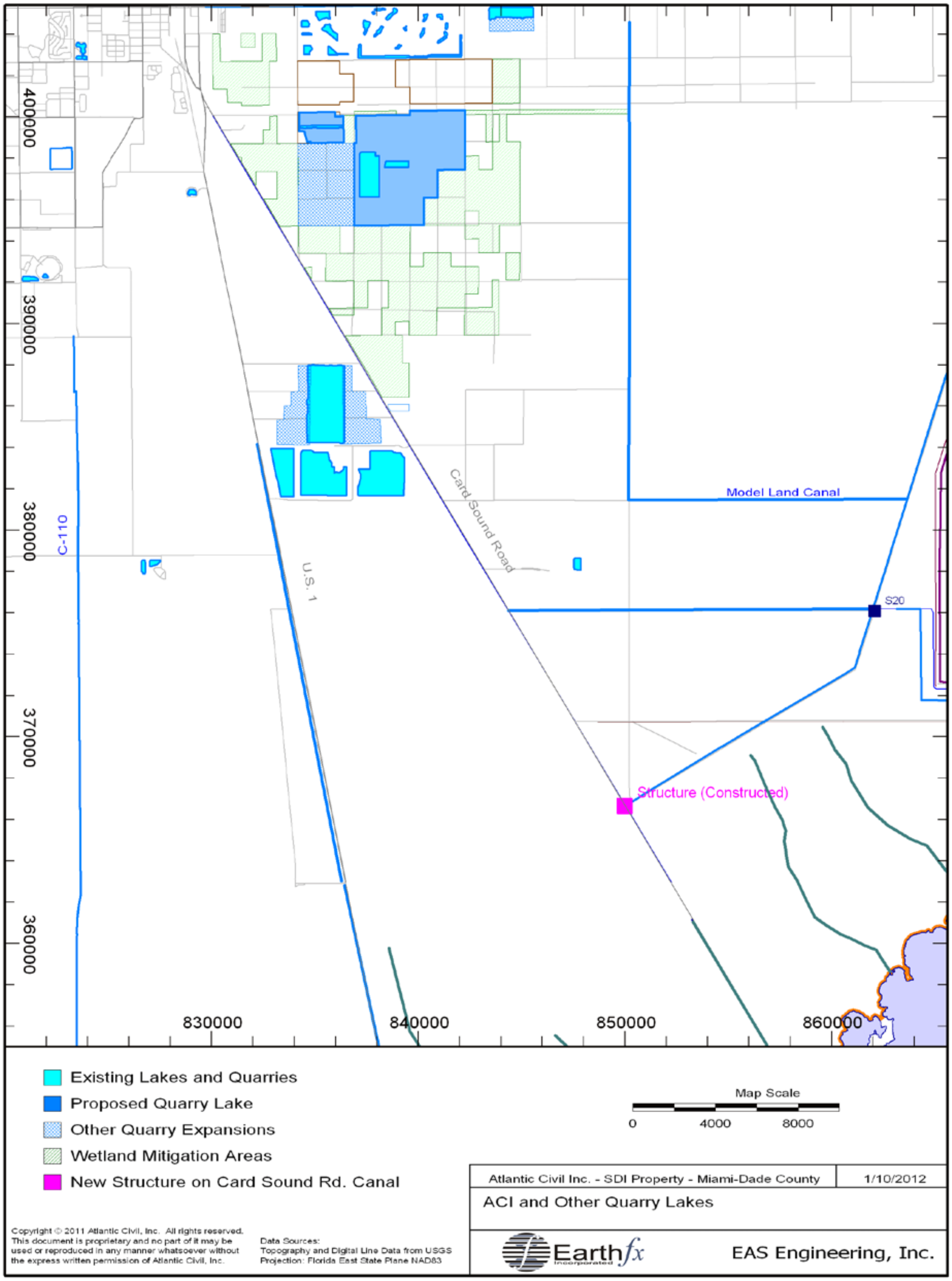

Figure 45: Conditions for "ACI and other Quarry Lakes" with proposed quarry lakes and wetland mitigation areas.

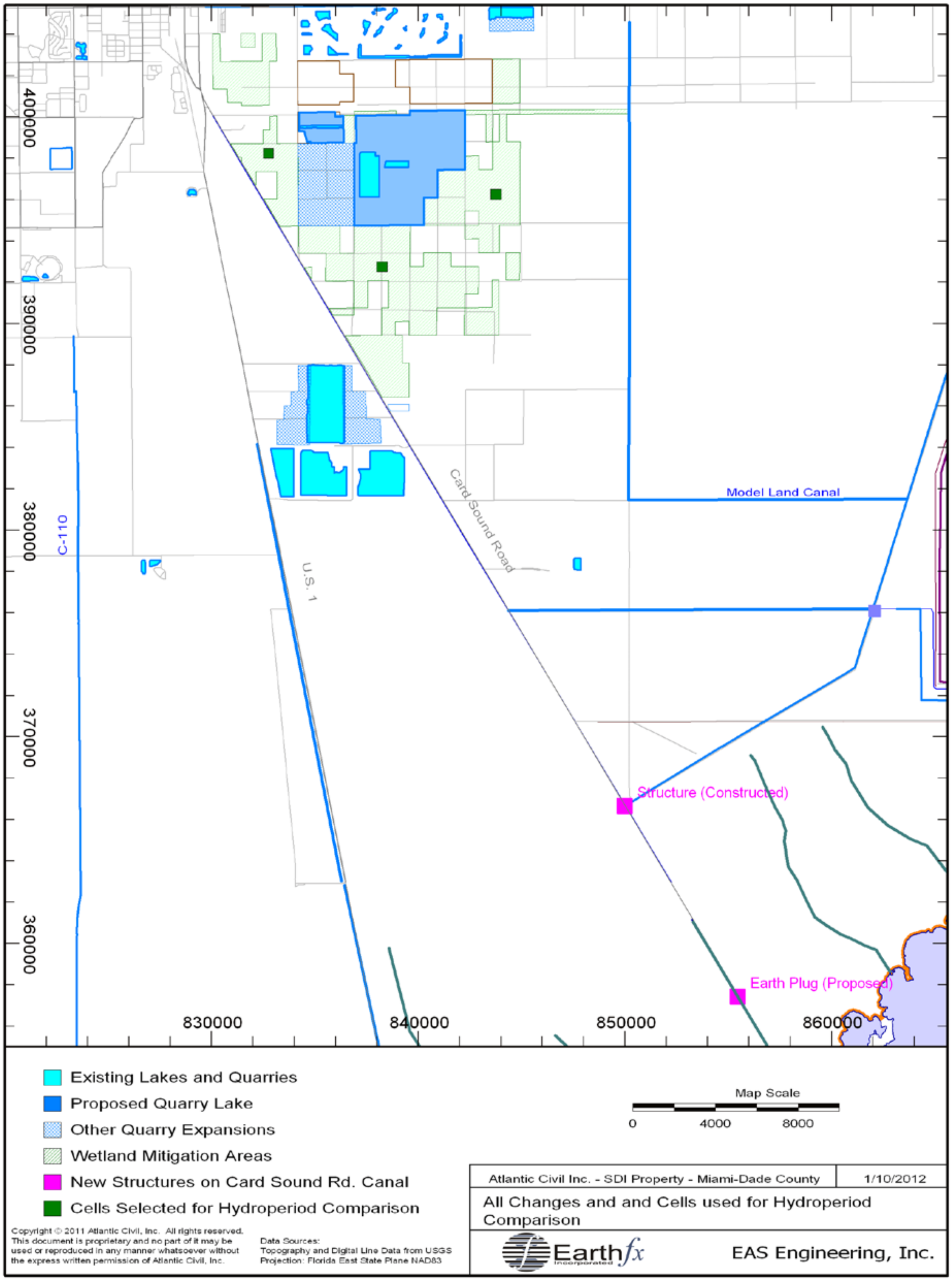

Figure 46: Proposed quarry, other quarry expansions, new structures, and cells selected for hydrograph comparison

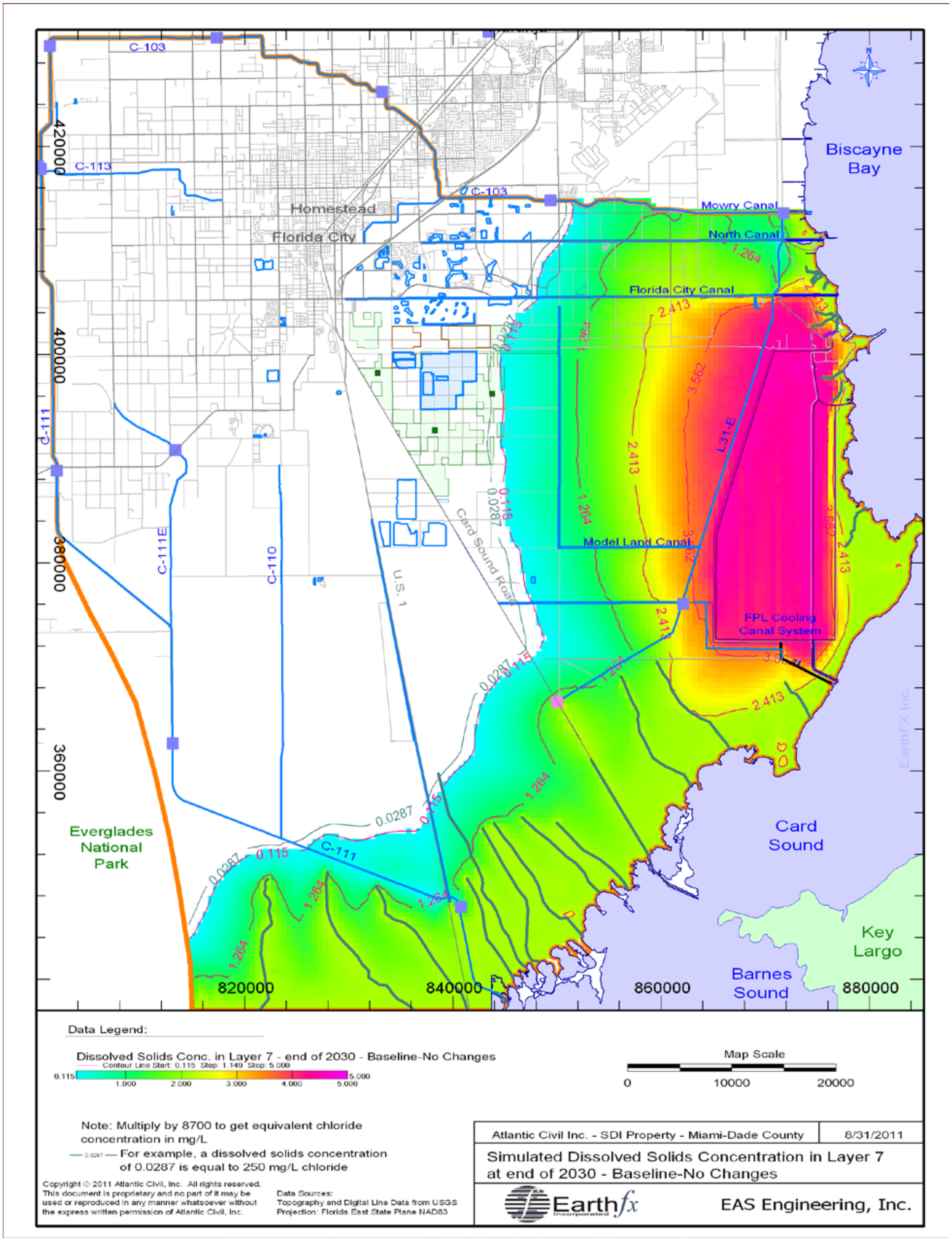

Figure 47: Simulated dissolved solids concentration in Layer 7 at end of 2011 to 2030 simulations - Baseline-No Changes scenario.

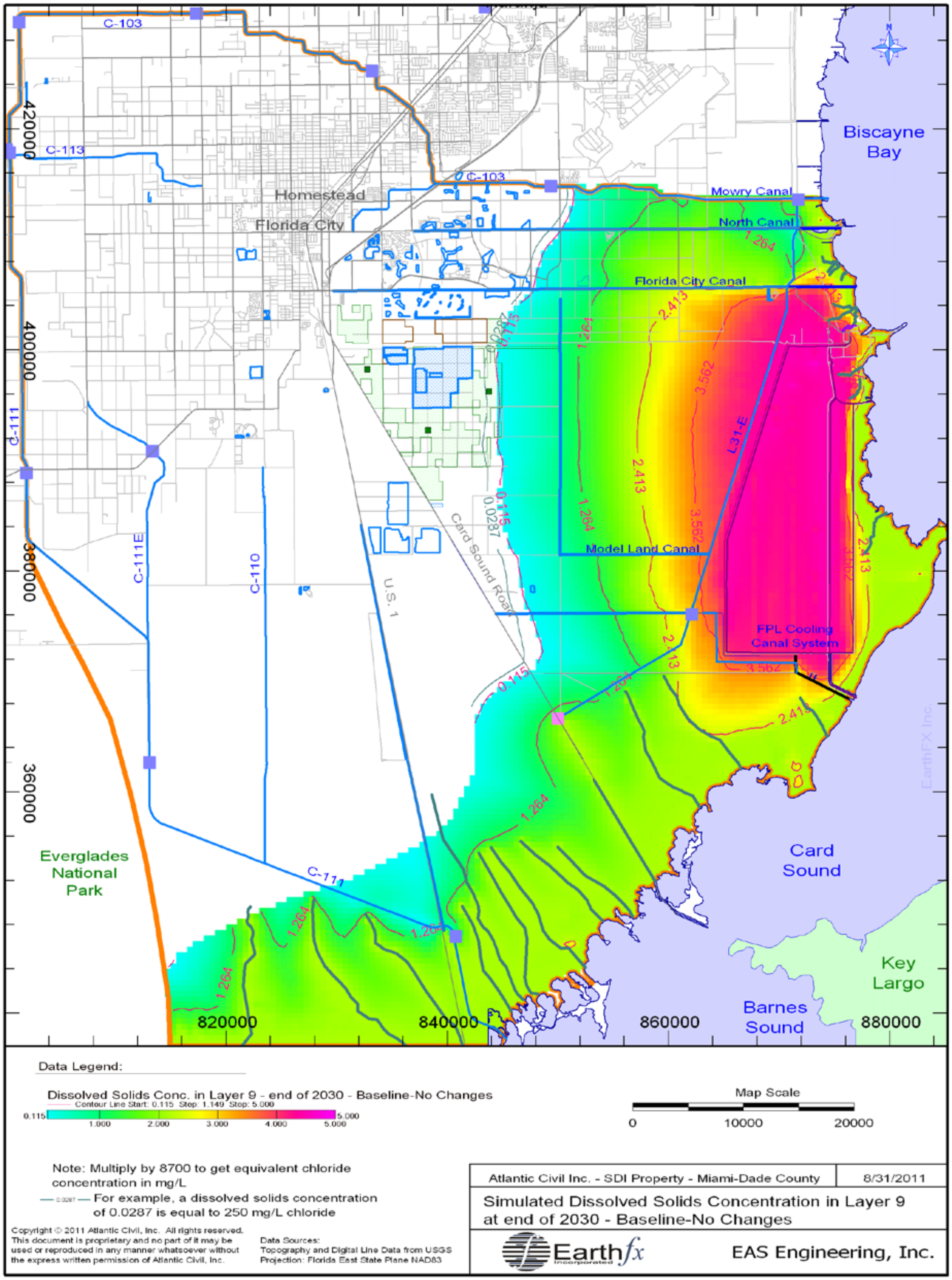

Figure 48: Simulated dissolved solids concentration in Layer 9 at end of 2011 to 2030 simulations - Baseline-No Changes scenario.

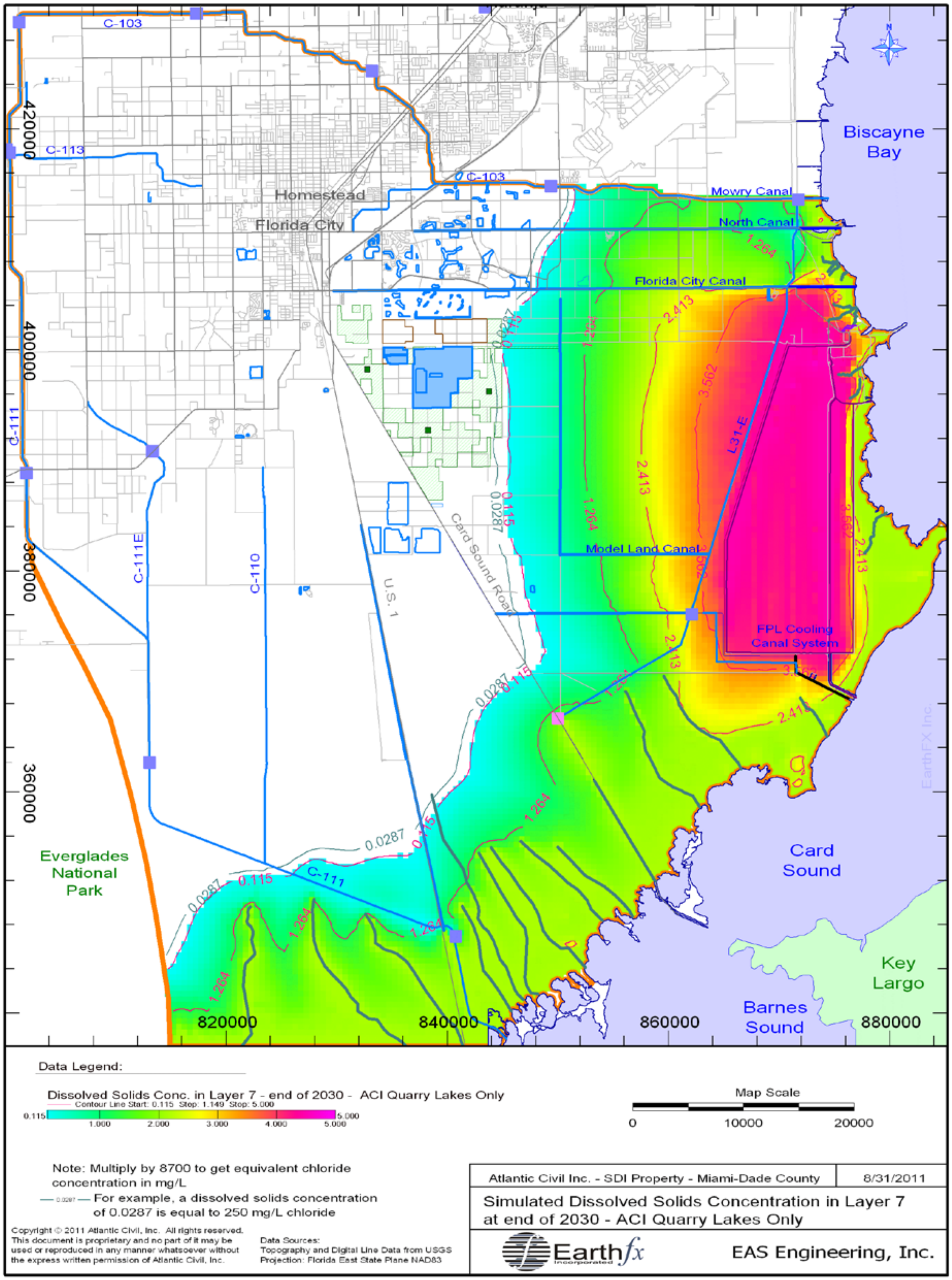

Figure 49: Simulated dissolved solids concentration in Layer 7 at end of 2011 to 2030 simulations - ACI Quarry Lakes Only scenario.

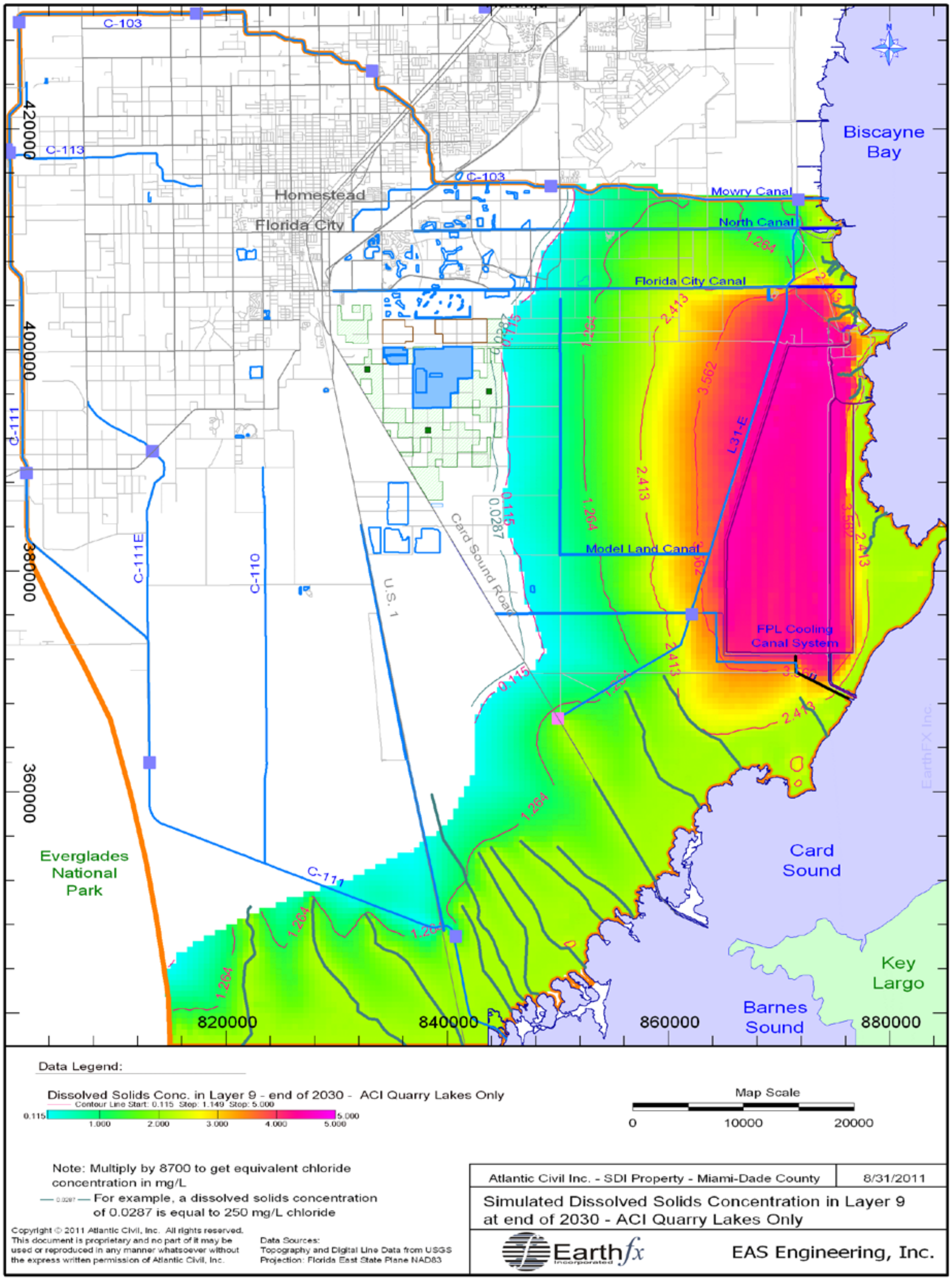

Figure 50: Simulated dissolved solids concentration in Layer 9 at end of 2011 to 2030 simulations - ACI Quarry Lakes Only scenario.

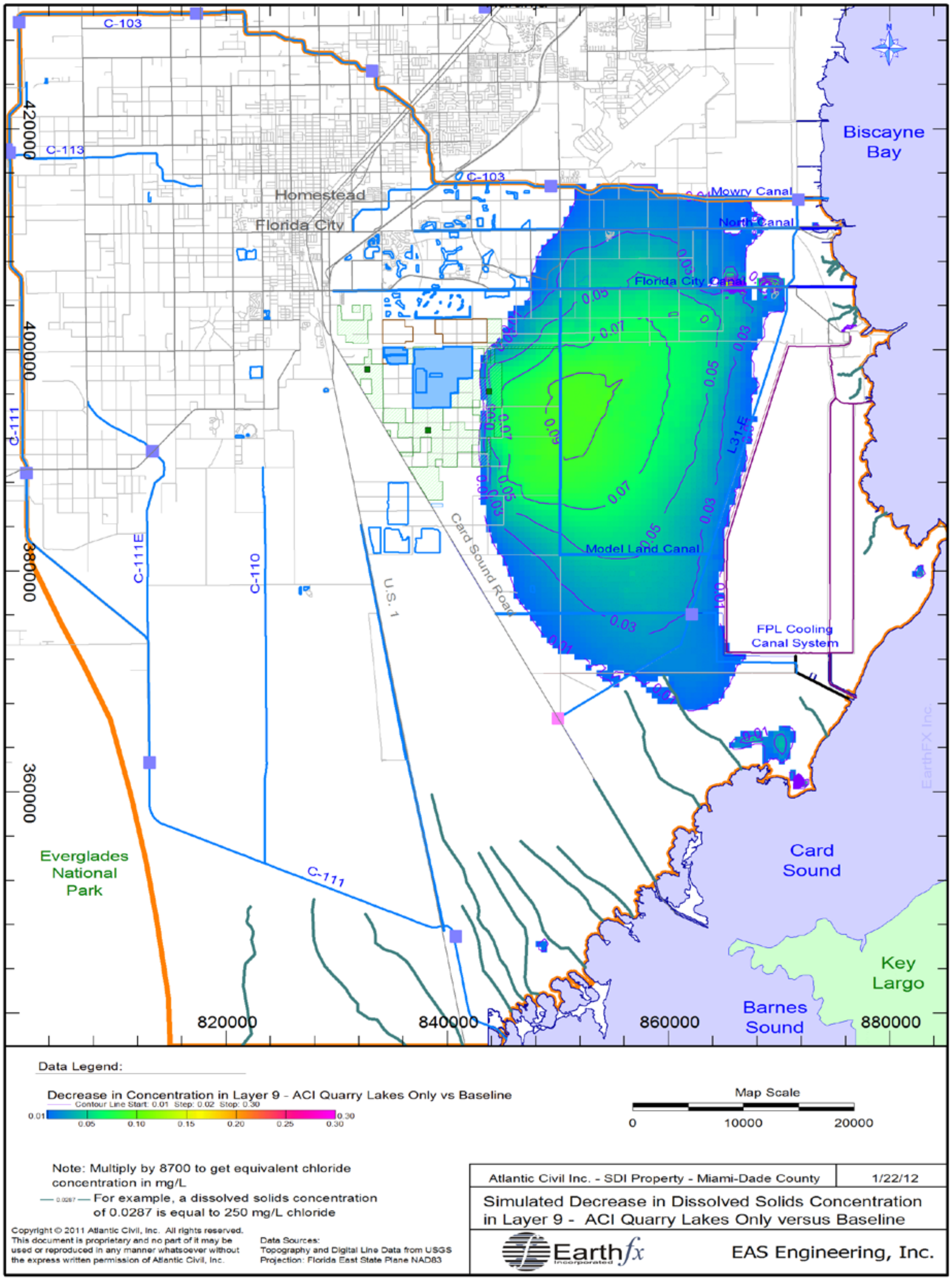

Figure 51: Simulated decrease in dissolved solids concentration in Layer 9 at end of 2011 to 2030 with the proposed quarry expansion but no other changes.

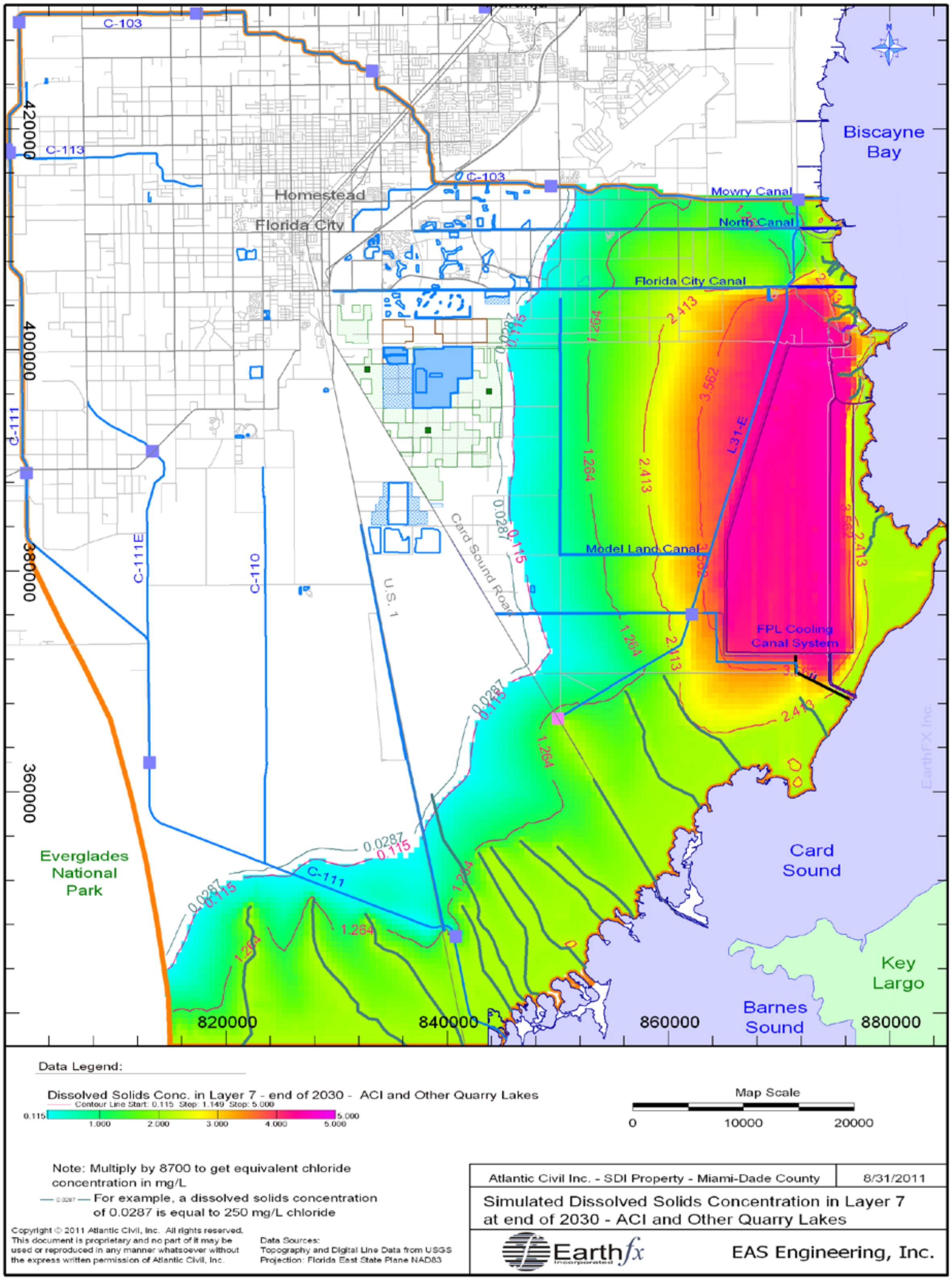

Figure 52: Simulated dissolved solids concentration in Layer 7 at end of 2011 to 2030 simulations - ACI and Other Quarry Lakes scenario.

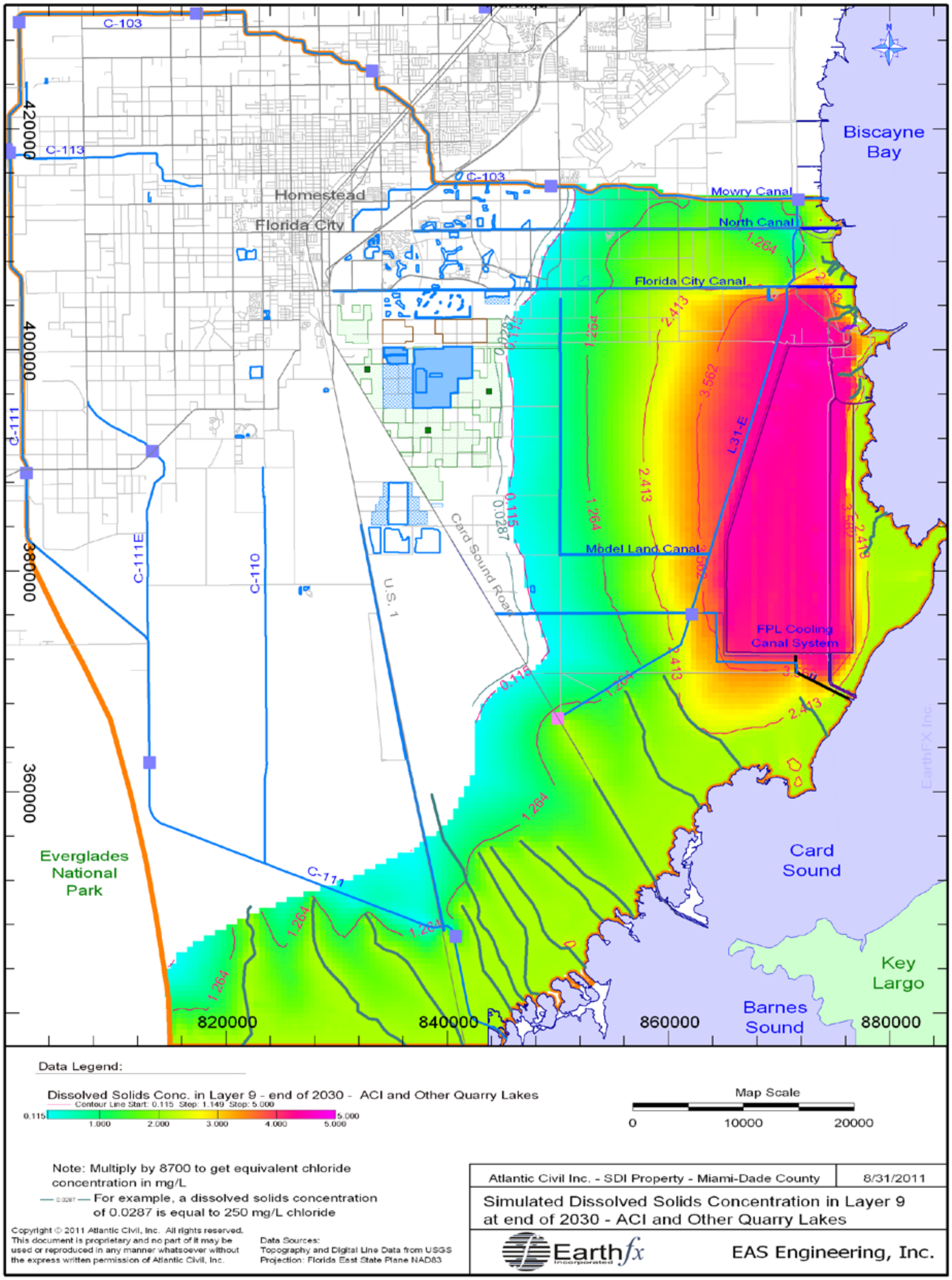

Figure 53: Simulated dissolved solids concentration in Layer 9 at end of 2011 to 2030 simulations - ACI and Other Quarry Lakes scenario.

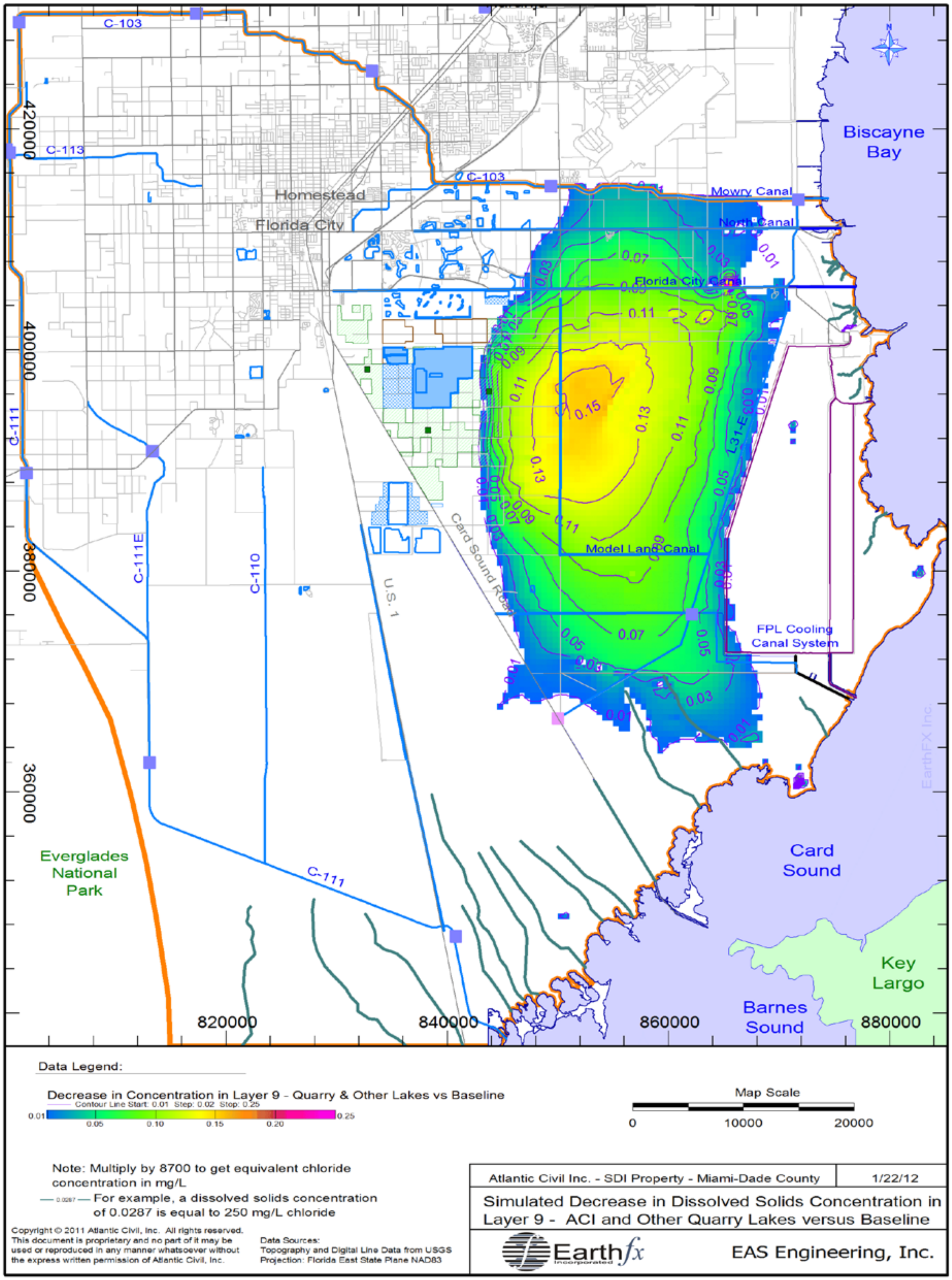

Figure 54: Simulated decrease in dissolved solids concentration in Layer 9 at end of 2011 to 2030 with all other lakes and the proposed quarry expansion.

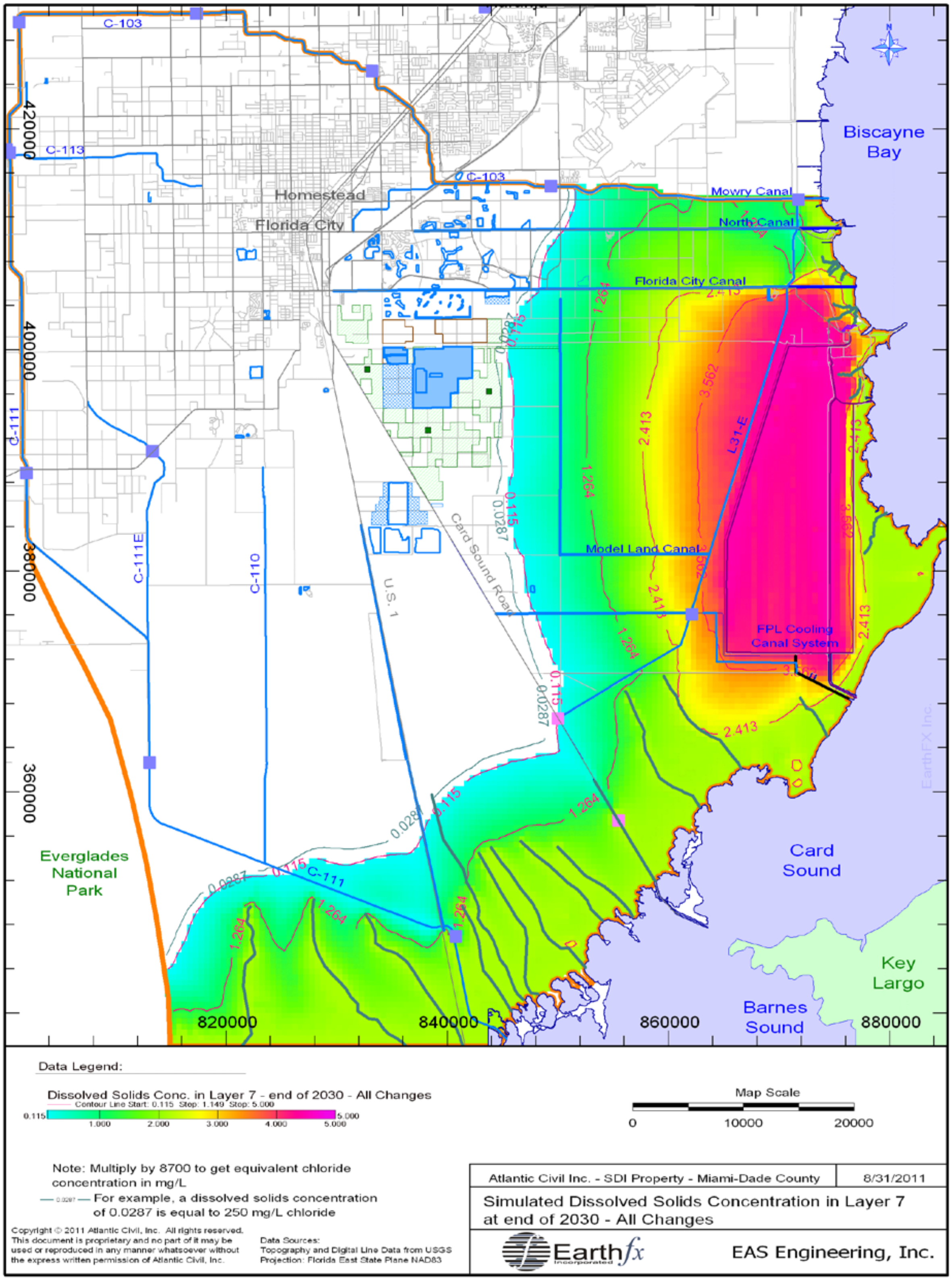

Figure 55: Simulated dissolved solids concentration in Layer 7 at end of 2011 to 2030 simulations - All Changes scenario.

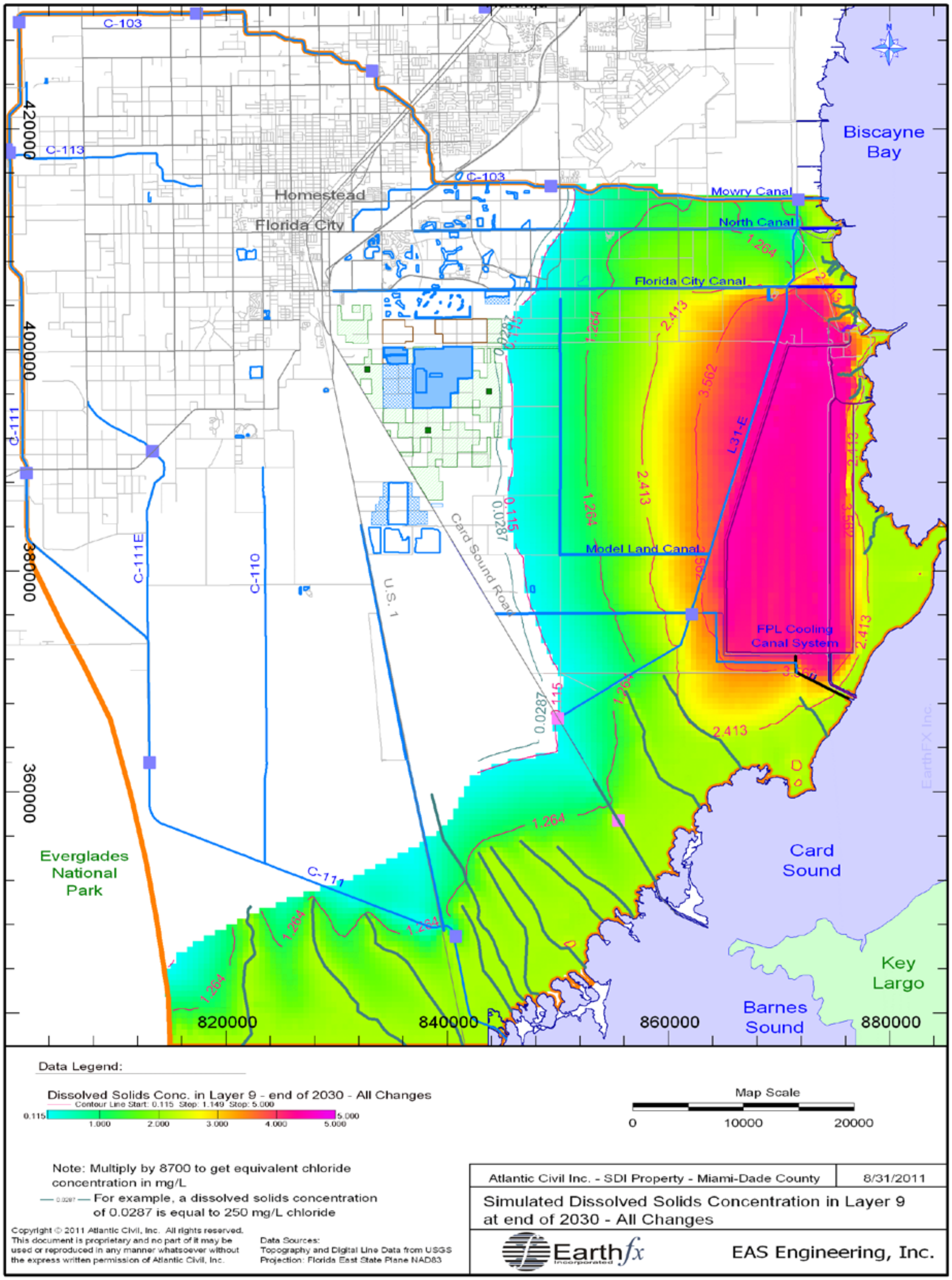

Figure 56: Simulated dissolved solids concentration in Layer 9 at end of 2011 to 2030 simulations - All Changes scenario.

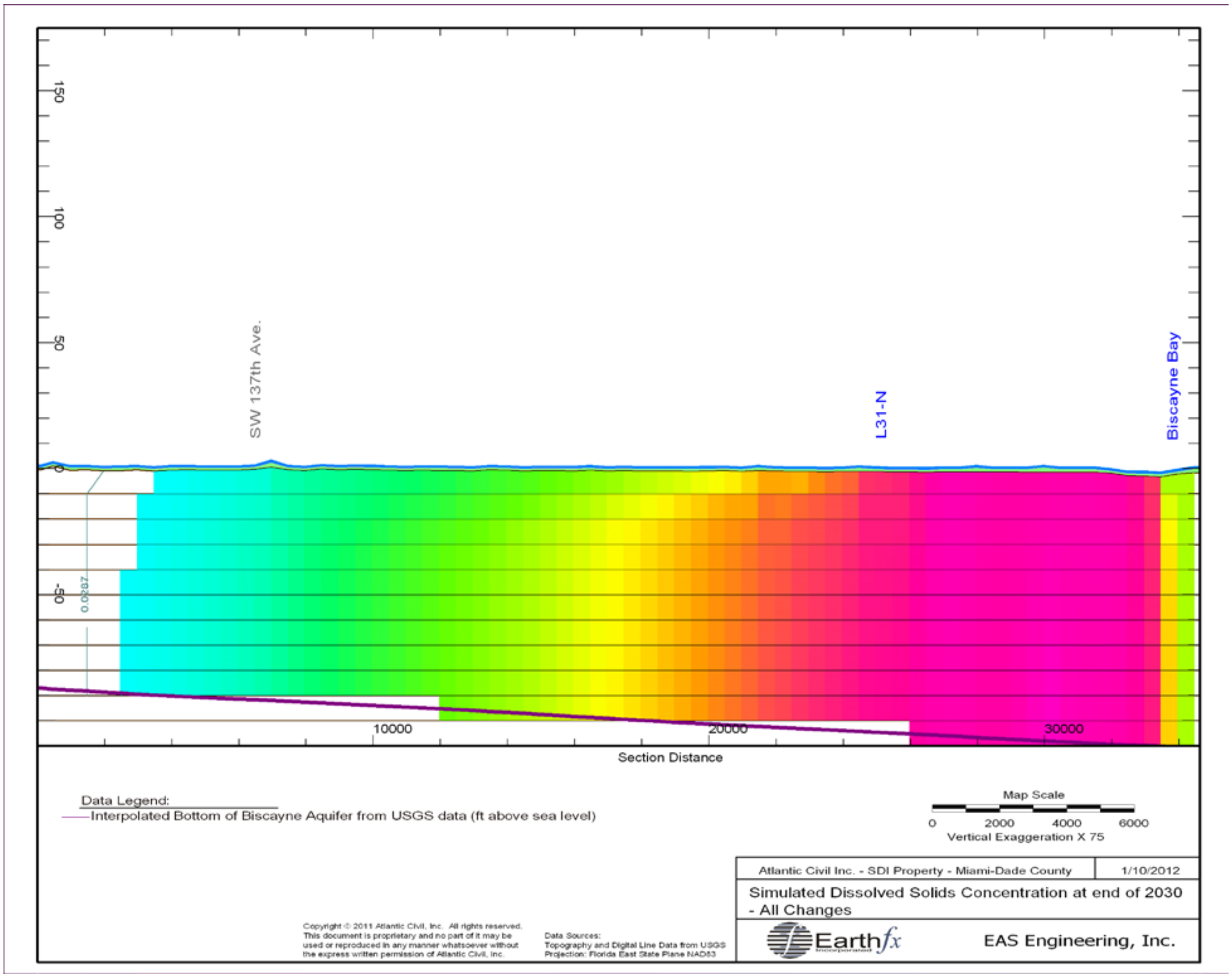

Figure 57: West-east section showing simulated dissolved solids concentration at end of 2011 to 2030 simulations - All Changes scenario

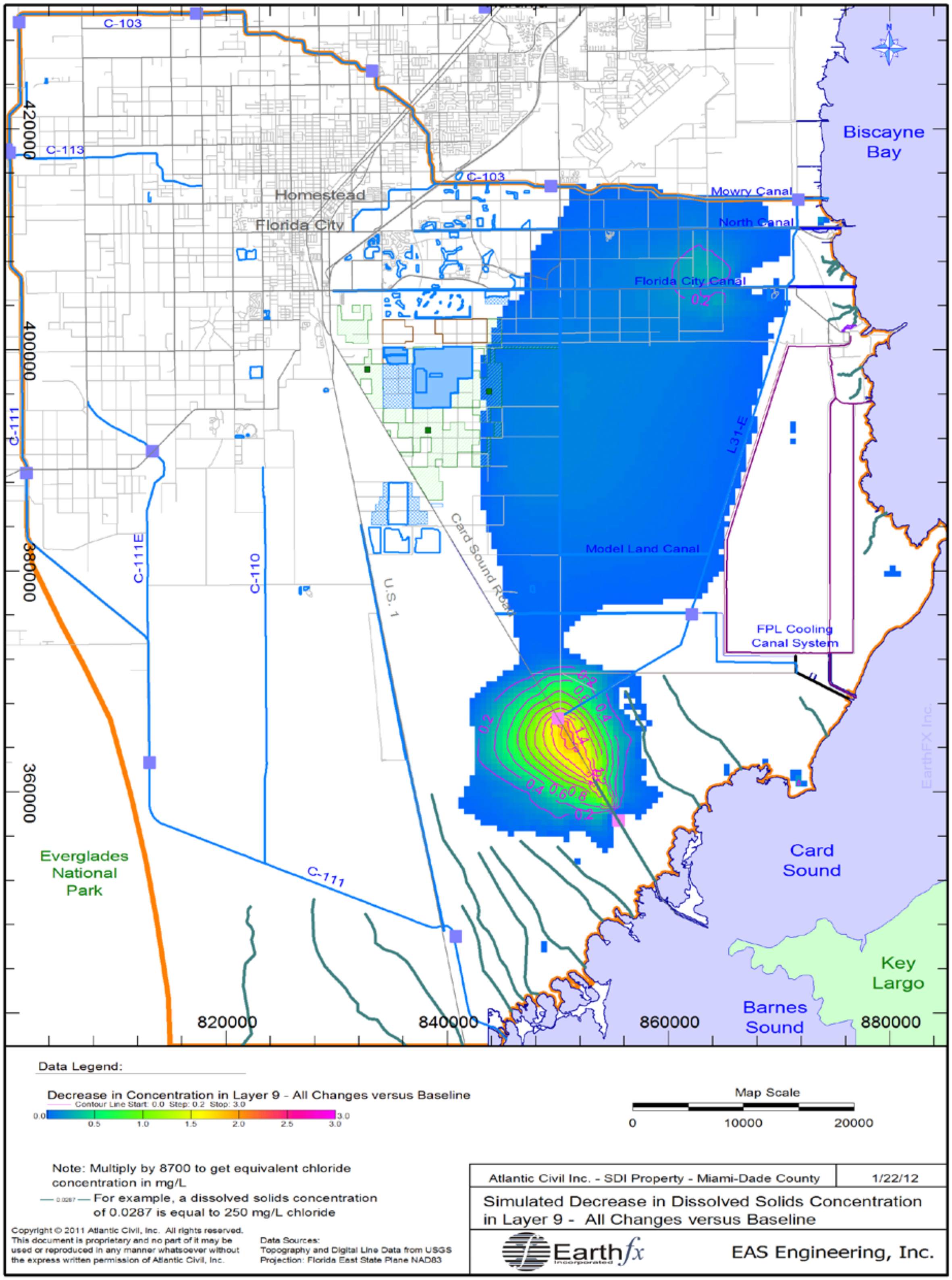

Figure 58: Simulated decrease in dissolved solids concentration in Layer 9 at end of 2011 to 2030 with all changes and the proposed quarry expansion.

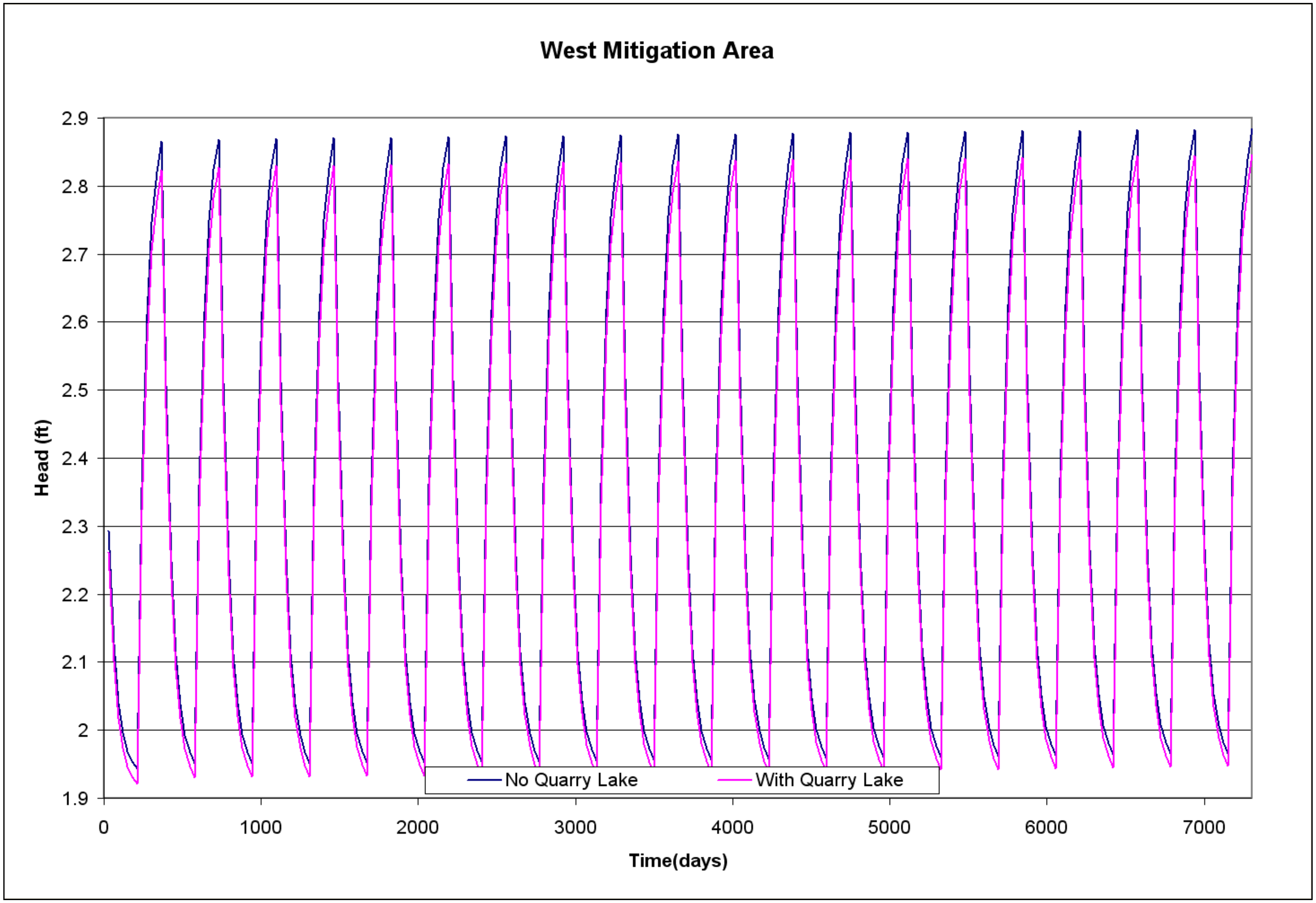

Figure 59: Hydrographs of heads in Layer 1, a surrogate for wetland stage, in the west wetland mitigation area.

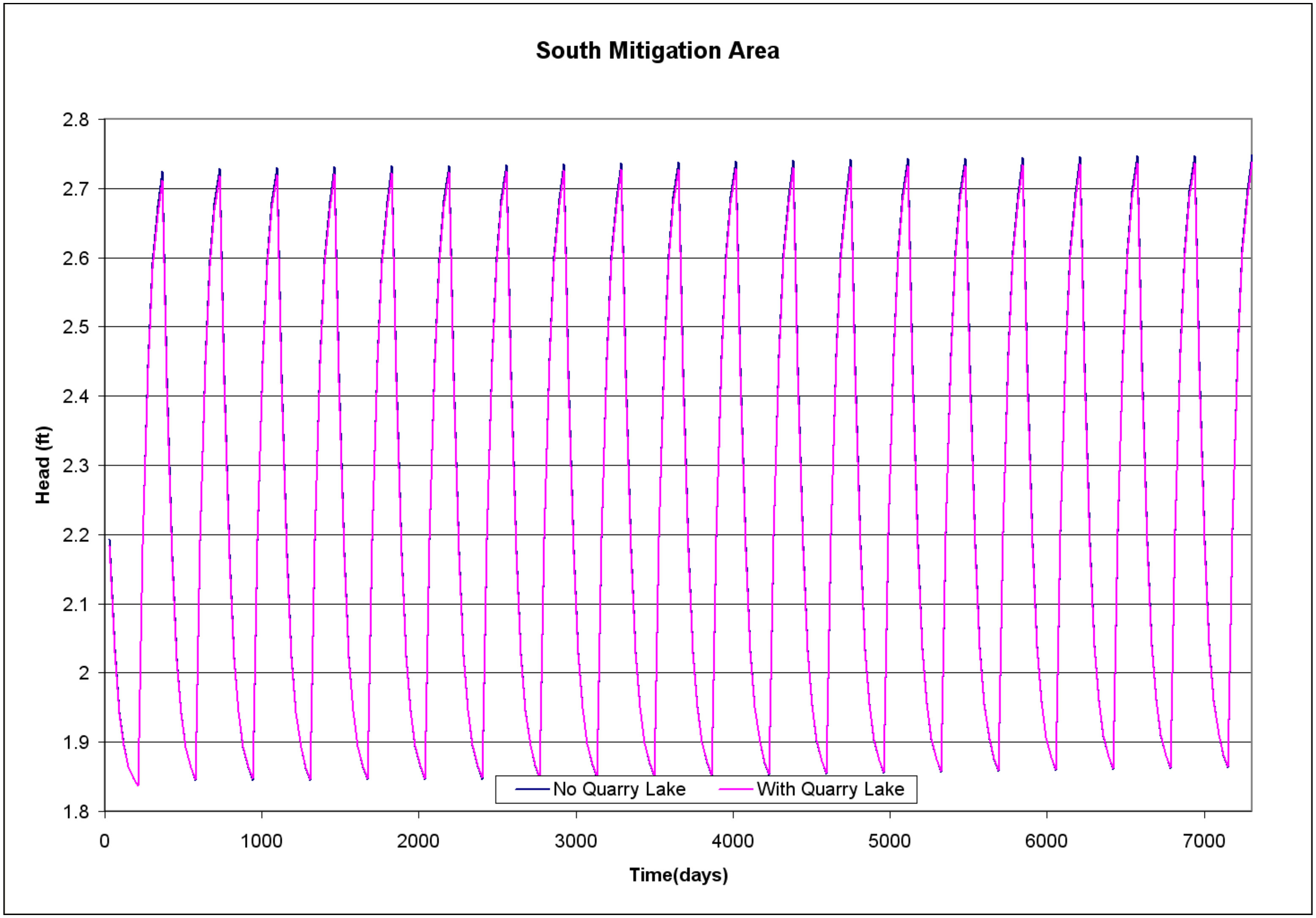

Figure 60: Hydrographs of heads in Layer 1, a surrogate for wetland stage, in the south wetland mitigation area.

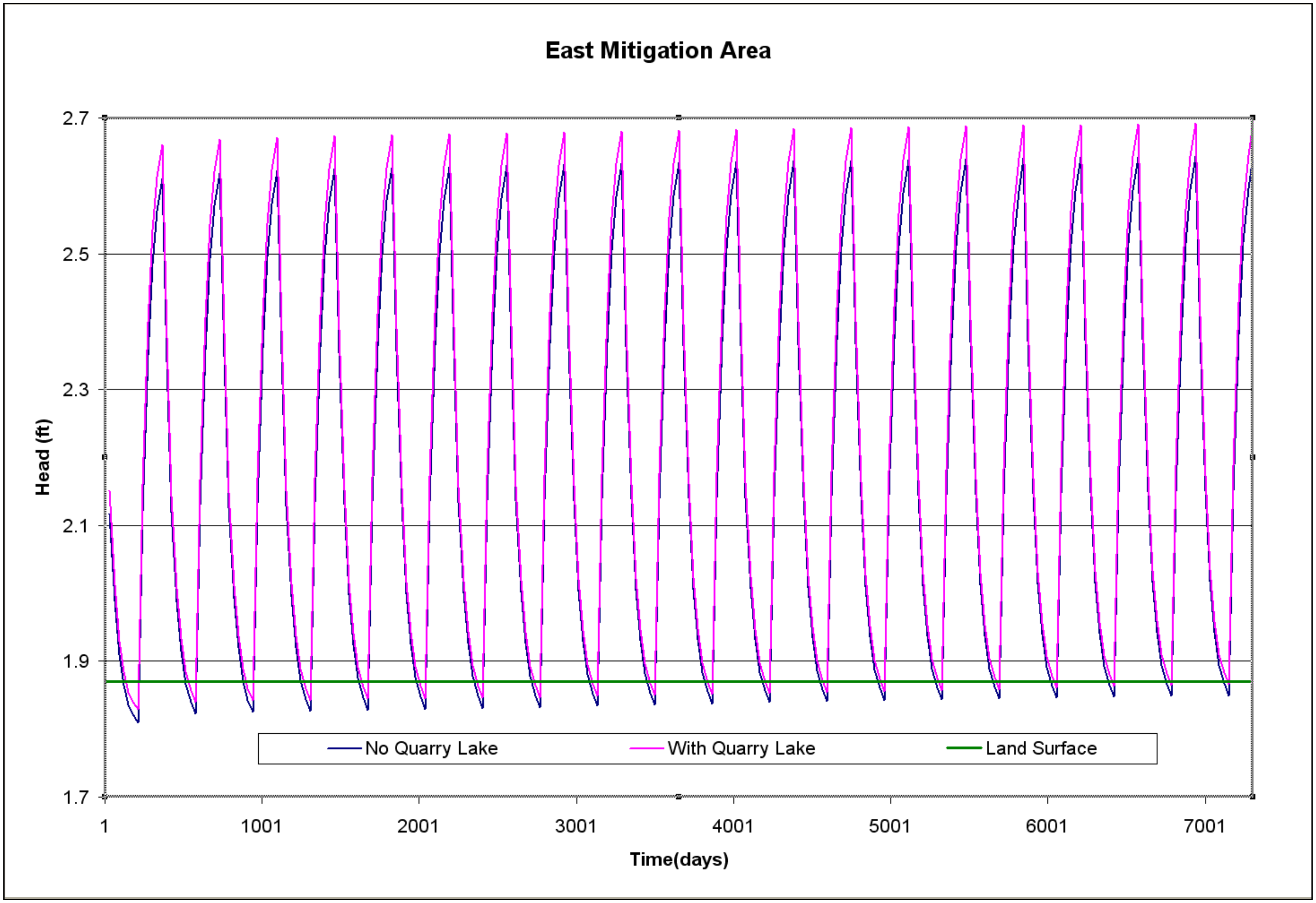

Figure 61: Hydrographs of heads in Layer 1, a surrogate for wetland stage, in the east wetland mitigation area (for "All Changes" scenarios).

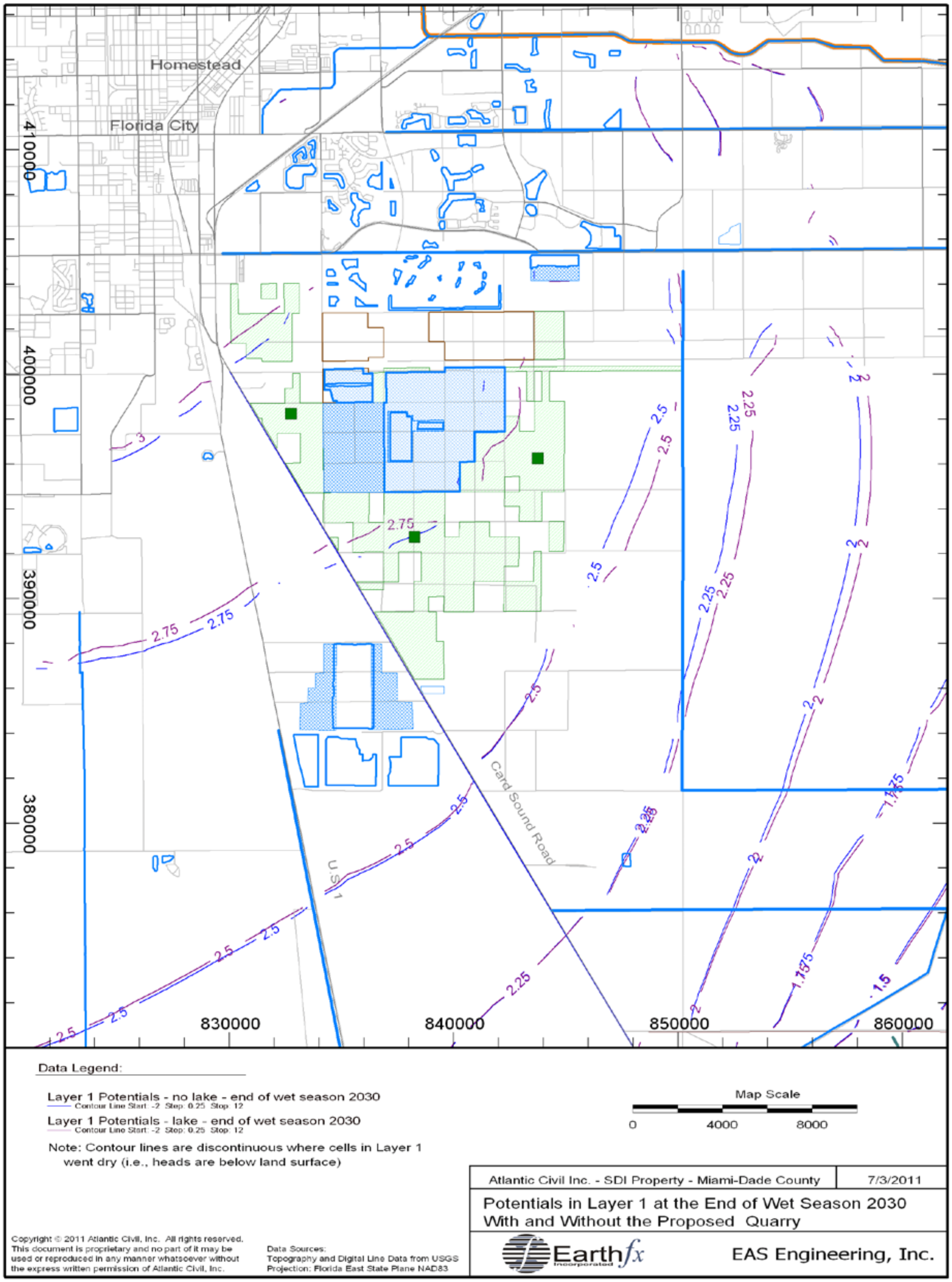

Figure 62: Potentials in Layer 1 with and without the quarry at the end of the 2030 wet season.

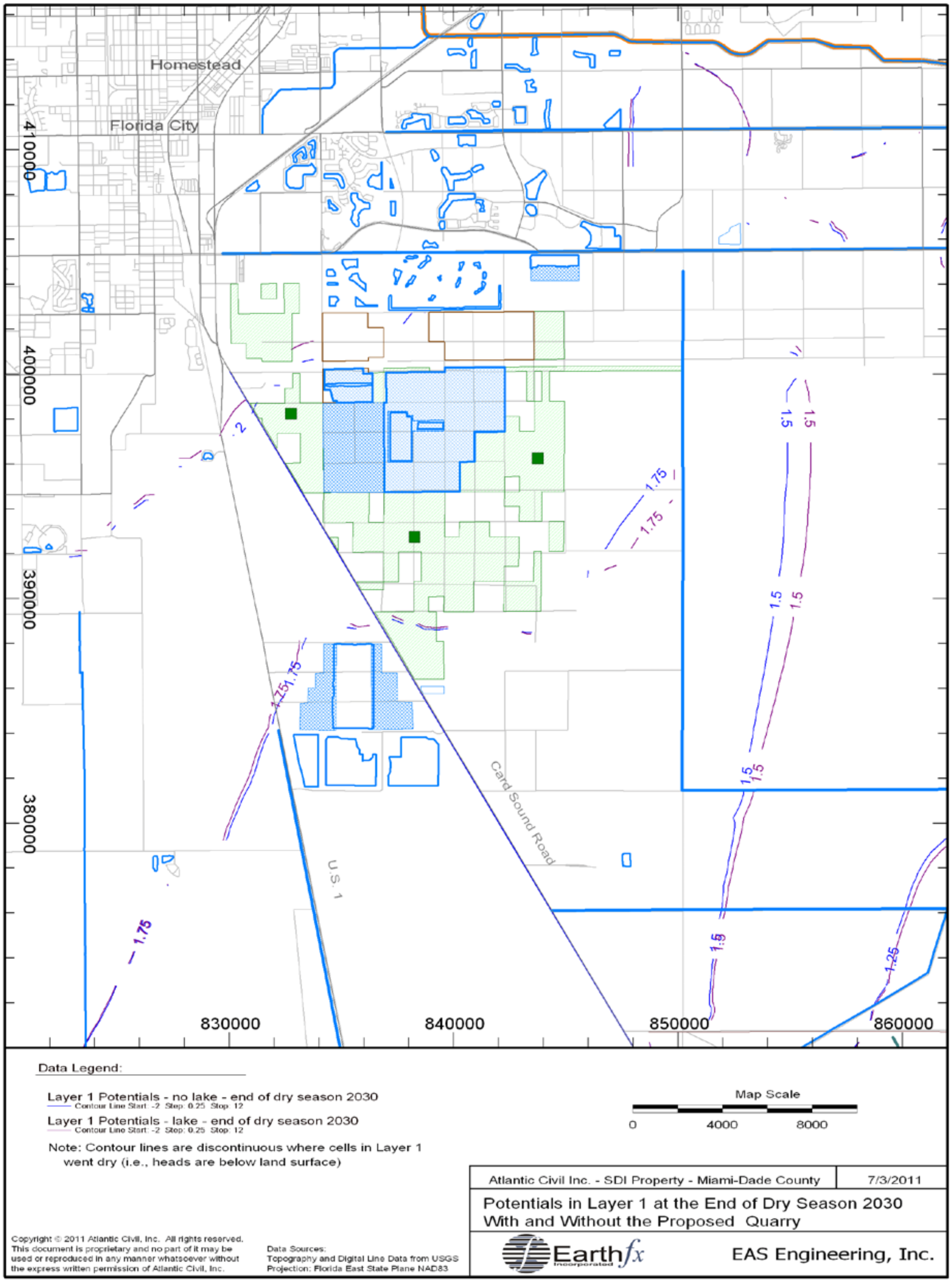

Figure 63: Potentials in Layer 1 with and without the quarry at the end of the 2030 dry season.

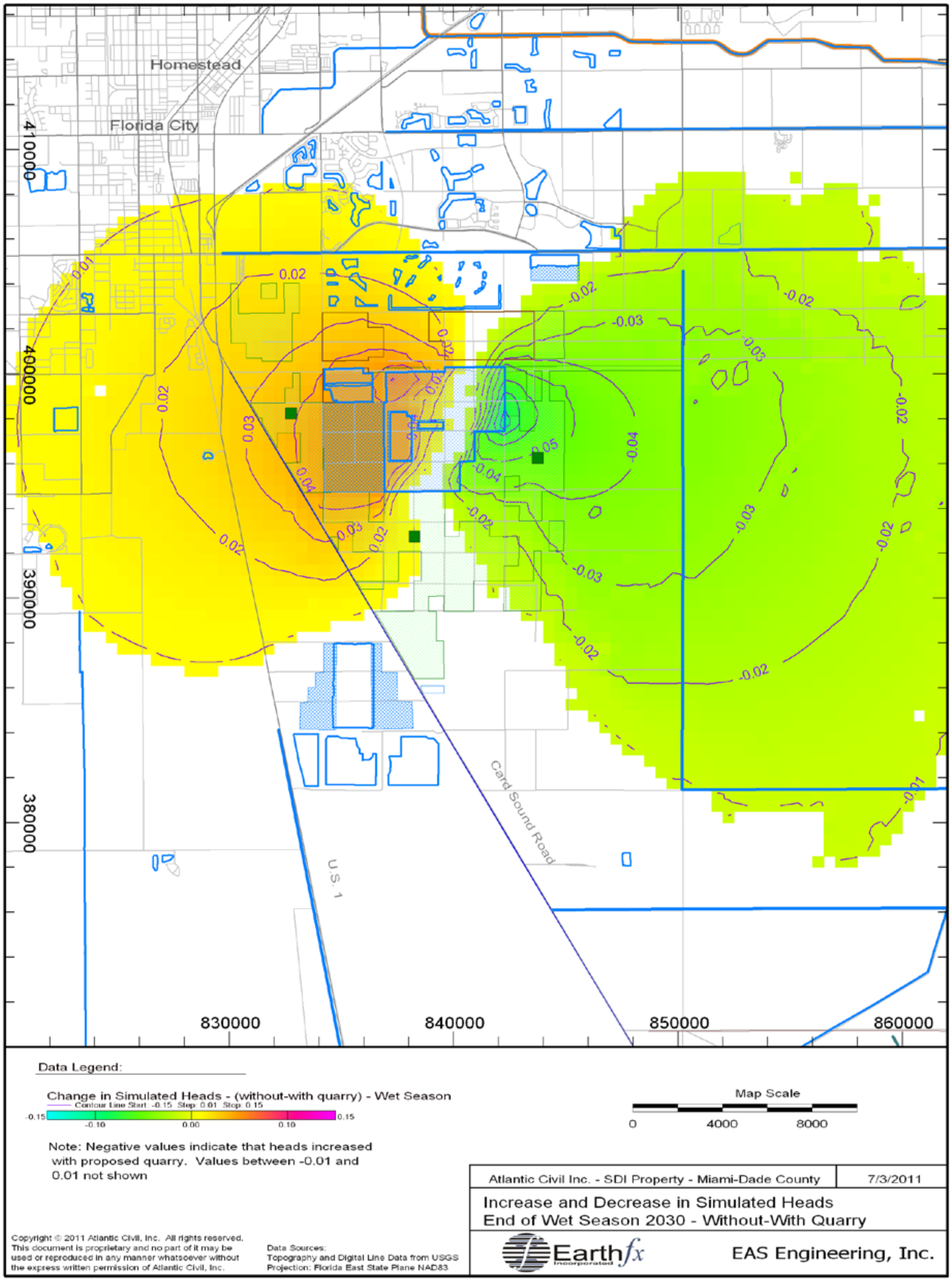

Figure 64: Change in simulated potentials at the end of the 2030 wet season (without - with quarry).

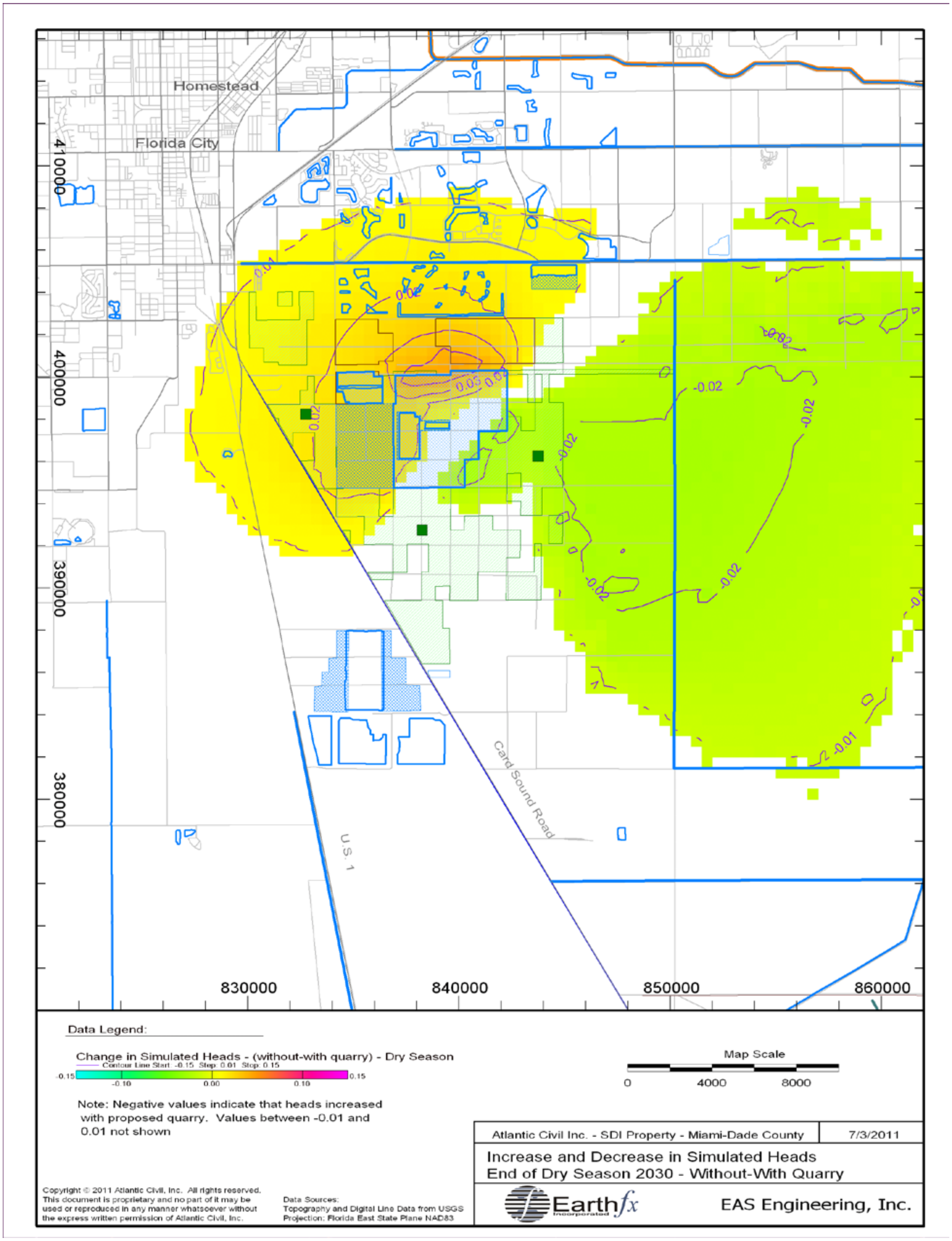

Figure 65: Change in simulated potentials at the end of the 2030 dry season (without - with quarry).

Technical Appendix A

Additional Groundwater Flow and Saltwater/Freshwater Interface Modeling for the Atlantic Civil Property South Miami-Dade County, FL

Prepared for:
EAS Engineering, Incorporated

Prepared by:

Earthfx Incorporated
3363 Yonge Street
Toronto, Ontario M4N 2M6

March 25, 2014

Earthfx Incorporated

Earth Science Information Systems

March 25, 2014

Edward A. Swakon, P.E., President
EAS Engineering, Inc.
55 Almeria Ave.
Coral Gables, FL 33134
eswakon@eas-eng.com

RE: Additional Groundwater Flow and Saltwater/Freshwater Interface Modeling for the Atlantic Civil Property, South Miami-Dade County, FL.

Dear Mr. Swakon:

We are pleased to provide the draft final technical appendix that describes additional modeling of groundwater flow and the saltwater/freshwater interface at the Atlantic Civil Property in South Miami-Dade County, Florida.

The model was applied to analyze the effects of an expanded quarry lake footprint and deeper excavation at the site (to 110 feet below sea level) and the mining of sands of the Tamiami Formation.

Improvements were made to the model to better represent the occurrence of sands and limestones within the upper portion of the Tamiami Formation included within the Biscayne Aquifer. Flow and transport within the ow-permeability materials underlying the Biscayne Aquifer are now modeled.

The report describes the results of our geologic analysis and revisions to the model. All the previous simulations, including the historic and predictive simulations, have been updated with the revised models. The analyses show that, in general, the effects of the quarry on the position of freshwater/saltwater interface are small and lead to small reductions in simulated chloride concentrations to the east of the quarry site.

We trust this technical appendix meets with your satisfaction. We look forward to the opportunity to work with you in the future on this and other projects.

Yours truly
Earth*fx* Incorporated

Dirk Kassenaar, M.Sc., P.Eng.

E.J. Wexler, M.Sc., M.S.E., (P.Eng.)

3363 Yonge St., Toronto, Ontario, Canada M4N 2M6
T: 416.410.4260 F: 416.481.6026
www.earthfx.com

Table of Contents

List of Figures

Additional Groundwater Flow and Saltwater/Freshwater Interface Modeling for the Atlantic Civil Property, South Miami-Dade County, FL

1 Introduction

1.1 Previous Work

Atlantic Civil Incorporated (ACI) is planning to expand an existing rock quarry site located east of Card Sound Road in South Miami-Dade County, Fl. In reviewing the application for a permit (SAJ-1995-06797 Rock Mining), the Corps of Engineers (COE) required that a cumulative impact assessment (CIA) be done for the site and surrounding area. A cumulative impact assessment was conducted and submitted in January 2012 that focused on the watershed containing the proposed quarry (primary watershed) and two adjacent watersheds (secondary watersheds), as shown in Figure 1.

A numerical model was developed to simulate regional groundwater flow and saltwater movement in the vicinity of the proposed quarry lake on the ACI property using the USGS SEAWAT code. The model used hydraulic properties and recharge rates based on the available field data and the results of previous modeling studies by the U.S. Geological Survey (USGS) and Earthfx. The model was calibrated by matching response in observation wells and the mapped position of the saltwater front.

The primary focus of the 2012 modeling effort was to examine the impact of the quarry development on the position of the saltwater front. The model simulated transient, density-dependent groundwater flow and solute transport and represented the history of change to the canal systems that greatly influenced groundwater flow and saltwater intrusion in the study area. Results of saltwater intrusion modeling were presented in a series of plan view maps and animations of dissolved solids concentrations. A secondary objective of the modeling effort was to confirm results of earlier Earthfx studies that showed construction of lakes on the ACI property would have no significant impacts on the surrounding wetland mitigation areas.

Model results indicated that groundwater levels in the "With ACI Quarry" simulation were slightly lower on the upgradient (west) side of the lake but slightly higher on the downgradient (east) side. The higher water levels in the east helped to reduce dissolved solids concentrations and prevented landward migration of the saltwater front in the vicinity of the proposed quarry expansion. Similarly, results for the other predictive scenarios for the period from 2010 to 2030, which included the proposed ACI quarry expansion along with the expansion of other nearby quarries and changes in the canal operations, showed that the construction of the ACI quarry will not cause landward movement of the salt front.

1.2 Need for Model Update

The ACI Quarry was represented in the previous modeling work (referred to as the “2012 model”) as being excavated to a depth of 70 ft below sea level (-70 ft). According to a revised design, the proposed quarry lake will now extend to a depth of 110 feet below mean sea level (-110 ft) level following the extraction of sands of the Tamiami Formation. Accordingly, the representation of the quarry excavation needed to be updated. The quarry lake is also to be expanded by 17 acres. The expanded footprint was also represented in the updated model.

The 2012 model represented the Biscayne Aquifer, which is comprised of the Miami Limestone, Fort Thompson Formation, and the permeable upper portion of the Tamiami Formation. The permeable upper portion of the Tamiami Formation, which consists of limestones and sands, was represented as a single, undifferentiated unit, with a uniform hydraulic conductivity of 3000 ft/d. Because the quarry will now be extracting Tamiami sands, it was important to update the model to properly simulate flow through the sands and the effects of their removal.

As a first step, a considerable effort was made to determine whether the sands were local, discontinuous units, or whether they could be mapped as a more regional unit. As will be described further on, available well logs were reviewed and the occurrence of sands and limestones within the permeable upper portion of the Tamiami Formation was mapped. These areas were assigned different hydraulic conductivity values in the updated model.

Finally, while the 2012 model extended to a depth of -110 ft (see Figure 4), the top of the low-permeability deposits in the Tamiami Formation was taken as a model boundary due to the sharp contrast in hydraulic conductivity between these beds and the overlying sands and limestones. To properly simulate the effect of the excavation below the previous model boundary, flow and solute transport through the low-permeability materials was simulated. Areas of the 2012 model that were designated as “inactive” because they fell below the top of the low-permeability deposits in the Tamiami Formation were considered to be active in the revised model.

All the historic and predictive simulations of transient, density-dependent groundwater flow and solute transport made with the 2012 model were updated using the revised model. Except for the revised hydraulic conductivities for upper Tamiami, the active lower Tamiami, and the revised quarry footprint, all other assumptions made for the 2012 model were held constant. Results of the modeling are presented in this Technical Appendix as a series of plan view maps and animations of dissolved solids concentrations.

2 Model Update

2.1 Review of Geologic Data for the Tamiami Formation and Revised Hydrostratigraphic Model

The 2012 conceptual model used five layers to represent the local hydrostratigraphy. These are labelled on the left side of Figure 4 and consisted of:

Conceptual Model Layer 1:	Surface Flow Layer
Conceptual Model Layer 2:	Surficial Soils – predominantly muck
Conceptual Model Layer 3:	Miami Limestone
Conceptual Model Layer 4:	Fort Thompson Formation
Conceptual Model Layer 5:	Permeable, contiguous beds of the Tamiami Formation

The numerical model used the two upper layers to represent Conceptual Model Layers 1 and 2. The limestone layers (Conceptual Model Layers 3 to 5) were represented using numerical model layers 3 to 13, each 10 feet thick, as shown on the right side of Figure 4.

The bottom of Conceptual Model Layer 5 in the 2012 Model was interpolated from the contour map of the base of the Biscayne aquifer in Fish and Stewart (1991). Layer 5 was presumed to include mostly limestones of Tamiami age but does include some of the sand beds as well.

A review of the geologic data within the quarry vicinity and studies in nearby areas (e.g. JLA Geosciences, Inc., 2010) was conducted to better understand the distribution of contiguous sand units at the top of the Tamiami Formation within the study area. Well logs were collected and reviewed for boreholes including:

- recently drilled on the ACI property: SDI 1, 2 and 3;
- ACI monitoring wells: 15, 16, and 17;
- borehole drilled by Florida Power and Light (FPL) in the vicinity of the Turkey Point facility: TPGW 1 to 14;
- USGS wells;
- Florida Keys Aqueduct Authority (FKAA) wells;
- Miami-Dade Water and Sewer Authority (MDWSA) wells.

Locations for boreholes with geological logs are shown in Figure 5. Borehole information was compiled in a database that includes location and elevation data and lithologic data with interval top and bottom depths converted to elevations above (or below) sea level. The borehole logs were viewed graphically in cross section, along with the bounding surfaces for the major geologic units and the bottom of the Biscayne aquifer, using VIEWLOG-GIS (v4.0) software.

Review of the data indicated that the sands occur in a wide band across the study area. Wells with occurrences of either sand (including sandstone) or limestone at the top of the Tamiami Formation within the Biscayne aquifer as delimited by Fish and Stewart (1991) were identified and the extent of the sand deposits was mapped. It must be noted that the sedimentology of the Tamiami Formation is complex and there is considerable variation within the unit, both in terms of sedimentary character and facies thickness. Refinements to the geologic and hydrostratigraphic bounding surfaces in the light of new data may be necessary for future studies, in particular, the lower bounding surface of the Biscayne aquifer.

2.2 Revised Numerical Model

The methods for assigning hydraulic conductivity values to the numerical model layers representing Conceptual Model Layers 3 and 4 (Miami Limestone and Fort Thompson Formation) as well as the upper model layers were kept the same as in the previous work (see Earthfx, 2012). The numerical model was revised where the numerical model layers represented the part of the Tamiami Formation in the Biscayne aquifer (Conceptual Model Layer 5).

Whereas the previous model had a uniform hydraulic conductivity value assigned to this unit, two hydraulic conductivity zones were established to represent the moderately permeable limestones and the moderately permeable sands. Properties were adjusted in initial model runs and final values of 3000 ft/d for the limestone and 10 ft/d for the sands were selected.

The previous model had an inherent assumption that the lower part of the Tamiami Formation (i.e., that was not considered part of the Biscayne aquifer) was composed primarily of low-permeability sands/marls and, as such, did not contribute significantly to groundwater flow in the study area. Because the proposed quarry would be excavated into these materials, it was decided that it would be better to represent at least the upper portion of the low-permeability material explicitly. Accordingly, areas that were designated as “inactive” because they fell below the base of the Biscayne aquifer were now considered to be active in the revised model. Properties for the low-permeability materials were adjusted in initial model runs and a final hydraulic conductivity value of 0.03 ft/d was selected.

Figure 6 shows the hydraulic conductivity of model Layer 6. This layer is all within the Fort Thompson Formation and, therefore, the properties are the same as they were in the previous model. Figure 7 shows the hydraulic conductivity of model Layer 7. There is some sand/marl of the Tamiami Formation in this layer (pink area) in the west. This area was inactive in the previous model. Note that there are separate colour scales to show the hydraulic conductivities of the two formations because of the vast differences in the range of values.

Figure 8 through Figure 10 show the hydraulic conductivities in model layers 8 through 10, respectively. The marls, sands, and limestones of the Tamiami as well as the small areas of the Fort Thompson Formation are present in these layers. Finally, Figure 11 through Figure 13 show the hydraulic conductivities in model layers 11 through 13, respectively. These layers are all within the upper or lower part of the Tamiami Formation. Layer 13 was almost completely inactive in the previous model, but now is fully active.

Figure 14 shows the model grid and boundary conditions. Unlike the previous model which had different boundary conditions (i.e., “inactive” cells) in the lower layers to represent where the lower portion of the Tamiami Formation subcropped in the layer (see Figure 17 in Earthfx, 2012), these zones are now active and the boundary conditions are identical in each layer.

No other model properties or boundary conditions were revised. Additional discussions regarding the model development, the SEAWAT code (Langevin and others, 2003), and calibration can be found in Earthfx (2012).

3 Simulations of Historical Conditions

Several historic periods were simulated with the 2012 Model to match the time-dependent development of the saltwater front in response to changes in the controlling stage or configuration of the canals and to increasing dissolved solids concentrations in the FPL cooling canals. The runs are described briefly in the table below.

Results of updated historical modeling are presented in this Technical Appendix as a series of figures showing revised saltwater concentrations at various depths and at critical times. Significant findings regarding the movement of the saltwater interface within the sands of the Tamiami Formation are discussed. Further discussions regarding the simulations can be found in Earthfx (2012).

Scenario	Key Features
Pre-development	No canals, only near-shore drainage. Higher head (6.5 ft) at northwest GHB boundary (see "Model Boundaries"). No Pumping.
1945-1968	Uncontrolled drainage canals (Mowry, Florida City, Model Land, U.S.1, and Card Sound Road. Near shore drainage modified in vicinity of the canals. Reduced head (4.5 ft) at northwest GHB boundary. No pumping.
1968-1972	SFWMD canals added. Changes in configuration of Mowry, Florida City, Model Land, and US 1 canals. Otherwise, same as above.
1973-1985	FPL Cooling Canal System added Municipal water supply and other pumping added. First of quarry lakes added between Card Sound Road and U.S. 1. Otherwise, same as above.
1986-1995	Additional quarry lakes added between Card Sound Rd. and U.S. 1. Pumping rates adjusted to reflect historical increases. Otherwise, same as above.
1996-2010	Additional quarry lakes added. Otherwise, same as above.

Dissolved solid concentrations are presented in units of lb/ft^3 and can be converted to equivalent chloride concentrations in mg/L by multiplying by 8700. For example, the 0.115 lb/ft^3 concentration is equivalent to 1000 mg/L of chloride which has been used by the USGS in defining the extent of the saltwater front. The 1000 mg/L isochlor has been used by the USGS for mapping of the edge of the saltwater front. This line has been used to define the position of the saltwater front on the figures discussed below.

3.1 Pre-development Conditions

Dissolved solid concentrations of 2.184 lb/ft^3 were set along the shoreline and the south model boundary for this simulation. Near-shore natural drainage features allow inland saltwater movement in Layers 2 and 3. Average wet season precipitation was assumed to be 0.0231 ft/day or 41.6 inches over a 5-month wet season and 0.0076 ft/day (19.1 inches) over a 7 month dry season. Average wet season maximum ET was assumed to be 0.0175 ft/day (31.5 in) and 0.01085 ft/day (27.3 inches) during the dry season. As noted, actual ET losses depend on the depth to the water table in each model cell. Concentrations in recharge to the groundwater system were assumed to be equal to zero. ET is treated differently than other sinks because the solute is left behind as the water evaporates while other sinks (such as wells) remove both water and solute.

The model was run from the starting conditions until reasonably stable conditions were achieved. Although the salt-water interface moves back and forth in response wet and dry cycles, the overall landward migration of the interface reaches a maximum within 16 years in most layers. The rapid movement to equilibrium in the models is due to the extremely high hydraulic conductivity of the Biscayne aquifer. Movement in the sands and marls was slower.

Simulated dissolved solids concentrations in Layer 7 at the end of the wet season under pre-development conditions are shown in Figure 15. Simulated dissolved solids concentrations in Layer

10 at the end of the wet season under pre-development conditions are shown in Figure 16. Layer 10, which is between 70 and 80 ft below sea level, was selected for display because it is the one with the greatest change in hydraulic conductivity values compared to the previous model. In both figures, the simulated concentrations (green lines) are similar to those in the previous model (red lines) although the front has not moved as far west in the areas mapped as having Tamiami sands. Also, the revised model contours are continuous whereas the previous model contours were truncated where the low-permeability Tamiami subcropped.

Figure 17 shows the simulated dissolved solids concentrations within each model layer along a west-east section line east of the ACI property (section line is shown in Figure 15). The figure illustrates that density effects have moved the toe of the saltwater front about 1000 ft further west at the base of the aquifer than near the top. The westward displacement increases with solute concentration and density.

3.2 1945 to 1967 Conditions

The simulation period from 1945 to 1967 represents a time with mostly uncontrolled drainage canals affecting the groundwater and surface water flow systems. The simulations for this period used reported average wet season and dry season precipitation for each individual year. Average wet season maximum ET and average dry season maximum ET were set based on long-term average values. Actual ET losses for each wet and dry season depend on the precipitation rate and the depth to the water table in each model cell. The general head boundary at the northwest corner of the model area was reduced to 4.5 ft above sea level to adjust for the drainage of the Everglades by the Miami River and canals north of the study area. Starting conditions for the simulation were the end of wet season heads and dissolved solids concentrations obtained from the pre-development simulations. As expected, nearly stable conditions were obtained within a relatively short time period.

Figure 18 shows the simulated dissolved solids concentration in Layer 10 at the end of the 22 year simulation period. The approximate location of the saltwater interface, as mapped by Parker and others (1955) is shown for comparison. Contours from the previous simulations are also plotted for comparison and show that the saltwater front has not spread as far landward within the Tamiami sands in the revised model simulations.

3.3 1968 to 1972 Conditions

The simulated end of wet season heads and dissolved solids concentrations for 1967 were used as starting conditions for the 1968 to 1972 simulations. This period is meant to represent the construction and initial operating period of the SFWMD drainage and flood control system which regulates the surface water and groundwater flow systems in the study area. Locations of the canals and structures are shown in Figure 19. To simplify the model, it was assumed that the entire system was operational in October 1967 although S-197 and the southern extension of C-111 were not opened until 1969.

Figure 19 shows the simulated dissolved solids concentration in Layer 10 at the end of the five-year simulation period. A comparison with Figure 18 shows that the simulated saltwater front has been pushed back across the study area except in the vicinity of the Card Sound Road canal which remained uncontrolled. Contours from the previous simulations are also plotted for comparison and show that the saltwater front still lies further landward within the Tamiami sands in the previous model simulations.

3.4 1973 to 1984 Conditions

The simulated end of wet season heads and dissolved solids concentrations for 1972 were used as starting conditions for the 1973 to 1984 simulations. The principal change represented in this period was the construction of the FPL cooling canal system and interceptor canal. To simplify the model, it was assumed that the entire system was operational at the start of 1973. Time-varying concentrations in the cooling canals were adjusted over the simulation period based on historic average wet season and dry season salinity values estimated from quarterly data reported by FPL. The simulations also include pumping by the Florida Keys Aqueduct Authority (FKAA), Florida City, City of Homestead Wittkop Park and Harris Field wellfields, and the South Dade Water System Everglades, Newton, and Redavo wellfields, along with several smaller users.

Figure 20 shows the simulated dissolved solids concentration in Layer 10 at the end of the 12-year simulation period. A comparison with Figure 19 shows that simulated saltwater front has been pushed further back across most of the study area. Some inland migration occurs in the area between the Model Land canal and L31-E west of the FPL cooling canals and a small westward movement was noted in the vicinity of the expanded quarry lake between Card Sound Road and US 1. The pushback is due to the continued infiltration of freshwater from the SFWMD canals, the control of saltwater encroachment into the tidal reaches of these canals and a series of wetter than average years between 1973 and the 1985 drought. Figure 20 also shows the 1985 saltwater front position as mapped by Klein and Waller (1985) for comparison.

Contours from the previous simulations are nearly identical to the previous model simulations except beneath the north end of the FPL cooling canals. The presence of Tamiami sands in this area has slowed the downward migration of saltwater in the revised model simulations.

3.5 1985 to 1996 Conditions

The simulated end of wet season heads and dissolved solids concentrations for 1984 were used as starting conditions for the 1985 to 1996 simulations. The principal change represented in this period was the expansion of the quarry lakes between Card Sound Road and US 1. Pumping of groundwater for cooling the City of Homestead Power Plant was added to the list of wells. Otherwise, the methods used to represent the canal systems, precipitation, and increased pumping were similar to previous simulations.

Figure 21 shows the simulated dissolved solids concentration in Layer 10 at the end of the 14-year simulation period. Careful comparison with the previous simulation (Figure 20) shows that the simulated saltwater front has stabilized and receded slightly across the study area mainly due to some extremely wet years during the period after the 1985 and 1989 droughts. A minor westward movement was noted in the vicinity of the expanded quarry lakes between Card Sound Road and US 1 primarily because of continued saltwater leakage from the uncontrolled Card Sound Road Canal. Figure 21 also shows the 1995 saltwater front position as mapped by Sonenshein (1996).

Contours from the previous simulations are nearly identical to the previous model simulations except in the northern end of the model. Landward migration of the saltwater front in the area in this area has slowed the downward migration of saltwater in the revised model simulations due to the reduced inputs from the FPL cooling canals.

3.6 1997 to 2010 Conditions

The simulated end of wet season heads and dissolved solids concentrations for 1996 were used as starting conditions for the 1997 to 2010 simulations. The principal change represented in this period was the construction of the quarry lake on the ACI property. All other lakes in the study area were also represented in these simulations. Otherwise, the methods used to represent the canal systems, precipitation, and increased pumping were similar to previous simulations. Dissolved solids concentrations in the FPL canals increased noticeably during the simulation period as compared to the previous period in which concentrations were relatively stable.

Figure 22 shows the simulated dissolved solids concentration in Layer 10 at the end of the 14-year simulation period. Comparison with the previous period (see Figure 21) shows that the simulated saltwater front has advanced west of the north extension of the Model Land Canal (east of the ACI property). The movement is mainly in response to the lower than average rainfall over the period (see Earthfx, 2012). Additional westward movement of the simulated salt front in the vicinity of the ACI property is also due, in part, to the higher concentrations in the FPL cooling canals. The advance was not as pronounced as in the previous model simulations, however. Figure 22 also shows the latest estimate of the 2010 saltwater front position as mapped by Prinos (2011) and Fitterman and others (2012).

4 Saltwater Front Response to Quarry Lake Development

The updated model was applied to analyze several scenarios with and without the proposed ACI quarry lake to determine the impact of quarry lake development. The model simulations considered the new proposed quarry expansion using the updated 582-acre footprint and the deeper depth of excavation (110 ft below sea level). Recent changes to the hydrologic system, such as the control structure constructed by FPL in the Card Sound Road canal, and other future projects, such as wetland mitigation, expansion of nearby quarries, and other planned modifications to the canal system were represented in some of the future scenarios, as shown in the table below.

Results of the revised modeling effort are documented in this Technical Appendix as a series of updated figures. As in the previous section, significant findings regarding the movement of the saltwater interface within the sands of the Tamiami Formation are discussed. Further discussions regarding the simulations can be found in Earthfx (2012).

All future simulations were started in 2010 to be consistent with the previous modeling work Simulated heads and concentrations at the end of the 1996-2010 model run were used as starting conditions for all simulations. Other assumptions included constant pumping rates at the existing wells and the use of long-term average (rather than observed) wet season and dry season precipitation. Concentrations in the FPL canals were assumed to increase linearly with time based on projections from the available data.

Scenario	Key Features
Baseline-No Changes	Construction of structure on Card Sound Road. Long-term average wet season/dry season precipitation. Constant pumping rates No expansion of quarries Concentrations in FPL canals based on linear projection. Otherwise same as 1996-2010 simulations.
ACI Quarry Lakes Only	Expanded ACI Quarry lakes (East and West) added. Otherwise same as Baseline-No Changes conditions.
ACI and Other Quarry Lakes	Expanded ACI Quarry lakes (East and West) added Expansion of other licensed quarries added. Otherwise, same as No Changes -Without Quarry conditions
All Changes	Expanded ACI Quarry lakes (East and West) added Expansion of other licensed quarries added. Construction of earth plug in lower reaches of Card Sound Rd. Canal. Changes to Florida City canal operations. Otherwise, same as No Changes-Without Quarry conditions
Original Footprint and Depth	Expanded ACI Quarry lakes (East and West) added. ACI Quarry lakes have original proposed depth and footprint. Otherwise same as Baseline-No Changes conditions.

Chloride concentrations and the position of the saltwater front (i.e., the 1000 mg/L chloride contour) were analyzed by comparing the gridded values used to generate the plan-view maps of predicted concentrations. Results of the three saltwater movement simulations with quarry lakes were compared against the results of the Baseline-No Changes simulation.

4.1 Baseline – No Changes Scenario

The "Baseline-No Changes" scenario only considered the existing lakes and quarries. The only modification was the addition of the control structure on the Card Sound Road canal built in 2010 (see Figure 23).

Figure 24 shows the simulated dissolved solids concentration in Layer 10 at the end of the 22-year baseline simulation period with no changes except the structure on Card Sound Road. Comparison with the starting conditions (see Figure 22) shows that concentrations in the Card Sound Road area have decreased due to the prevention of saltwater migration up the Card Sound Road canal and to increased potentials. The decrease is not as dramatic as in the previous model, however, because of the longer time required to flush the contaminants from the Tamiami sands. At the same time, the saltwater front has advanced westward in the vicinity of the ACI site primarily due to the assumed linear increase in solute concentrations in the FPL canals and the continued leakage of hypersaline water. The advance is not as far as in the previous model, again, due to the presence of the Tamiami sands which slow the movement of the hypersaline water from the FPL canals.

4.2 ACI Quarry Lake Only

For the "ACI Quarry Lakes Only" scenario (Figure 25), the lakes were assumed to be excavated through the Biscayne aquifer to the final depth of 110 ft below sea level. Hydraulic conductivity and anisotropy factors for Layers 2 through 13 were modified in the expanded footprint of the proposed lake. Otherwise, conditions were the same as for the “Baseline-No Changes" scenario.

Figure 26 shows the simulated dissolved solids concentration in Layer 10 at the end of the 22-year "ACI Lakes Only" simulation period with no additional changes except the expansion of the ACI east and west quarry lake footprints. Visual comparison with the previous simulation shows only minor change. To better quantify the simulated changes, the gridded concentration values at the end of the "ACI Quarry Lakes Only" simulation were subtracted from the gridded concentration values at the end of the "Baseline-No Changes" simulation. Results for Layer 10, presented in Figure 27, showed no increases and only a minor decrease in dissolved solids concentration (maximum value of 0.13 lb/ft^3 or about 1,130 mg/L chloride) in the area east of the ACI property where concentrations were projected to reach 15,900 mg/L without the quarry.

The simulated decrease is due to slightly higher heads on the downgradient (east) side of the quarry lake that help to hold back the advance of the saltwater front. For example, Figure 28 shows the difference in the simulated potentials (i.e. groundwater levels, in ft) in Layer 7 at the end of 2030 between the ACI Lakes Only and Baseline-No Changes scenarios. The increases in potentials are small (0.0 to 0.06 ft) but over time have caused a measurable decrease in the landward movement of the salt front. The patterns of decreases in simulated dissolved solids concentration (Figure 27) are much more complex than those obtained from the previous model, primarily because of the effects of the Tamiami sands on the movement of solutes.

4.3 ACI Quarry Lake and Other Quarry Lakes

For the "ACI and Other Lakes" scenario (Figure 29), hydraulic conductivity and anisotropy factors for Layers 2 through 8 were modified in the footprint of the other expanded quarries. These lakes were kept at the same depth as in the previous model. Extinction depths for all quarry lake footprints were changed to reflect that evaporation occurs at the maximum rate over the lakes. Otherwise, conditions were the same as for the “ACI Quarry Lakes Only " scenario.

Figure 30 shows the simulated dissolved solids concentration in Layer 10 at the end of the 22-year "ACI and Other Quarry Lakes" simulation period with expansion of the east and west quarry lakes and the addition of all other future quarry expansions in the study area. Again, visual comparison of this simulation with the baseline simulation shows only minor change. Subtracting the two results (Figure 31) shows a further decrease in dissolved solids concentration in Layer 10 (maximum value of 0.153 lb/ft^3 or about 1330 mg/L chloride) in the area east of the ACI property where concentrations were simulated to reach 16,710 mg/L without the quarry. The decrease is still due primarily to the slightly higher heads on the downgradient (east) side of the quarry lake that help to hold back the advance of the saltwater front.

4.4 All Changes including ACI Quarry Lake and Other Quarry Lakes

For the "All Changes" scenario (Figure 32) all changes made for the "ACI and Other Lakes" scenario were made. In addition, construction of a proposed earth plug in lower reaches of Card Sound Road Canal and proposed changes to the operation of the Florida City canal were simulated.

Figure 33 shows the simulated dissolved solids concentration in Layer 10 at the end of the 22-year "All Changes" simulation period with the expansion of the east and west quarry lakes, the addition of all other future quarry expansions in the study area, the addition of the earth plug in the lower reaches of the Card Sound Road canal, and changes to operations of the Florida City canal. The most noticeable change is the reduction of dissolved solids concentrations in the area between the earth plug and the new control structure (Figure 32). Subtracting the two results for Layer 9 confirms the change in the vicinity of the plug (maximum value of 1.8 lb/ft^3 or about 15,750 mg/L chloride), shows a slight decrease in the vicinity of the Florida City canal (maximum value of 0.32 lb/ft^3 or about 2780 mg/L chloride), and shows the minor decrease in dissolved solids concentration (maximum value of 0.13 lb/ft^3 or about 1100 mg/L chloride) in the area east of the ACI property where concentrations were simulated to reach 8,440 mg/L without the quarry (Figure 33). It is important to note the scale change in the color-contouring which goes from 0.1 to 3.0 lb/ft^3 rather than from 0.1 to 0.3 0 lb/ft^3 as on Figure 27 and Figure 31.

4.5 Changes due to Expanding and Deepening the ACI Quarry Lake

Figure 36 shows the simulated dissolved solids concentration in Layer 10 at the end of the 22-year "Original Footprint and Depth" simulation period. The simulation is similar to the "ACI Lakes Only" scenario except, in this case, the original ACI quarry lake depth and footprint were used. Visual comparison with the previous simulation (Figure 30) shows only minor change. To better quantify the simulated changes, the gridded concentration values at the end of the "ACI Quarry Lakes Only" simulation were subtracted from the gridded concentration values at the end of the "Original Footprint and Depth" simulation". Results for Layer 10, presented in Figure 37, showed a slight increase in the concentration of up to 0.012 lb/ft^3 (100 mg/L) near Card Sound Road and small decreases of up to 0.045 lb/ft^3 (390 mg/L) to the east of the quarry lake.

4.6 Discussion

As was noted in Earthfx (2012), a number of simplifying assumptions were necessary to conduct these simulations. They include the simplification of recharge and ET processes as well as all the assumptions used in representing the lakes, the SFWMD canals and other drainage canals, the FPL cooling canals, and the aquifer properties and boundaries (see Earthfx, 2012). The procedures followed were similar to those employed in previous modeling studies of groundwater flow and saltwater encroachment (e.g., Merritt (1997) and Langevin (2001)) and built on a significant amount of data collected over the years. These simplifications are not expected to have a significant impact on the conclusions based on the model results. .

The model consistently indicated that small decreases in simulated concentrations will occur east of the ACI property in all scenarios. The magnitude of these decreases should be taken as approximations, however. Based on the repeatability of the results, even with the significant revisions to the model, it is reasonable to assume that any changes in the position of the saltwater front induced by the quarry lake will be insignificant when compared to the impacts caused by drought, changes in canal operations, and changes in the increasing trend in concentrations in the FPL cooling canals. The model results for all scenarios evaluated for the period from 2010 to 2030, including the proposed ACI quarry lake expansion, expansion of other quarries in the study area, and other possible future changes to canal operations, showed no increase in the salt front movement.

5 Limitations

Services performed by Earth*fx* Inc. were conducted in a manner consistent with that level of care and skill ordinarily exercised by members of the environmental engineering and consulting profession.

This report presents the results of data compilation and computer simulations of a complex geologic setting. Models constructed from this data are limited by the quality and completeness of the information available at the time the work was performed. The applicability of the simplifying assumptions may or may not be applicable to a variety of applications.

It should be recognized that the passage of time affects the information provided in this report. Environmental conditions and the amount of data available can change. Discussions relating to the conditions are based upon information that existed at the time the conclusions were formulated. Consistent with the foregoing, Earthfx Inc. used its best professional efforts to consider and evaluate all reasonably relevant and accessible data during its efforts to prepare this report. Data reviewed for this report was evaluated in its reported state; it was beyond the scope of this project to review each data measurement or to audit the reported data.

All of which is respectively submitted,

EARTHFX INC.

Report prepared by:

E.J. Wexler, M.Sc., M.S.E., P.Eng.
Director of Modelling Services
Earthfx Incorporated

6 REFERENCES

Earthfx Incorporated, 2012, Simulation of groundwater flow and saltwater movement in the vicinity of the Atlantic Civil Property, South Miami-Dade County, FL: prepared for Atlantic Civil Incorporated in support of Application Number SAJ-1995-6797(mining), Earthfx Inc., January 30, 2012.

Fish, J.E., and Stewart, Mark, 1991, Hydrogeology of the surficial aquifer system, Dade County, Florida: U.S. Geological Survey Water-Resources Investigations Report 90-4108, 50 p.

Fitterman, D.V., Deszcz-Pan, M., and Prinos, S.T., 2012, Helicopter electromagnetic survey of the Model Land Area, Southeastern Miami-Dade County, Florida: U.S. Geological Survey Open-File Report 2012–1176, 77 p.

JLA Geosciences, Inc., 2010, Geology & hydrogeology report for FPL Turkey Point Plant - Groundwater, surface water, & ecological monitoring plan, FPL, Turkey Point Plant, Homestead, Florida: prepared for Florida Power and Light, October 2010.

Klein, H. and Waller, B.G., 1985, Synopsis of saltwater intrusion in Dade County, Florida, through 1984: U.S. Geological Survey (USGS) Water-Resources Investigations Report 85-4104.

Langevin, C.D., 2001, Simulation of ground-water discharge to Biscayne Bay, southeastern Florida: U.S. Geological Survey Water-Resources Investigations Report 00-4251, 127 p.

Langevin, C.D., Shoemaker, W.B., and Guo, W., 2003, MODFLOW-2000, The U.S. Geological Survey modular ground-water model - documentation of the SEAWAT-2000 version with the variable density flow process (VDF), and the integrated MT3DMS transport process (IMT); U.S. Geological Survey Open File Report 03-426, 43 p.

Merritt, Michael L., 1997, Simulation of the water-table altitude in the Biscayne aquifer, southern Dade County, Florida, water years 1945-89: U.S. Geological Survey Water-Supply Paper 2458, prepared in cooperation with the Metro-Dade Department of Environmental Resources Management, 148 p.

Parker, G.G., Ferguson, G.E., Love, S.K., and others, 1955, Water resources of southeastern Florida: U.S. Geological Survey Water-Supply Paper 1255, 965 p.

Prinos, S.T., ed., 2011, Approximate inland extent of the saltwater interface in the Biscayne aquifer in 2011, Miami-Dade County, FL: U.S. Geological Survey Arc-GIS shapefile. (Available at http://www.envirobase.usgs.gov/FLIMS/SaltFront/viewer.htm.)

Sonenshein, R.S. 1996. Delineation of saltwater intrusion in the Biscayne Aquifer, Eastern Dade County, Florida, 1995: USGS Water Resources Investigation Report 96-4285.

FIGURES

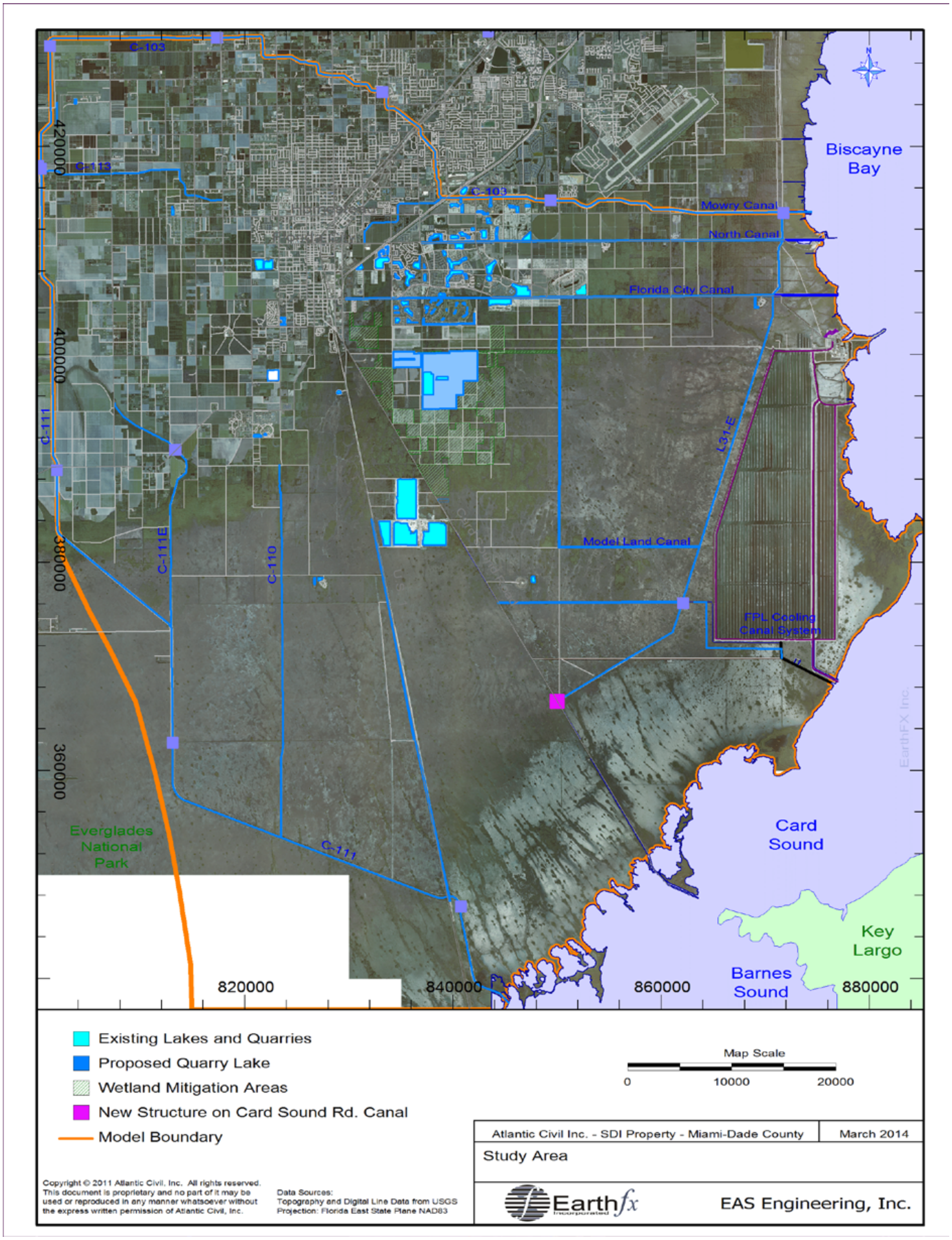

Figure 1: Location of proposed quarry and lateral extent of the 2012 Model.

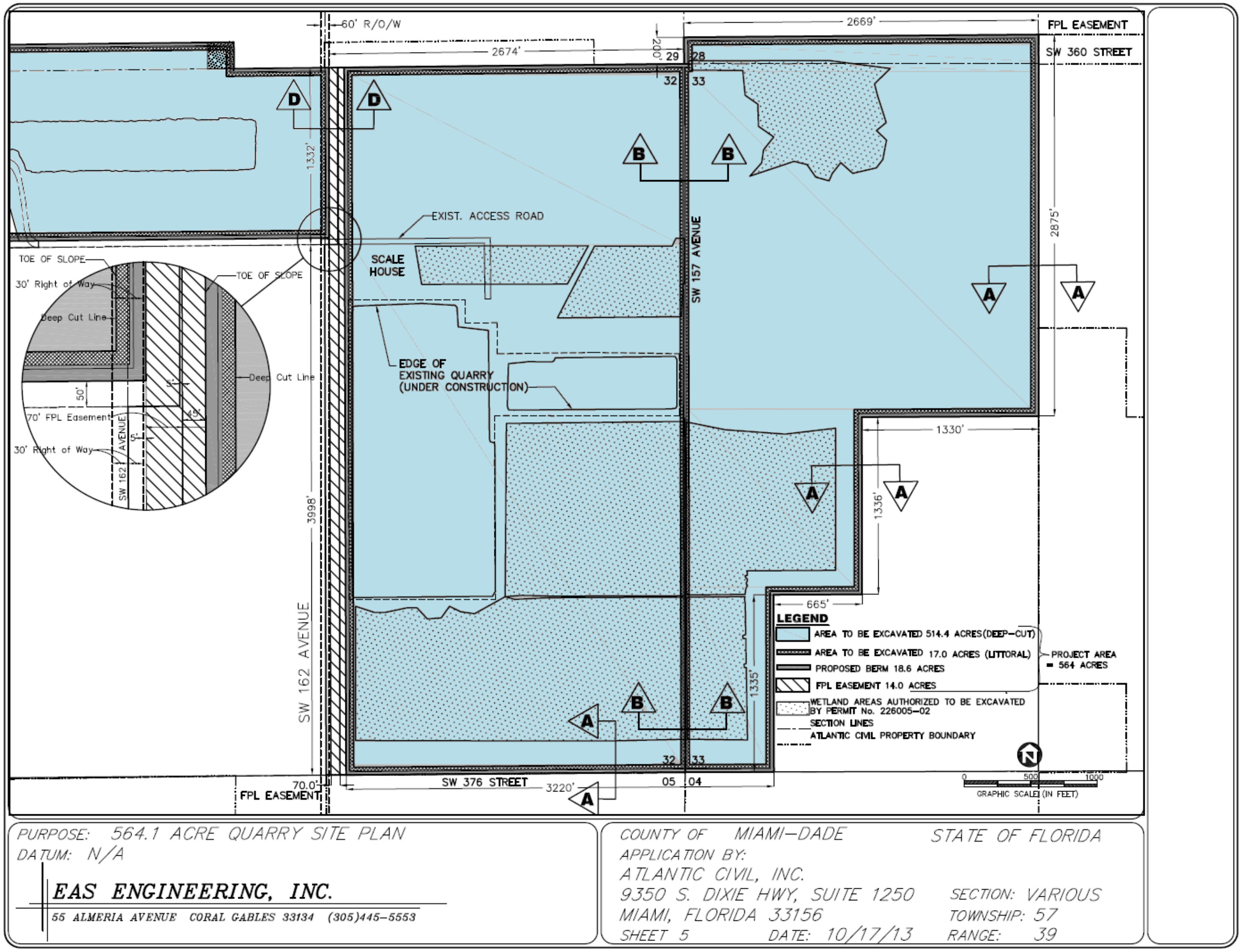

Figure 2: Revised proposed quarry lake footprint (modified from EAS Engineering, 2013).

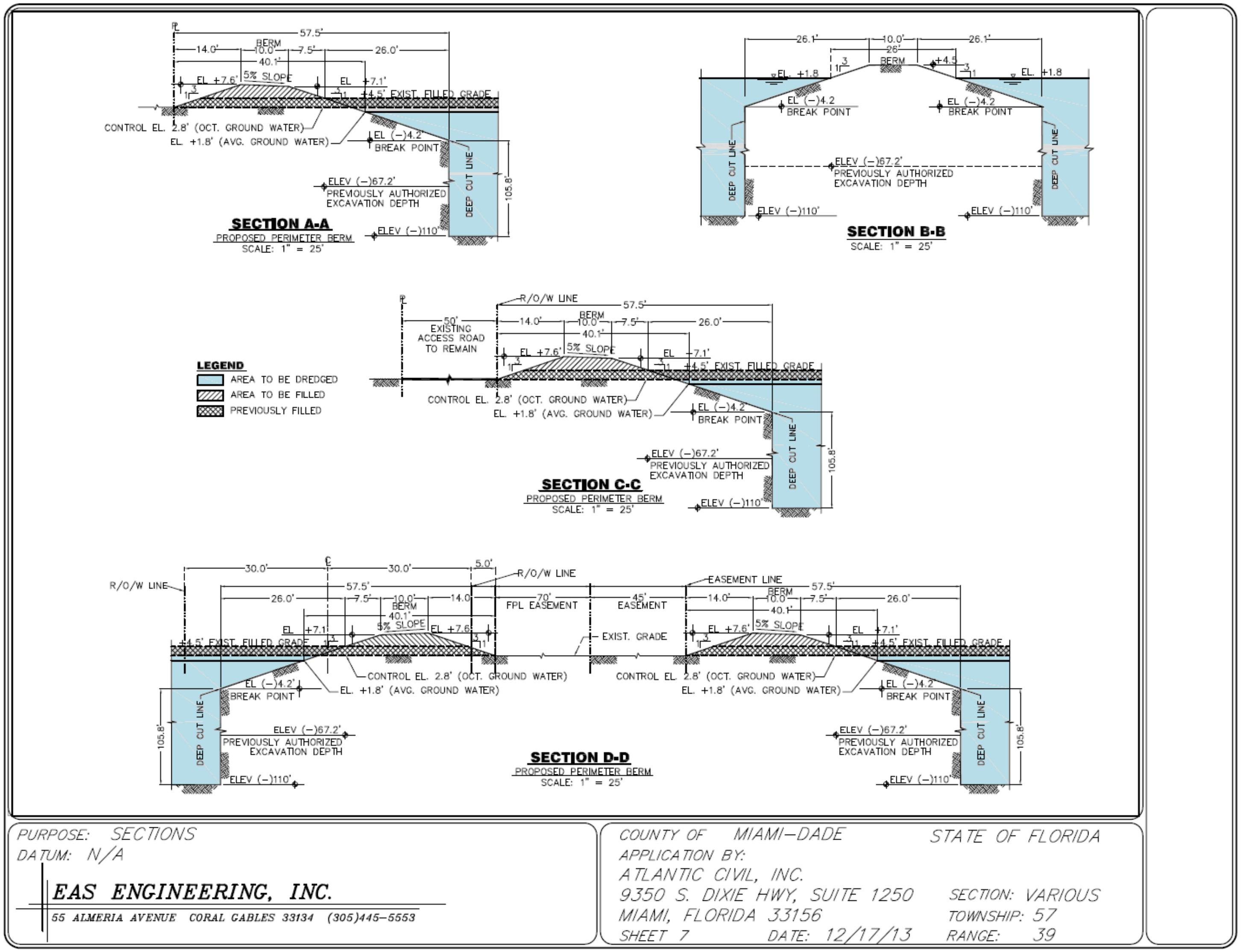

Figure 3: Revised proposed quarry lake depth (modified from EAS Engineering, 2013).

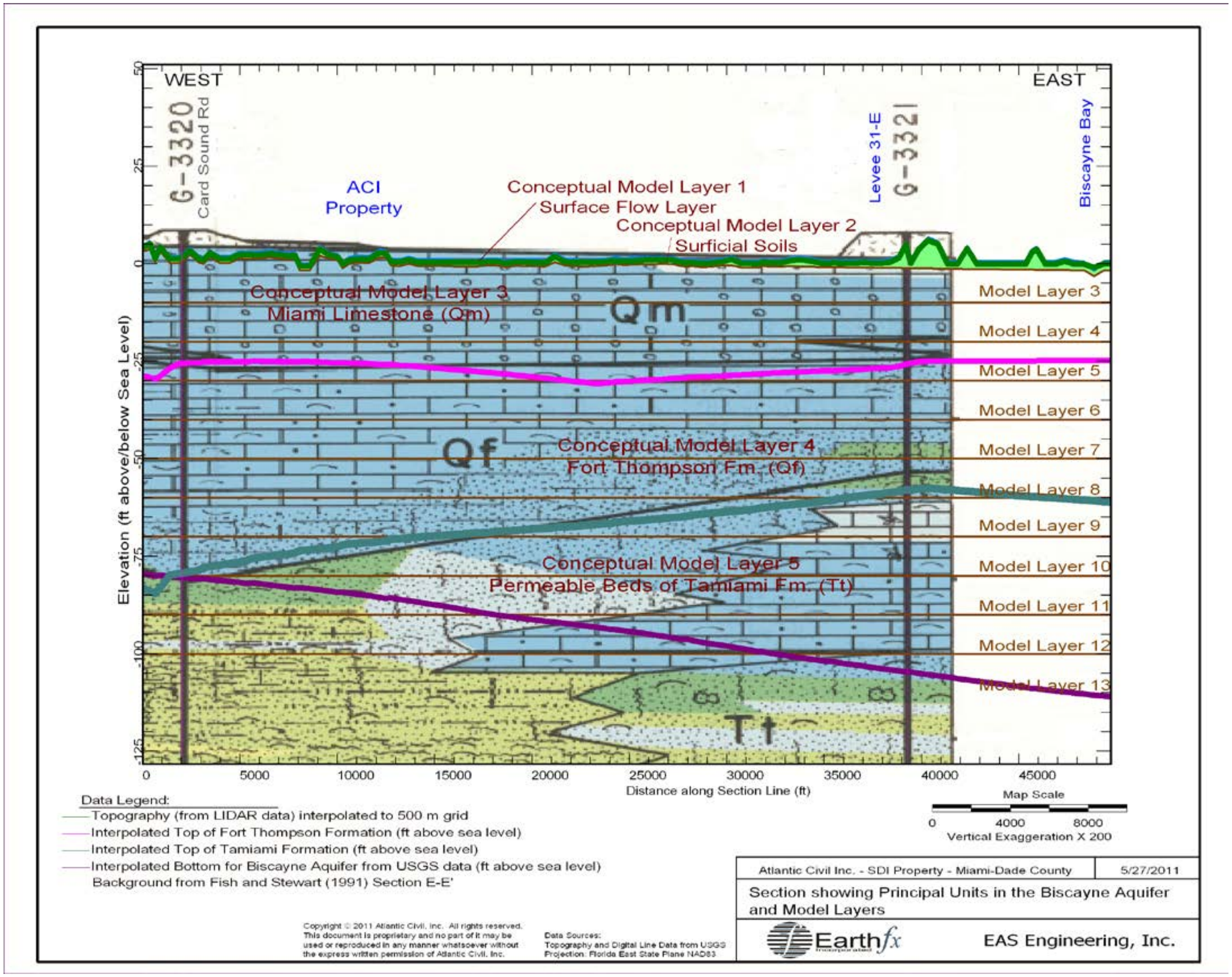

Figure 4: Local stratigraphy and vertical extent of the 2012 Model.

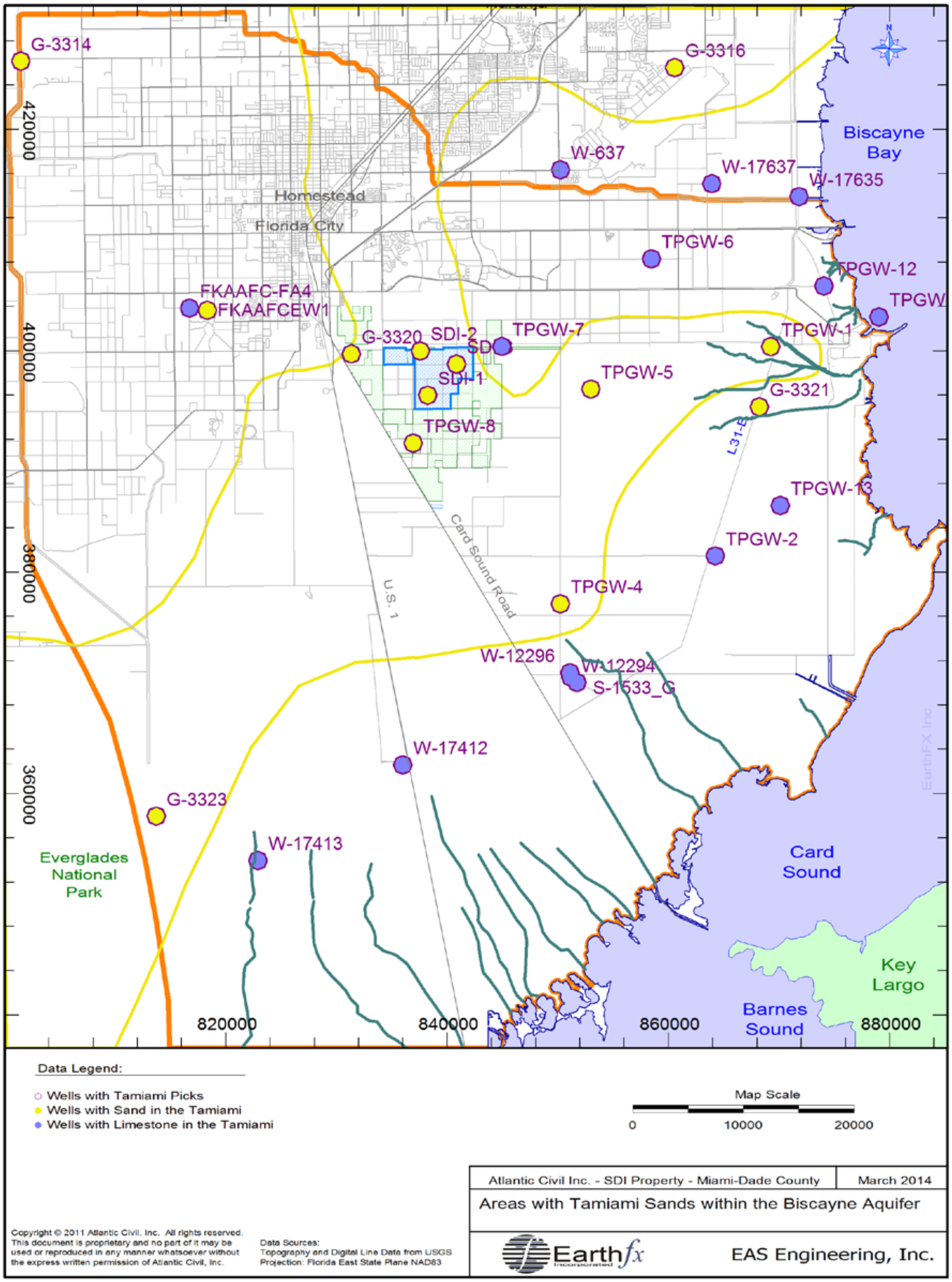

Figure 5: Areas with Tamiami Formation sands in the Biscayne Aquifer.

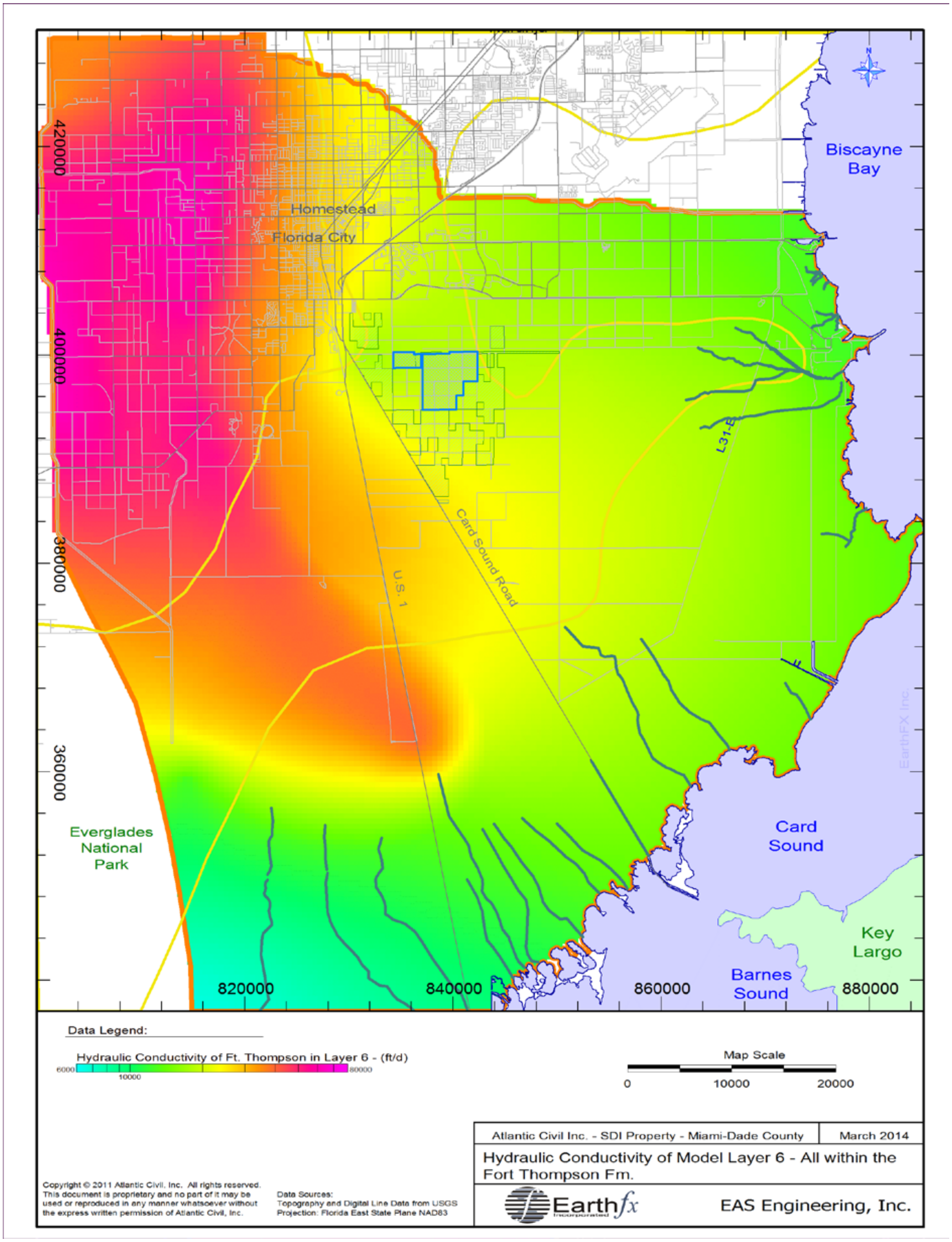

Figure 6: Hydraulic conductivity of model Layer 6, assumed to be all within the Fort Thompson Formation. Values are same as in previous model.

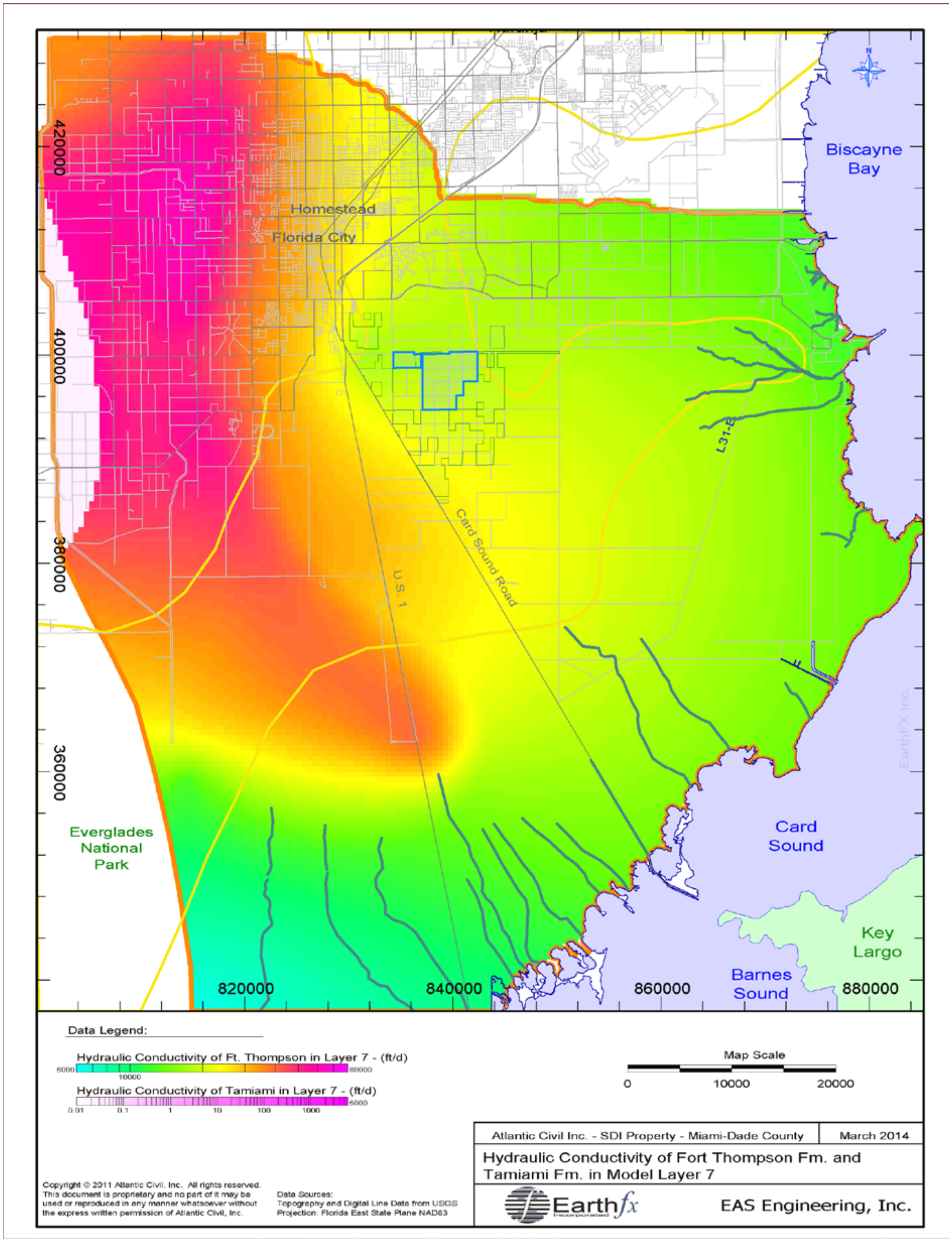

Figure 7: Hydraulic conductivity of Layer 7. Note the two color scales to represent the Fort Thompson and Tamiami Formations.

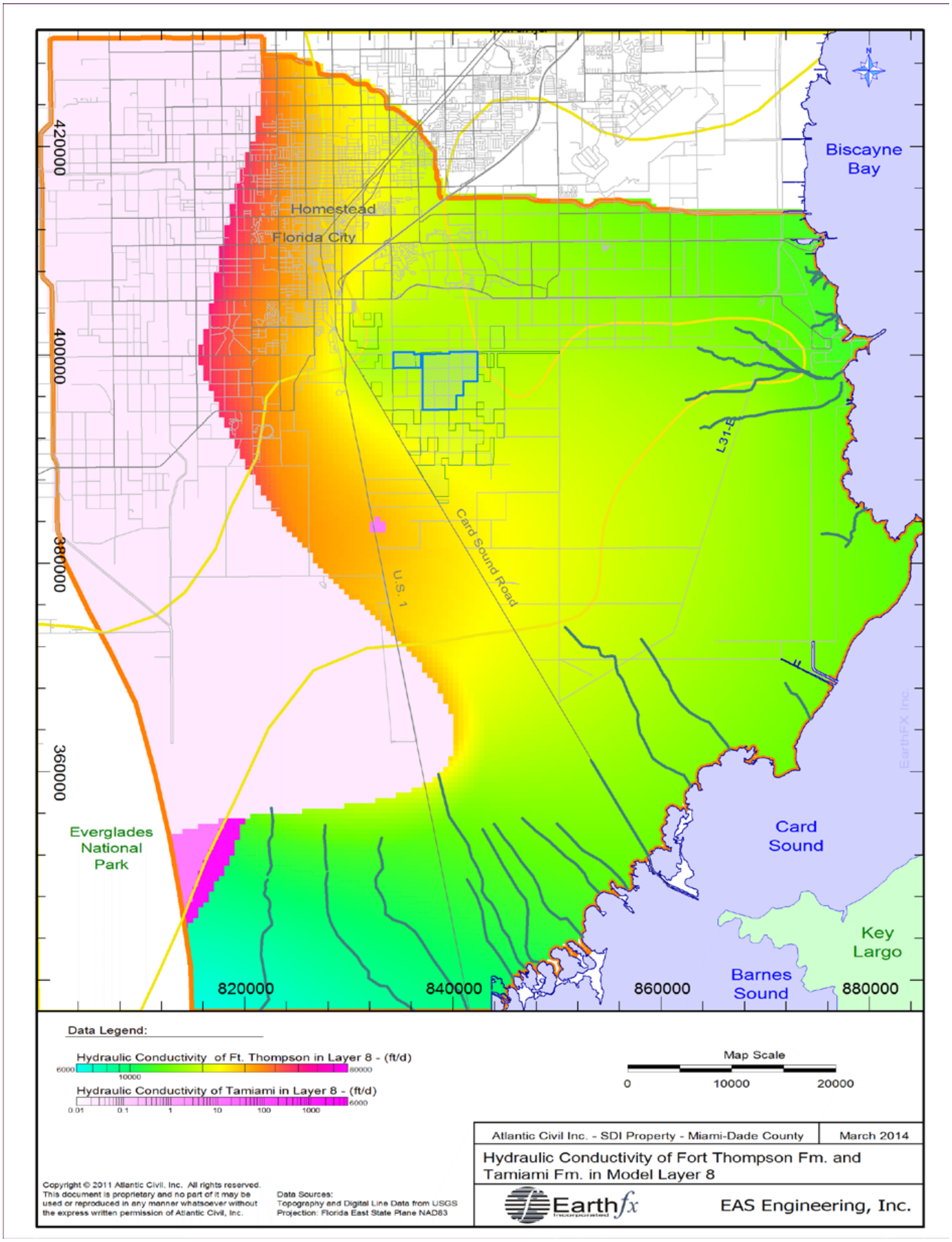

Figure 8: Hydraulic conductivity of Layer 8. Note the two color scales to represent the Fort Thompson and Tamiami Formations.

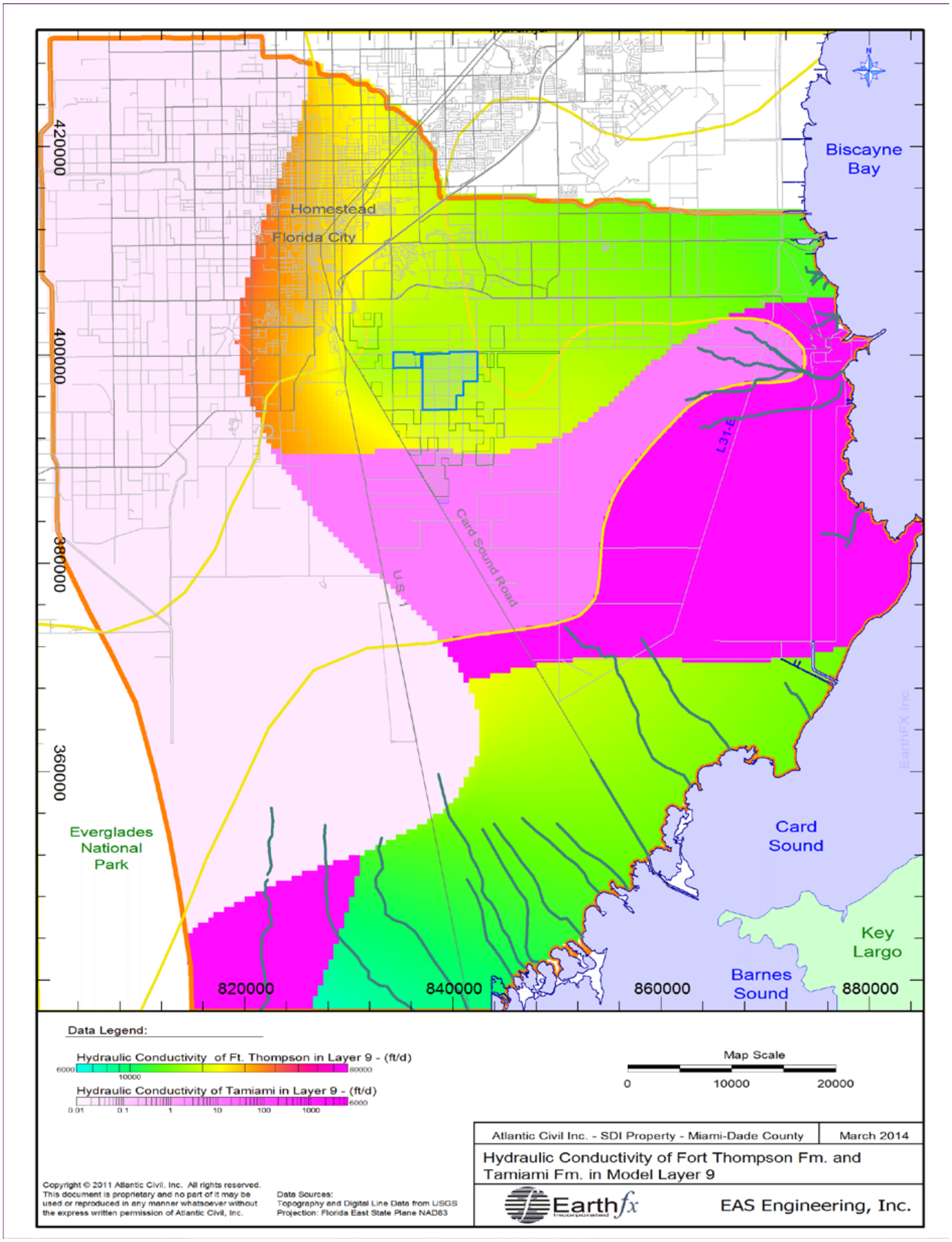

Figure 9: Hydraulic conductivity of Layer 9. Note the two color scales to represent the Fort Thompson and Tamiami Formations.

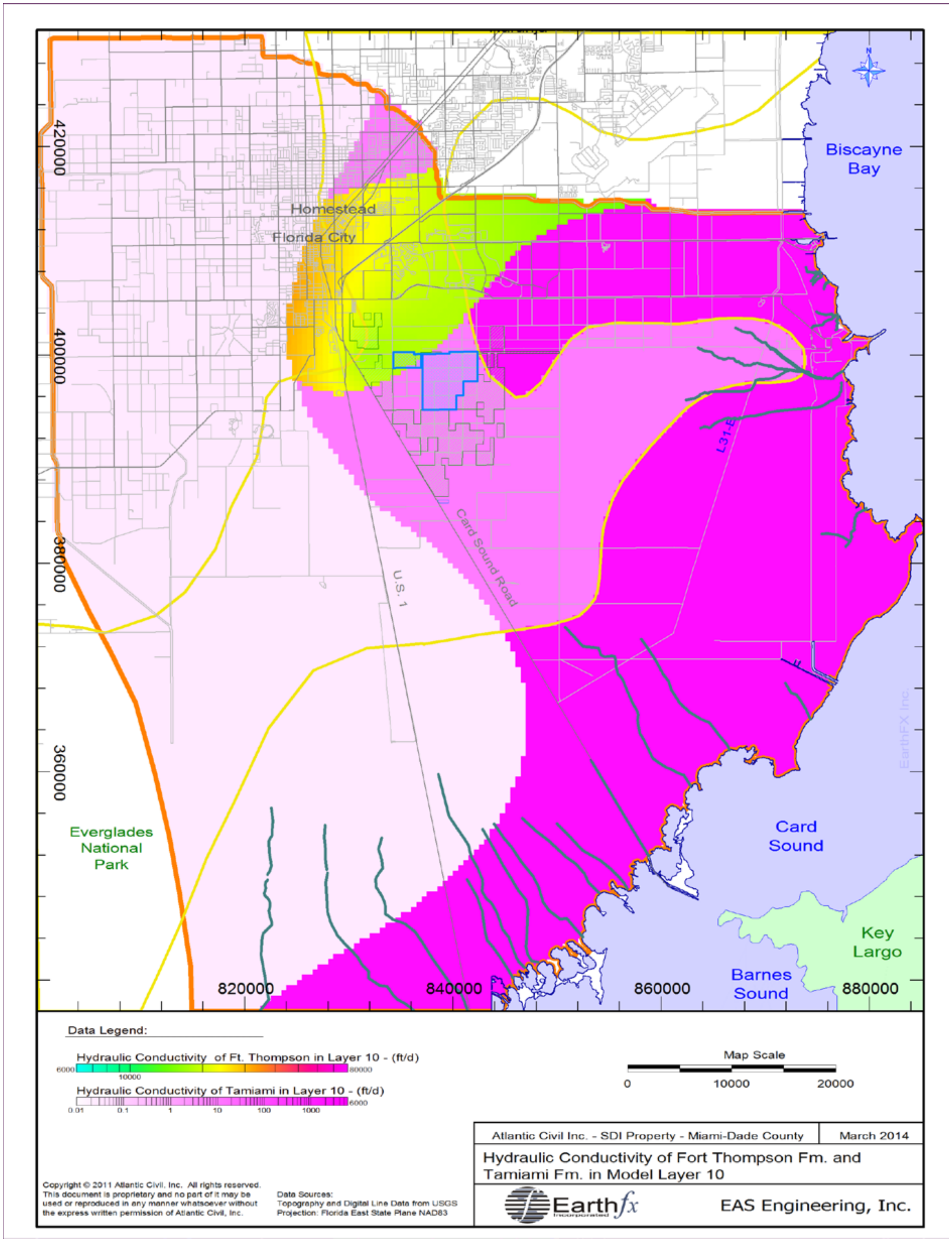

Figure 10: Hydraulic conductivity of Layer 10. Note the two color scales to represent the Fort Thompson and Tamiami Formations.

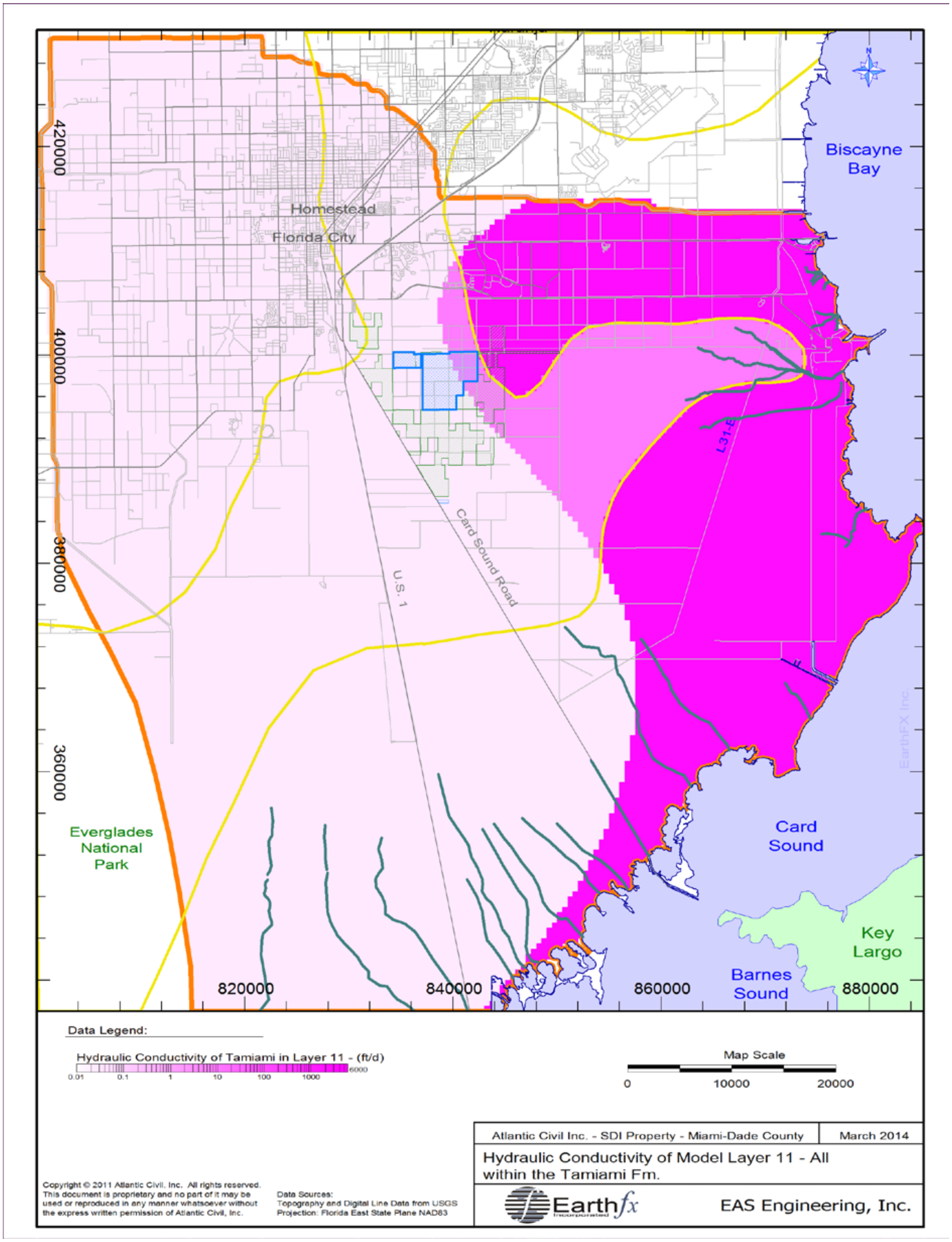

Figure 11: Hydraulic conductivity of Layer 11, assumed to be all within the Fort Thompson Formation.

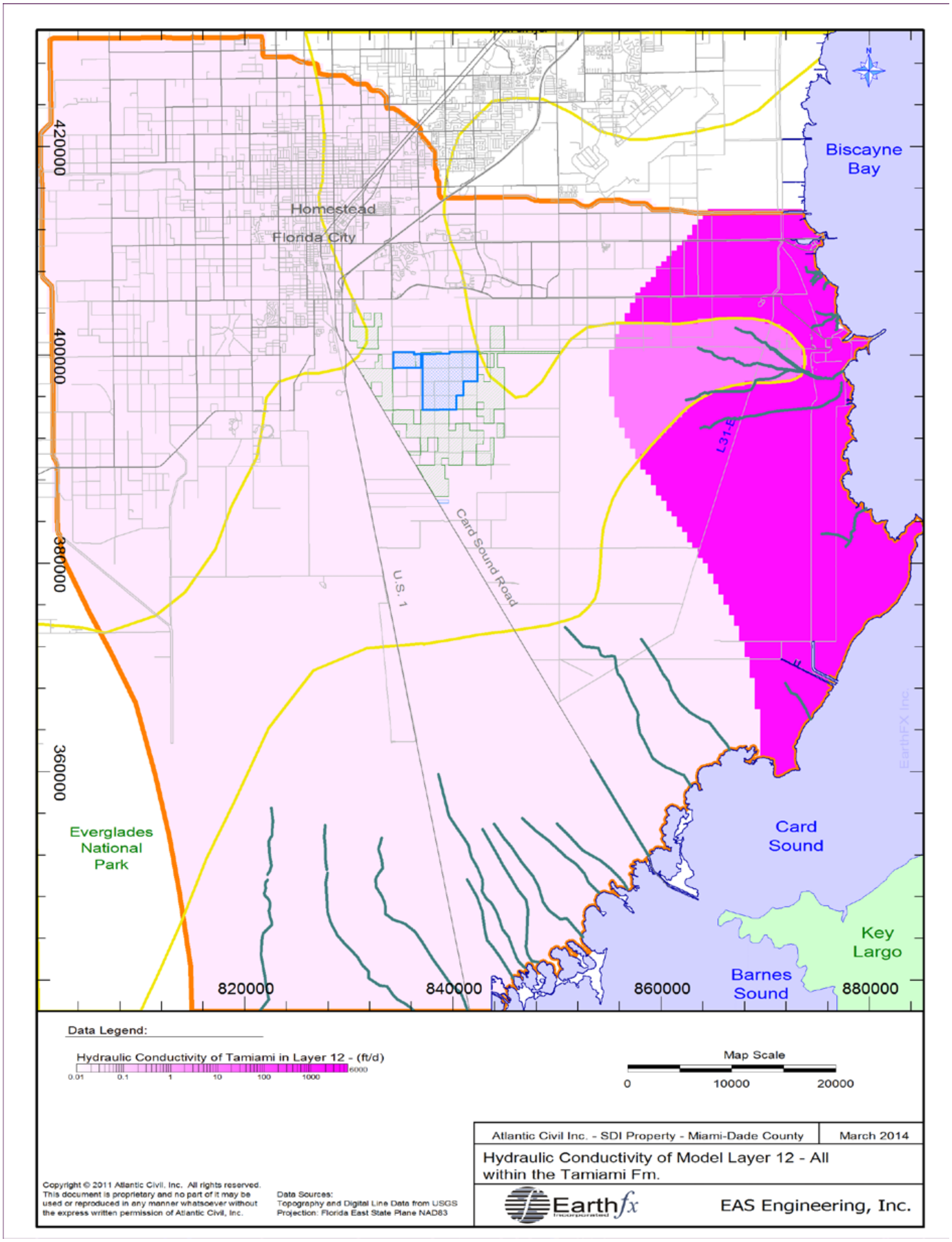

Figure 12: Hydraulic conductivity of Layer 12, assumed to be all within the Fort Thompson Formation.

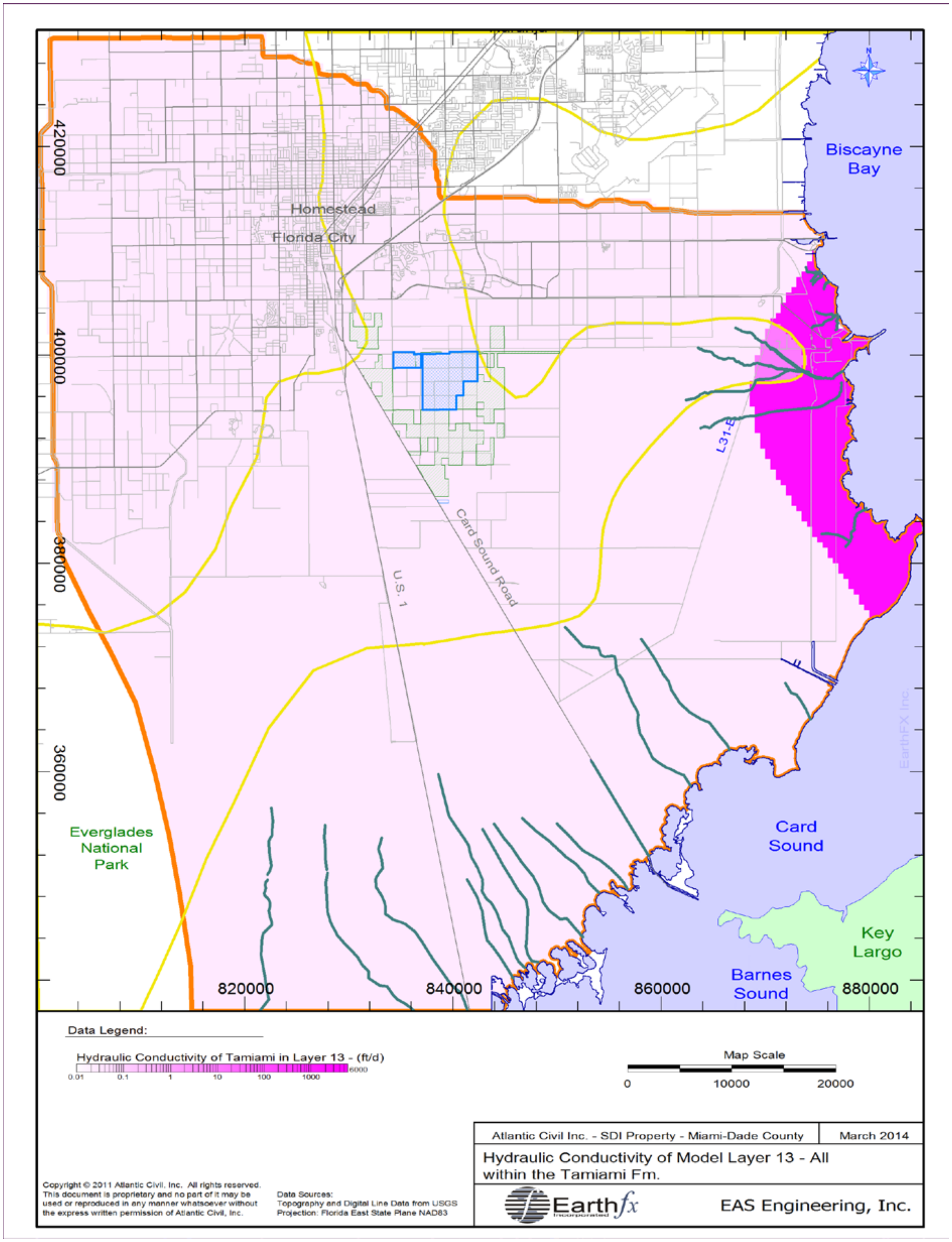

Figure 13: Hydraulic conductivity of Layer 13, assumed to be all within the Fort Thompson Formation.

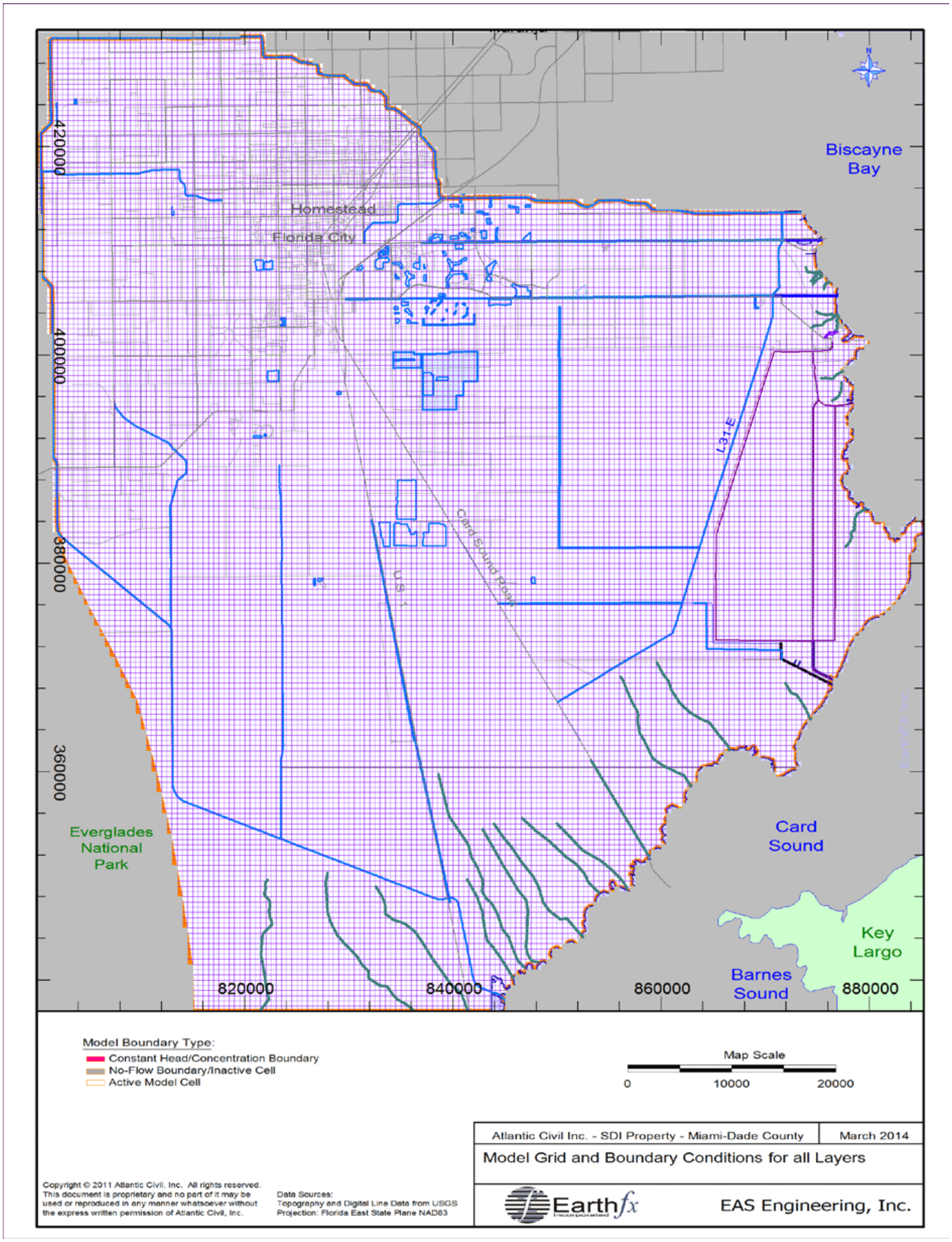

Figure 14: Model grid and boundary conditions for all layers.

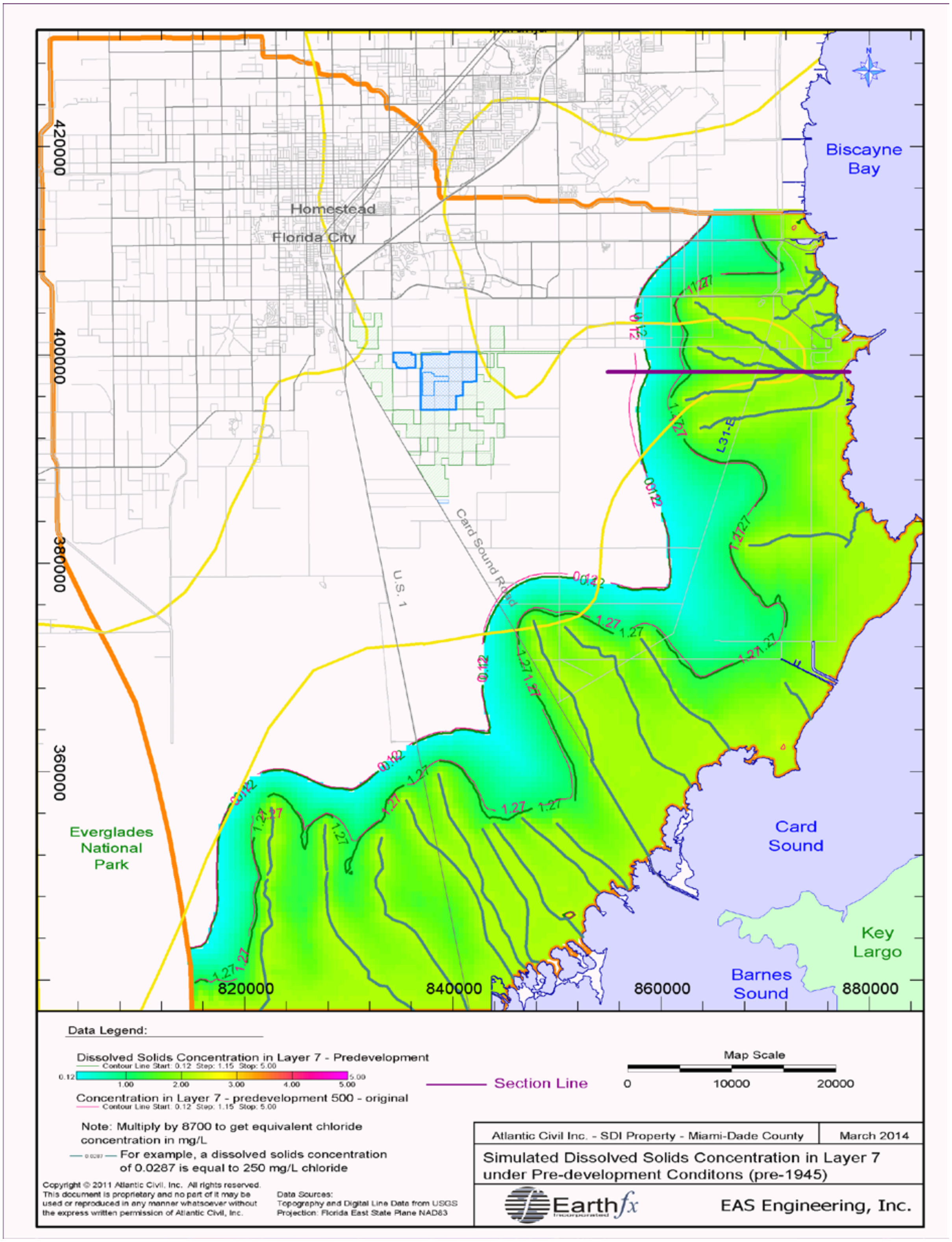

Figure 15: Simulated dissolved solids concentration in Layer 7 at the end of the wet season under pre-development conditions.

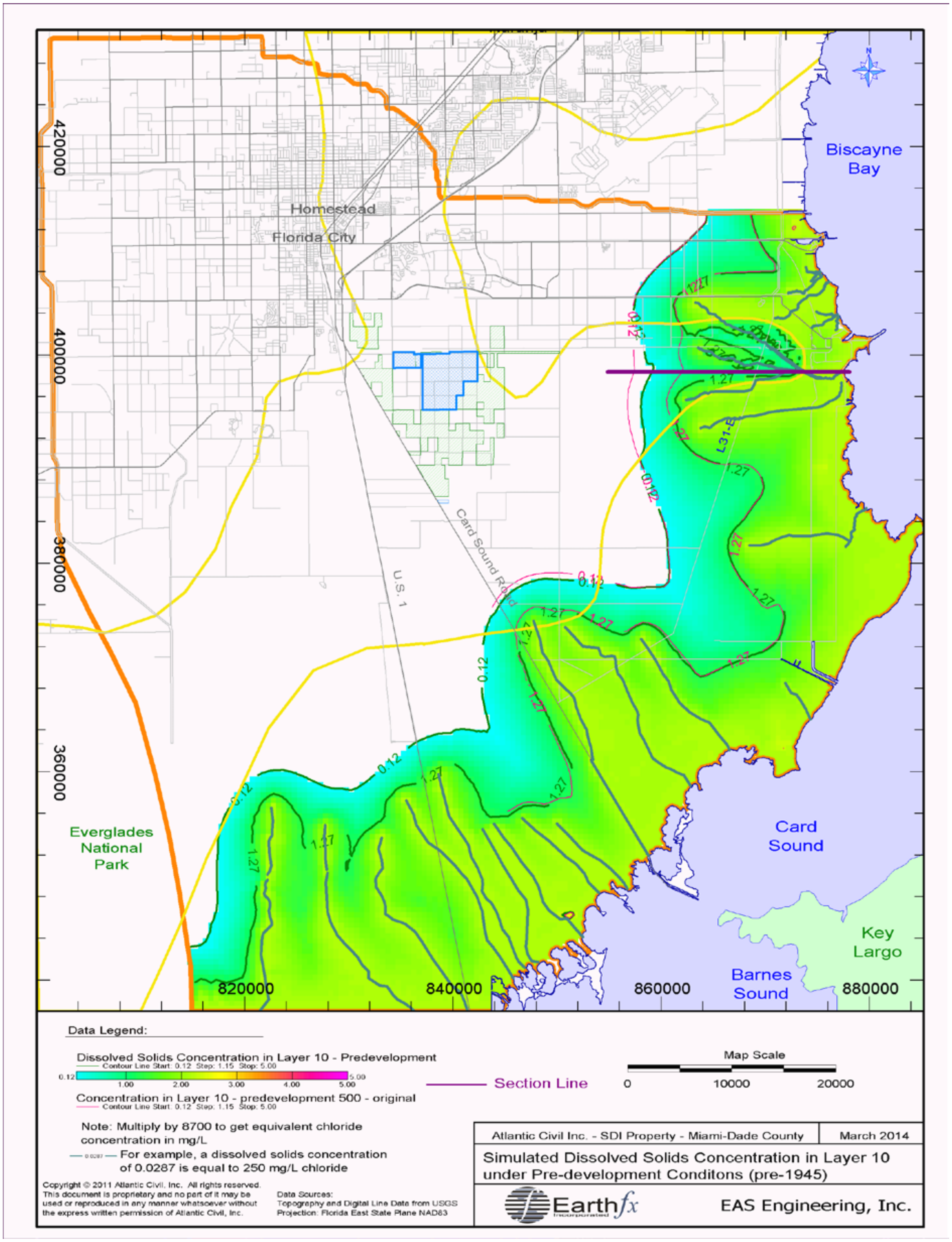

Figure 16: Simulated dissolved solids concentration in Layer 10 at the end of the wet season under pre-development conditions.

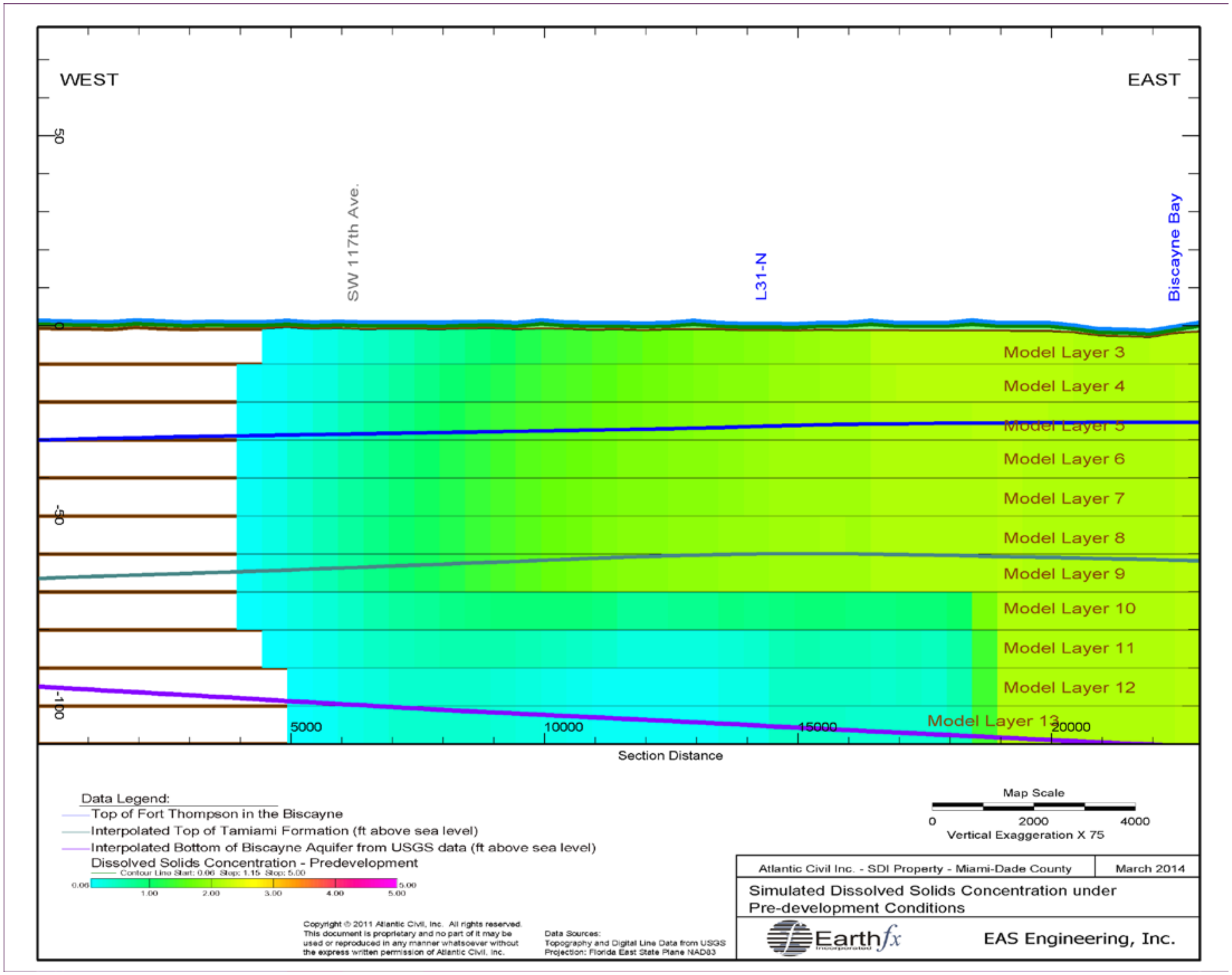

Figure 17: Simulated dissolved solids concentration with depth – pre-development conditions (Section line shown on Figure 15)

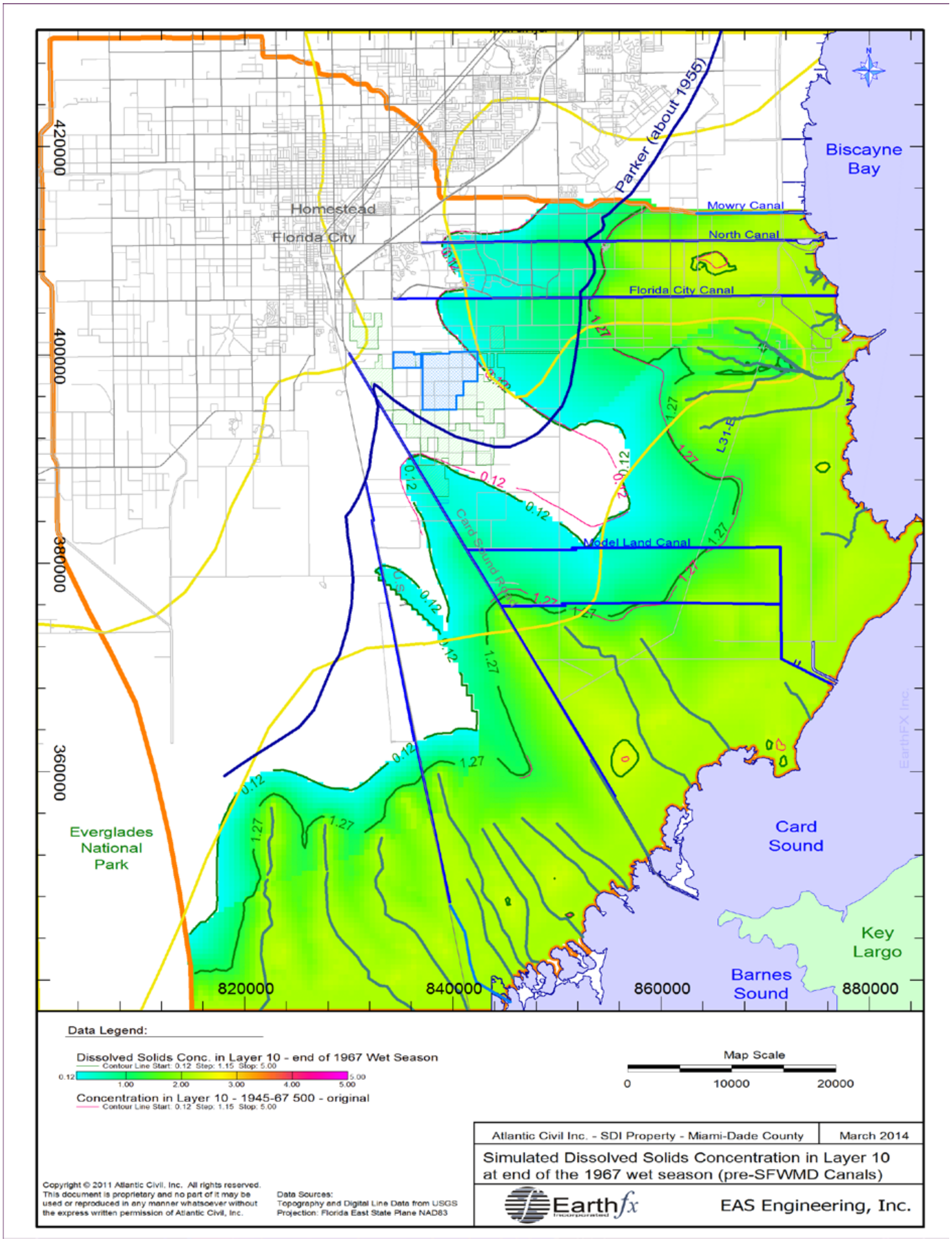

Figure 18: Dissolved solids concentration in Layer 10 at end of 1945 to 1967 simulations.

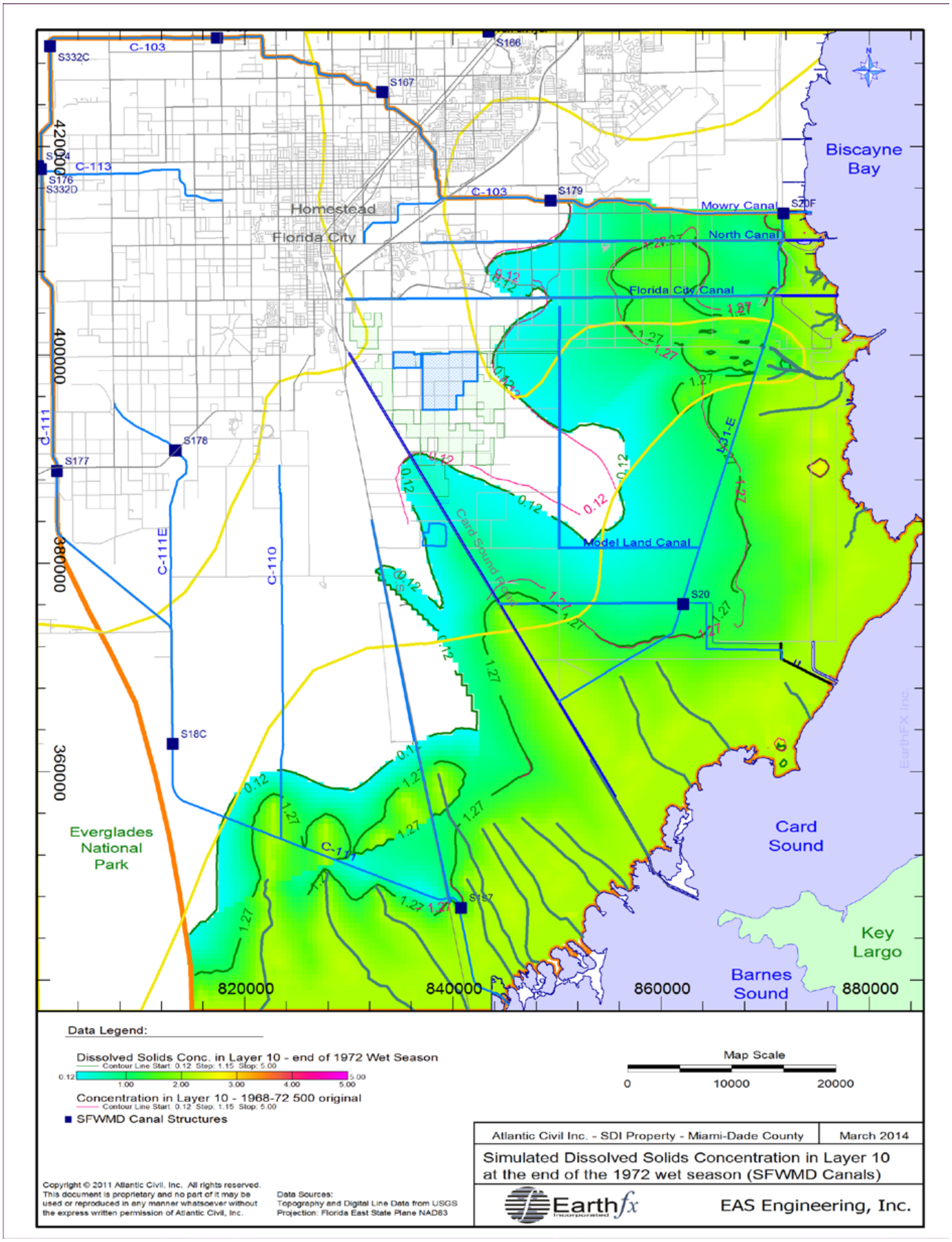

Figure 19: Dissolved solids concentration in Layer 10 at end of 1968 to 1972 simulations.

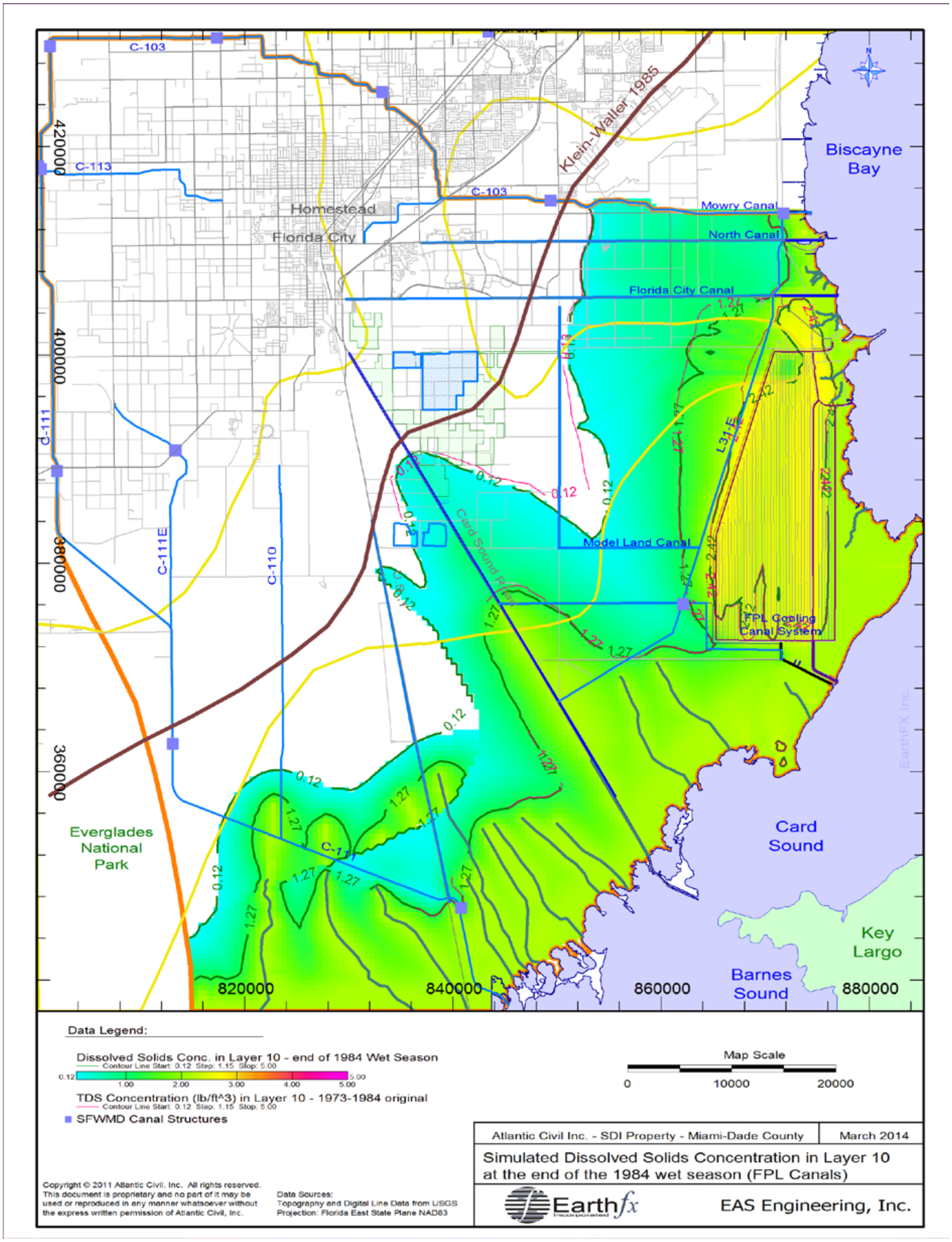

Figure 20: Dissolved solids concentration in Layer 10 at end of 1973 to 1984 simulations.

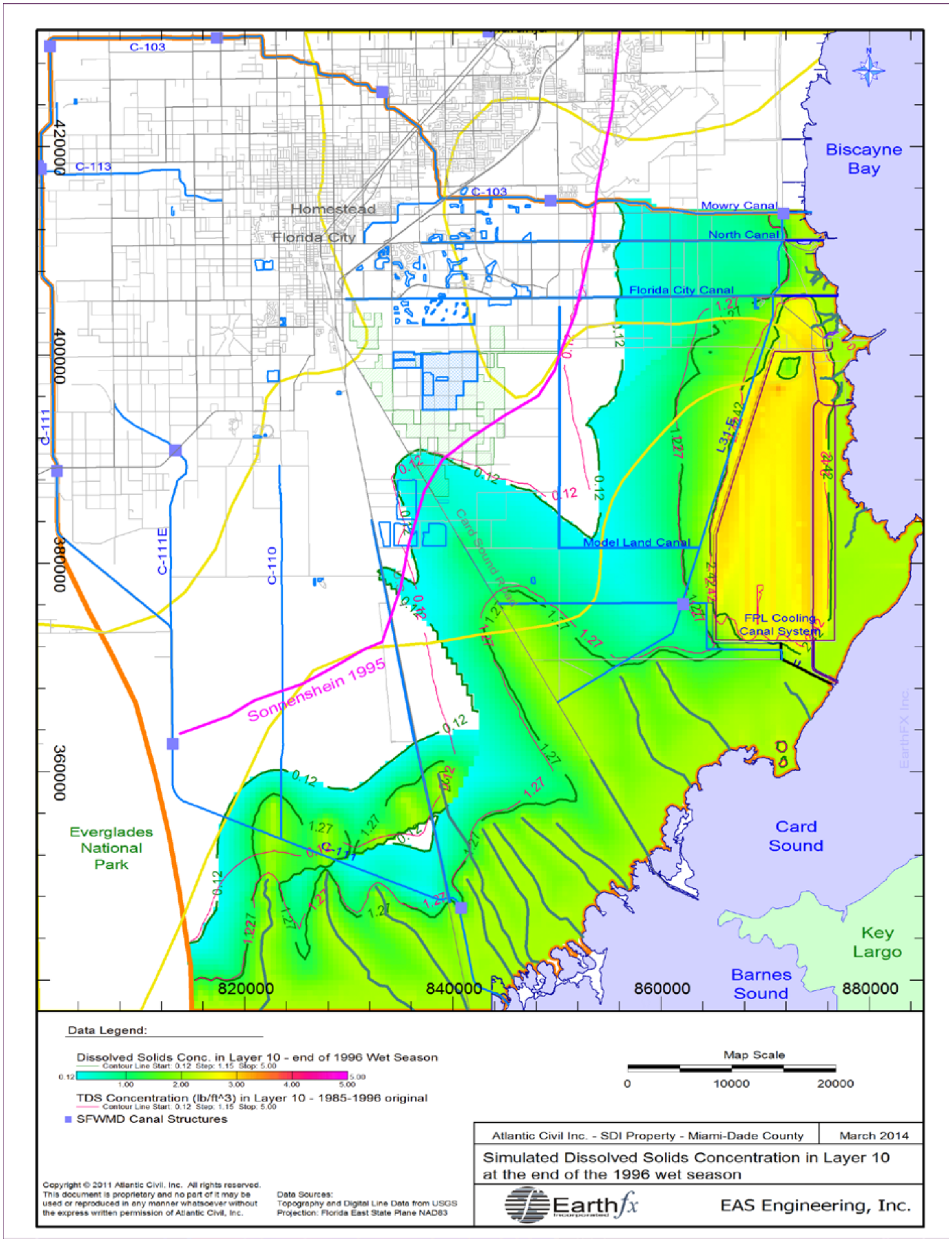

Figure 21: Dissolved solids concentration in Layer 10 at end of 1985 to 1996 simulations.

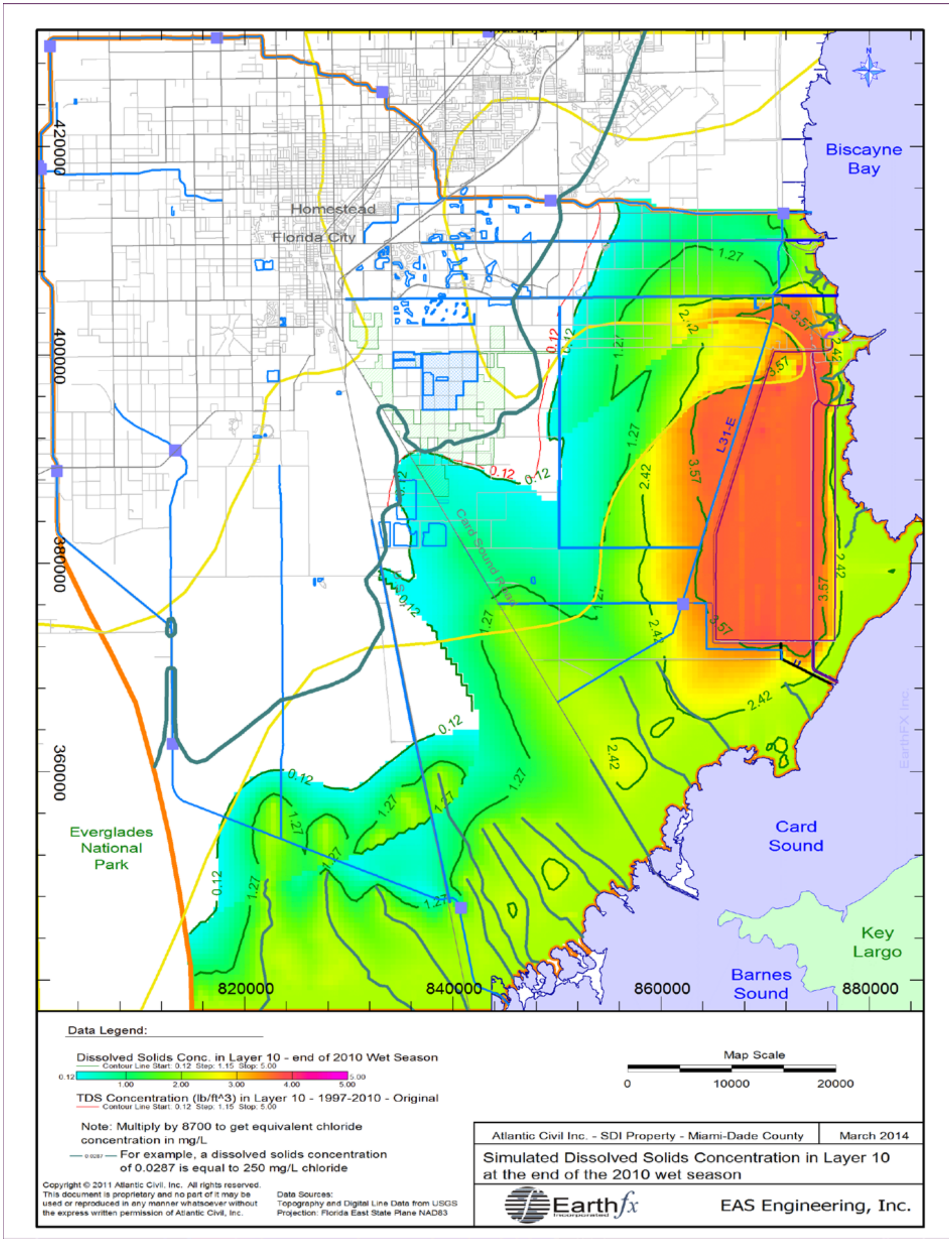

Figure 22: Dissolved solids concentration in Layer 10 at end of 1997 to 2010 simulations.

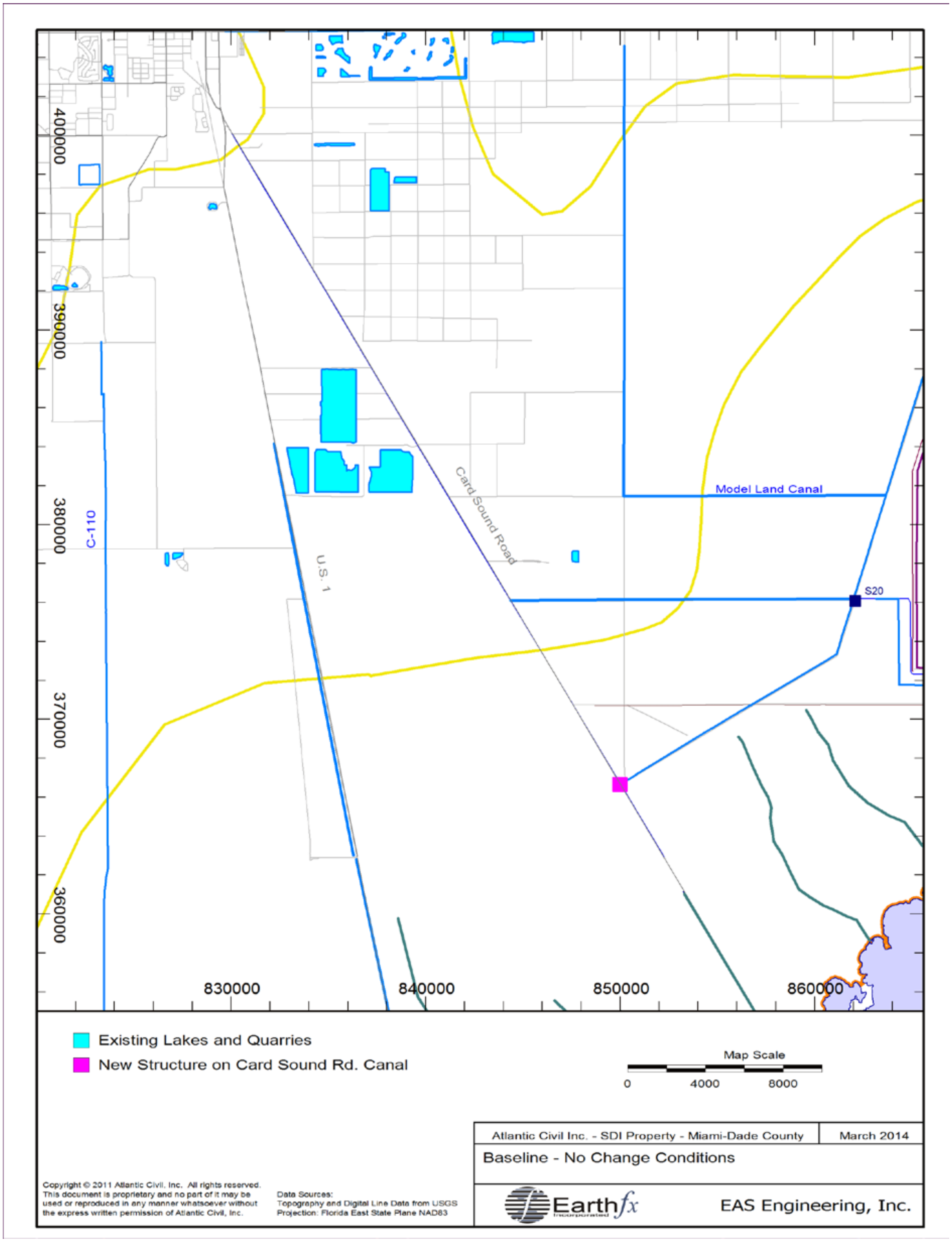

Figure 23: Baseline conditions with existing lakes and new structure on Card Sound.

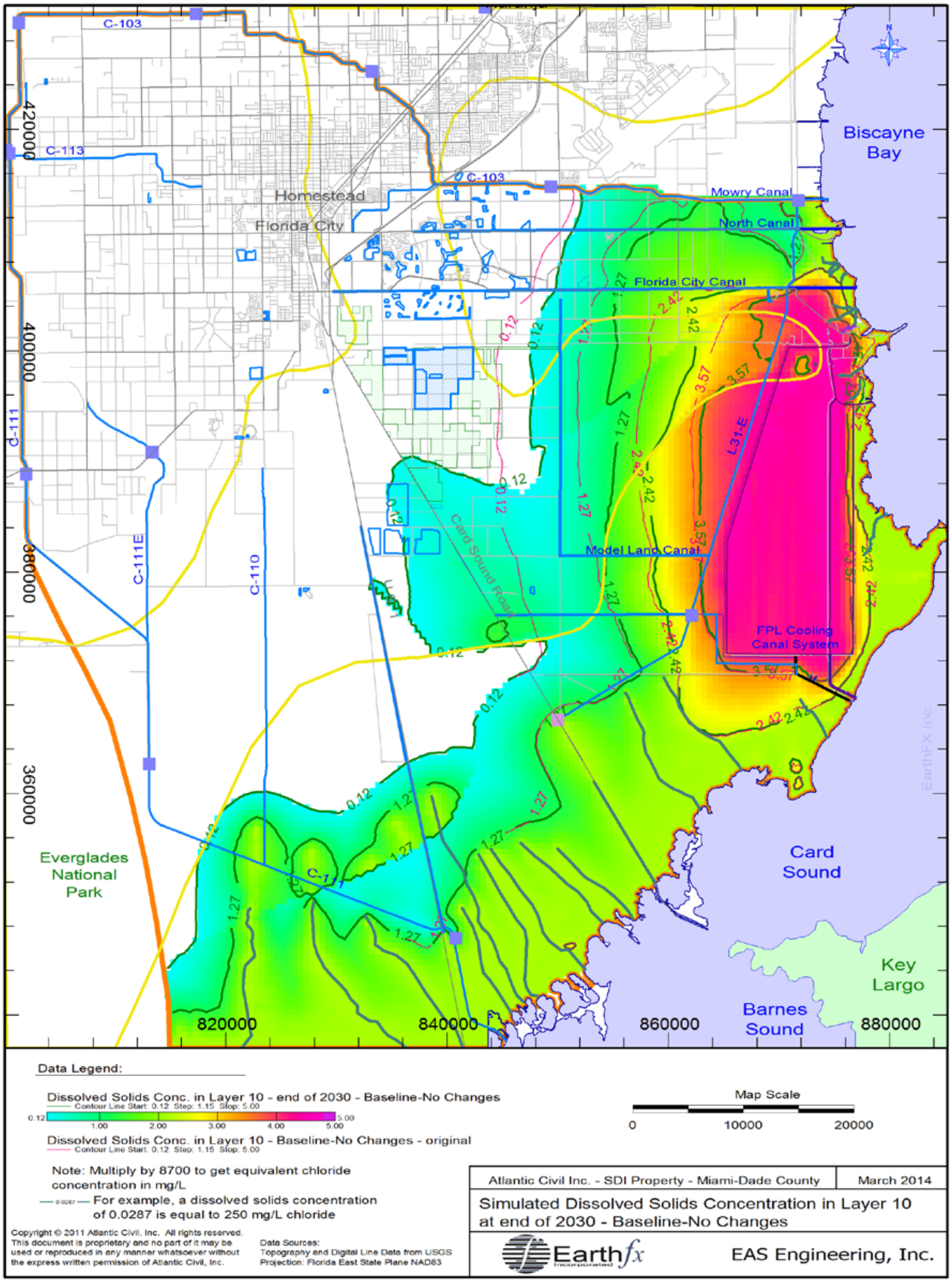

Figure 24: Simulated dissolved solids concentration in Layer 10 at end of 2011 to 2030 simulations - Baseline-No Changes scenario.

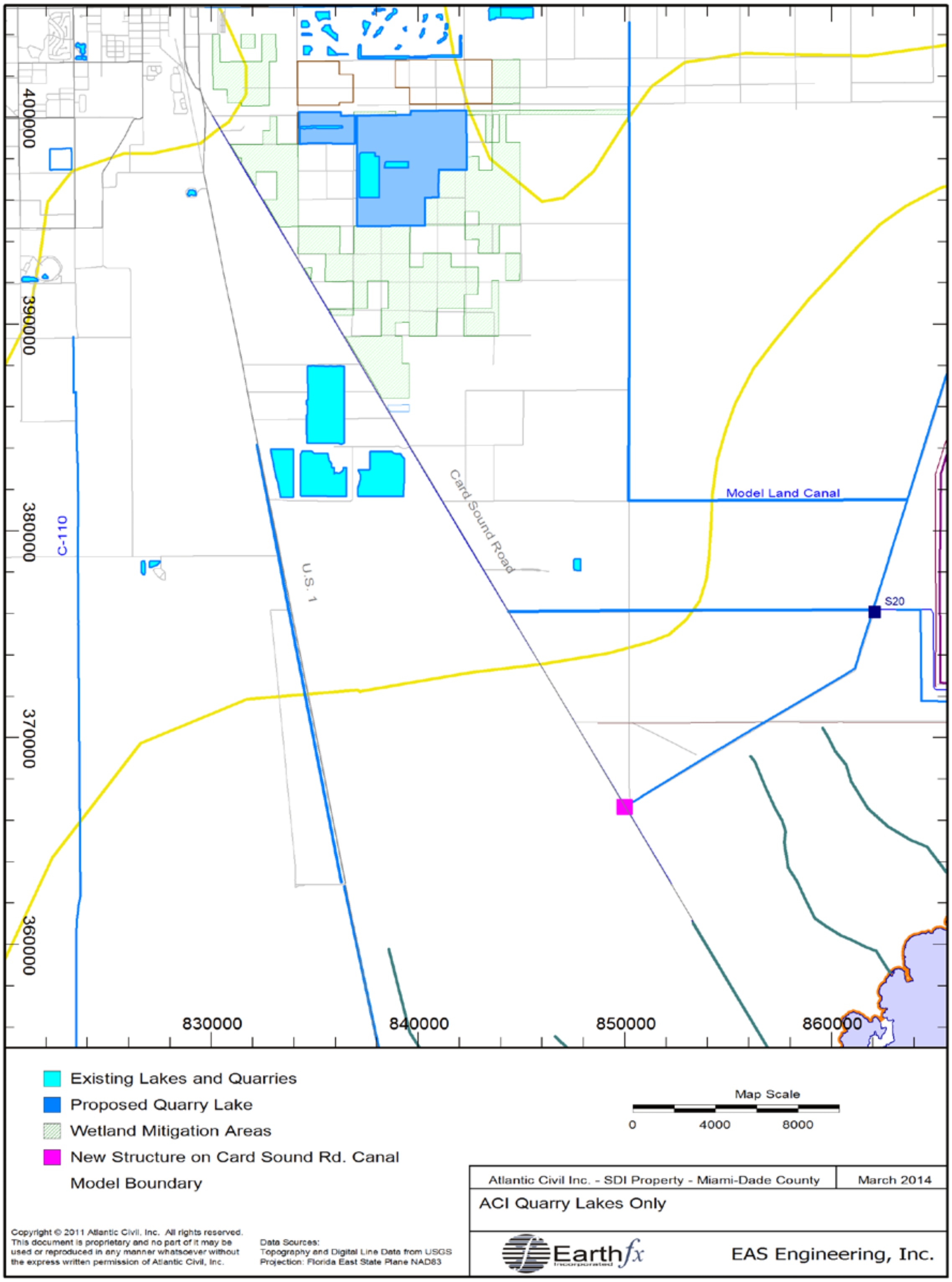

Figure 25: Conditions for "ACI Quarry Lakes Only" with proposed quarry lakes and wetland mitigation areas.

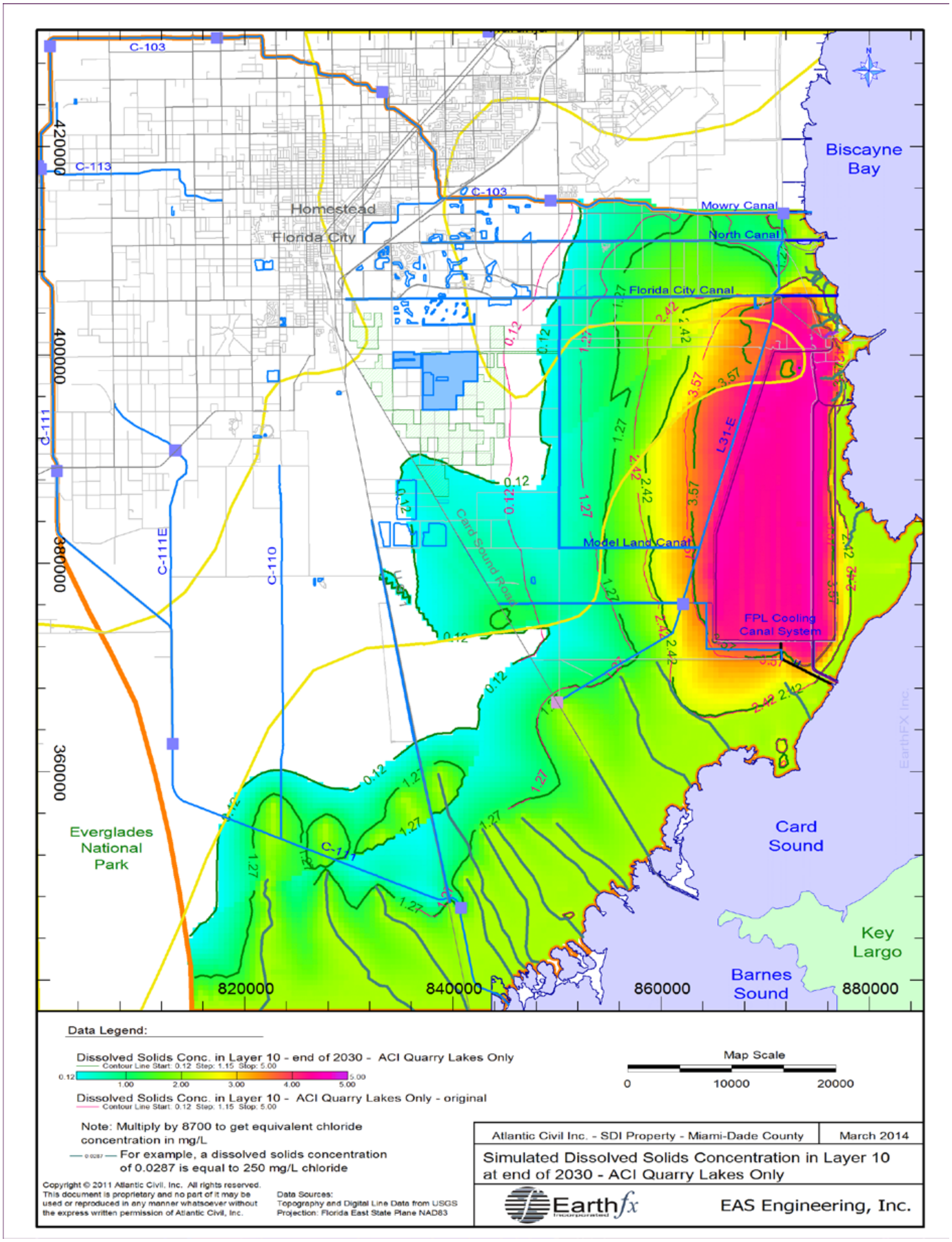

Figure 26: Simulated dissolved solids concentration in Layer 10 at end of 2011 to 2030 simulations - ACI Quarry Lakes Only scenario.

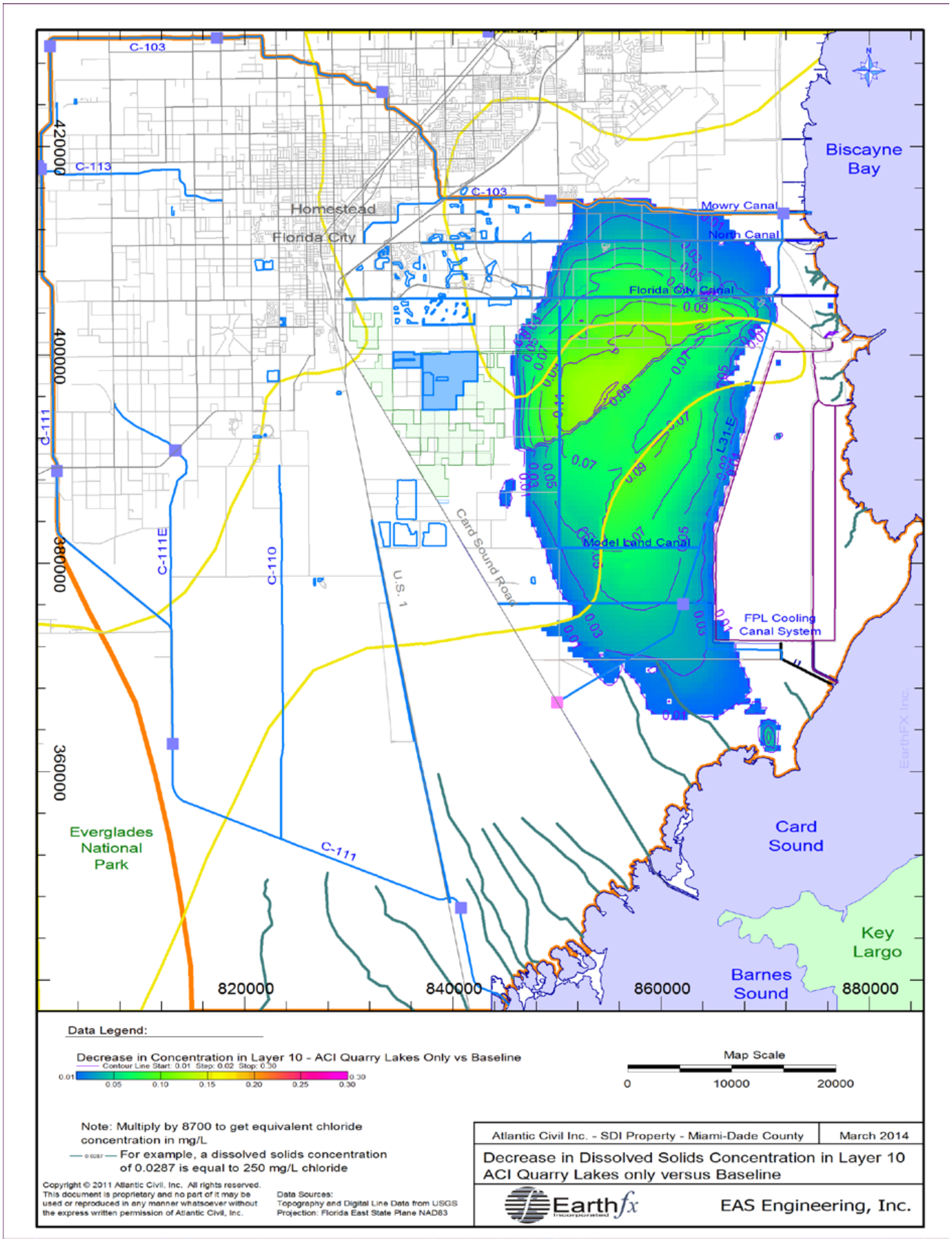

Figure 27: Simulated decrease in dissolved solids concentration in Layer 10 at end of 2011 to 2030 with the proposed quarry expansion but no other changes.

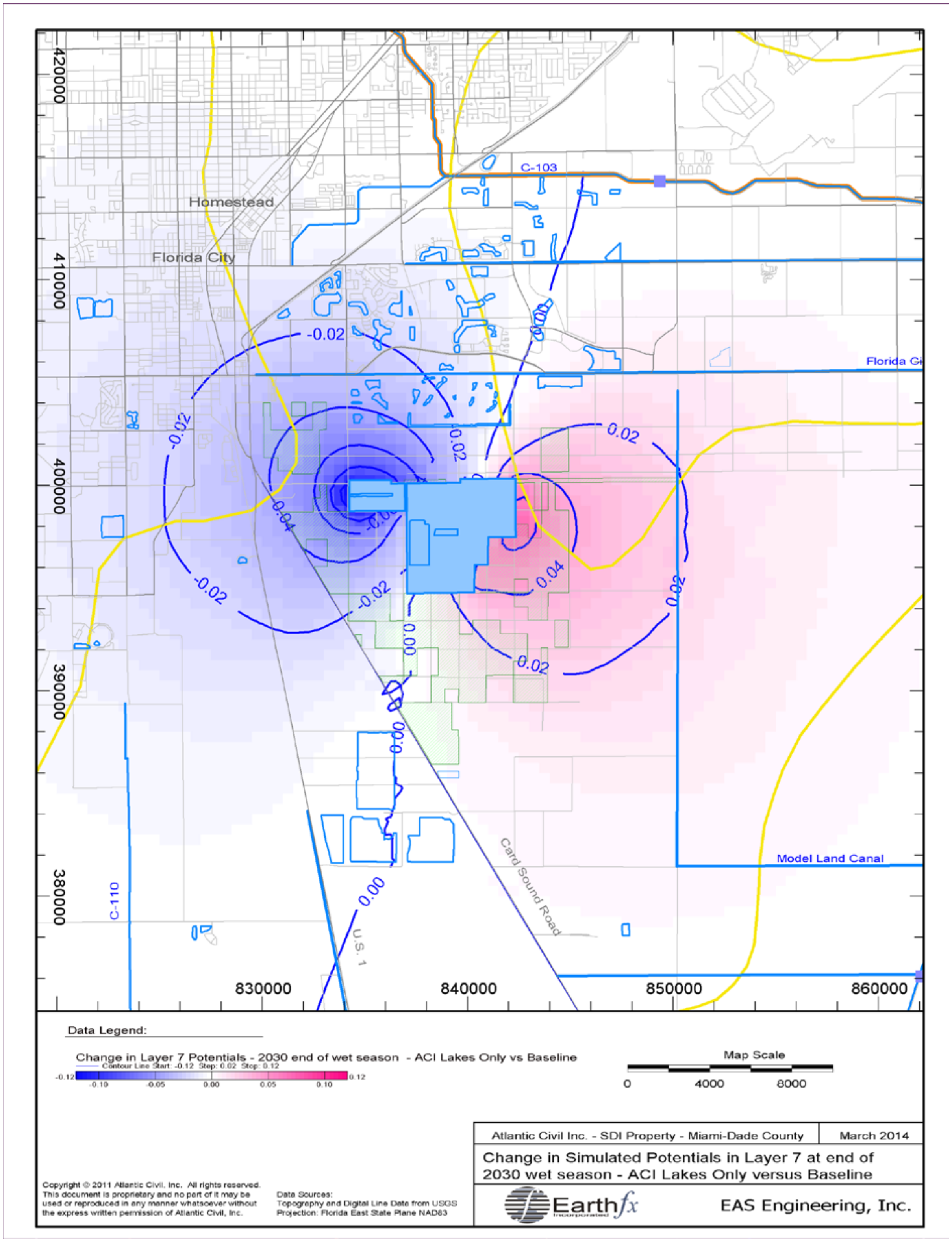

Figure 28: Change in simulated potentials in Layer 7 at the end of the 2030 wet season – ACI Lakes Only verses Baseline-No Changes.

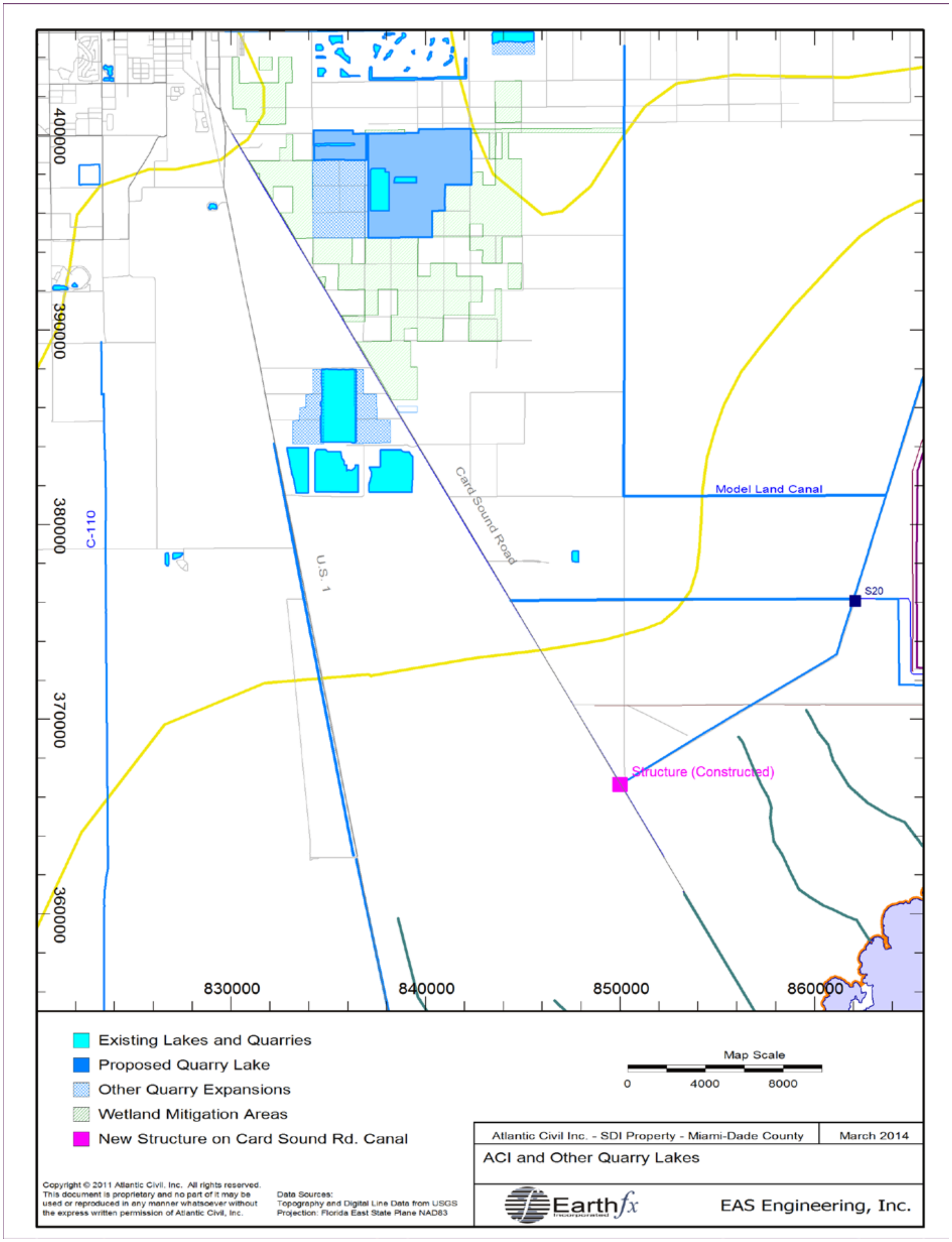

Figure 29: Conditions for "ACI and other Quarry Lakes" with proposed quarry lakes and wetland mitigation areas.

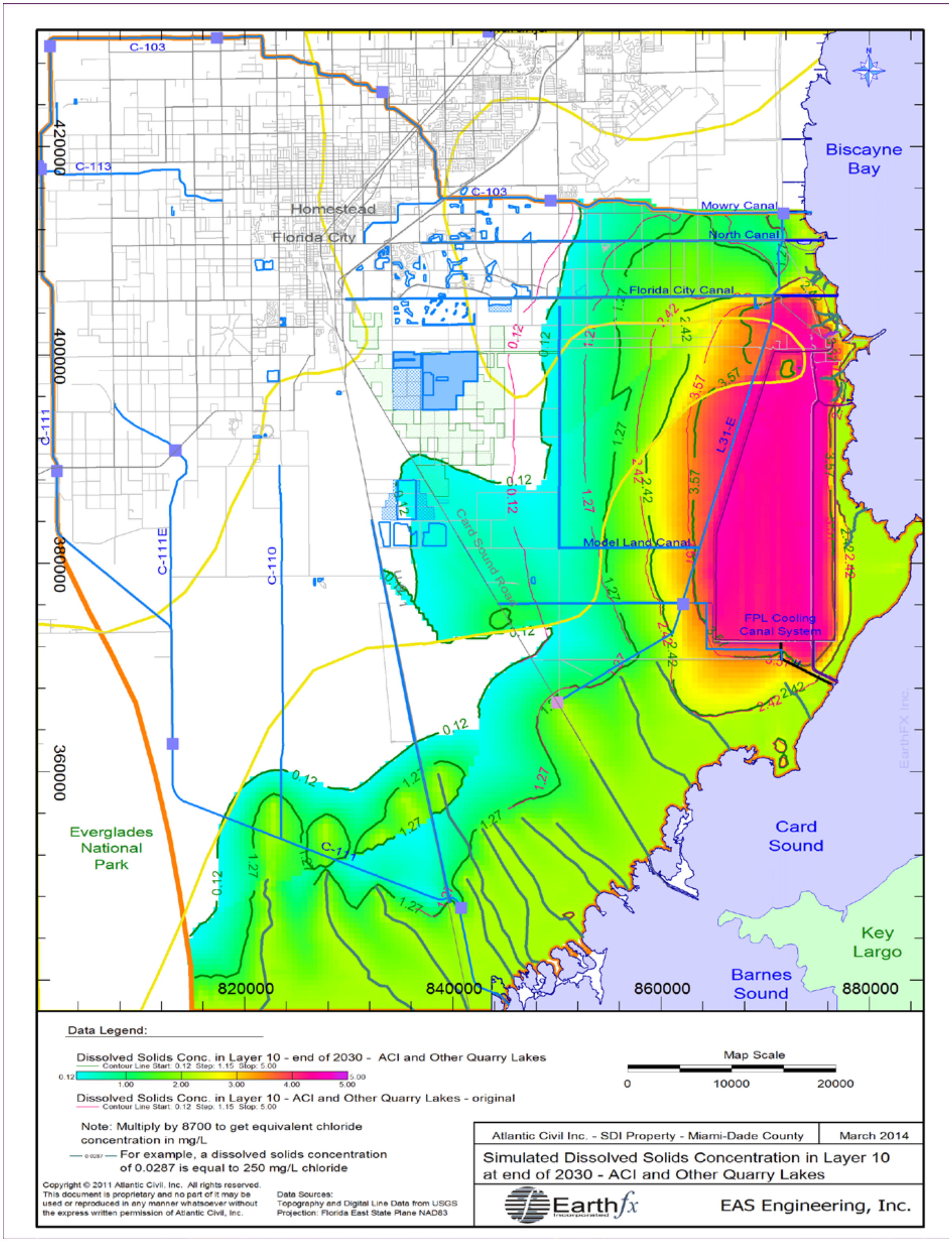

Figure 30: Simulated dissolved solids concentration in Layer 10 at end of 2011 to 2030 simulations - ACI and Other Quarry Lakes scenario.

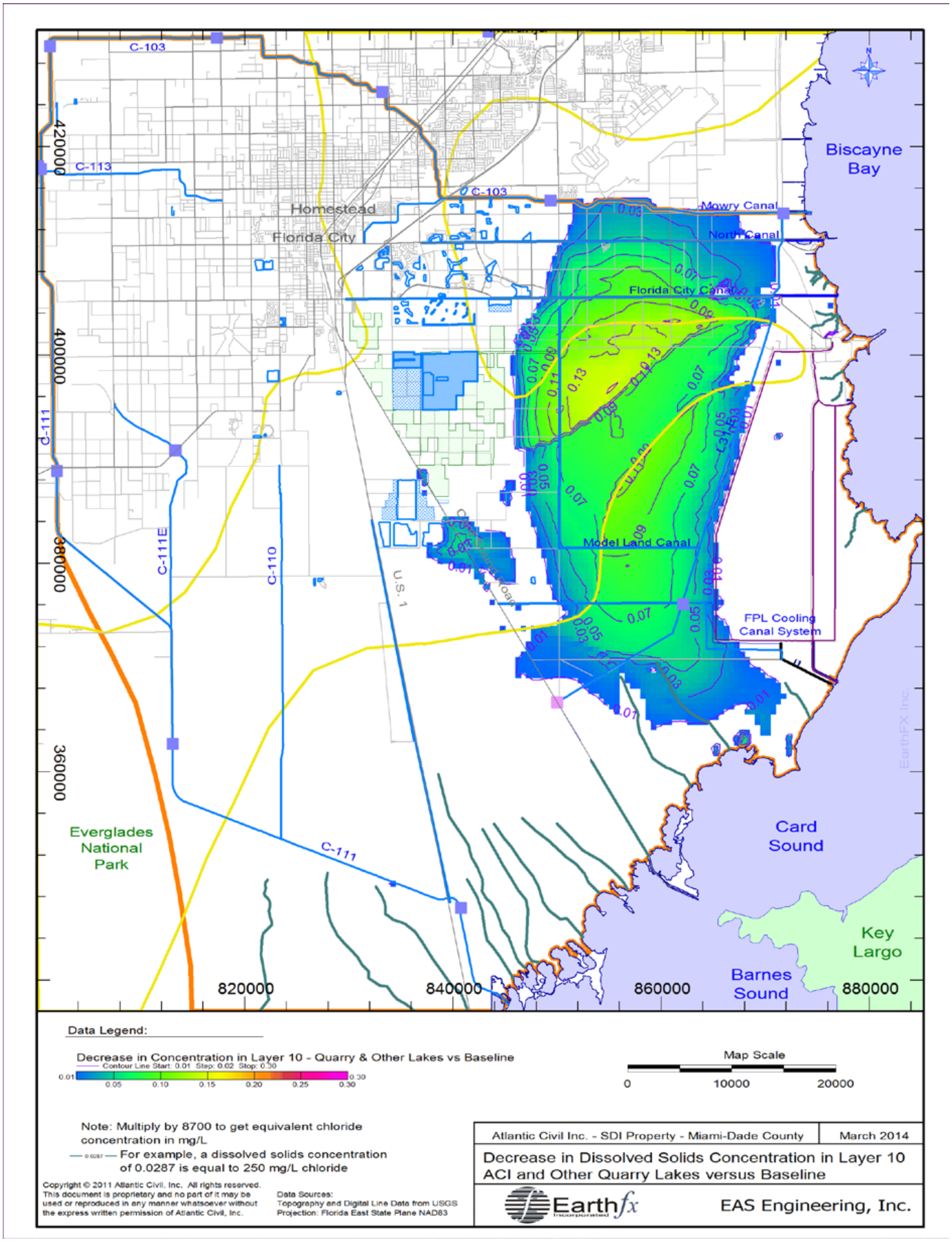

Figure 31: Simulated decrease in dissolved solids concentration in Layer 10 at end of 2011 to 2030 with all other lakes and the proposed quarry expansion.

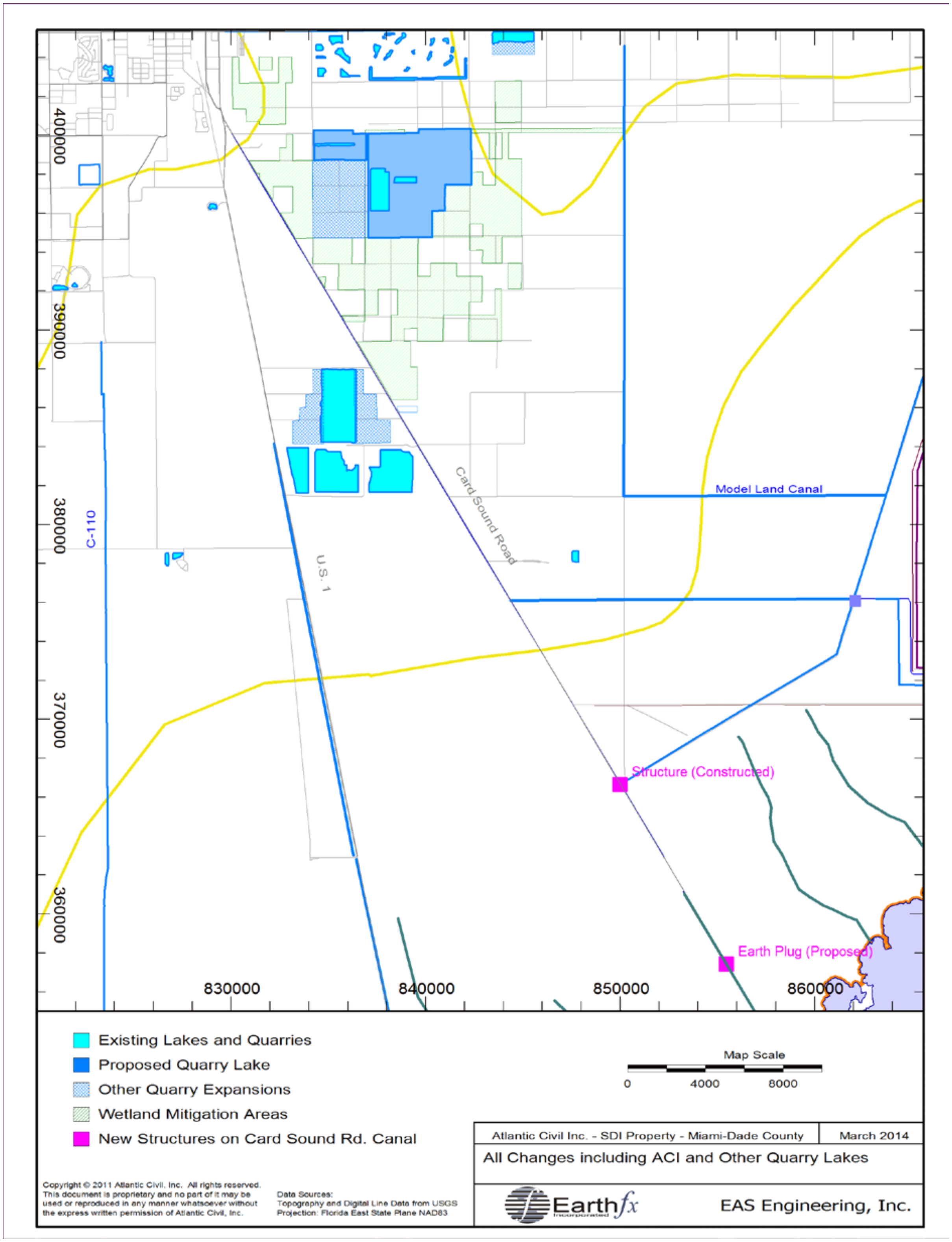

Figure 32: All changes including proposed quarry, other quarry expansions, and new structures.

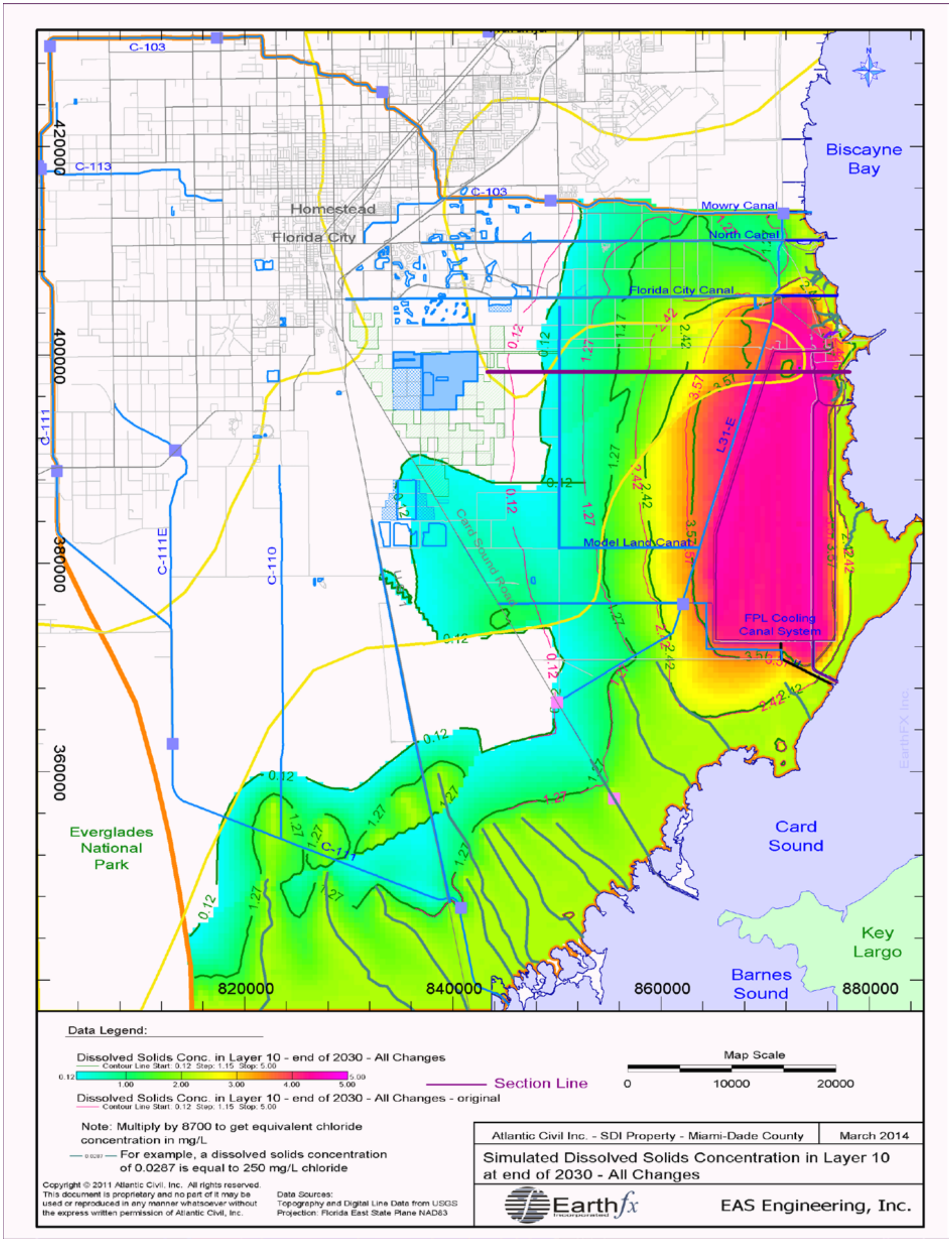

Figure 33: Simulated dissolved solids concentration in Layer 10 at end of 2011 to 2030 simulations - All Changes scenario.

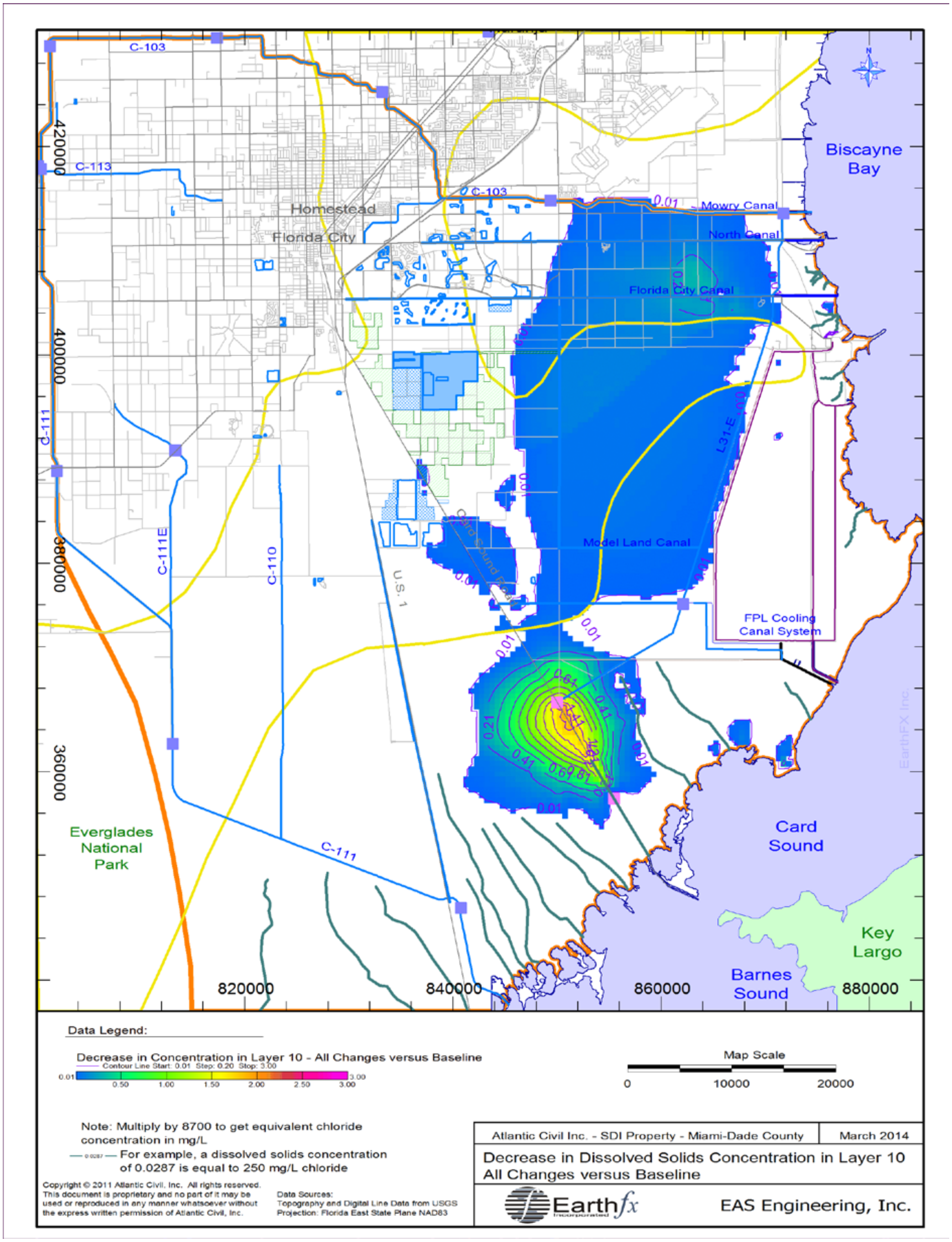

Figure 34: Simulated decrease in dissolved solids concentration in Layer 10 at end of 2011 to 2030 with all changes and the proposed quarry expansion. Note the change in color scale from Figure 31.

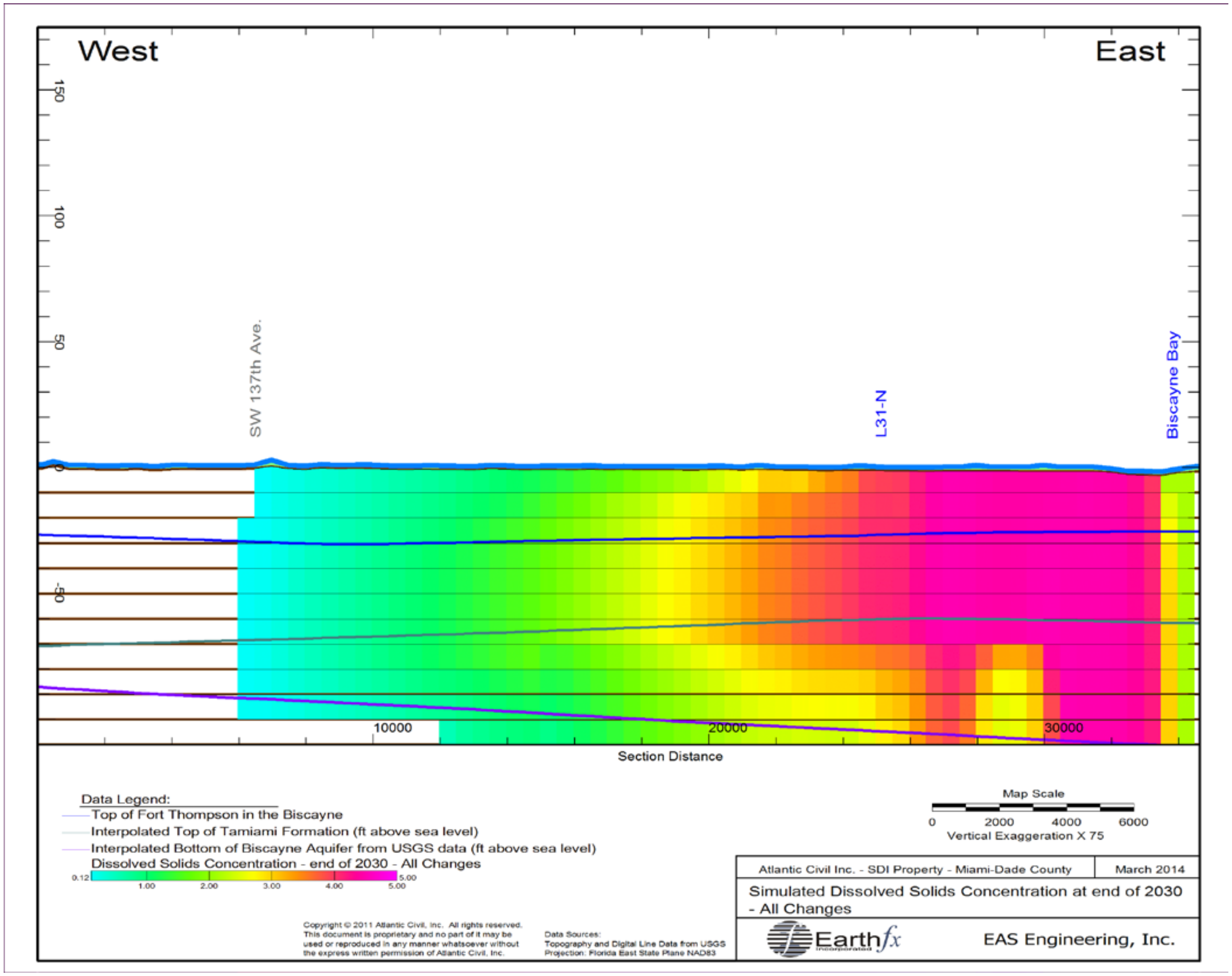

Figure 35: West-east section showing simulated dissolved solids concentration at end of 2011 to 2030 simulations - All Changes scenario. Section line shown on Figure 33.

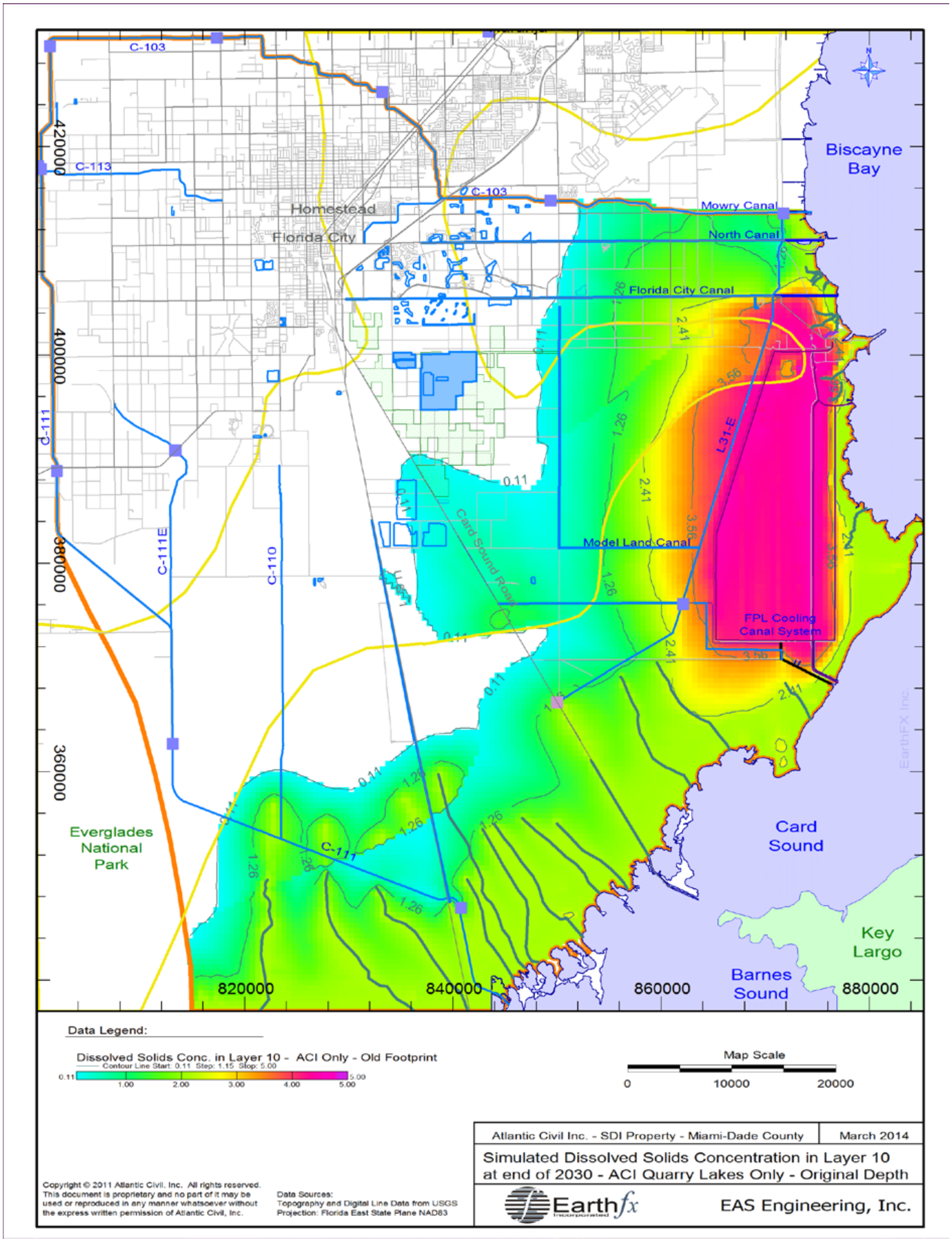

Figure 36: Simulated dissolved solids concentration in Layer 10 at end of 2011 to 2030 with the proposed quarry expansion but no other changes – original quarry lake footprint and depth.

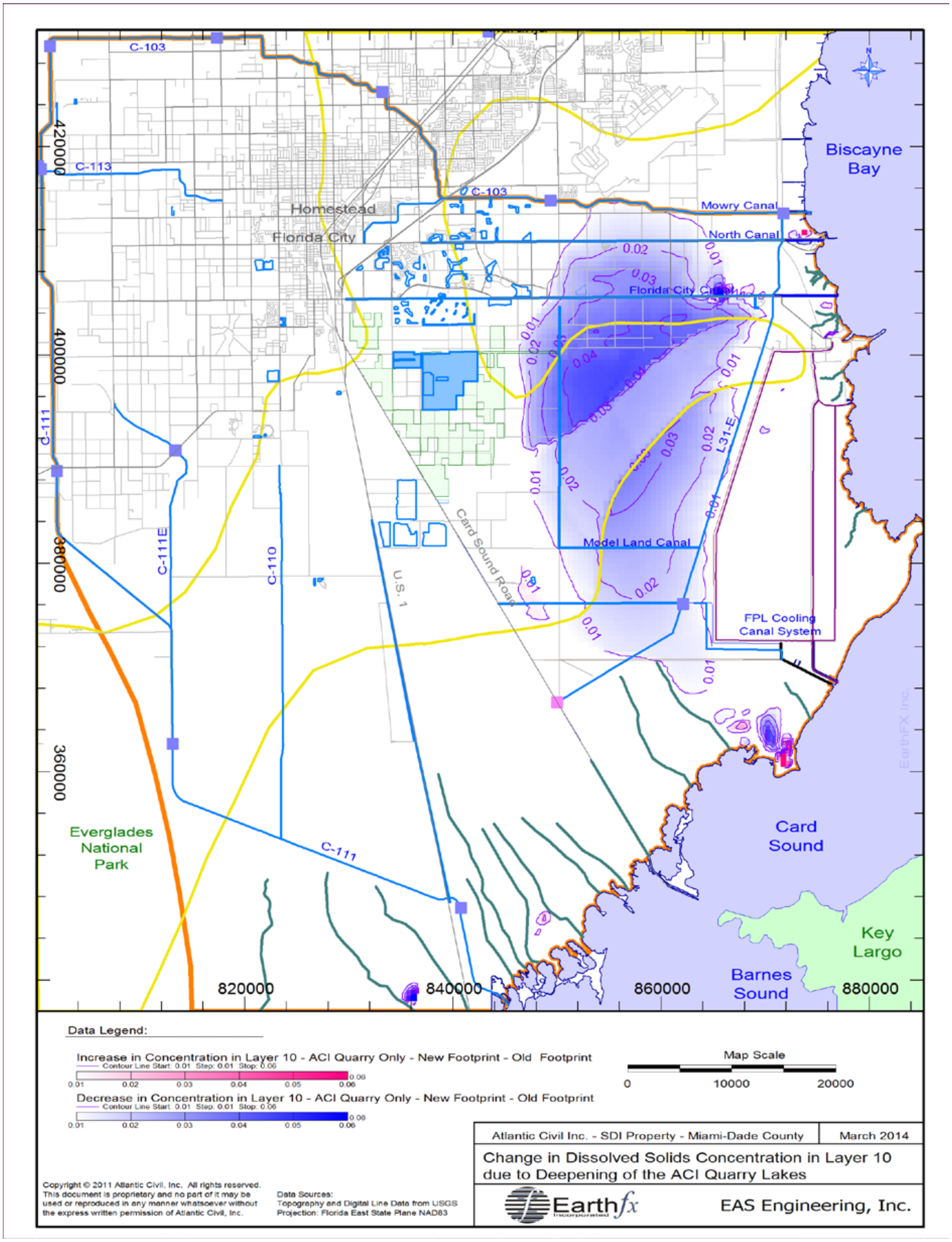

Figure 37: Simulated increase (red) and decrease (blue) in dissolved solids concentration in Layer 10 at end of 2011 to 2030 due to deepening the proposed quarry lakes.

Privileged and Confidential

Review of the FPL Three-Dimensional Groundwater Flow and Saltwater Transport Model

Prepared for:

Lewis, Longman, and Walker, P.A.
EAS Engineering, Incorporated

Prepared by:

Earthfx Incorporated
3363 Yonge Street
Toronto, Ontario M4N 2M6

June 5, 2016

Earth Science Information Systems

March 25, 2014

Edward A. Swakon, P.E., President
EAS Engineering, Inc.
55 Almeria Ave.
Coral Gables, FL 33134
eswakon@eas-eng.com

RE: Additional Groundwater Flow and Saltwater/Freshwater Interface Modeling for the Atlantic Civil Property, South Miami-Dade County, FL.

Dear Mr. Swakon:

Attached is a interim review of a three-dimensional groundwater flow and saltwater transport model of the Biscayne aquifer in the South Dade area developed by Tetra-Tech to analyze saltwater contamination in the in the vicinity of the Florida Power and Light Company (FPL) Turkey Point Cooling Canal System (CCS). As stated by Tetra Tech, the purpose of the model was to (1) support the design of a Recovery Well System (RWS) to intercept, capture, and contain the hypersaline plume north and west of the CCS; support authorization through the appropriate regulatory processes; and demonstrate that it will not create adverse impacts to groundwater, wetland (hydroperiod or water-stage), or other environmental resources, and (2) to continue to assess the status and efficacy of the system operation in meeting the objectives of the Consent Agreement.

It should be noted that we received the model input and output files much before receiving the report documenting model development. Much of the time to date was spent on analyzing the model input files to determine the approach taken, model assumptions, and parameter values. The documentation received is still light on specifics, and working through the inputs is still the best way to understand the model limitations and biases.

We trust this progress report meets with your satisfaction. We look forward to the opportunity to work with you in the future on this and other projects.

Yours truly
Earth*fx* Incorporated

Dirk Kassenaar, M.Sc., P.Eng.

E.J. Wexler, M.Sc., M.S.E., (P.Eng.)

Table of Contents

List of Figures

List of Tables

Review of the Florida Power and Light Three-Dimensional Groundwater Flow and Saltwater Transport Model

1 Executive Summary

Earthfx Incorporated reviewed a three-dimensional variable-density groundwater flow and transport model which was developed by Tetra Tech, Incorporated on behalf of Florida Power and Light Company (FPL). The model simulates groundwater flow in the vicinity of the FPL Turkey Point Nuclear Generating Station and the cooling canal system (CCS). The model also simulates the movement of the saltwater interface and the plume of hypersaline groundwater emanating from the CCS.

Although dismissed out-of-hand in their report (Tetra Tech, 2016), the FPL model appears to be based on the procedures and design of a model developed by Earthfx Incorporated for the same area on behalf of Atlantic Civil Incorporated (ACI). The model boundaries, basic grid design, division of the simulation periods, and other features are identical to the ACI model. The FPL report does not acknowledge these contributions in their report. Where the FPL model deviated from the ACI model, the simplifications made by Tetra Tech generally decreased the reliability and predictive capability of the model, as discussed further below.

Under the Fifth Supplemental Agreement between FPL and SFWMD (Resolution No. 2009-1000), FPL was required to develop "a SFWMD-approved fully-coupled 3-D surface and groundwater density dependent flow model incorporating FPL operational components to evaluate the best alternatives for abatement, mitigation or remediation". Under the recent (October 2015)) Consent Agreement between FPL and DERM, FPL was required to develop refined variable density dependent groundwater/surface water model. The FPL model, however, only considers groundwater flow and is not a fully-coupled surface water and groundwater model. A coupled model would have a surface-water submodel to simulate hydrologic processes such as precipitation, evapotranspiration, overland runoff, groundwater recharge, flow in the canals, and water levels in the CCS and other lakes, as well as the influence of the shallow groundwater system on these processes. Instead, groundwater recharge, CCS levels, and canal levels are specified as "known" inputs to the model.

Key differences between the FPL and ACI models include (1) extension of the active model area under Biscayne Bay so that impacts of hypersaline water on the bay can be considered, and a slightly higher level of grid refinement in the vicinity of the CCS where grid cells 200 ft on a side are used instead of a uniform 500 ft cell size. The increased grid resolution represents the one major improvement over the ACI model.

The FPL model layers are deformed to follow the base of the Biscayne Aquifer. Despite their claim to represent regional aquifer characteristics; their model layers with properties based solely on local aquifer testing and assume those values are constant across the entire model area. The transmissivities for the Fort Thompson Formation do not match aquifer regional aquifer characteristics as reported in USGS reports which increase dramatically to the west of the CCS. Transmissivity values are generally lower by a factor of 3 to 4 compared to aquifer transmissivity values mapped by Merritt (1997) and much lower than the calibrated transmissivity values in Hughes and White (2014). This has a noticeable effect on the predicted water levels; for example, the simulated heads at the FKAA wellfield exceed 6 ft below sea level in an area known have extremely high transmissivity. As well, the low transmissivity values assumed in the FPL model contribute to the unrealistic high simulated heads seen periodically in the Model Land area. Tetra Tech acknowledged that the low transmissivity values were a reason for the model's inability to match the westward extent of the saltwater plume. They increased the values in later model runs but did not attempt to match the observed values.

Unlike the ACI model, the FPL model does not account for sheet flow that can occur periodically in the Model Land area. This is another contributing factor to the unrealistic high simulated heads seen in the area. The FPL model does not represent lakes.

Surface water features were represented by MODFLOW “rivers” and “drains”. The exact method for assigning and adjusting conductance values is unclear and appears to be applied in an inconsistent manner. The values assigned appear to favor limiting leakage of saltwater from the CCs and favoring capture by the interceptor drain and dilution by leakage from L31-E.

The FPL model does not allow net recharge to decrease below zero and does not account for groundwater losses due to evapotranspiration from deeper root systems when the water table is near surface. The model does not properly represent seasonal conditions in which ET losses exceed groundwater recharge from rainfall. This is a key process in south Dade County and is responsible for the accelerated westward movement of the natural saltwater interface and the body of hypersaline water.

The calibrated FPL model was able to represent observed chloride concentrations in 2010 in the CCS vicinity reasonably well. Chloride values below Biscayne Bay are higher than observed, however. Use of the model in a predictive capability for areas west of the CCS should be viewed with caution in light of the model simplifications discussed in this review.

2 Introduction

2.1 Previous Work

Earthfx Incorporated (2012, 2014) developed a numerical model on behalf of Atlantic Civil Incorporated (ACI) to simulate regional groundwater flow and saltwater movement in the vicinity of the ACI property using the USGS SEAWAT code. The model was developed in support of an application to expand the quarry and, at the request of US Army Corps of Engineers, the model was used to conduct a cumulative impact assessment (CIA) for the site and surrounding area.,

The model used hydraulic properties and recharge rates based on the available field data and the results of previous modeling studies by the U.S. Geological Survey (USGS) and Earthfx. The model was calibrated by matching response in observation wells and the mapped position of the saltwater front. The model was reviewed by the US Army Corps of Engineers – Jacksonville.

The primary focus of the modeling effort was to examine the impact of the quarry development on the position of the saltwater front but considered the effect of other water use in the area. The model simulated transient, density-dependent groundwater flow and solute transport and represented groundwater extraction for water supply and agriculture, the history of change to the South Florida Water Management District (SFWMD) canal systems, and the cooling canal system (CCS) operated by Florida Power and Light (FPL). The model was calibrated to match observed history of groundwater levels and the position of the freshwater/saltwater (FW/SW) interface. Results of saltwater intrusion modeling were presented in a series of plan view maps and animations of dissolved solids concentrations. Results of predictive scenarios for the period from 2010 to 2030, which included the proposed ACI quarry expansion along with the expansion of other nearby quarries, changes in SFWMD canal operations, and increased salinity in the CCS, showed that the construction of the ACI quarry will not cause landward movement of the salt front. However, results clearly indicated that increased salinity in the CCS caused movement of a body of high salinity groundwater westward from the CCS to toward the ACI property.

The model was reviewed by the US Army Corps of Engineers – Jacksonville. Copies of the Earthfx (2012, 2014) reports describing model calibration and applications and copies of all model input files and model results were provided to FPL as part of the discovery process for a series of licensing hearings related to operations of the FPL Turkey Point Nuclear Generating Station and the CCS.

2.2 FPL 2-D SEAWAT Model

Prior to 2016, FPL had developed two key models, a spreadsheet-based water balance model to calculate water levels and salinity in the CCS under historic and future conditions, and a two-dimensional cross-section model using the USGS SEAWAT code (Langevin *et al*., 2008).

The 2-D model was built directly from a simplified model prepared by Hughes and Langevin (Hughes *et al.*, 2010) for a theoretical analysis of the relative importance of temperature or salinity in the vertical movement of hypersaline water beneath the CCS. The 2-D model represented a roughly east-west section through the CCS extending from C-111 in the west to about 1 mile offshore beneath Biscayne Bay.

The model represented the CCS, L31-E, the interceptor ditch, and Biscayne Bay. It did not represent other SFWMD canals, agricultural ditches, pumping, and seasonal variation in groundwater recharge and evapotranspiration. It did not represent the variation in hydraulic conductivity or aquifer thickness away from the CCS. Because it was a cross-section model, it assumed that flow over the entire length of the section was parallel to the section and that no cross-flow occurs, an unrealistic assumption given the highly transient flow patterns in the area. The 2-D model was used primarily for “proof-of-concept” analyses of salt-water migration beneath the CCS.

2.3 FPL 3-D SEAWAT Model

Under the Fifth Supplemental Agreement between FPL and SFWMD (Resolution No. 2009-1000), FPL was required to develop a SFWMD-approved fully-coupled 3-D surface and groundwater density dependent flow model incorporating FPL operational components to evaluate the best alternatives for abatement, mitigation or remediation. It is presumed that the 3-D model prepared by FPL is in partial fulfillment of this requirement.

It should be noted at the outset that the model only considers groundwater-flow and is not a fully-coupled surface water and groundwater model, as required. A coupled model would have a surface-water submodel to simulate hydrologic processes such as precipitation, evapotranspiration, overland runoff, groundwater recharge, flow in the canals, and water levels in the CCS and other lakes, as well as the influence of the shallow groundwater system on these processes. Instead, groundwater recharge, CCS levels, and canal levels are specified as “known” inputs to the model.

The 3-D FPL model appears to have been based very closely on the previous work by Earthfx for ACI. Extensions and refinements were made to the model as will be discussed further on. Simplifications were also made and will also be discussed.

2.3.1 Model Extent and Grid

The extent of the FPL model (Figure 1a) is bounded to the west and south by the C-111 canal system and to the north by C-103 and Mowry canals. The model extends 3 to 4 miles east of Biscayne Bay. The ACI model (Figure 1b) has identical boundaries to the west and north. The model extended further south to represent saltwater intrusion and groundwater discharge to Florida Bay. The ACI model was truncated at the shoreline of Biscayne Bay. The assumption made was that freshwater discharging past the shoreline would ultimately discharge to the Bay and that there was no need to model it explicitly.

The FPL model uses a finite difference grid with square cells 500 ft on a side over much of the model area with refinement to 200 ft cells in the vicinity of the CCS (Figure 2a). The ACI model, which was not specifically focussed on the CCS, used a uniform 500 ft cell size (Figure 2b). The origins (upper left corner) of the two grids) differ by about 700 ft.

2.3.2 Model Layers

The FPL Model has 11 layers (Figure 3a). The top of the first layer represents land surface and the bottom represents the base of the Fort Thompson Formation. The layers are deformed although the basis for the layer deformation is not provided. The base of the model generally follows that of the base of the Biscayne Aquifer and appears to follow the generalized surface of Hughes and White (2014) although the source of the data is not provided.

Table 1: Uniform Layer Properties used in FPL Model

Model Layer	Unit	Horizontal Hydraulic Conduc-tivity (ft/d)	Vertical Hydraulic Conduc-tivity (ft/d)	Specific Storage (per ft)	Specific Yield	Longi-tudinal Disper-sivity (m)	Horiz. Trans-verse Disper-sivity (m)	Vert. Trans-verse Disper-sivity (m)
1	Sediment	250 / 100*	10	1x10-6	0.2	20	2.0	0.02
2	Miami Lime-stone	250	50	1x10-6	0.2	20	2.0	0.02
3		350	50	1x10-6		20	2.0	0.02
4		20,000	2000	1x10-6		20	2.0	0.02
5	Ft. Thomp-son Fm.	1400	200	1x10-6		20	2.0	0.02
6		1400	200	1x10-6		20	2.0	0.02
7		1400	200	1x10-6		20	2.0	0.02
8		60,000	6000	1x10-6		20	2.0	0.02
9		1400	200	1x10-6		20	2.0	0.02
10		1400	200	1x10-6		20	2.0	0.02
11		1400	200	1x10-6		20	2.0	0.02
* Higher value for terrestrial sediments; lower value for marine sediments in Biscayne Bay								

Except for Layer 1, each model layer is assigned a uniform value of hydraulic conductivity (Figure 3a). The FPL report indicates that "…*the aquifer characteristic data for the model were derived from two aquifer performance tests conducted at Turkey Point and regional aquifer characteristics as reported in USGS reports (Klein and Stewart, 1996; Fish and Stewart, 1991; Langevin, 2001). Aquifer characteristics data from both on-site tests identified lower than regional permeability values for the Biscayne Aquifer, which could be related to clastics encountered in the Ft Thompson at these sites*".

It should be noted that the aquifer properties used do not vary spatially and appear to be based solely on the local testing which was noted to be lower than regional values. The transmissivities for the Fort Thompson Formation used in the FPL model (Figure 4a) therefore do not match aquifer regional aquifer characteristics as reported in USGS reports which increase dramatically to the west of the CCS. Transmissivity values are generally lower by a factor of 3 to 4 compared to aquifer transmissivity values mapped by Merritt (1997) and much lower than the calibrated transmissivity values in Hughes and White (2014). This has a noticeable effect on the predicted water levels, as will be discussed further on.

The upper three layers are assumed to represent the Miami Limestone, although this is not stated. There does not appear to be a specific representation of the muck and marl soils in the study area, although the vertical hydraulic conductivity of Layer 1 is reduced compared to Layers 2 and 3. The horizontal hydraulic conductivity of Layer 1 is reduced from 250 ft/d t 100 ft/d below Biscayne Bay. . Vertical hydraulic conductivity values were assigned to be about a factor of 10 lower than the horizontal hydraulic conductivity values (Figure 5a). There is no layer to represent overland flow that can occur in the wet season.

The ACI model has 13 layers and goes to a depth of -110 ft (Figure 3b). The 2012 ACI model follows the base of the Biscayne Aquifer as mapped by Merritt (1997). The model was revised to include the mapped sands (Pinecrest Sands) in the Tamiami Formation that are in contact with the Biscayne aquifer. The layers are not deformed, rather, the hydraulic conductivities are varied within each layer based on the aquifer materials (Figure 3b) and to match maps of aquifer transmissivity developed by Merritt (1997) based on work by Fish and Stewart (1991). Transmissivities (Figure 4b) are higher by about a factor of 2 in the CCS vicinity compared to the aquifer test values used by FPL. Vertical hydraulic conductivity values were assigned to be about a factor of 100 lower than the horizontal hydraulic conductivity values (Figure 5b).

The upper layers of the ACI model represent the overburden soils (Layer 2) and the Miami Limestone (Layer 3). The base of Layer 1 is at land surface and the layer was assigned a very high hydraulic conductivity. The method followed that of Merritt (1997) for representing wet season overland flow in the area east of Card Sound.

2.3.3 Model Boundaries

Biscayne Bay is defined as a time-varying Constant Head (CHD) boundary (Figure 6). The assigned head values are based on recorded water levels at two stage measurement stations in Biscayne Bay. For the steady-state analysis, heads were held constant at -0.71 ft above NAVD. Values were varied i between -0.64 and -0.71 ft in the transient simulations.

The MODFLOW River package is used to simulate the primary canals (e.g. C-111, C-103, and L-31E). River stages are based on water level data at canal flow control structures (where available) from 1968 to present, and water levels recorded in the CCS from 2010-2015. Locations of the rivers represented in the steady-state simulation are shown in Figure 6a as dark blue lines. A minor point is that FPL should not have represented C-111 and C103 in the steady-state model simulations as these canals were not active prior to 1968. Figure 6b shows the location of rivers in the FPL model for the post 1973 simulations.

Figure 7 shows the conductance values for rivers and drains in the FPL model. The maximum value is shown for rivers penetrating more than 1one layer. Tetra Tech indicated that river conductance values (equal to the wetted area times the hydraulic conductivity divided by the riverbed sediment thickness) were calculated using the upper layer hydraulic conductivities and either the surface area of the canal bottom within the model cell or the exposed area based on canal depth, for deeper canals. It is assumed that the values were assigned through an automated process but specific details related to the method of calculating conductance were not provided. Further on in their report, Tetra Tech indicates that conductance values were adjusted on a reach-by reach basis as part of the calibration process.

Values ranged from 80 ft2/d to 200 ft2/d for the North and Florida City Canals. Values for the C-111 and C103 canals on the model boundary ranged from to 50,000 to 567,000 depending on cell size. The values seem to be on the low side. For example, a cell with 500 ft of canal, with a layer 1 thickness of 4.5 ft, and a hydraulic conductivity value of 250 ft/d, and an assumed clogged side zone thickness of 2 ft would have a conductance value of 562,500 which is about equal to the highest value. Most of the other cells had values lower by a factor of 2 to 10 despite similar properties.

L-31E conductance values ranged from 109 ft2/d to over 2,300,000 ft2/d. High values, generally over 100,000 ft2/d, were assigned to cells in Layers 3 and 4. The higher values are assumed to be related to the higher hydraulic conductivity of Layer 4. The exact methodology for assigning values is unclear and does not appear consistent with the method for assigning values to the boundary canals. The higher conductance values favor dilution of saltwater emanating from the CCS.

The MODFLOW River package was also used to simulate the Cooling Canal System (CCS). Conductance values varied from about 102 ft2/d to 33,333 ft2/d. The values assigned also appear to be affected by whether the cells are representing open water in the CCS or the bermed areas (Figure 7b). Cells were assigned relatively low conductance values compared to L-31E, the interceptor drain, or the boundary canals. Even cells in layers 3 and 4 which should reflect the high hydraulic conductivity of Layer 4 were assigned low values. The low values favor limiting the leakage of saltwater from the CCS

The MODFLOW Drain package is used to represent secondary canals (e.g., Model Land, Card Sound Road, C-110, and C-113) and the Interceptor Ditch. Drain elevations are based on water level data at flow control structures (where available), DEM-based topographic gradients (e.g. Card Sound Road Canal), or measured water levels in the Interceptor Ditch. Locations of the drains represented in the steady-state simulation are shown in Figure 6a as lighter blue lines. Figure 6b shows the location of surface water features represented in the FPL model for the post 1973 simulations.

Drain conductance values for the CCS are shown in Figure 7a and Figure 7b. Values generally ranged between 1,000,000 and 4,200,000 ft2/d. The higher values were for Layer 3 but cells in Layers 1 and 2 also had values at or above 2,000,000 ft2/d. As noted above, the conductance values are much larger than those applied to the CCS even though the settings are similar. The high values favor intercepting the saltwater emanating from the CCS.

Natural drainage features and canals that had no control structures, such as the Card Sound Road (pre-2011) and the North, Florida City, and Model Land canals, and the borrow canal along U.S. 1 (pre-1968) were treated in the ACI model as zones of high hydraulic conductivity rather than as rivers or drains. The levels in these canals are affected by the groundwater system rather than by control structures and they, in turn, affect groundwater levels. Drains on the other hand, only allow one-way drainage from the aquifer. The larger SFWMD canals along the boundary of the model were simulated using the MODFLOW RIVER module in post-1968 simulations.

Lakes are not represented in the FPL model. Because SEAWAT does not incorporate any of the MODFLOW lake modules, these were represented in the ACI model with zones of extremely high transmissivity, as was first done in the model by Merritt (1997).

The perimeter of the FPL model is represented by General Head Boundaries (GHBs). GHB boundaries were assigned to all perimeter model cells not containing a River or Constant Head boundary. The same heads assigned to the overlying River or CHD cells are assigned to the underlying GHB cells. In our view, the west boundary should have been represented using a flow divide rather than a specified inflow.

Concentrations were simulated as terms of relative salinity, where a relative salinity of 1 is equivalent to 35 PSU (seawater concentration) and an equivalent chloride concentration of 19,400 mg/L. A value of 1 was applied in Biscayne Bay, the lower reach of C-111 and the uncontrolled portions of Mowry, North, and Florida City Canals. This is similar to the ACI model, although C-111 was assumed to be controlled by S-197 in the post-1972 simulations. As well, because Card Sound Road is simulated as a one-way drain in the FPL model, there is no possibility for it to affect concentrations in the aquifer. Card Sound Road, the US 1 borrow canal, and coastal inlets were simulated as uncontrolled features in the ACI model which allowed saltwater to move inland in the canals and affect concentrations. The movement of saltwater into the Card Sound Road canal was observed as far back as 1945 (Parker *et al*., 1955) and has been noted on all FW/SW maps produced by the USGS.

2.3.4 Groundwater Recharge and Discharge

The recharge rates for the steady-state model range from 0 to 0.0062 in/d (2.25 in/yr) with 0 values everywhere except in the northwest corner representing the Homestead area (Figure 8). According to FPL, seasonal recharge rates were calculated based on the methodology described in Hughes and White (2014). NEXRAD precipitation and evapotranspiration data were used to estimate the base groundwater recharge rates from 1996-2015. Average seasonal rates used in the seasonal model prior to 1996 were based on the seasonal average rates from 1996-2015. Rates used in this period are shown in Figure 9a for the wet season and Figure 9b for the dry season. The seasonal and monthly transient model Recharge Packages reference external .DAT files which contain arrays of stress period-specific recharge rates. As in other model packages, the predictive recharge data file repeats the monthly model’s simulated period between 2011 and 2015.

It should be noted that the FPL model does not allow net recharge to decrease below zero and therefore does not account for groundwater losses due to evapotranspiration from deeper root systems when the water table is near surface. This is a key process in south Florida, and, in particular south Dade County. This phenomenon was noted as far back as 1945. For example, Klein (1965) noted that “A cone of depression to below sea level apparently develops whenever a drought is sufficiently extended. An earlier indication that water levels in southern Dade County declined below sea level during a drought was shown in a water-level contour map for May 19, 1945 (Parker and others, 1955, p.210-211). The 1945 map showed only the northeast part of the cone of depression, but otherwise was similar to the cone of May 1962” (reproduced here in Figure 10).

The ACI model follows the approach of Merritt and Langevin and uses the MODFLOW evapotranspiration module to calculate groundwater ET as a function of potential ET and depth to the water table. This allows the ACI model to recreate the westward gradients that occur in the Model Land area under drought conditions. The inability of the FPL model to match the westward extent of the salt water plume from the CCS is due in part felt that the lack of FPL model representing these seasonal westward gradients.

Groundwater extraction was simulated in the FPL model using the MODFLOW Well Package and includes municipal, industrial and agricultural groundwater pumping. Rates and locations, shown in Figure 11a were determined from SFWMD data. Wells included in the ACI model (Figure 11b) were also included in the FPL model and were pumped at the permitted rates.

2.3.5 Steady-State Model results – Pre 1968

The simulated steady state heads and concentrations are presented in Figure 12. The simulated heads appear reasonable in the Model Land area as they are strongly constrained by the specified river stages for the C-111 and C-103 boundary canals and by drainage to the Model Land canal. The North, Florida City, and Card Sound Road canals have less influence because of the lower assigned conductance values. Heads are lowered significantly by pumping for at the FKAA wellfield. This is likely due to not representing the high transmissivities in this area.

The simulated relative salinity values have been transformed to chloride concentrations for display purposes in Figure 12b by assuming a 19,000 mg/L chloride concentration for seawater. As expected, there is no influence of the Card Sound Road canal on the concentrations. The effect of assuming that C-111 has the same salinity as Biscayne Bay is noted in the southwest part of the model. Otherwise, the values are similar to those simulated in the ACI model.

The steady-state model results were meant primarily to provide starting conditions for the transient simulations. However, they also provide a good way of assessing the basic building blocks of the FPL model.

2.3.6 Seasonal Model – 1968 to 2010

The FPL Model simulates transient groundwater flow, salt and heat transport for a period of approximately 42 years. As in the ACI Model, the period is broken into 84 seasonal stress periods.

Simulated heads in the vicinity of the FKAA wellfield for Layer 5 in Stress Period 81 are shown in Figure 14. The simulated heads are 6 ft below sea level. The low values are related to the unrealistic assumption in the FPL model that hydraulic conductivity values are the same as those determined by aquifer testing at the CCS. Fish and Stewart found the area shown to be of extremely high transmissivity.

This existence of a high transmissivity zone in the vicinity of the FKAA was recognized by Tetra Tech and was given as a one of the reasons for not using Water level data from G-864 and G-864A in the model calibration "…the lack of any observed response to the 40 ac-ft/day increase (i.e. 20 ac-ft/day to 60 ac-ft/day) in FKAA pumping between 1974 and 2010—which would suggest atypical, exceptionally high transmissivities in this area.". The characterization of the transmissivities as atypical is inconsistent with the long-recognized trend of increasing transmissivity to the west of the CCS. Tetra Tech notes that they doubled the transmissivity values across the model to better match the westward movement, but changing the values uniformly is not the correct approach to representing a spatially variable transmissivity.

Simulated heads in the area between C-110 and the CCS for Layer 2 in Stress Period 74 are shown in Figure 15a. The simulated heads are more than 1 ft above land surface. The high heads are related to the lack of a method for representing overland flow in the area as was done in the Merritt and ACI models. These high heads likely contribute to the model's inability to match the westward movement of the saltwater plume from the CCS.
The seasonal model was used to calculate groundwater salinity values from 1969 to 2010. The CCS was assumed to start operations in 1973 with Biscayne Bay water. Chloride concentrations assigned to the river cells used to represent the CCS were varied over time to simulate changes in CCS salinity (Figure 13).

The FPL model matches 2010 observed chloride concentrations in the CCS vicinity reasonably well (Figure 16). Chloride values below Biscayne Bay are higher than observed, however, indicating that either the transmissivities are too high east of the CCS, the discharge from the CCS is too high, or that inflows into the CCS from Biscayne Bay are underestimated. Use of the model in a predictive capability for areas west of the CCS should be viewed with caution in light of the model simplifications discussed in this review.

3 Limitations

Services performed by Earth*fx* Inc. were conducted in a manner consistent with that level of care and skill ordinarily exercised by members of the environmental engineering and consulting profession.

This report presents the results of data compilation and computer simulations of a complex geologic setting. Models constructed from this data are limited by the quality and completeness of the information available at the time the work was performed. The applicability of the simplifying assumptions may or may not be applicable to a variety of applications.

It should be recognized that the passage of time affects the information provided in this report. Environmental conditions and the amount of data available can change. Discussions relating to the conditions are based upon information that existed at the time the conclusions were formulated. Consistent with the foregoing, Earthfx Inc. used its best professional efforts to consider and evaluate all reasonably relevant and accessible data during its efforts to prepare this report. Data reviewed for this report was evaluated in its reported state; it was beyond the scope of this project to review each data measurement or to audit the reported data.

All of which is respectively submitted,

EARTHFX INC.

Report prepared by:

E.J. Wexler, M.Sc., M.S.E., P.Eng.
Director of Modelling Services
Earthfx Incorporated

LICENSED PROFESSIONAL ENGINEER
E.J. WEXLER
100132311
PROVINCE OF ONTARIO

4 REFERENCES

Earthfx Incorporated, 2012, Simulation of groundwater flow and saltwater movement in the vicinity of the Atlantic Civil Property, South Miami-Dade County, FL: prepared for Atlantic Civil Incorporated in support of Application Number SAJ-1995-6797(mining), Earthfx Inc., January 30, 2012.

Fish, J.E., and Stewart, M., 1991, Hydrogeology of the surficial aquifer system, Dade County, Florida: U.S. Geological Survey Water-Resources Investigations Report 90-4108, 50 p.

Hughes, J.D., Langevin, C.D., and Brakefield-Goswami, L., 2010. Effect of Hypersaline Cooling Canals on Aquifer Salinization: Hydrogeology Journal vol. 18, no. 1: 25-38. DOI 10.1007/s10040-009-0502-7.

Hughes J.D. and White, J.T., 2014. Hydrologic Conditions in Urban Miami-Dade County, Florida, and the Effect of Groundwater Pumpage and Increased Sea Level on Canal Leakage and Regional Groundwater Flow. U.S. Geological Survey Scientific Investigations Report 2014–5162, 175 p., http://dx.doi.org/10.3133/sir20145162.

Klein, H. and Waller, B.G., 1985, Synopsis of saltwater intrusion in Dade County, Florida, through 1984: U.S. Geological Survey (USGS) Water-Resources Investigations Report 85-4104.

Langevin, C.D., 2001, Simulation of ground-water discharge to Biscayne Bay, southeastern Florida: U.S. Geological Survey Water-Resources Investigations Report 00-4251, 127 p.

Langevin, C.D., Shoemaker, W.B., and Guo, W., 2003, MODFLOW-2000, The U.S. Geological Survey modular ground-water model - documentation of the SEAWAT-2000 version with the variable density flow process (VDF), and the integrated MT3DMS transport process (IMT); U.S. Geological Survey Open File Report 03-426, 43 p.

Langevin, C.D., Thorne, D.T., Jr., Dausman, A.M., Sukop, M.C., and Guo, Weixing, 2008, SEAWAT Version 4: A Computer Program for Simulation of Multi-Species Solute and Heat Transport: U.S. Geological Survey Techniques and Methods Book 6, Chapter A22, 39 p.

Merritt, Michael L., 1997, Simulation of the water-table altitude in the Biscayne aquifer, southern Dade County, Florida, water years 1945-89: U.S. Geological Survey Water-Supply Paper 2458, prepared in cooperation with the Metro-Dade Department of Environmental Resources Management, 148 p.

Parker, G.G., Ferguson, G.E., Love, S.K., and others, 1955, Water resources of southeastern Florida: U.S. Geological Survey Water-Supply Paper 1255, 965 p.

Tetra Tech Incorporated, 2016, A Groundwater Flow and Salt Transport Model of the Biscayne Aquifer, June 2016, 53 p.

FIGURES

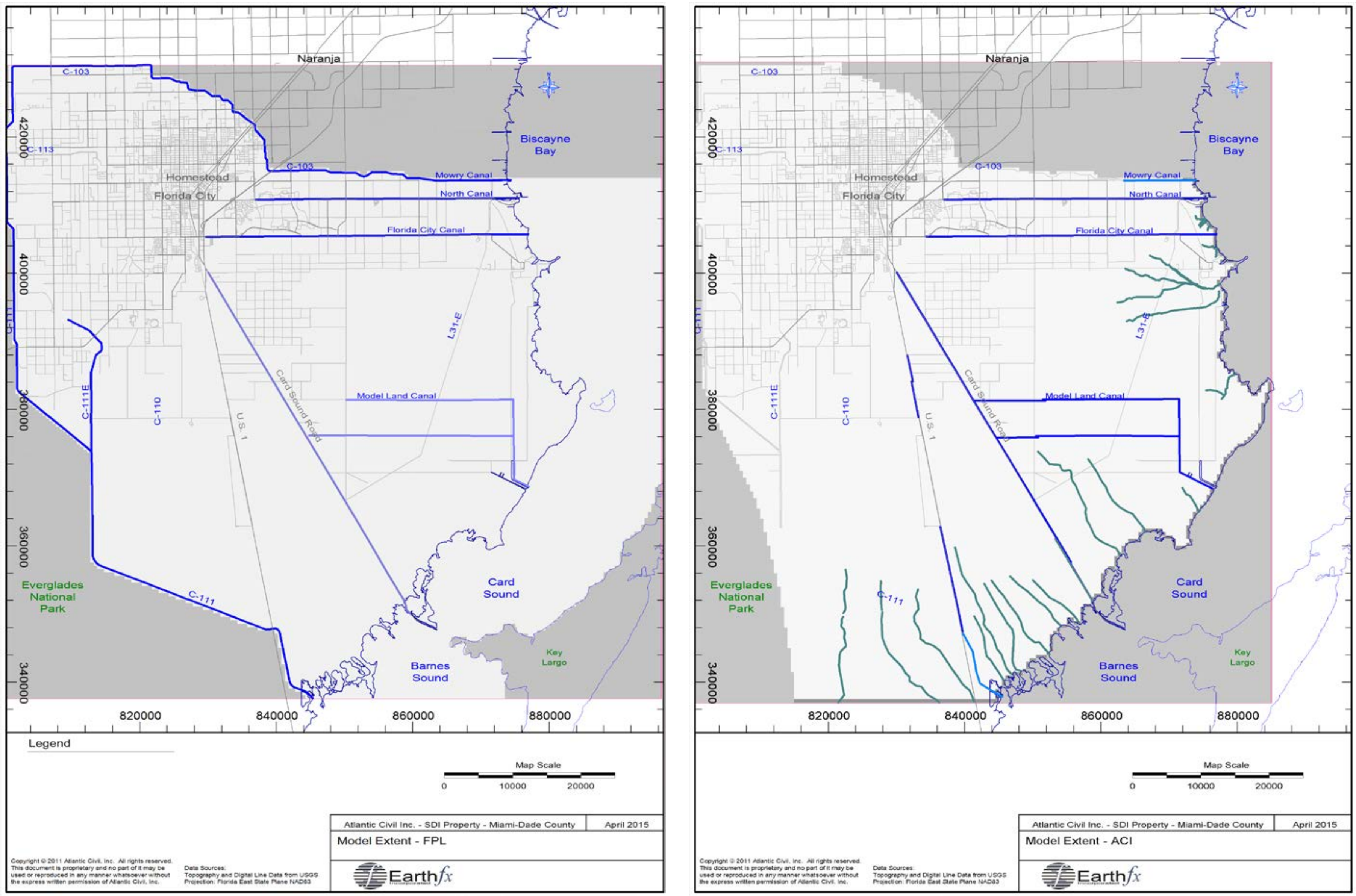

Figure 1: Extent of (a) the FPL model and (b) the ACI model.

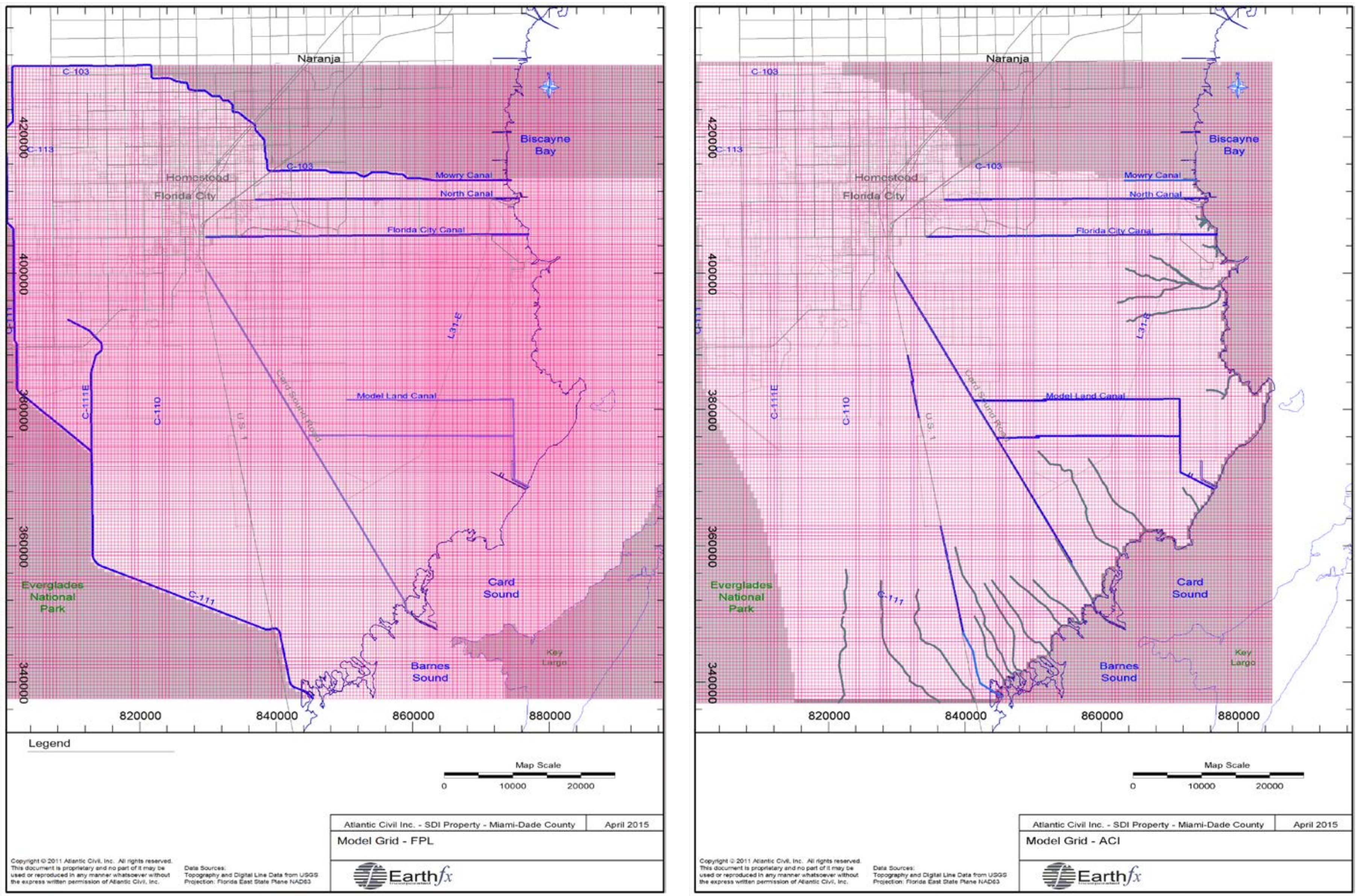

Figure 2: Model grid (a) FPL Model and (b) ACI Model.

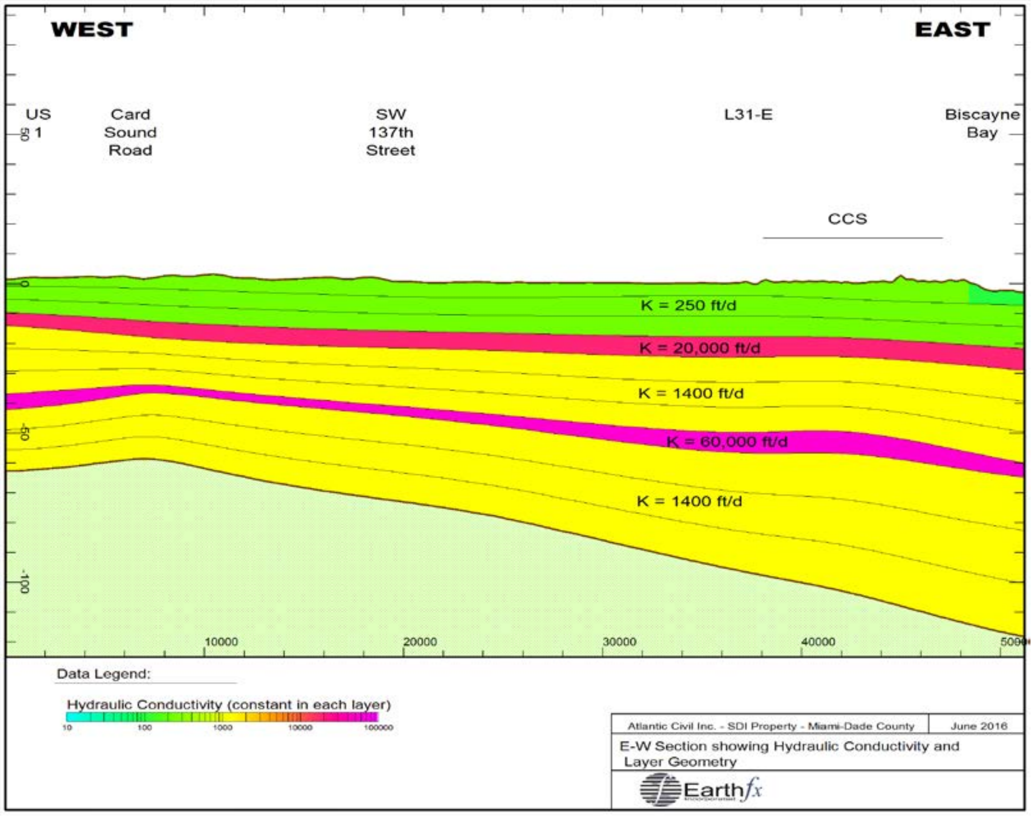

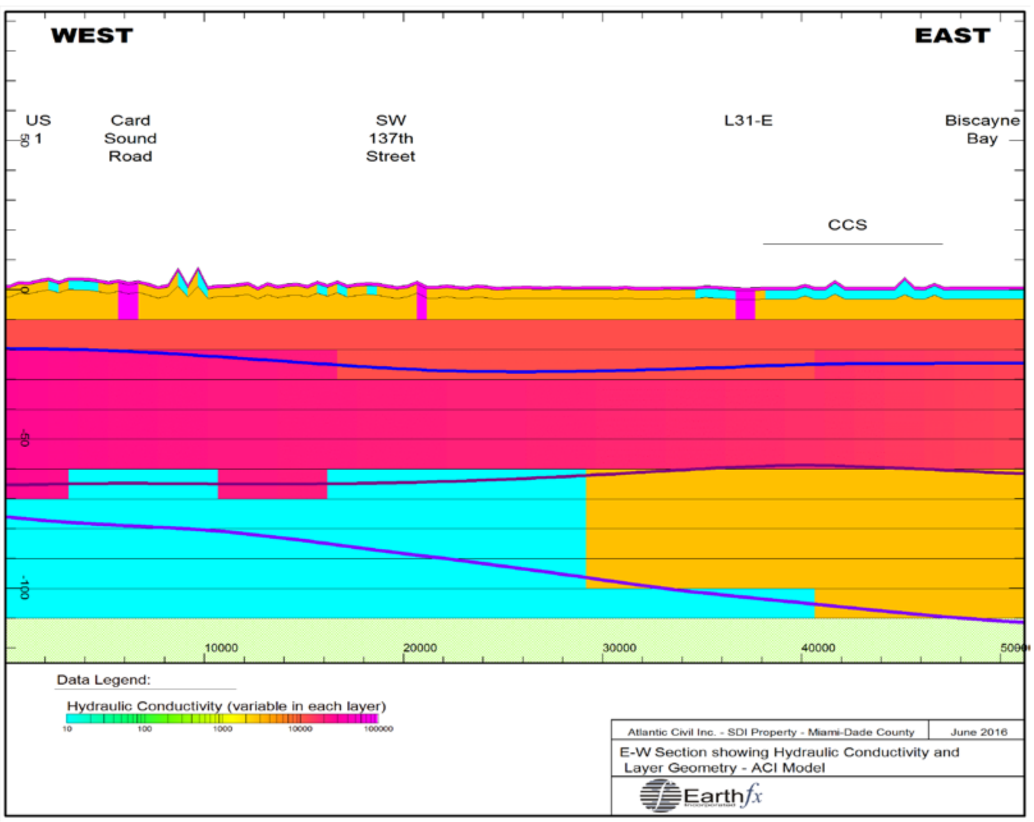

Figure 3: Layer geometry and hydraulic conductivity values (a) FPL Model and (b) ACI Model.

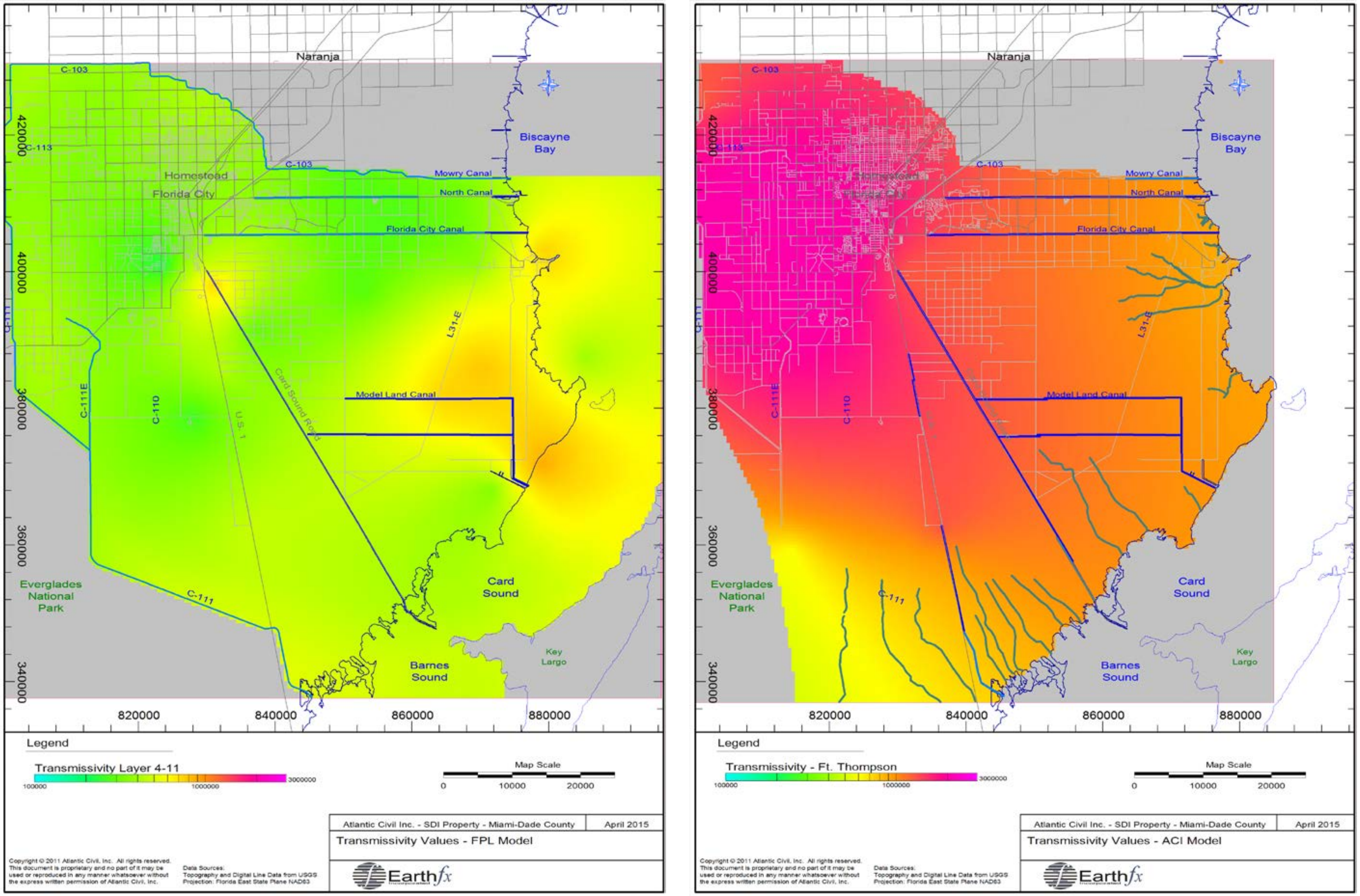

Figure 4: Transmissivity values for the Ft. Thompson Formation in the Biscayne aquifer (a) FPL Model and (b) ACI Model.

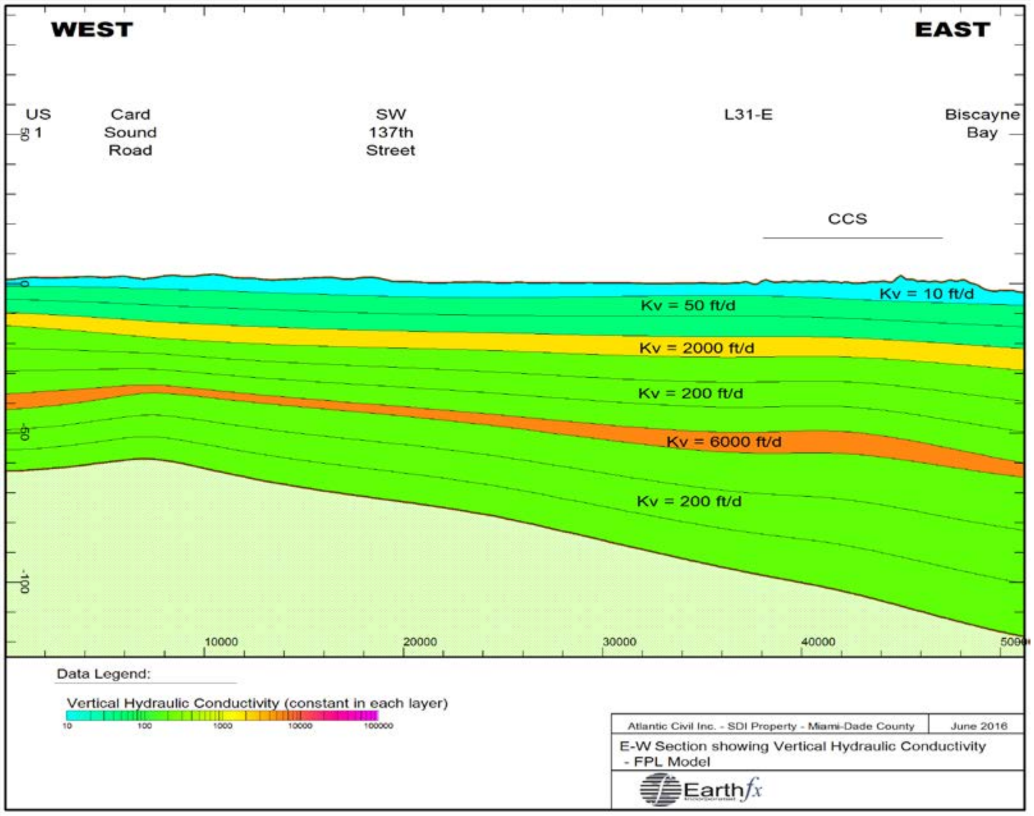

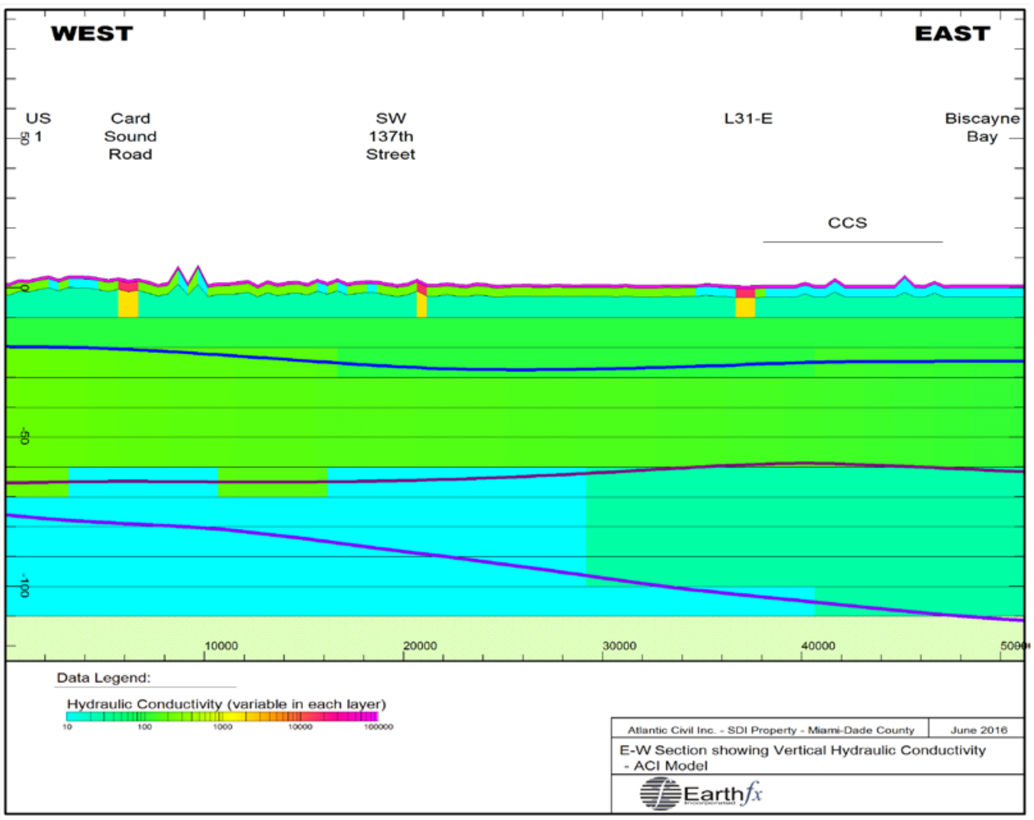

Figure 5: Vertical hydraulic conductivity values (a) FPL Model and (b) ACI Model.

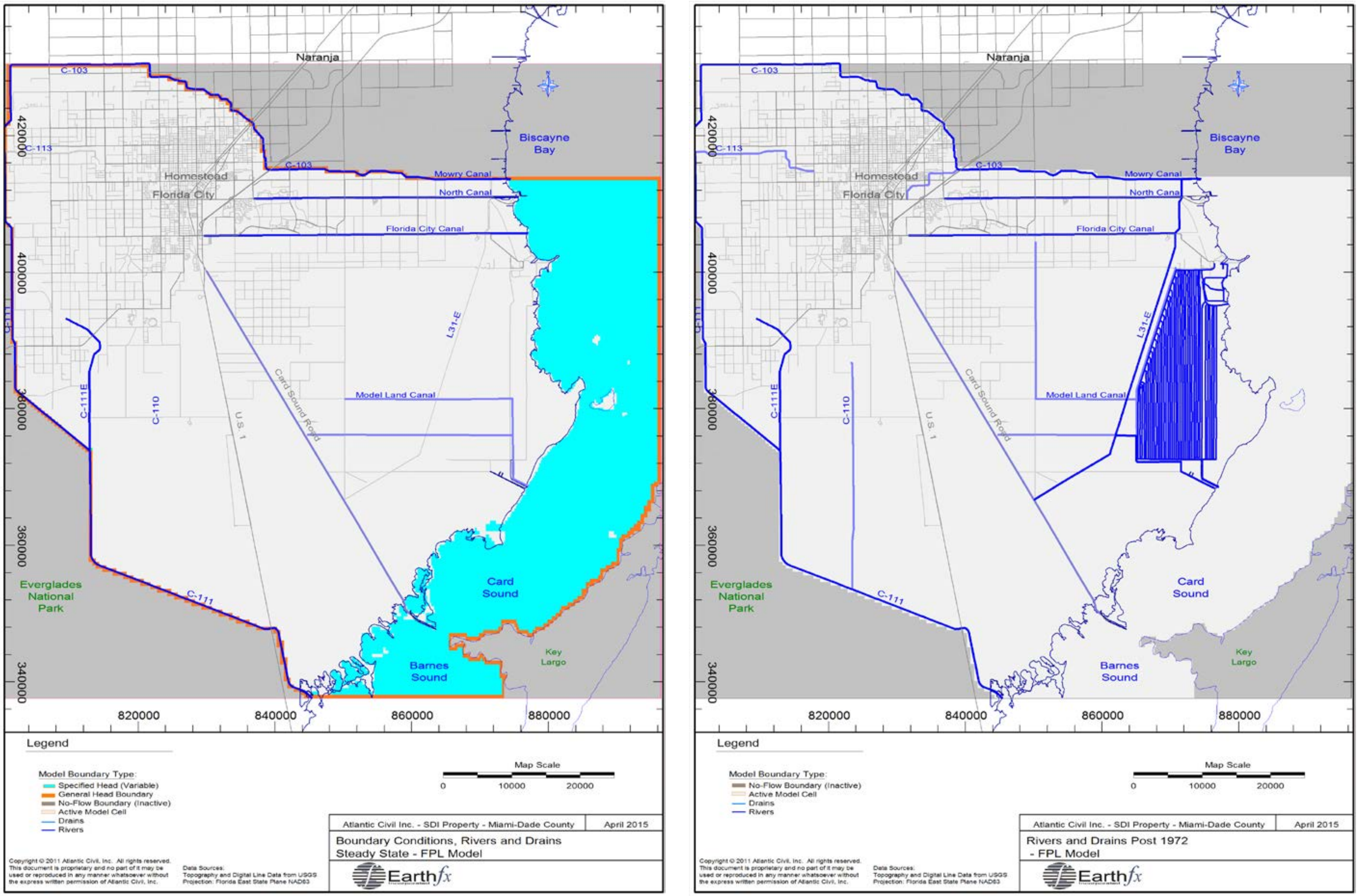

Figure 6: (a) FPL Model boundary conditions and location of drains and rivers - steady-state model and (b) Drains and rivers - post 1973 model.

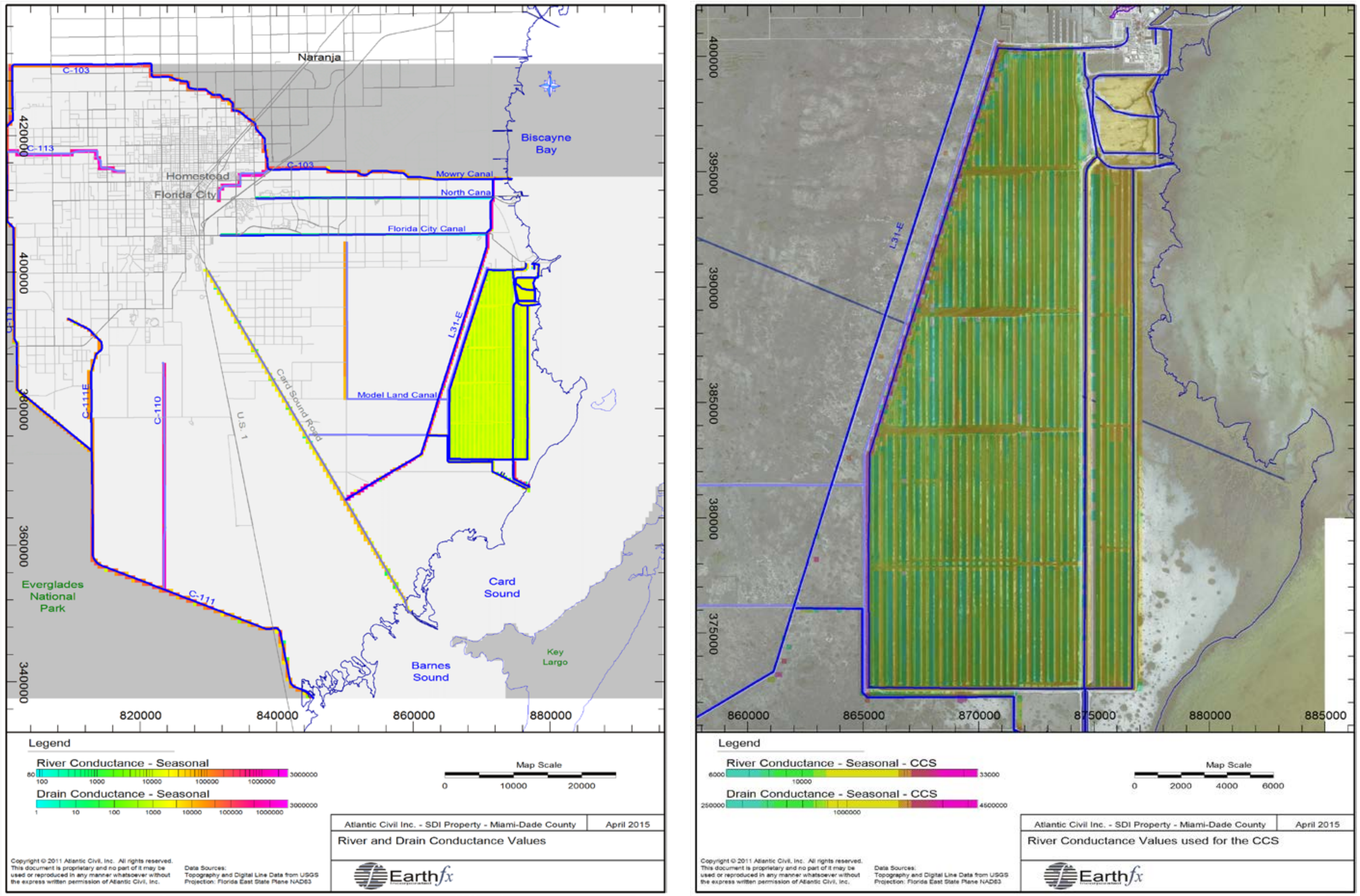

Figure 7: (a) Conductance values for rivers and drains in the FPL model and (b) Conductance values used for the CCS.

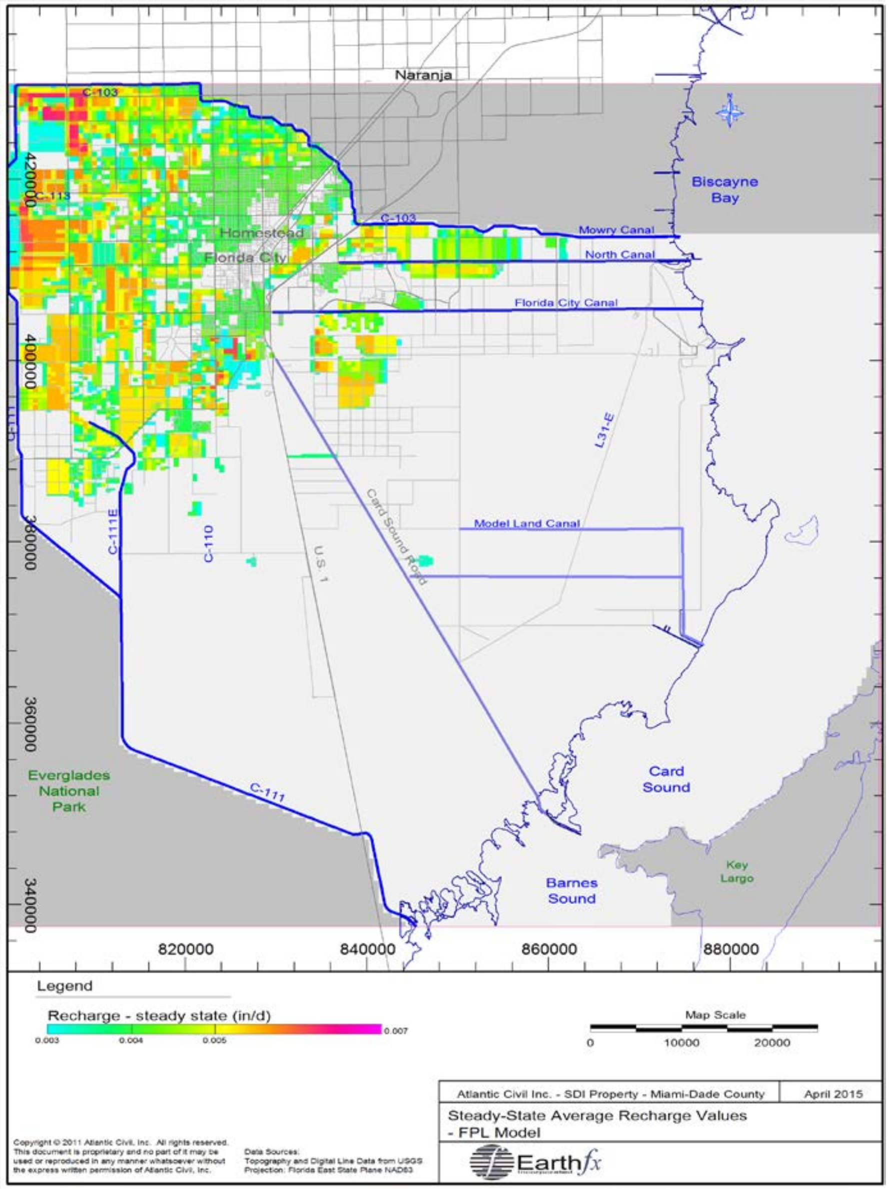

Figure 8: Average recharge rates for the steady-state model.

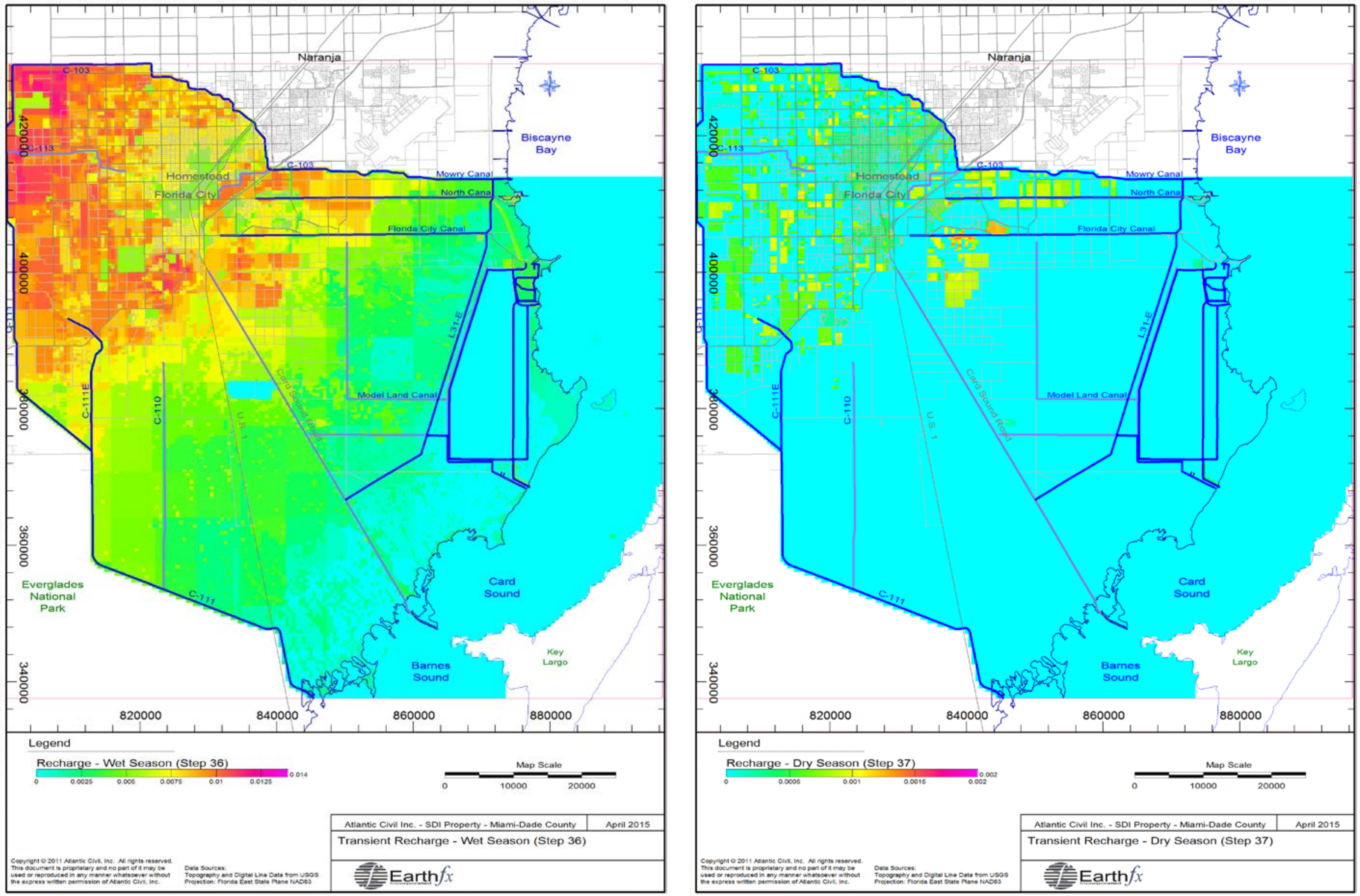

Figure 9: Applied seasonal recharge (a) wet season, and (b) dry season (note different scales).

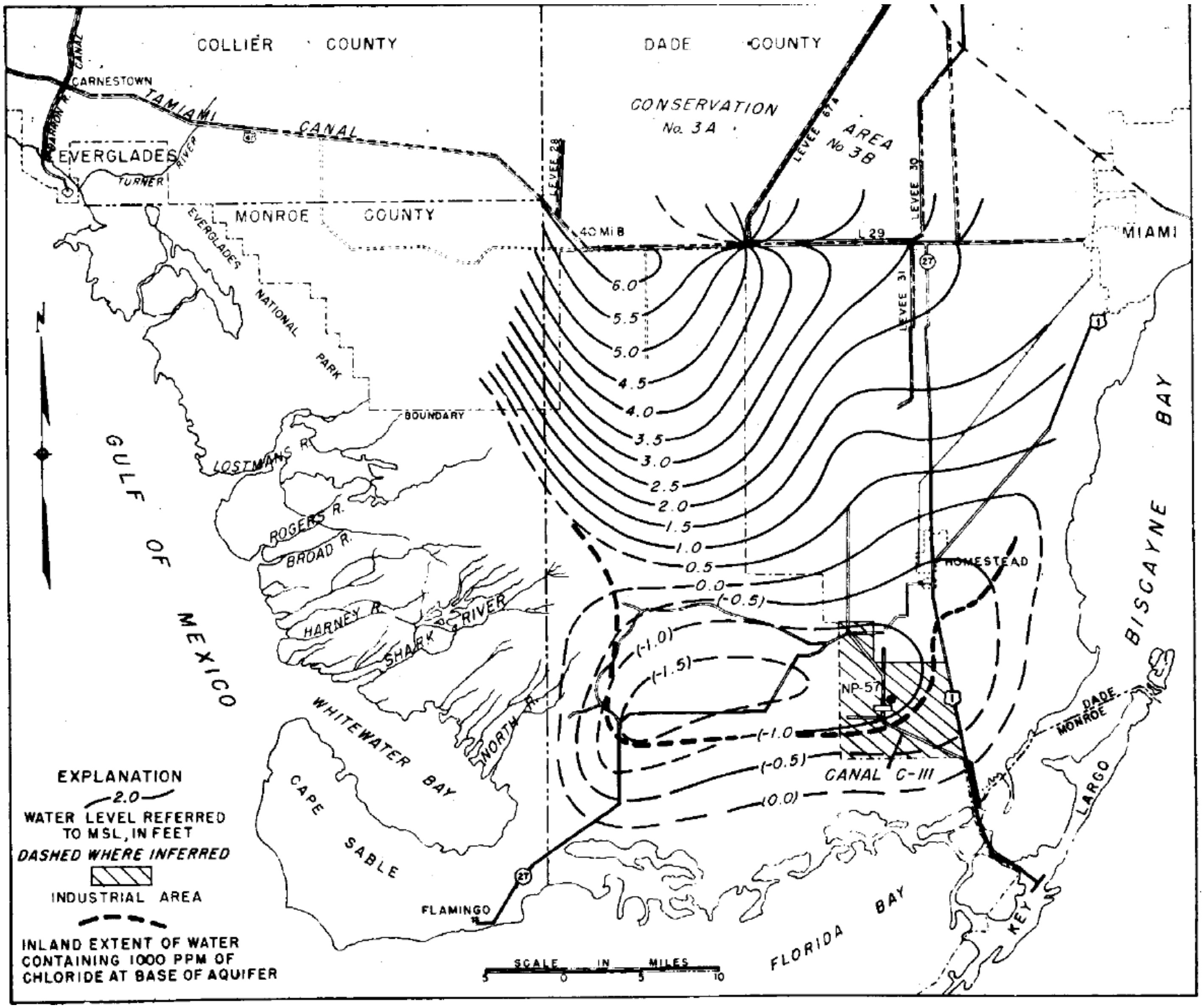

Figure 10: Water table map for May 1962, from Klein (1965).

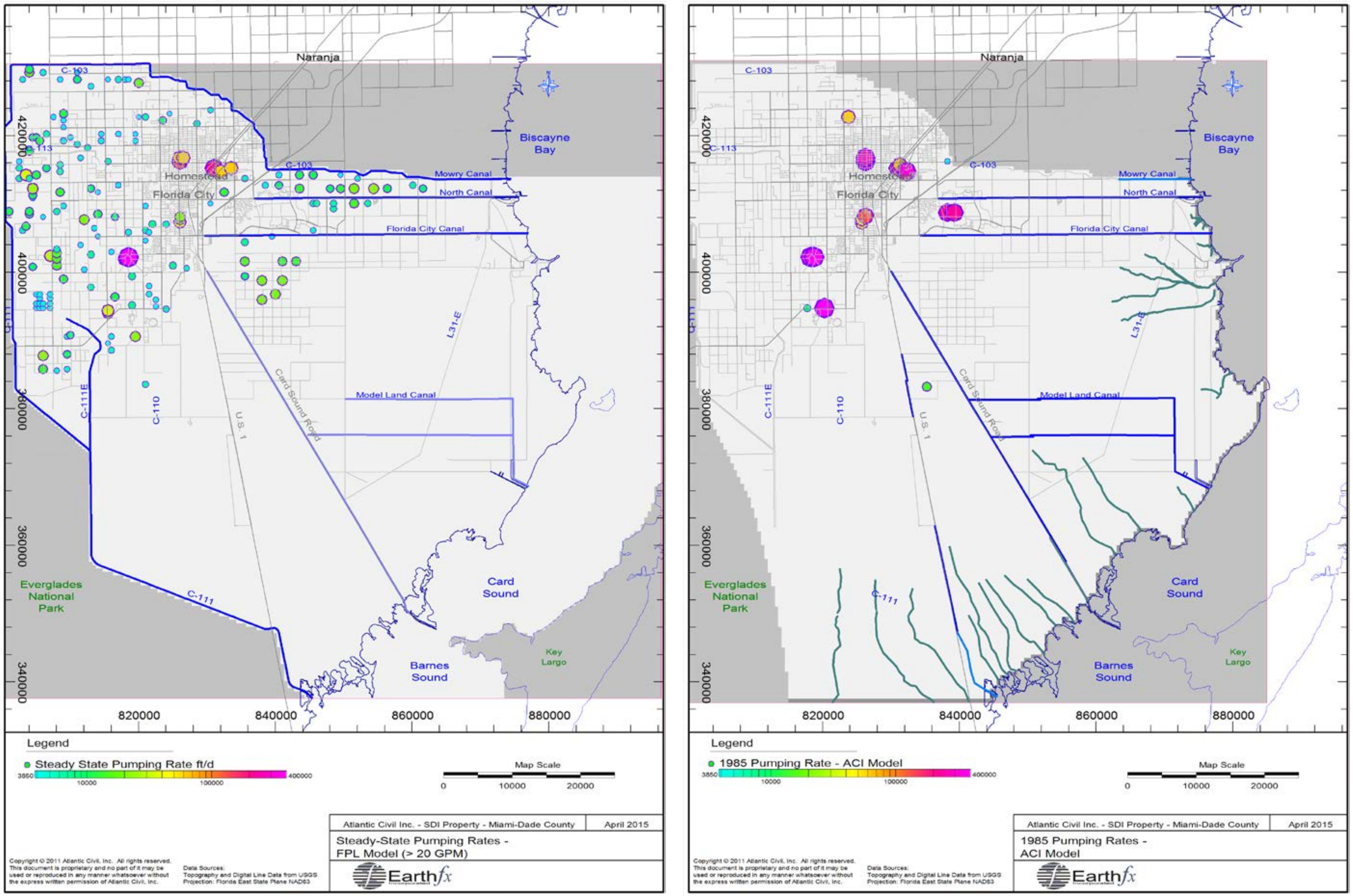

Figure 11: (a) Steady state pumping rates in the FPL Model and (b) 1985 pumping rates in the ACI Model.

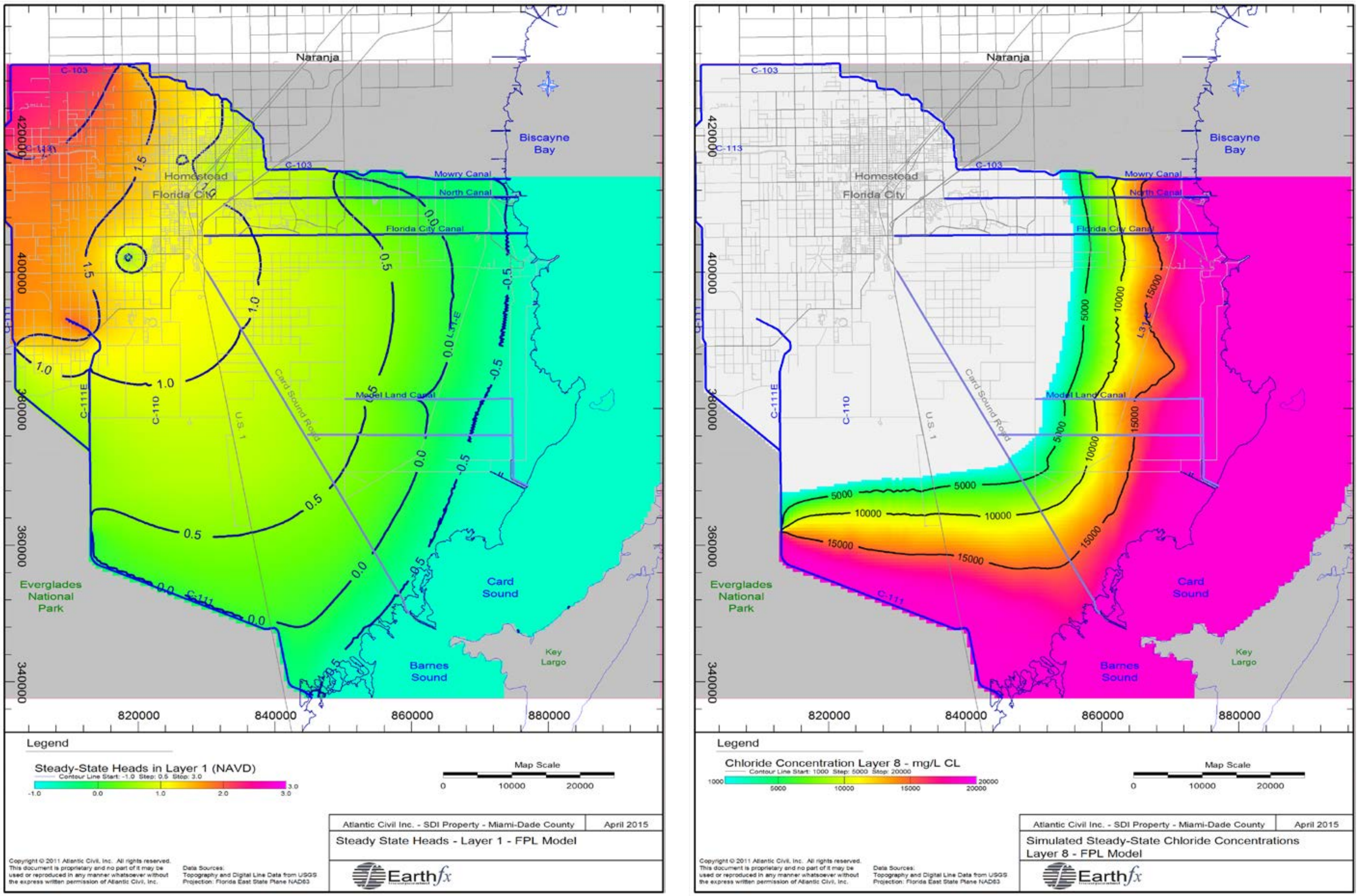

Figure 12: Simulated steady state model results (a) heads in Layer 1 and (b) chloride concentrations in Layer 8.

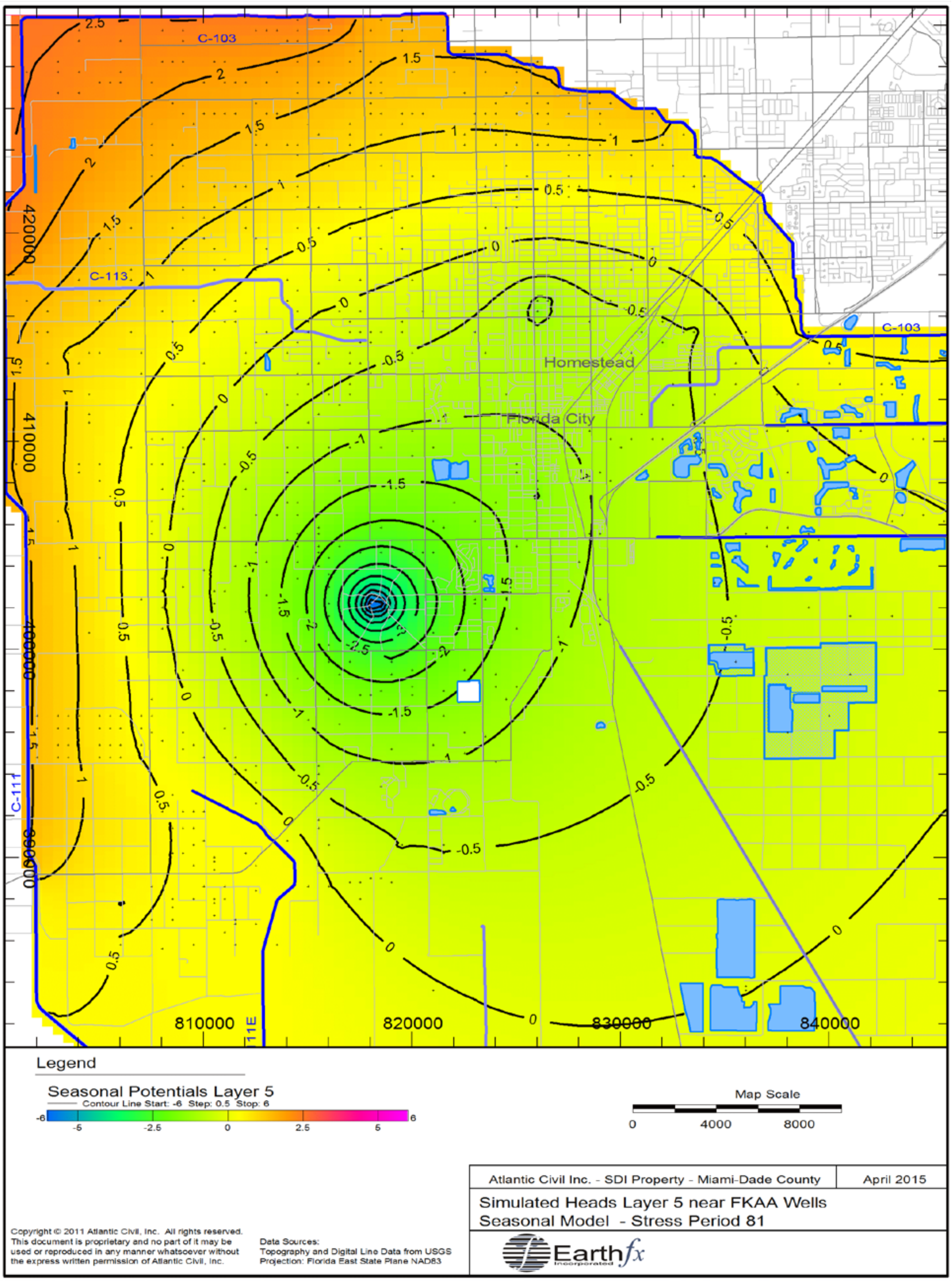

Figure 13: Simulated heads in Layer 5 in the Seasonal Model at Stress Period 81.

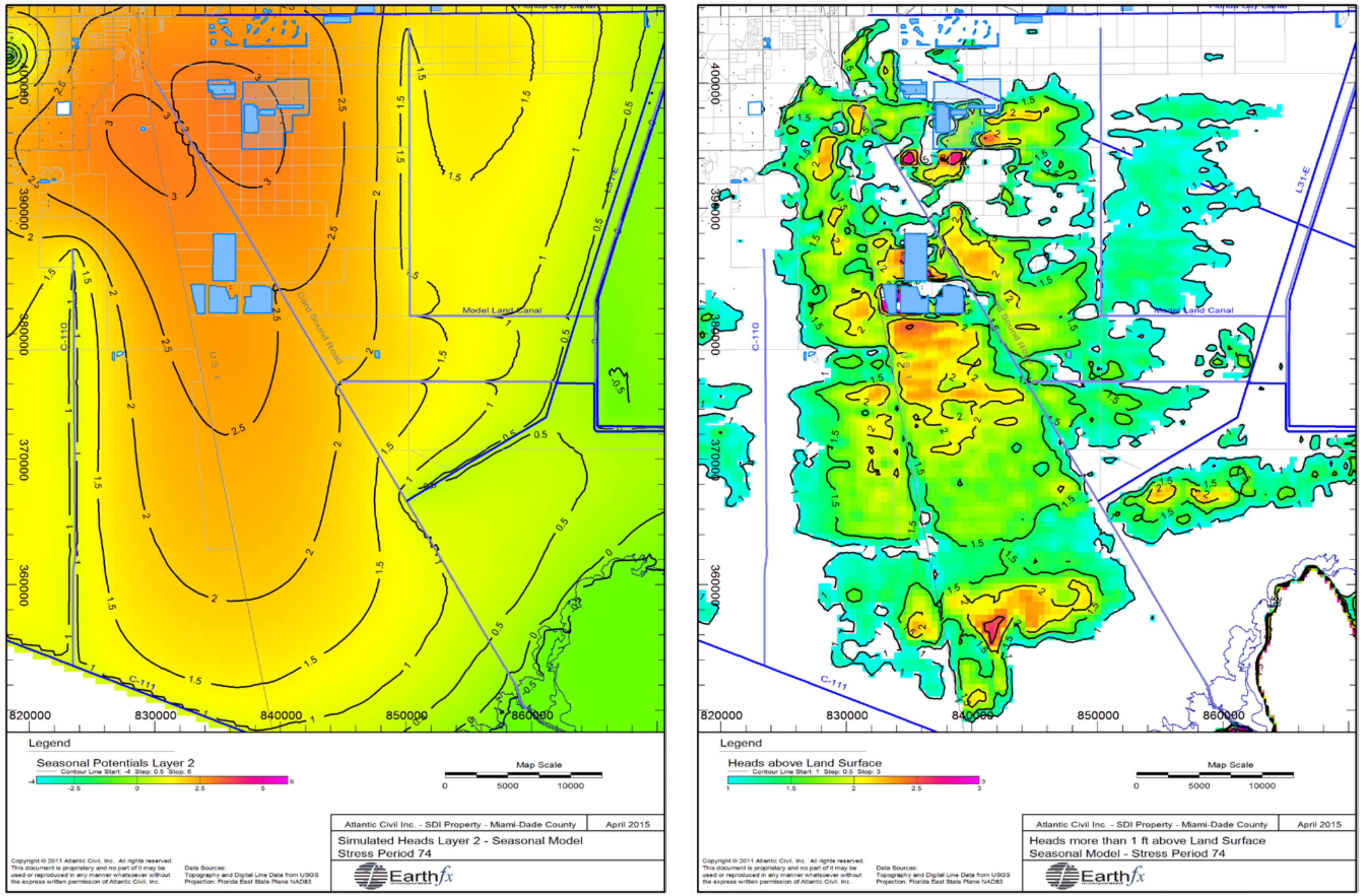

Figure 14: (a) Simulated heads in Layer 2 in the area between C-110 and the CCS for Stress Period 74 and (b) Simulated heads more than 1 ft above land surface.

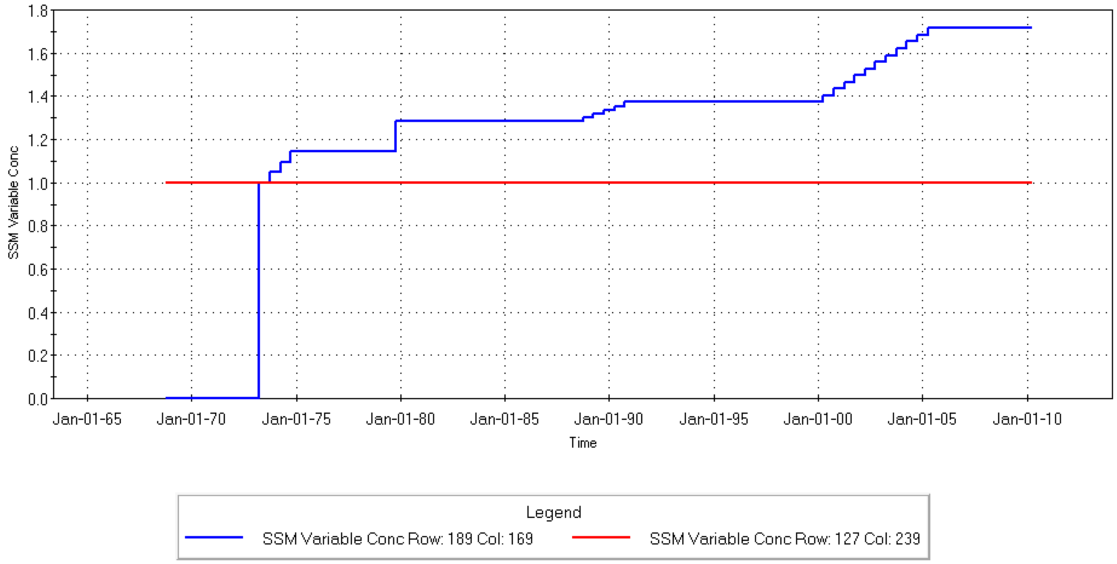

Figure 15: Relative salinity values applied to the CCS in the FPL model (Values above 1 represent hypersaline water).

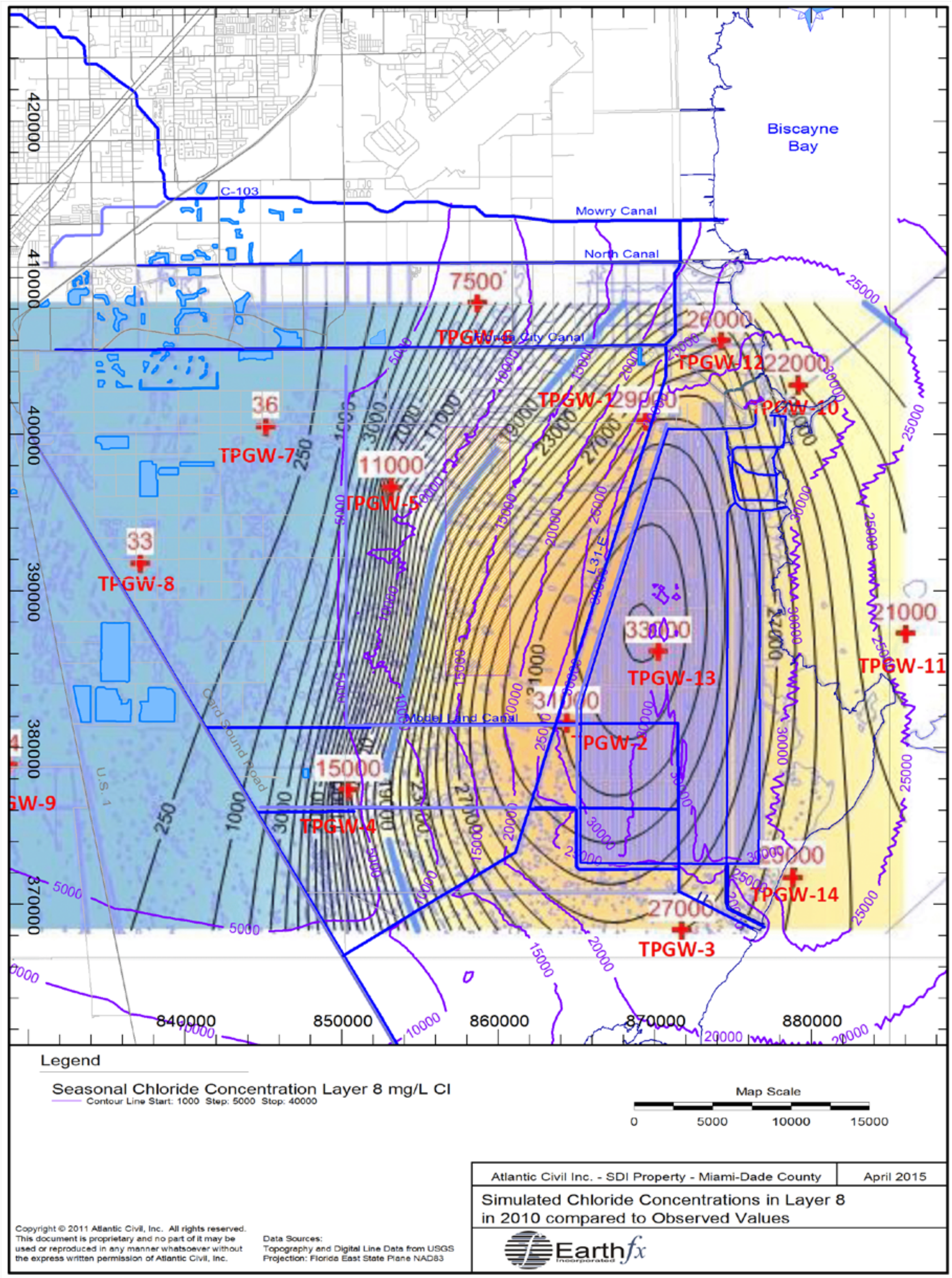

Figure 16: Simulated chloride concentrations in 2010 in Layer 8 and observed values in December 2010.